UNIVERSITY OF ALBERTA

Role of brain-derived neurotrophic factor (BDNF) in the generation of central sensitization and neuropathic pain.

by

Van Bich Lu ©

A thesis submitted to the Faculty of Graduate Studies and Research
in partial fulfillment of the requirements for the degree of

Doctor of Philosophy

Department of Pharmacology

Edmonton, Alberta, Canada
Fall 2007

Library and
Archives Canada

Published Heritage
Branch

395 Wellington Street
Ottawa ON K1A 0N4
Canada

Bibliothèque et
Archives Canada

Direction du
Patrimoine de l'édition

395, rue Wellington
Ottawa ON K1A 0N4
Canada

Your file Votre référence
ISBN: 978-0-494-33021-0
Our file Notre référence
ISBN: 978-0-494-33021-0

NOTICE:
The author has granted a non-exclusive license allowing Library and Archives Canada to reproduce, publish, archive, preserve, conserve, communicate to the public by telecommunication or on the Internet, loan, distribute and sell theses worldwide, for commercial or non-commercial purposes, in microform, paper, electronic and/or any other formats.

The author retains copyright ownership and moral rights in this thesis. Neither the thesis nor substantial extracts from it may be printed or otherwise reproduced without the author's permission.

AVIS:
L'auteur a accordé une licence non exclusive permettant à la Bibliothèque et Archives Canada de reproduire, publier, archiver, sauvegarder, conserver, transmettre au public par télécommunication ou par l'Internet, prêter, distribuer et vendre des thèses partout dans le monde, à des fins commerciales ou autres, sur support microforme, papier, électronique et/ou autres formats.

L'auteur conserve la propriété du droit d'auteur et des droits moraux qui protège cette thèse. Ni la thèse ni des extraits substantiels de celle-ci ne doivent être imprimés ou autrement reproduits sans son autorisation.

In compliance with the Canadian Privacy Act some supporting forms may have been removed from this thesis.

While these forms may be included in the document page count, their removal does not represent any loss of content from the thesis.

Conformément à la loi canadienne sur la protection de la vie privée, quelques formulaires secondaires ont été enlevés de cette thèse.

Bien que ces formulaires aient inclus dans la pagination, il n'y aura aucun contenu manquant.

Canada

To my wonderful family: Dad, Mom, Ha and Linh,
Without your love and patience, I would not be where I am or who I am today.

And to the grandfather I never had the chance to meet,
who believed with hard work the possibilities are infinite.

ABSTRACT

Using an organotypic slice culture preparation of rat spinal cord slices, the effect of brain-derived neurotrophic factor (BDNF) on dorsal horn neurons, at comparable levels and durations as those found in animal models of neuropathic pain, was assessed.

Prolonged exposure to elevated levels of BDNF produced an increase in overall dorsal horn excitability as a result of neuronal type-specific changes in excitatory and inhibitory synaptic transmission. BDNF decreased synaptic excitation of identified inhibitory neurons but increased synaptic excitation of putative excitatory dorsal horn neurons.

The actions of BDNF on excitatory synaptic activity are sufficient to initiate Ca^{2+} oscillations and spontaneous bursts of activity during extracellular recordings. BDNF also induced changes in inhibitory synaptic activity, but these changes were not as influential as the changes in excitatory synaptic activity on overall dorsal horn excitability. Under our experimental conditions, neither the reversal of the chloride gradient nor the induction of classical long-term potentiation contributed to the action of BDNF.

The selectivity and pattern of synaptic changes induced by BDNF are very similar to the changes observed in an animal model of neuropathic pain. These and other findings from our laboratory strongly implicate BDNF in the central sensitization of the spinal cord that may underlie the development of chronic neuropathic pain.

ACKNOWLEDGEMENTS

There are some very special people who have helped me along this journey and I would like to thank them at this time.

First and foremost, I would like to thank my supervisors Drs. Peter Smith and Bill Colmers. Thank you Peter for having me in the lab. Your enthusiasm and cheerfulness reminds me that there is a bright side to every bump in the road of life and a good laugh can make for a very smooth trip. Thank you Bill for your continuous input and suggestions. I will always remember your kindness as a mentor and a friend. I would also like to thank my supervisory committee members, Drs. Bill Dryden and Klaus Ballanyi, for sharing their expertise and knowledge. I have learnt so much from them and thank them both for their generosity. In addition, I would like to thank the other members of my thesis defence examining committee, Dr. Michael Salter from the University of Toronto and Dr. Brad Kerr from the Department of Anaesthesiology at the University of Alberta, for taking the time out of their very busy schedules to read and review this thesis. I appreciate their expert advice and comments on my thesis.

Also, a special thanks to Dr. Laura Ballerini and her lab at the International School for Advanced Studies (SISSA) in Trieste, Italy for the excellent training in the preparation of the organotypic spinal cord slice cultures. Her expert knowledge in slice culturing has been invaluable to this project and her continual support and personal communication is much appreciated.

In addition, I wish to thank the gracious members in the Ballanyi laboratory, especially Ms. Araya Ruangkittisakul and Ms. Nicoleta Bobocea. Their kindness and commitment is truly "inspiring", much like their work. I wish them the best of luck in their future endeavours.

I also must thank Dr. Nina Pronchuk and Ms. Honey Chan. Their expertise in immunohistology and confocal microscopy has been extremely helpful in establishing new techniques in our lab.

Finally, many thanks go out to the members, and friends, from the Smith lab. To past members Drs. Tim Moran and Chris Ford for helping me learn the 'ins' and 'outs' of patching, and to Drs. Kwai Alier and Sridhar Balasubramanyan for all the relevant discussions regarding our projects, and the non-relevant discussions too. To current lab members: Pat Stemkowski, Ken Wong, Lele (Yishen) Chen and James Biggs, I greatly appreciate their kindness and friendship. I look forward to reading about their future successes which is much deserved. And I would like to thank Ms. Briana Napier for all her help over the summer, and wish her all the best in what will be a bright future.

TABLE OF CONTENTS

CHAPTER 1 GENERAL INTRODUCTION 1

1.1 What is Pain? 2

- *1.1.1 Pain provides an evolutionary advantage* 2
- *1.1.2 Good and bad pain* 3
- *1.1.3 Pain as a disease* 5
- *1.1.4 Two facets of pain* 6

1.2 The Nociceptive Signalling Pathway 7

- *1.2.1 Classification of primary afferent neurons* 9
- *1.2.2 Classification of dorsal horn neurons in Lamina II* 11
  - *1.2.2.1 Morphology* 11
  - *1.2.2.2 Electrophysiology* 13
  - *1.2.2.3 Immunohistochemistry* 15
  - *1.2.2.4 Summary of the classification of dorsal horn neurons* 15

1.3 Animal Models of Neuropathic Pain 16

1.4 Pathophysiology of Neuropathic Pain 17

- *1.4.1 Central sensitization* 19
- *1.4.2 Possible chemical mediators of central sensitization* 20

1.5 The Neurotrophin: Brain-Derived Neurotrophic Factor (BDNF) 22

- *1.5.1 Behavioural tests support the role of BDNF in initiating neuropathic pain* 25
- *1.5.2 Changes in the levels of BDNF in animal pain models* 26

1.5.3 Mechanism of BDNF action 28

1.6 Problems with Previous Research and Statement of Hypothesis 29

1.7 Technique for the Chronic Application of BDNF: the Organotypic Cultures (OTCs) of Spinal Cords 31

1.7.1 Background on organotypic cultures (OTCs) 32

1.7.2 Special considerations for OTCs of spinal cord tissue 34

1.8 Techniques to Identify Neuronal Populations within the Dorsal Horn: Electrophysiology and Biocytin Cell Fills 35

1.9 Conclusions and Statement of Problem 36

1.10 References 49

CHAPTER 2 GENERAL METHODS 62

2.1 Preparation of Organotypic Slice Cultures 63

2.1.1 Serum-free culture conditions 65

2.2 Treatment Protocol of Defined Medium OTCs (DMOTCs) with BDNF 66

2.3 Electrophysiology 66

2.4 Histology and Immunohistochemistry 68

2.5 Fluorescent Calcium Imaging 69

2.6 Analysis and Statistical Tests 70

2.7 Drugs 71

2.8 References 81

CHAPTER 3 CHARACTERIZATION OF DORSAL NEURONS IN DEFINED-MEDIUM ORGANOTYPIC CULTURES OF RAT SPINAL CORDS.. 82

3.1 Introduction 83

3.2 Methods 85

3.2.1 Defined-medium organotypic cultures (DMOTCs) of spinal cord slices 85

3.2.2 Electrophysiology 85

3.2.3 Histology and immunohistochemistry... 88

3.3 Results... 89

3.3.1 Observation of living neurons under IR-DIC optics.............................. 89

3.3.2 Populations of dorsal horn neurons 89

3.3.3 Morphology and immunohistochemical staining................................... 90

3.3.4 Passive membrane properties 92

3.3.5 Membrane excitability 93

3.3.6 Synaptic pharmacology.. 94

3.3.7 Time-course of development 96

3.3.8 Antagonist-induced bursting activity 97

3.3.9 Spontaneous synaptic activity 97

3.4 Discussion... 99

3.4.1 Neuronal phenotypes in DMOTC slices 100

3.4.2 GAD as an immunochemical marker of inhibitory dorsal horn neurons .. 101

3.4.3 Development of inhibitory synaptic transmission............................... 102

3.4.4 Increased synaptic activity and spontaneous excitability in DMOTCs 103

3.4.5 Altered I-V relationship in DMOTCs... 104

3.5 Conclusions 104

3.6 References 123

CHAPTER 4 BDNF AND NEURONAL EXCITATION 127

4.1 Introduction 128

4.2 Methods 129

4.2.1 Defined-medium organotypic cultures (DMOTCs) of spinal cord slices .. 129

4.2.2 Electrophysiology 130

4.2.3 Data analysis, modeling and statistical testing 132

4.2.4 Drugs and chemicals 133

4.3 Results 134

4.3.1 Classification of neurons in the superficial dorsal horn of the cultures 134

4.3.2 No effect of BDNF on passive membrane properties 134

4.3.3 Minimal effects of BDNF on active membrane properties 135

4.3.4 Effects of BDNF on sEPSCs 135

4.3.5 Effects of BDNF on mEPSCs 137

4.3.6 BDNF-induced alterations in the frequency of presynaptic action potentials does not account for changes in sEPSCs of tonic and delay neurons 138

4.3.7 Further analysis of the mechanism of action of BDNF on tonic cells 139

4.3.8 Further analysis of the mechanism of action of BDNF on delay cells 141

4.3.9 Alterations in synaptic activity can affect spontaneous action potential activity of dorsal horn neurons 142

4.4 Discussion 143

4.4.1 Neuronal type-specific effects of BDNF on excitatory synaptic transmission 145

4.4.2 Effect of BDNF on tonic neurons 146

4.4.3 Effect of BDNF on delay neurons 147

4.4.4 Effect of BDNF on irregular, phasic and transient neurons 149

4.4.5 BDNF-induced increase in overall dorsal horn excitability? 151

4.5 Conclusions 152

4.6 References 175

CHAPTER 5 BDNF AND NEURONAL INHIBITION 181

5.1 Introduction 182

5.2 Methods 183

5.2.1 Defined-medium organotypic cultures (DMOTCs) of spinal cord slices .. 183

5.2.2 Electrophysiology 184

5.2.3 GAD staining 185

5.2.4 Data analysis and statistical testing 186

5.2.5 Drugs and chemicals 187

5.3 Results 188

5.3.1 Effect of BDNF on sIPSCs 188

5.3.2 Effect of BDNF on mIPSCs 189

5.3.3 BDNF-induced alterations in presynaptic action potential activity of inhibitory neurons can account for some of the changes in sIPSC population 190

5.3.4 Further analysis of the mechanism of BDNF action on tonic cells 192

5.3.5 Further analysis of the mechanism of BDNF action on delay cells 193

5.3.6 Effect of BDNF on postsynaptic receptors mediating 'tonic' inhibitory conductances 194

5.3.7 Effect of BDNF on presynaptic inhibition of excitatory transmission 195

5.3.8 Changes in network excitability cannot be attributed to BDNF-induced reversal of inhibition 196

5.3.9 GAD-positive neurons correlate well with tonic firing neurons 197

5.4 Discussion 199

5.4.1 Neuronal type-specific effects of BDNF on inhibitory synaptic transmission 200

5.4.2 Effect of BDNF on inhibition of tonic neurons 201

5.4.3 Effect of BDNF on inhibition of delay neurons 202

5.4.4 Effect of BDNF on inhibition of irregular, phasic and transient neurons . 203

5.4.5 Effect of BDNF on GAD-positive neurons 204

5.5 Conclusions 205

5.6 References 222

CHAPTER 6 BDNF AND MORPHOLOGICAL CLASSES OF NEURONS 225

6.1 Introduction 226

6.2 Methods 226

6.3 Results 227

6.3.1 No effect of BDNF on distribution of morphologically and electrophysiologically classified populations of dorsal horn neurons 227

6.3.2 Minimal neuronal sprouting induced by BDNF 227

6.3.3 Effect of BDNF on synaptic activity of TIC neurons 228

6.3.4 Effect of BDNF on synaptic activity of DR neurons 229

6.3.5 Effect of BDNF on synaptic activity of DV neurons 230

6.4 Discussion 230

6.4.1 Effect of BDNF on TIC neurons 231

6.4.2 Effect of BDNF on DR neurons 233

6.4.3 Effect of BDNF on DV neurons 234

6.5 Conclusions 235

6.6 References 246

CHAPTER 7 BDNF AND OVERALL DORSAL HORN EXCITABILITY 249

7.1 Introduction 250

7.2 Methods 251

7.2.1 Defined-medium organotypic cultures (DMOTCs) of spinal cord slices .. 251

7.2.2 Calcium imaging 252

7.2.3 Electrophysiology 252

7.2.4 Drugs and chemicals 253

7.2.5 Data analysis and statistical testing 254

7.3 Results 254

7.3.1 Enhanced depolarization-evoked Ca^{2+} responses from BDNF-treated DMOTC slices 254

7.3.2 BDNF-induced Ca^{2+} oscillations 255

7.3.3 BDNF-induced Ca^{2+} oscillations parallel an increase in extracellular activity 255

7.3.4 BDNF-induced Ca^{2+} oscillations depend on extracellular Ca^{2+} and voltage-gated Ca^{2+} channels 256

7.3.5 BDNF-induced Ca^{2+} oscillations dependent on action potential generation through TTX-sensitive Na^{+} channels 257

7.3.6 BDNF-induced Ca^{2+} oscillations mediated by AMPA/kainate receptors but not NMDA receptors 258

7.3.7 Large Ca^{2+} oscillations induced following removal of inhibition 258

7.4 Discussion 259

7.4.1 Ca^{2+} imaging techniques 259

7.4.2 BDNF enhances overall dorsal horn excitability 260

7.4.3 The mechanism of BDNF-induced Ca^{2+} oscillations 261

7.5 Conclusions 263

7.6 References 278

CHAPTER 8 GENERAL DISCUSSION AND FINAL CONCLUSIONS 282

8.1 BDNF Instigates Central Sensitization 284

8.1.1 Similar alterations in dorsal horn neurons observed in a nerve injury model of neuropathic pain 286

8.1.2 Blocking BDNF attenuates dorsal horn excitability 288

8.1.3 BDNF is a chemical mediator of central sensitization 290

8.2 BDNF and Synaptic Plasticity 292

8.3 BDNF-induced Alterations in Inhibition is Not as Significant as Alterations in Excitation to Dorsal Horn Excitability 294

8.3.1 Consequences of alterations in inhibitory synaptic activity to delay neurons 295

8.3.2 Assessing contribution of inhibition to overall neuronal activity 296

8.3.3 Limited effect of BDNF-induced changes in inhibition on overall dorsal horn excitability 298

8.4 Organotypic Culture of Spinal Cord Slices: Studying "Pain in a Dish" 299

8.5 Final Conclusions 300

8.6 References 314

APPENDIX PUBLISHED PAPERS 321

A1. *Substantia Gelatinosa* neurons in defined-medium organotypic slice cultures are similar to those in acute slices from young adult rats. 322

A2. Neuron type-specific effects of brain-derived neurotrophic factor in rat superficial dorsal horn and their relevance to 'central sensitization'. 337

LIST OF TABLES

Table 1-1 38

Table 1-2 40

Table 3-1 106

Table 3-2 108

Table 4-1 154

Table 4-2 156

Table 6-1 237

Table 8-1 303

LIST OF FIGURES

Figure 1-1 42

Figure 1-2 44

Figure 1-3 46

Figure 1-4 48

Figure 2-1 74

Figure 2-2 76

Figure 2-3 78

Figure 2-4 80

Figure 3-1 110

Figure 3-2 112

Figure 3-3 114

Figure 3-4 116

Figure 3-5 118

Figure 3-6 120

Figure 3-7 122

Figure 4-1 158

Figure 4-2 160

Figure 4-3 162

Figure 4-4 164

Figure 4-5 166

Figure 4-6 168

Figure 4-7 170

Figure 4-8 172

Figure 4-9 174

Figure 5-1 207

Figure 5-2 209

Figure 5-3 211

Figure 5-4 213

Figure 5-5 215

Figure 5-6 217

Figure 5-7 219

Figure 5-8 221

Figure 6-1 239

Figure 6-2 241

Figure 6-3 243

Figure 6-4 245

Figure 7-1 265

Figure 7-2 267

Figure 7-3 269
Figure 7-4 271
Figure 7-5 273
Figure 7-6 275
Figure 7-7 277

Figure 8-1 305
Figure 8-2 307
Figure 8-3 309
Figure 8-4 311
Figure 8-5 313

LIST OF ABBREVIATIONS

ACC: anterior cingulated cortex

ANOVA: analysis of variance

ANOVA-SNK: ANOVA with Student Newman-Keuls

BDNF: brain-derived neurtrophic factor

B+S: bicuculline and strychnine

CCI: chronic constriction injury

CGRP: calcitonin-gene related peptide

CNQX: 6-cyano-7-nitroquinoxaline-2,3-dione

CNS: central nervous system

CSF: cerebral spinal fluid

D-AP5: D(-)-2-Amino-5-phosphonopentanoic acid

DMEM: Dulbecco's Modified Eagle Medium

DMOTC: defined medium organotypic culture

DMSO: dimethyl sulfoxide

DR: delay radial

DRG: dorsal root ganglion

DV: delay vertical

E_{Cl}: equilibrium potential for chloride ions

eEPSC/eIPSC: evoked excitatory / inhibitory postsynaptic current

EPSP/IPSP: excitatory / inhibitory postsynaptic potential

ERK: extracelluar signalling kinase

FBS: fetal bovine serum

fMRI: functional magnetic resonance imaging

GABA: γ-aminobutyric acid

GAD: glutamic acid decarboxylase

HBSS: Hanks' balanced salt solution

IASP: Internation Association for the Study of Pain

IB4: isolectin B4

IC: islet-central

I-C: insular cortex

IEI: inter-event interval

IL-1β: interleukin-1β

I_{NaP}: persistent sodium current

IR-DIC: infrared differential interference contrast

I-V: current-voltage

KCC2: K^+/Cl^- cotransporter

KS: Kolmogorov-Smirnov

LPS: lipopolysaccharide

LTP: long-term potentiation

MCM: microglial-conditioned medium

MEG: magnetoencephalography

mEPSC/mIPSC: miniature excitatory / inhibitory postsynaptic current

NBQX: 2,3-dihydroxy-6-nitro-7-sulfamoyl-benzo[f]quinoxaline-2,3-dione

NF200: neurofilament 200

NGF: nerve growth factor

NGS: normal goat serum

NMDA: N-methyl-D-aspartate

NSAIDS: non-steroidal anti-inflammatory drugs

OTC: organotypic culture

$p75^{NTR}$: p75 neurotrophin receptor

PAG: periaqueductal grey

PBS: phosphate buffered saline

PET: positron emission tomography

PFC: prefrontal cortex

PKCγ: protein kinase Cγ

R_{input}: input resistance

RMP: resting membrane potential

SI: primary somatosensory cortex

SII: secondary somatosensory cortex

sEPSC/sIPSC: spontaneous excitatory / inhibitory postsynaptic current

sEPSP/sIPSP: spontaneous excitatory / inhibitory postsynaptic potential

TIC: tonic islet-central

Trk: tropomyosin receptor kinase

TrkB-d5: TrkB extracellular binding domain 5

TTX: tetrodotoxin

vGLUT1 or 2: vesicular glutamate transporter 1 or 2

VPL: ventroposterolateral

VPM: ventroposteromedial

WHO: World Health Organization

χ^2: Chi-squared

CHAPTER 1

GENERAL INTRODUCTION

1.1 What is Pain?

The International Association for the Study of Pain (IASP) defines pain as, "an unpleasant sensory and emotional experience associated with actual or potential tissue damage, or described in terms of such damage". Most people would agree that pain is an unpleasant experience one would rather not suffer through in their daily lives. However, what might escape appreciation is the need for pain for our survival and the perpetuation of the human species.

1.1.1 Pain provides an evolutionary advantage

Pain is part of our body's defence against perils in our surroundings. This signal is a powerful warning system that alerts our brain to dangers in our environment and provides vital sensory information on the noxious elements in our surroundings. Since prolonged contact with harmful agents can produce tissue damage that may impede normal functioning, alerting the brain to such dangers is advantageous for survival.

In addition, pain serves as an important protective mechanism from further tissue damage. If there is tissue damage or injury, the sensation of pain persists until the injured tissue has completely healed. This prevents the exacerbation of the initial injury and additional damage from the use of injured tissue. It also allows proper healing mechanisms to occur without disruption. The importance of pain in the prevention of further tissue damage is illustrated in people with 'congenital insensitivity to pain' (Manfredi et al., 1981; Nagasako et al., 2003). This is a rare disorder where individuals are unable to process normal physical pain. As a result of this genetic disease, there is no pain signal alerting the brain of tissue damage and thus, no negative feedback signalling to deter the use of injured tissue. People with this condition typically have a short lifespan as they succumb to injuries that are not properly attended to or treated.

Besides providing a response to noxious stimuli, pain signalling also provides a means by which we learn about our environment. The negative reinforcement of a noxious stimulus with pain is the basis for producing long-lasting memories concerning harmful elements in our surroundings. By adapting to the various cues and stimuli in our environment, we can avoid the adverse elements in our surroundings and thus become more successful survivors. Thus, pain provides an evolutionary advantage and is vital for our survival.

1.1.2 Good and bad pain

Pain can be classified into two main categories. The first category is acute pain which includes the body's immediate pain response as well as the pain endured while aggravating previous tissue damage. This type of pain serves the important biological function of alerting the brain of immediate tissue damage or injury that requires attention, and has been referred to as "good pain".

The second category of pain is of the chronic variety. Chronic pain, as the name implies, is a condition of persistent long-lasting pain that may invoke different pain signalling mechanisms compared to acute pain. Chronic pain which accompanies prolonged tissue damage, such as burns, is one adaptive mechanism for dealing with long-term injuries and this type of chronic pain normally subsides as the injury eventually resolves itself. Unfortunately, in other forms of chronic pain such as fibromyalgia or arthritis, the source of injury is more difficult to localize and may involve ongoing inflammation in the region which activates pain signalling pathways. Furthermore, some forms of chronic pain do not accompany any apparent or prolonged tissue damage. For instance, chronic pain of idiopathic origin can arise with no initiating tissue damage (Diatchenko et al., 2006; Sen and Christie, 2006). In other cases, damage to pain signalling neurons themselves can initiate abnormal pain signals that outlast the original injury. This type of chronic pain is known as neuropathic pain.

An example of neuropathic pain is phantom-limb pain where amputation induces chronic pain mechanisms as a result of activity from damaged nerves that originally innervated the lost limb (Flor, 2002). Chronic neuropathic pain can arise from direct injury to neurons *per se* (Kim et al., 1997; Kim and Chung, 1992), or as a result of diseases such as diabetic neuropathy (Chen and Pan, 2002) and cancer (Mantyh and Hunt, 2004). Since this type of pain persists or occurs in the absence of tissue damage, it has no biological purpose. Furthermore, this type of pain can be long-lasting or even permanent and thus significantly reduce the quality of life of those affected. Thus, this type of chronic pain is often referred to as "bad pain" or "the disease of pain".

Normal acute pain can be appropriately managed with conventional analgesics such as non-steroidal anti-inflammatory drugs (NSAIDS) like ibuprofen, which target cyclooxygenases and block the production of prostaglandins, or opioids like morphine and codeine, which attenuate the release of neurotransmitters. However, these treatments are not very effective for chronic neuropathic pain because there is altered pain signalling. Thus, the mechanisms utilized for acute pain relief do not necessarily apply to chronic neuropathic pain. In fact, opioids are only effective in one-third of neuropathic pain patients (Gilron et al., 2005; Raja et al., 2002). Currently, treatments for the management of chronic neuropathic pain include anticonvulsants and antidepressants (Laird and Gidal, 2000; Sindrup et al., 2005), but these treatments still have limited effectiveness. Thus, novel and effective treatments for the management of chronic neuropathic pain are desperately needed.

1.1.3 Pain as a disease

The World Health Organization (WHO) recognizes pain as a significant detractor to a healthy life (World Health Organization, 2003). Although pain is not a leading cause of death or disease worldwide, it is associated with many diseases which claim the lives of millions of people each year (Bond and Breivik, 2004). For instance, 80% of the 67 million patients dying of cancer annually suffer from pain (Harstall and Ospina, 2003). In addition, pain is a major health concern in all parts of the world. There are people in developing countries with severe, chronic pain as a result of disease, famine or conflict.

Chronic pain is prevalent in North American society. According to the American Chronic Pain Society, chronic pain is the primary cause of disability in the United States and approximately 50 million Americans suffer from chronic pain (American Pain Foundation, 2007). It accounts for over $20 billion in costs annually for direct health care expenditures in America. In Canada, over 18% of the population suffers from chronic pain (Chronic Pain Association of Canada, 2007). The estimated cost of chronic pain to the Canadian health care system (disability, medical expenses) is over $10 billion which does not include social costs such as loss of income and productivity.

As mentioned previously, the number of effective treatments available for sufferers of chronic neuropathic pain does not meet the demand. In order to find new treatments and reduce the devastating impact of chronic pain on people's lives, we must understand the pathology of this disease.

1.1.4 Two facets of pain

The definition of pain, mentioned previously, highlights two important aspects of pain: a sensory or nociceptive component, and an emotional or affective component of pain. Direct injury to the body can trigger a pain signal, but emotional and other psychological triggers can also produce a painful experience. For example, recollecting past painful experiences or even empathizing with another person's pain can produce pain similar to actual tissue damage.

Therefore, pain represents the complex interaction of an organism's physiological and emotional response to tissue damage or noxious stimulation. Due to the subjective nature of a person's emotions, pain can be difficult to measure across subjects. As quoted from a study on pain management in primary health care facilities, "pain is whatever the experiencing person says it is, and exists whenever s/he says it does" (McCaffery, 1972). Further complicating the study of pain is our relatively poor understanding of the cognitive processing of pain that occurs in higher brain regions such as the cortex and amygdala.

Despite these challenges, some human pain studies incorporate this emotional component of pain in their studies. Most often, these studies utilize pain questionnaires and patient interviews where patients rate their pain as well as how their pain has affected their daily routine (Melzack, 1975; Thomas et al., 1996). These studies provide much needed insight into the magnitude of a patient's pain and how disruptive diseases such as chronic pain are to daily living. However, a heavy reliance on human patients communicating their pain presents a challenge when dealing with other species. Animal pain models, much like animal models for other diseases, are a convenient tool to study the pathology and development of diseases under controlled repeatable conditions. Unfortunately, studying the emotional manifestation of pain in animals is technically difficult and subjective to the observational skills of the experimenter as well. Consequently, a minority of animal pain studies explore this affective component of pain.

On the other hand, nociception, or the body's physiological processing of noxious stimuli, has been studied in extensive detail. The sensory nervous system develops and behaves in a similar manner across individuals. Also, responses from sensory nerves can be measured and quantified objectively, resulting in less variation amongst subjects, either humans or rodents. Therefore, the majority of studies in pain research focus on nociception and nociceptive processing of noxious stimuli.

1.2 The Nociceptive Signalling Pathway

Understanding normal nociceptive processing can aid in the study of pain diseases because perturbations along this pathway are major contributors to long-lasting pain syndromes.

Nociceptive signals are initiated by activation of specialized receptors, known as nociceptors, by noxious levels of chemical, thermal or mechanical stimuli. These signals from activated nociceptors are conducted down primary afferent nerves which then synapse on to dorsal horn neurons of the spinal cord. There are different classes of nociceptive primary afferents which will be discussed in detail in the next section.

The grey matter of the spinal cord is divided into 10 layers or laminae. Laminae I to VI make up the dorsal horn of the spinal cord, which receives inputs from nociceptive primary afferents fibres. Lamina II of the spinal cord, also known as the *substantia gelatinosa*, contains local excitatory and inhibitory interneurons. The neurons in this region serve an important role in integrating nociceptive information and some neurons synapse on to projection neurons in Lamina I. Most of the axons of these projection neurons cross the midline and ascend to the anterolateral quadrant of the spinal cord. These axons then proceed to the higher brain regions via the spinoreticular tract, which terminates in the brainstem, or the spinothalamic tract, which terminates in the thalamus. The spinothalamic tract is subdivided into the lateral spinothalamic tract which terminates in the ventroposterolateral (VPL) nucleus of the thalamus, and the medial spinothalamic tract which terminates in the ventroposteromedial (VPM) nucleus of the thalamus. Neurons along the lateral spinothalamic tract convey somatotopical information to the somatosensory cortex, thus permitting accurate localization of pain. Sensory information from the other tracts, the spinoreticular and medial spinothalamic tracts, do not provide the precise location of pain but are involved in alerting the brain of noxious stimuli and possibly the affective components of pain.

Pain involves the complex interplay of nociception, cognition, emotion, and behaviour; therefore not surprisingly, various brain regions are involved in pain perception and no discrete pain centre has been identified in the brain. Nociceptive processing in higher brain regions can be studied by utilizing brain imaging techniques such as positron emission tomography (PET), magnetoencephalography (MEG) and functional magnetic resonance imaging (fMRI). These imaging studies revealed that normal nociceptive processing involves a network of cortical areas termed the "pain matrix". These areas include the primary and secondary somatosensory cortices (SI and SII), the insular cortex (I-C), the anterior cingulated cortex (ACC), the thalamus and the prefrontal cortex (PFC). Parts such as the SI, SII and thalamus are likely involved in the sensory-discriminative aspects of pain whereas the ACC and I-C are part of the limbic system involved in the affective or emotional aspects of pain. PFC areas that are activated during nociception are implicated in the cognitive aspects of pain. Other areas activated during processing of nociceptive information include the brainstem, basal ganglia and cerebellum.

Complementing the ascending pain signalling pathway are the descending analgesic pathways. These pathways serve a vital role for the survival of an organism as it allows for suppression of overwhelming pain in stressful situations to allow proper cognitive functioning for escape and survival. One of the best studied descending pathways involves activation of neurons in the periaqueductal grey (PAG) area. PAG neurons project to the rostral ventral medulla which then projects to the dorsal horn of the spinal cord through the dorsolateral funiculus where they inhibit nociceptive transmission in the dorsal horn.

1.2.1 Classification of primary afferent neurons (summarized in Table 1-1)

Primary afferent fibres, which have their cell bodies located in the dorsal root ganglion (DRG), can be classified into different groups based on their cell body size and the extent of axonal myelination. Aβ fibres, which carry low-threshold mechanoceptor or touch information, typically have a "large" soma diameter of 40 μm or greater and have large heavy myelinated axons. Aδ fibres have "medium" sized soma diameters between 30 and 40 μm and their axons are thinly myelinated. Finally, C fibres have "small" diameter cell bodies less than 30 μm and also have small calibre axons that lack myelination. Since Aδ and C fibres differ in their extent of myelination, they have different conduction velocities, 20 m/s and slower than 2 m/s respectively.

The nociceptive Aδ and C fibres also contain different nociceptors. Nociceptors on Aδ fibres are either high-threshold mechanoreceptors, which are sensitive to noxious mechanical stimuli such as sharp objects, or mechanothermal nociceptors, which are sensitive to mechanical and extreme temperature (>52°C) stimuli. Coupled with the relatively fast conduction velocity of Aδ fibres, these nociceptive neurons are responsible for alerting the brain quickly of very noxious stimuli which have the potential of causing serious tissue damage, which is sometimes referred to as 'first pain'. On the other hand, C fibre nociceptors are polymodal or respond to a broad spectrum of mechanical or thermal stimuli. These nociceptors are also sensitive to a wide range of chemical stimuli from bradykinin to an increase in proton concentration. Both of these mediators are usually released from and indicate injured tissue, and therefore the slow signals C fibres conduct is often referred to as 'second pain'.

As well, nociceptive neurons terminate and innervate different layers of the dorsal horn of the spinal cord. Specifically, the Aδ fibres send inputs into Lamina I and Lamina V (Light and Perl, 1979a; Light and Perl, 1979b), and C fibres have some terminals in Lamina I but mainly terminate in Lamina II (Sugiura et al., 1986).

Besides soma diameter, various markers have been used to differentiate between different primary afferents populations. For instance, neurofilament 200 (NF200) is a commonly used marker for large and medium sized cells. It is an intermediate filament protein and a major constituent of the cytoskeleton in axons of myelinated A-fibres. Isolectin B4 (IB4) is a commonly used marker for a subpopulation of unmyelinated C fibres. IB4 is a plant lectin from *Griffonia simplicifolia*, which binds a carbohydrate marker found on a select population of non-peptideric C fibres. The peptidergic population of C fibres can be identified by staining for neuropeptides contained within select populations of primary afferents such as calcitonin-gene related peptide (CGRP) and substance P. Both peptides are found in nociceptive primary afferents and are highly colocalized. The function of these neuropeptides in nociceptive transmission will be elaborated on in a later section.

1.2.2 Classification of dorsal horn neurons in Lamina II

1.2.2.1 Morphology

Some of first studies characterizing Lamina II neurons describe their anatomy and morphology within the dorsal horn. These studies described different cell types according to cell body shape and size, but the defining morphological characteristic of neurons in the dorsal horn is the orientation of dendrites. Although these studies were conducted in various animal species, a number of similar phenotypes are described.

The "islet" cells described in the dorsal horn of cats and rats typically have long dendrites that reside almost exclusively within Lamina II and project predominantly in the rostrocaudal orientation (Bennett et al., 1980; Cervero and Iggo, 1980; Gobel, 1975; Gobel, 1978; Grudt and Perl, 2002; Todd and Lewis, 1986). Recurrent dendritic branches, where one branch turns back towards the soma, occur in islet cells as well

(Gobel, 1978). Islets cells typically have few dendritic spines and comprise approximately 30% of the neurons in Lamina II (Gobel, 1978).

"Central" cells share many characteristics with islet cells. They have small cell bodies (7-14 µm) with two main dendritic trees emerging from opposite poles of the cell body. The longest dendrites project along the rostrocaudal plane with dendrites also along the dorsoventral and to a much lesser extent mediolateral plane. Similar "border" cells have been described by Gobel (1978) which lay near layers II and III and its dendritic tree is limited to this region and runs mainly rostrocaudally. In comparison to islet cells, the dendritic tree of central cells does not appear to extend as far rostrocaudally as islet cells and have a moderately extensive branching. Because of this likeness, others have called these cells "small islets" (Todd and Lewis, 1986). Since islet and central neurons have dendritic trees oriented along the same rostrocaudal axis and the difficulty discerning length of projections in transverse sections of the spinal cord, this has led to the combined grouping of "islet-central" neurons (Figure 1-1; Balasubramanyan et al., 2006).

"Vertical" cells possess a distinctive dorsoventral orientation with sparse wide dendrites (Figure 1-1; Grudt and Perl, 2002). This cell morphology has been previously described as "stalked" cells with short, thick branching dendrites which also project dorsoventrally (Bennett et al., 1980; Cervero and Iggo, 1980; Gobel, 1975; Gobel, 1978; Todd and Lewis, 1986). These cells are the most common type of neuron in Lamina II accounting for half the neurons in this region (Gobel, 1978).

Finally, Grudt and Perl (2002) describe another group of neurons in the *substantia gelatinosa* where their dendritic trees radiate in all directions, hence the name "radial" cells (Figure 1-1). Todd and Lewis (1986) describe a similar class of "spiny" neurons which have short dendrites extending in almost all orientations. Their dendrites often have many dendritic spines which form a very compact dendritic tree. Interestingly, similar "multipolar" cells have been described along the border of Lamina I and II in the superficial dorsal horn of rats (Prescott and De Koninck, 2002).

All four major cell morphologies identified in the *substantia gelatinosa* of the spinal cord, primarily receive monosynaptic C fibre input except for vertical cells where a large percentage of neurons receive both Aδ and C fibre inputs (Yasaka et al., 2007). The orientation of vertical cells and the ability of the dendritic tree to project more dorsally, possibly into Lamina I, could contribute to increased Aδ fibre inputs.

1.2.2.2 Electrophysiology (summarized in Table 1-2)

A number of different electrophysiological properties can be measured using whole-cell recordings, and the action potential firing pattern has been used as a defining characteristic of dorsal horn neurons. The pattern of action potential discharges is determined by the population of ion channels present and could indicate the behaviour of neurons when activated. In general, there are five main action potential firing patterns described in dorsal horn neurons. "Tonic" neurons exhibit continuous action potential discharges in response to depolarizing current pulses. The frequency and action potential height remain consistent throughout stimulation. "Delay" neurons have a sustained pause before the onset of action potential firing. This delay prior to action potential discharges truncates as stimulation intensity increases but is consistently present. "Phasic" neurons display an initial burst of action potentials before accommodation or cessation of firing.

"Transient" or single-spike neurons fire only a single action potential regardless of the intensity of current stimulation. Finally, "irregular" neurons do not exhibit any clear relationship between action potential discharge pattern and intensity of depolarization stimulus.

More recently, a combination of morphological and electrophysiological techniques have been used to characterize dorsal horn neurons (Balasubramanyan, 2006; Grudt and Perl, 2002; Prescott and De Koninck, 2002 in the superficial dorsal horn) (summarized in Figure 1-2). Whole-cell recordings provide access and measurement of a cell's neuronal properties, and also allow for the filling of cells with dye that can be visualized for real-time or *post-hoc* morphological analysis. A large percentage of islet neurons appear to have a tonic firing pattern. Central neurons fired with a phasic pattern. Vertical neurons can display a tonic firing pattern, but some also fire with a "delay" firing pattern. Radial or multipolar cells typically have a "delay" firing pattern as well.

Insight into the neurotransmitter content and thus phenotype of Lamina II neurons came from studies using simultaneous paired recordings of synaptically connected neurons (Lu and Perl, 2003; Lu and Perl, 2005). An islet tonic cell makes a specific inhibitory connection with central phasic cells in the dorsal horn of the spinal cord. Central phasic neurons have been shown to release glutamate when activated to produce excitatory postsynaptic responses (Lu and Perl, 2005), though some report GABAergic phasic firing neurons (Heinke et al., 2004). Vertical 'delay' neurons appear to excite a class of Lamina I, substance P-positive, projection neurons (Lu and Perl, 2005).

1.2.2.3 Immunohistochemistry

Specific populations of dorsal horn neurons may exclusively express certain proteins and this can be exploited in order to classify neurons in this region. For example, γ-aminobutyric acid (GABA), which is the main inhibitory neurotransmitter in the central nervous system, has been identified in islet neurons in the dorsal horn, but not in central cells (Todd and McKenzie, 1989). In addition, the rate-limiting enzyme in the synthesis of GABA, glutamic acid decarboxylase (GAD), is a commonly used marker for the identification of inhibitory GABAergic neurons. Two isoforms of GAD are known, GAD65 and GAD67, and both have been found in the dorsal horn of the spinal cord (Mackie et al., 2003).

Currently, there is no broad spectrum marker for excitatory dorsal horn neurons. Although markers such as protein kinase Cγ (PKCγ) (Polgar et al., 1999) and vesicular glutamate transporter 2 (vGLUT2) (Todd et al., 2003) have been identified in select populations of excitatory dorsal horn neurons.

New experimental tools, which use these protein markers to identify different neuronal populations, are now available for the study of neurons within the dorsal horn. Genetically altered animals, which couple protein expression with fluorescence, make it possible to identify and target select populations of neurons for electrophysiological study (Dougherty et al., 2005; Hantman et al., 2004; Heinke et al., 2004).

1.2.2.4 Summary of the classification of dorsal horn neurons

Currently, there is no strict classification scheme for Lamina II neurons; although, various techniques have been utilized to characterize the different neurons within this region. Some of the difficulty in categorizing neurons may be the heterogeneity of neurons in this region. Within Lamina II alone, there are several different cell morphologies and action potential firing patterns consistently described in the literature. Also complicating the identification of distinct neuronal phenotypes is the overlapping features shared by different neurons in the dorsal horn. For instance, some islet and vertical neurons in Lamina II exhibit a similar tonic firing pattern.

Despite this, recognizing different neurons in the dorsal horn and utilizing what is known about these different neuronal groups can aid in understanding the roles different dorsal horn neurons have in nociceptive processing. We know the most common cell types in the *substantia gelatinosa* region of the dorsal horn and there is good evidence identifying the inhibitory and excitatory interneurons on the basis of firing pattern, neurotransmitter content and morphology (Heinke et al., 2004; Lu and Perl, 2003; Lu and Perl, 2005; Todd and McKenzie, 1989). Even though the precise details of dorsal horn physiology are not completely known, the current state of knowledge is sufficient for rational studies of transmission of nociceptive information and how this signalling pathway is altered in neuropathic pain states.

1.3 Animal Models of Neuropathic Pain

As mentioned earlier, animal models have been useful in elucidating the mechanisms involved in neuropathic pain. Most of these models involve injuring peripheral nerves which can induce long-lasting neuronal changes and chronic pain, similar to what is observed in humans during neuropathic pain. For example, the chronic constriction injury (CCI) model of neuropathic pain involves damaging the sciatic nerve of animals by placing loose ligatures (Bennett and Xie, 1988) or a tube (Mosconi and Kruger, 1996) around the nerve. The level of chronic pain in animals can be measured and signs associated with neuropathic pain can be assessed using a variety of behavioural tests. Hyperalgesia, an exaggerated or excessive pain response, and allodynia, a normally non-noxious stimulus now perceived as noxious, can be identified and nociceptive withdrawal thresholds can be quantified as well. The use of animal models allows for the study of specific cellular or biochemical mechanisms involved in changes to nociceptive processing during neuropathic pain states.

1.4 Pathophysiology of Neuropathic Pain

Studying changes in nociceptive signalling following peripheral nerve injury has shed some light on the progression of neuropathic pain (summarized in Figure 1-3). Following peripheral nerve injury, there are a number of changes in the primary afferents which conduct sensory information from the periphery to central neurons. There is a significant increase in the excitability of primary afferents measured as a decrease in threshold or rheobase and increased frequency of action potential firing (Abdulla and Smith, 2001b). Spontaneous ectopic firing also occurs and is generated from the site of injury, or neuroma, as well as intrinsically from primary afferent fibres (Amir and Devor, 2003; Wall and Devor, 1983). Enhanced excitability of primary afferents is observed in all populations of primary afferents but the most profound increase in excitability is observed in the small diameter C fibres (Abdulla and Smith, 2001b). The changes in excitability have been attributed to changes in ionic conductances of primary afferents, specifically a reduction in potassium and high-voltage activated calcium currents

(Abdulla and Smith, 2001a) and an increase or altered sodium channel expression (Abdulla and Smith, 2002; Waxman et al., 1994).

The increased excitability of primary afferents following peripheral nerve injury has consequences on the central neurons they innervate. Dorsal horn neurons, which have normally limited activity, become spontaneously active and show enhanced excitability following nerve injury (Dalal et al., 1999; Kohno et al., 2003; Laird and Bennett, 1993). Also, there are reports of loss of inhibitory tone in the dorsal horn (Baba et al., 2003; Moore et al., 2002; Sivilotti and Woolf, 1994) and even a reversal of inhibitory transmission to excitation (Coull et al., 2003) as mechanisms contributing to neuropathic pain. Studies examining the specific changes in identified populations of Lamina II dorsal horn neurons have described a selective increase in the excitatory drive to presumed excitatory 'delay' neurons, and a converse decrease in excitatory drive to putative inhibitory tonic neurons (Balasubramanyan et al., 2006). This would result in an overall increase in excitatory tone in the dorsal horn. Presumably, the increase in excitability of primary afferents and the dorsal horn of the spinal cord augments pain signals in the brain and is responsible for chronic neuropathic pain.

Neuroimaging studies indicate that the same brain structures within the pain matrix which are involved in normal nociceptive processing are also activated during neuropathic pain (Chen et al., 2002; Ducreux et al., 2006; Maihofner et al., 2004; Peyron et al., 2004); but the activation patterns and the level of activity are altered. For instance, in neuropathic pain patients, there are changes in the SI region and a reorganization of cortical maps (Chen et al., 2002). There is an expansion of somatosensory regions such that they become sensitive to neighbouring areas. Also, following spinal cord injury, there are changes within the thalamus observed with imaging studies that have been correlated with an increase in bursting and spontaneous activity of thalamic neurons (Lenz et al., 1989; Lenz et al., 1994). These changes in neuronal activity can be attributed to changes in sodium channel expression in thalamic neurons following injury (Hains et al., 2005; Hains et al., 2006).

1.4.1 Central sensitization

Following nerve injury, the changes in nociceptive transmission begin in the primary afferents and then continue on to the dorsal horn neurons of the spinal cord. The persistence of neuropathic pain even after the initial injury has healed may be a consequence of altered nociceptive signalling further downstream of the original injury.

Therefore, a vital step in the development of neuropathic pain is the initiation of long-lasting changes in central dorsal horn neurons. These mechanisms are responsible for enhancing the excitability of dorsal horn neurons that could persist regardless of continuous input from injured primary afferents. It also provides a means of linking increased excitability in primary afferents to the dorsal horn neurons they innervate. This priming of central neurons by injured primary afferents is known as "central sensitization" (Woolf, 1983; Woolf and Chong, 1993). The mechanisms responsible for central sensitization may underlie the induction and development of intractable chronic neuropathic pain. Therefore, key mediators of central sensitization within the spinal cord are potential therapeutic targets for the treatment of chronic neuropathic pain.

1.4.2 Possible chemical mediators of central sensitization

The main neurotransmitter released from primary afferents is glutamate. There are also a number neuropeptides present in nociceptive neurons; but, the most abundant neuropeptides are CGRP and the tachykinins such as substance P and tachykinin A (Nestler et al., 2001). CGRP is not synthesized in all nociceptive neurons, but is found in subsets of Aδ and C fibre neurons. On the other hand, substance P is found in over 20% of dorsal root ganglion neurons (Levine et al., 1993) and is colocalized with glutamate in primary afferent nerve terminals that innervate the superficial dorsal horn (De Biasi and Rustioni, 1988; Hokfelt et al., 1975b). Release of substance P has been demonstrated following noxious stimulation (Hokfelt et al., 1975a) and it can excite dorsal horn neurons or modulate excitatory glutamatergic activity (Levine et al., 1993). Substance P can also enhance inflammation by increasing vasodilatation and vascular permeability of extravasant white blood cells. Substance P has been implicated in neuropathic pain in animal studies (Cahill and Coderre, 2002), but unfortunately human clinical trials have failed to show significant analgesia following administration of substance P receptor antagonists (Hill, 2000). Other neuropeptides are also found in primary afferent terminals, but their endogenous role in nociceptive signalling remains to be elucidated.

There are some major differences between classical neurotransmitters, such as glutamate and GABA, and neuropeptides. One is the energy expenditure required for the synthesis, transport, and release of neuropeptides is much greater than for neurotransmitters. The synthesis of neuropeptides requires protein translation at the endoplasmic reticulum near the nucleus in the neuronal soma. Newly synthesized neuropeptides are then packaged in vesicles and then anterogradely transported and stored in terminals until released. On the other hand, neurotransmitter synthesis occurs in the cytoplasm with enzymes located at nerve terminals in close proximity to release sites. Neurotransmitters are typically stored in small vesicles which are easily prompted to release its contents upon depolarization. But neuropeptide storage vesicles usually require high frequency stimulation to release these larger molecules. Also, the replenishment of neuropeptide stores following release requires *de novo* synthesis of neuropeptides and not simple reuptake or recycling as is the case for neurotransmitters. This process is much slower and again requires more energy. The advantage of having this alternative, but energy expensive signalling system is the ability of neuropeptides to transmit signals over long distances and for longer durations than neurotransmitters. Neuropeptides are capable of volume transmission, or the extrasynaptic spread of activity beyond its release sites. Combined with the ability of neuropeptide receptors to activate signal transduction pathways, this may lead to long-lasting and far-reaching neuropeptide signalling.

Chemical mediators released from hyperactive primary afferents likely play a role in initiating central sensitization. Following peripheral nerve injury, there is enhanced activity in nociceptive primary afferents and their central terminals are bombarded with action potentials. These levels are not normal and can lead to excessive neurotransmitter release, as well as trigger the release of neuropeptides which are not normally released during regular nociceptive signalling (summarized in Figure 1-4). The ability of neuropeptides to signal long distances and activate receptors coupled to signal transduction pathways can result in long-distance and long-lasting alterations in nociceptive neurons. These changes can lead to sensitization of dorsal horn neurons and further maladaptive or pathophysiological changes which may ultimately result in a neuropathic pain state.

1.5 The Neurotrophin: Brain-Derived Neurotrophic Factor (BDNF)

Based on their properties, neuropeptides seem capable of inducing the changes in dorsal horn neurons associated with chronic neuropathic pain. Also, they are ideally localized to mediate central sensitization, an activity-dependent increase in the excitability of central neurons. One particular neuropeptide located in nociceptive afferent terminals which has garnered much attention is brain-derived neurotrophic factor (BDNF).

BDNF is a neurotrophin that belongs to the family of neurotrophic factors. Neurotrophic factors are a class of growth factors which act selectively on neurons. They have actions on peripheral and central neurons, but may have biological roles in non-neuronal cells. They can promote the survival, differentiation and growth of neurons. Neurotrophins are a family of small proteins that share a high degree of homology and similar receptor signalling mechanisms. Members of this group include nerve growth factor (NGF), BDNF, neurotrophin-3, 4/5, 6 and 7.

Neurotrophins, such as BDNF, are present in different forms. BDNF is synthesized as a proto-peptide and cleavage of this pro-sequence by trypsin or metalloproteinases produces biologically active BDNF. This pro-neurotrophin form is assumed to have no activity; however, recent reports suggest this isoform is involved in proper protein folding and sorting and may actually have its own biological activity (Teng and Hempstead, 2004; Wiesmann and de Vos, 2001).

There are two classes of neurotrophin receptors. The high affinity binding receptor belongs to the tropomyosin receptor kinase (Trk) receptor class. Trk receptors are 140 kD proteins with an extracellular ligand binding domain, a single transmembrane helix, and a cytoplasmic domain with intrinsic tyrosine kinase activity. Three different Trk receptors have been described and selectively bind different neurotrophins with high affinity ($K_d = 10^{-11}$). BDNF and neurotrophin 4/5 specifically bind TrkB. The second receptor all neurotrophins bind with equal affinity is the low affinity ($K_d = 10^{-9}$) p75 neurotrophin receptor ($p75^{NTR}$). In addition, these receptors bind the pro-form of neurotrophins with greater affinity than truncated neurotrophins. The role of $p75^{NTR}$s in neurotrophin signalling is beginning to be understood and it appears that these receptors can signal on their own or interact with Trk receptors to allow full activation of the Trk receptor (Dechant and Barde, 2002; Dobrowsky and Carter, 2000; Teng and Hempstead, 2004).

BDNF can have diverse and sometimes opposite effects mediated by its two receptors. For instance, axonal regeneration of motoneurons requires BDNF signalling through its TrkB receptor but is severely attenuated by increased $p75^{NTR}$ expression and signalling following nerve injury (Boyd and Gordon, 2001). Similarly in dorsal root ganglion cells, BDNF-induced apoptosis decreased dramatically in $p75^{NTR}$ null (-/-) mice (Zhou et al., 2005). Therefore, BDNF signalling through $p75^{NTR}$ seems to be associated with cell death and not axonal growth.

Neurotrophins have global effects on survival and differentiation of neurons; however, strong evidence suggests that neurotrophins can also modulate fast synaptic transmission (for review see Poo, 2001). For instance, BDNF increases spontaneous excitatory synaptic activity (Lohof et al., 1993) and directly affects ion channels such as sodium channel gating (Blum et al., 2002; Rose et al., 2004). Moreover, BDNF can modulate the response of neurotransmitters over longer periods. The best characterized neuromodulatory effect of BDNF is the potentiation of glutamate responses at N-methyl-D-aspartate (NMDA) receptors (Jarvis et al., 1997). BDNF can also play a role in maintaining neuronal phenotype and function, and be involved in morphological changes at synapses which underlie some forms of learning and memory (Xu et al., 2004).

BDNF is found throughout the brain, and is also found in certain populations of primary afferent fibres. BDNF is predominantly expressed in small diameter DRG neurons which express the high-affinity NGF receptor TrkA (Cho et al., 1997; Karchewski et al., 2002; Michael et al., 1997). NGF stimulation has been shown to increase BDNF synthesis in these neurons (Apfel et al., 1996; Cho et al., 1997; Michael et al., 1997), and since NGF release is commonly associated with inflammation, BDNF may play a role in inflammation-induced pain. Interestingly, only 2% of BDNF-expressing DRGs also contain TrkB receptors (Michael et al., 1997) implying little autocrine signalling in BDNF-expressing neurons. BDNF is also co-localized with CGRP in small diameter nociceptive neurons (Michael et al., 1997). Approximately 55% of BDNF-immunoreactive cells colocalized with CGRP. Also, the low affinity neurotrophin receptor p75^{NTR} has been colocalized with BDNF in non-CGRP expressing neurons (Luo et al., 2001). This may indicate two distinct classes of BDNF-expressing primary afferent fibres.

BDNF is located in secretory granules or large dense-core vesicles and co-stored with other neuropeptides such as CGRP and substance P (Salio et al., 2007). Release of neuropeptide content from these vesicles occurs via the regulatory secretory pathway which responds to synaptic stimulation (Brigadski et al., 2005). High frequency stimulation is usually sufficiently to trigger the release of neuropeptides from vesicles; however, release of neurotrophins into the dorsal horn requires a pattern of repeated high frequency bursts (Lever et al., 2001) which may occur following peripheral nerve injury. Also, inflammation-induced release of NGF can upregulate the levels of BDNF in expressing DRG neurons. So, BDNF is found in nociceptive primary afferent terminals, and its levels in the dorsal horn can be significantly altered by conditions that arise following nerve injury or inflammation. Consequently, BDNF is one neuropeptide which may play a prominent role in initiating changes in nociceptive signalling which can lead to central sensitization of dorsal horn neurons.

1.5.1 Behavioural tests support the role of BDNF in initiating neuropathic pain

Some of the most compelling evidence for the role of BDNF in neuropathic pain comes from behavioural studies. Intrathecal injection of BDNF produces thermal hyperalgesia in animals, which is mediated by TrkB signalling (Groth and Aanonsen, 2002; Yajima et al., 2005). Moreover, behavioural responses are attenuated by administering BDNF-sequestering proteins or by blocking BDNF action on TrkB receptors in nerve injured animals (Coull et al., 2005; Fukuoka et al., 2001; Yajima et al., 2002) as well as in models of inflammation-induced pain (Groth and Aanonsen, 2002; Mannion et al., 1999; Matayoshi et al., 2005; Thompson et al., 1999). Thus, BDNF plays a relevant role in inducing chronic pain states and may be a common factor mediating long-lasting alterations in nociceptive signalling in the various animal pain models.

1.5.2 Changes in the levels of BDNF in animal pain models

BDNF has been shown to be released in animal models of neuropathic pain. Following peripheral nerve injury, there is a significant increase in the concentration of BDNF in the cerebral spinal fluid (CSF) near the spinal dorsal horn (Miletic and Miletic, 2002; Walker et al., 2001). Microprobe measurements reveal the most concentrated release of BDNF in Lamina II of the dorsal horn; however, following peripheral nerve injury there is a spread of BDNF beyond the superficial layers that penetrates into the deeper laminae (Walker et al., 2001). With these studies, it is unclear if this spread is due to migration of BDNF or release of BDNF from other primary afferents which terminate in the deeper laminae.

There are also changes in the expression of BDNF following peripheral nerve injury. Generally, there is an upregulation of BDNF mRNA and a corresponding increase in BDNF protein synthesis in the DRG and primary afferent terminals in the dorsal horn of the spinal cord. Though, depending on the neuropathic pain model, different populations of DRG neurons are responsible for this increase in BDNF expression. Nerve injury models that involve deforming or crushing nerves usually have a similar profile: a marked increase in BDNF expression in all sizes of DRG neurons (Cho et al., 1998; Ha et al., 2001; Obata et al., 2003). Other models involving cutting or ligating nerves had a more complex profile: medium and large diameter DRG cells show an increase in BDNF production but have either no change or a decrease in BDNF in small diameter DRGs (Cho et al., 1998; Karchewski et al., 2002; Michael et al., 1999; Zhou et al., 1999). The differences in expression of BDNF with different models of nerve injury could arise from loss of retrograde signalling as a result of severing neuronal axons. NGF released during inflammation is a major contributor to BDNF production in afferent C fibres, and this may be lost following axotomy of peripheral nerves. The other nerve injury models may simply damage peripheral nerves, but allow axonal signalling to continue.

In addition to release of BDNF from damaged primary afferent terminals, production of BDNF from spinal microglia following nerve injury has been shown (Dougherty et al., 2000; Ikeda et al., 2001). The synthesis and release of chemical mediators from activated microglia has been suggested to play a prominent role in neuropathic pain states (Coull et al., 2005; Hains and Waxman, 2006; Narita et al., 2006; Tsuda et al., 2005). Since BDNF is one of the molecules released following activation of spinal microglia, perhaps BDNF plays a role in inducing the mechanisms involved in producing chronic neuropathic pain. Regardless the source of BDNF, elevated levels of BDNF from either neuronal and non-neuronal cells can persist 4-7 days post-injury (Ha et al., 2001; Ikeda et al., 2001; Miletic and Miletic, 2002).

Receptors for BDNF, both TrkB and $p75^{NTR}$ receptors, are found normally in the dorsal horn (King et al., 2000; Salio et al., 2005). The expression of receptors is enhanced following nerve injury (Delcroix et al., 2003; King et al., 2000; Liebl et al., 2001) and receptor activation (Pezet et al., 2002b) has also been demonstrated. So, increased levels of BDNF and their targets in animal models of neuropathic pain suggest enhanced BDNF signalling following nerve injury. Thus, the effects of elevated BDNF signalling can provide clues as to the mechanisms of central sensitization which can lead to chronic neuropathic pain.

1.5.3 Mechanism of BDNF action

Many electrophysiological studies have examined the acute effects of BDNF on dorsal horn neurons. BDNF can enhance spinal reflex excitability (Kerr et al., 1999; Mannion et al., 1999; Thompson et al., 1999), which is a measure of nociceptive afferent input into the dorsal horn. BDNF selectively enhances C-fibre afferent inputs into the dorsal horn and not A-fibre inputs. BDNF can also facilitate excitatory synaptic currents, specifically currents mediated through NMDA receptors (Garraway et al., 2003; Kerr et al., 1999). In addition, BDNF is able to increase the frequency of synaptic currents by activating a class of sodium channels located on the presynaptic terminals of nociceptive primary afferents (Matayoshi et al., 2005). Thus, acutely applied BDNF (≤ 30min) is capable of increasing nociceptive signalling in the dorsal horn which may lead to an increase in the excitability of this region, or central sensitization.

The molecular signal transduction pathways activated in animal models of neuropathic pain also provide clues on BDNF action in the dorsal horn. High intensity C-fibre activity and noxious stimulation activates the extracelluar signalling kinase (ERK) which is mediated by activation of TrkB receptors, and not via other neuropeptide receptors such as NK1 receptors (Lever et al., 2003b; Pezet et al., 2002b). Activation of this pathway has been shown to lead to phosphorylation of the NMDA receptor subunit NR1 (Slack et al., 2004; Slack and Thompson, 2002). These pathways activated by BDNF have been suggested to lead to chronic changes in dorsal horn neurons and this may precipitate the abnormalities in nociceptive signalling observed in neuropathic pain.

Other studies however, have suggested that there is a loss of BDNF in some nerve injury models and it is this loss which is responsible for altered nociceptive signalling.

For instance, BDNF can enhance the release of GABA in the dorsal horn (Lever et al., 2003a; Pezet et al., 2002a) and the reduction of BDNF signalling could contribute to the loss of GABAergic tone observed during neuropathic pain.

Interestingly, differential and opposite effects of BDNF have been reported in separate populations of wide dynamic range neurons in the deeper spinal laminae which receive inputs from nociceptive Aδ fibres (Hains et al., 2002). The level of expression of different BDNF receptors could explain the differential effects of BDNF, but the phenotype of these neurons and if the overall effect of BDNF would be pro- or antinociceptive is still unclear.

So, there are conflicting views on the role of BDNF in the dorsal horn. Most behavioural studies would suggest BDNF is pro-nociceptive in nerve injury models of neuropathic pain (Coull et al., 2005; Fukuoka et al., 2001; Yajima et al., 2002). However, it remains a challenge reconciling the different mechanisms of action proposed for BDNF and what is ultimately the end result of BDNF on dorsal horn excitability.

1.6 Problems with Previous Research and Statement of Hypothesis

There are limitations to previous studies that investigated the role and mechanism of BDNF action on nociceptive transmission in the dorsal horn. For instance, a detailed account of changes induced by BDNF on specific populations of dorsal horn neurons is lacking. It is unknown if the changes induced by BDNF are selective for excitatory or inhibitory populations of dorsal horn neurons even though specificity of BDNF action has been reported (Hains et al., 2002; Zhou et al., 2005). The interpretation of BDNF's effect on dorsal horn excitability depends on the type of dorsal horn neurons affected. The main obstacle in these earlier studies was probably the lack of understanding of dorsal horn physiology. However, recent studies have identified populations of dorsal horn neurons and provided a good indication as to the phenotype of these populations (Grudt and Perl, 2002; Heinke et al., 2004; Lu and Perl, 2003; Lu and Perl, 2005). Using these characteristics, we can identify and study specific populations of dorsal horn neurons. Furthermore, we can examine the effects of BDNF with consideration of distinct neuronal phenotypes within the spinal dorsal horn.

Another major limitation of these studies is the short duration of BDNF treatment. The application of BDNF in a majority of these studies does not correspond to the duration of BDNF elevation found in whole-animal studies. Typically, BDNF is released and remains at elevated levels up to a week following sciatic nerve CCI; whereas most studies applying exogenous BDNF lasted only a few hours. Therefore these studies more likely examined the acute effects of BDNF and not the long-term consequences of BDNF exposure on dorsal horn signalling mechanisms. In order to understand the actions of BDNF on dorsal horn neurons, comparable BDNF treatments periods must be applied in order to correlate these studies with the situation encountered in nerve injury models of neuropathic pain.

Hence, the aim of this thesis project is to provide a detailed analysis of the effects of long-term BDNF exposure on known, identified populations of dorsal horn neurons. The duration of BDNF exposure on dorsal horn neurons will be lengthened compared to previous studies in order to parallel conditions which are actually found during induction of neuropathic pain.

Prolonged BDNF exposure is hypothesized to enhance the excitability of dorsal horn neurons in the spinal cord which can lead to central sensitization of nociceptive signalling. These alterations induced by BDNF are likely long-lasting, possibly even permanent changes in neuronal plasticity and may underlie the mechanisms involved in chronic, intractable neuropathic pain.

1.7 Technique for the Chronic Application of BDNF: the Organotypic Cultures (OTCs) of Spinal Cords

In order to study the consequences of long-term BDNF exposure on dorsal horn neurons, techniques that allow for the proper study of this network must be used. Therefore, I must first establish a system that allows for the long-term application of BDNF in order to be comparable with studies utilizing nerve injury models of neuropathic pain. This system must also be amendable to morphological, electrophysiological and immunohistochemical techniques that allow for the identification of dorsal horn neurons. Finally, preservation of the dorsal horn network would be ideal in order to maintain connectivity and thus communication between neurons. This will allow for the study of changes in synaptic transmission within the dorsal horn, along with the study of changes in the properties of individual neurons.

BDNF levels in the spinal dorsal horn can be elevated experimentally through a number of different means. For instance, following peripheral nerve injury, the levels of BDNF have been shown to be significantly elevated in the dorsal horn (Miletic and Miletic, 2002; Walker et al., 2001). Also, activated spinal microglia are capable of synthesizing and releasing BDNF in close proximity to dorsal horn neurons (Coull et al., 2005; Dougherty et al., 2000; Ikeda et al., 2001). While these stimuli for releasing BDNF may be physiologically relevant to the actual situation occurring during neuropathic pain, it may also stimulate the release of a multitude of other chemical mediators which could produce its own effect on dorsal horn neurons. In order to attribute the changes observed in dorsal horn neurons solely to the actions of BDNF, its levels should be selectively enhanced.

There are few experimental systems which allow for chronic application of BDNF to mimic the situation that occurs in nerve injury models and allow the long-term studies of spinal dorsal horn neurons. Acutely prepared spinal cord slices, which are most commonly used, only remain viable for a period of hours not days needed to expose dorsal horn neurons to BDNF. Thus, *in vitro* cell culture techniques are a well-suited alternative for studies involving long-term applications of BDNF.

The *in vitro* model which best suits our purpose is the organotypic spinal cord slice culture system. With this preparation, transverse spinal cord slices are isolated from animals and the entire slice is maintained in culture. Since the cytoarchitecture of the whole slice and synapses between neurons remains intact, neuronal networks and local circuits remain functional and active. The ability to study dorsal horn neurons in an arrangement closely resembling their actual network will provide valuable information regarding the effects of BDNF on overall nociceptive signalling.

1.7.1 Background on organotypic cultures (OTCs)

OTCs have been used for the study of neurons for some time. Various methods have been developed for the preparation of OTCs from the roller-tube technique

(Gahwiler, 1981; Gahwiler et al., 1998) to the membrane-interface chambers (Stoppini et al., 1991) and each have their own advantages and caveats.

Roller-tube cultures involve plating slices on to glass coverslips and placing slices into tubes filled with culture medium. During incubation, the tubes are continuously rotated in a roller drum at slow speeds. The slow rotation provides alternative aeration and feeding of cultures, and also optimizes the thinning of slice cultures. These roller-tube cultures thin down to single cell layer thickness (50 μm) and are ideal for optical studies (Gahwiler et al., 1997). Furthermore, the rotation of slices also serves to wash the clot above the slice used to anchor it initially to the glass coverslip; thus allowing easy access for electrophysiological recordings.

The popular Stoppini technique, involves culturing slices on a thin, porous membrane at the interface between the air and culture medium. This allows sufficient aeration of slices above the slice and feeding of slices from below on the side attached to the membrane. These cultures do not thin to the same extent as roller-tube cultures (100-150 μm) (Stoppini et al., 1991), but do preserve the three-dimensional organization of the slice and are ideal for morphological studies or even biochemical studies which require larger amounts of tissue. These membrane OTCs are maintained as stationary cultures which are easily accessible and permit chronic stimulation studies or experimental measurements to be taken over a long time course.

Both methods for the preparation of OTCs, the roller-tube and Stoppini technique, allow for the study of nervous tissue in culture. Both systems preserve the various neurons and non-neuronal cells in a co-culture system reminiscent of their arrangement *in situ*. The clear advantage of accessibility of neurons in roller-tube OTCs to electrophysiological and imaging techniques makes this an attractive system for the study of neuronal signalling within the dorsal horn. Moreover, this preparation system is capable of maintaining long-term cultures which is ideal for the proposed time-course of BDNF treatment (Figure 2-3B). Therefore, organotypic cultures of spinal cords will be prepared by the roller-tube technique in order to study the effects of long-term BDNF exposure on dorsal horn neurons.

1.7.2 Special considerations for OTCs of spinal cord tissue

Methods for establishing roller-tube OTCs of spinal cord tissue have been described (Braschler et al., 1989) with some modifications to the techniques for preparing OTCs from other brain tissues (Gahwiler, 1981; Gahwiler et al., 1998). Some of the changes in procedure were attributed to differences and challenges associated with cultures of spinal tissue.

The major difference between OTCs of spinal cords and other nervous tissue is the number of different tissues present in these cultures. Surrounding the spinal cord during preparation of slices is precursor bone and muscle tissue. The role of these other tissues in this co-culture system is unclear, as they can develop and grow within healthy cultures. Unfortunately, they can easily overgrow and overtake the entire culture. Therefore, in order to prevent their excess growth, each spinal cord slice must be trimmed of excess ventral tissue prior to plating on to glass coverslips.

Also, the dorsal root ganglia (DRGs) which are destined for the periphery are present in cultures derived from an embryonic source. The DRGs appear to play a vital role in maintaining neuronal connectivity within the dorsal horn and therefore must be preserved whilst preparing cultures. Therefore, spinal cord slices with intact DRGs have a better chance of survival and should be selected for culturing.

Because of the number of different tissues present in spinal cord co-cultures, the metabolic demand of these OTC slices is much higher than other preparations of OTCs from brain tissue. Consequently, the roller drum must be set at a higher rotation speed in order to accommodate feeding and aeration of spinal cord slice cultures. Also, the osmolarity of the medium must be lowered to comparable levels found in the CSF.

1.8 Techniques to Identify Neuronal Populations within the Dorsal Horn: Electrophysiology and Biocytin Cell Fills

Previous studies utilized the electrophysiological properties of neurons to classify distinct populations of dorsal horn neurons (Balasubramanyan et al., 2006; Grudt and Perl, 2002; Prescott and De Koninck, 2002). Specifically, the action potential firing pattern of neurons in response to depolarizing current injections was used. This is a convenient and relevant means of identifying neuronal populations because the output of neurons determines behaviour and function in neuronal signalling. The action potential firing patterns described for dorsal horn neurons (Table 1-2) will be used in this study.

Also, the firing patterns of neurons have been correlated with distinct cell morphologies. The structural and spatial arrangement of dendrites has been assumed to contribute to the functional role of these neurons (Bennett et al., 1980; Gobel, 1978), and consistent firing patterns with these cell morphologies has been found (Figure 1-2). In parallel with electrophysiological identification of dorsal horn neurons, the morphology of neurons can be examined by filling neurons with biocytin during intracellular recordings. These biocytin cell fills can be processed and visualized following electrophysiological experiments to identify the morphology of recorded neurons.

1.9 Conclusions and Statement of Problem

The dorsal horn of the spinal cord is an important centre for the integration of nociceptive information and alterations in this region can have significant consequences on nociceptive signalling to the brain. BDNF is one mediator implicated in neuropathic pain because its synthesis and expression are altered in chronic pain states. Also, BDNF can activate signalling cascades which can alter gene expression, at sites distant from its release. Therefore, BDNF is a mediator situated at a prime location and possesses the ideal properties to participate in central sensitization and the development of neuropathic pain. However, this role of BDNF remains to be firmly established. I have therefore examined the long-term effects of BDNF on identified dorsal horn neurons.

Table 1-1: Summary table of the classification of primary afferent fibres.

Primary afferent fibres carry sensory information from specialized receptors in the periphery, or nociceptors, into the dorsal horn of the spinal cord. These primary afferents can be classified based on their properties summarized in this table. Most notably, the soma diameter of primary afferent cell bodies located in the dorsal root ganglion (DRG) provides the classification names for primary afferent fibres. The main primary afferents involved in nociceptive signalling are the Aδ and C fibres.

	Aβ	**Aδ**	**C**
Neuronal classification	Large	Medium	Small
Soma diameter	>40 μm	30-40 μm	<30 μm
C_{in}	>90 pF	70-90 pF	<70 pF
Myelination	heavy	thin	none
Conduction velocity	40 m/s	6-30 m/s	<2 m/s
Information sent	light touch, hair bending	nociception	nociception
Nociceptors present	low-threshold mechanoceptors	high-threshold mechanoceptors, mechanothermal nociceptors	polymodal (mechanical, thermal, chemical stimuli)
Spinal cord innervations	Lamina III and IV	Lamina I, II and V	Lamina II, few Lamina I
Staining markers	NF200	NF200	IB4 (non-peptidergic) CGRP (peptidergic)

Table 1-2: Summary table of the electrophysiological classification of dorsal horn neurons.

Different categories of dorsal horn neurons can be identified based on their action potential discharge pattern in response to depolarizing current steps (Grudt and Perl, 2002). The firing pattern of neurons can encode specific signals to subsequent neurons along the nociceptive signalling pathway. Therefore, the action potential firing pattern of neurons can be used to identify populations of neurons that may share similar functions in transmitting nociceptive information in the dorsal horn.

Firing pattern	**Criteria**	**Sample trace**
Tonic	fires action potentials (APs) throughout current injection, APs equidistant and amplitude heights are similar	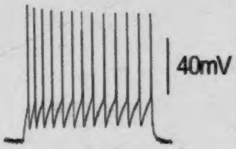
Delay	initial pause or delay before firing APs	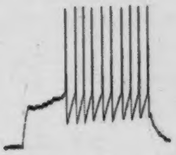
Phasic	three or more AP bursts at the beginning, but quiescent for the rest of stimulation	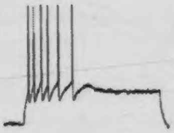
Transient	single or two APs at most fired at beginning of stimulation	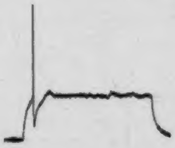
Irregular	does not follow any of the other listed patterns	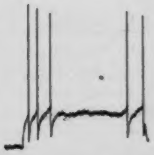

Figure 1-1: Morphological classes of dorsal horn neurons.

This diagram illustrates the main cell morphologies described in the *substantia gelatinosa*, or Lamina II, region of the spinal dorsal horn (Balasubramanyan, 2006; Grudt and Perl, 2002). The dashed line in the orientation map indicates the plane of depth or the plane that would run through the page. The lower right panel shows a close up view of the dorsal horn.

Islet and central cells are characterized by long, thin dendrites that project in the rostrocaudal orientation and their dendrites are mainly restricted within the Lamina II. Central cells' dendritic tree is typically shorter than that of islet cells. However as mentioned, transverse spinal cord slice preparations make the differentiation between islet and central neurons challenging; therefore, the common group of islet-central cells is used. Radial cells have short dendrites which project in all orientations. Lastly, vertical cells have thick dendrites which project predominantly in the dorsoventral orientation.

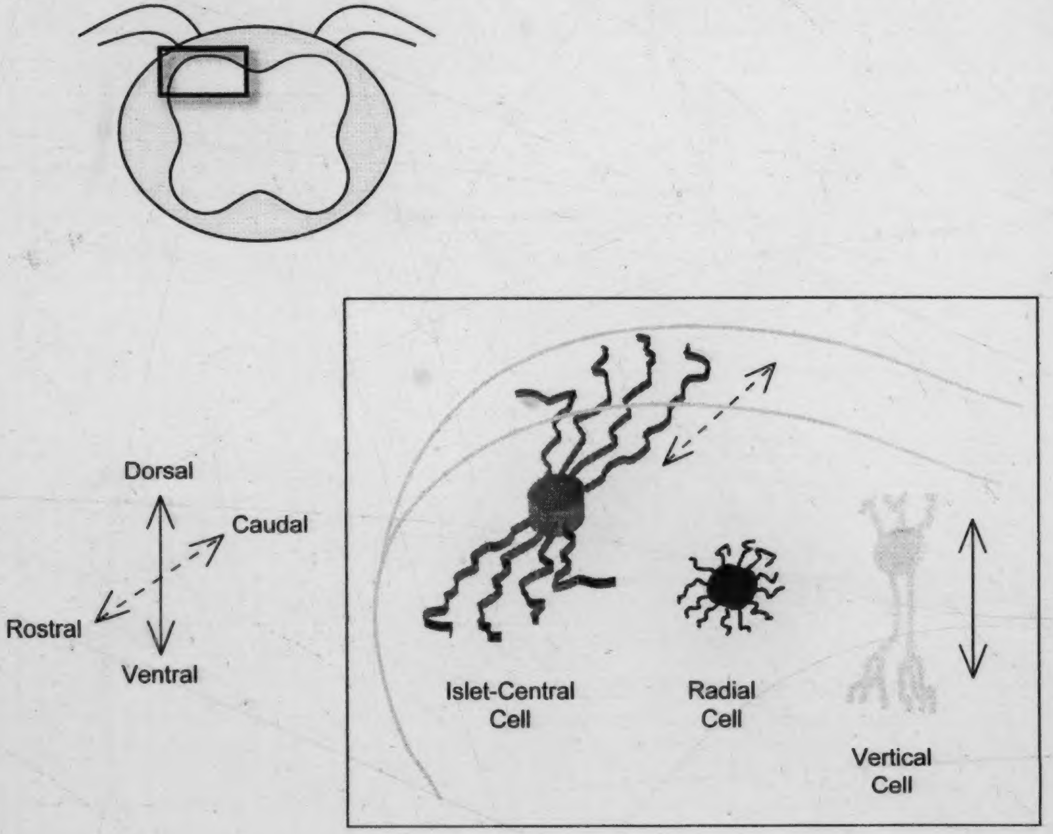
Dorsal
Caudal
Rostral
Ventral
Islet-Central Cell
Radial Cell
Vertical Cell

Figure 1-2: The morphology and electrophysiological characteristics of the main classes of neurons identified.

Based on studies from Grudt and Perl (2002) and Prescott and De Koninck (2002), these main morphological and electrophysiological categories of dorsal horn neurons have been described. Of the three main dorsal horn neuron morphologies described, some of the same action potential firing patterns are observed.

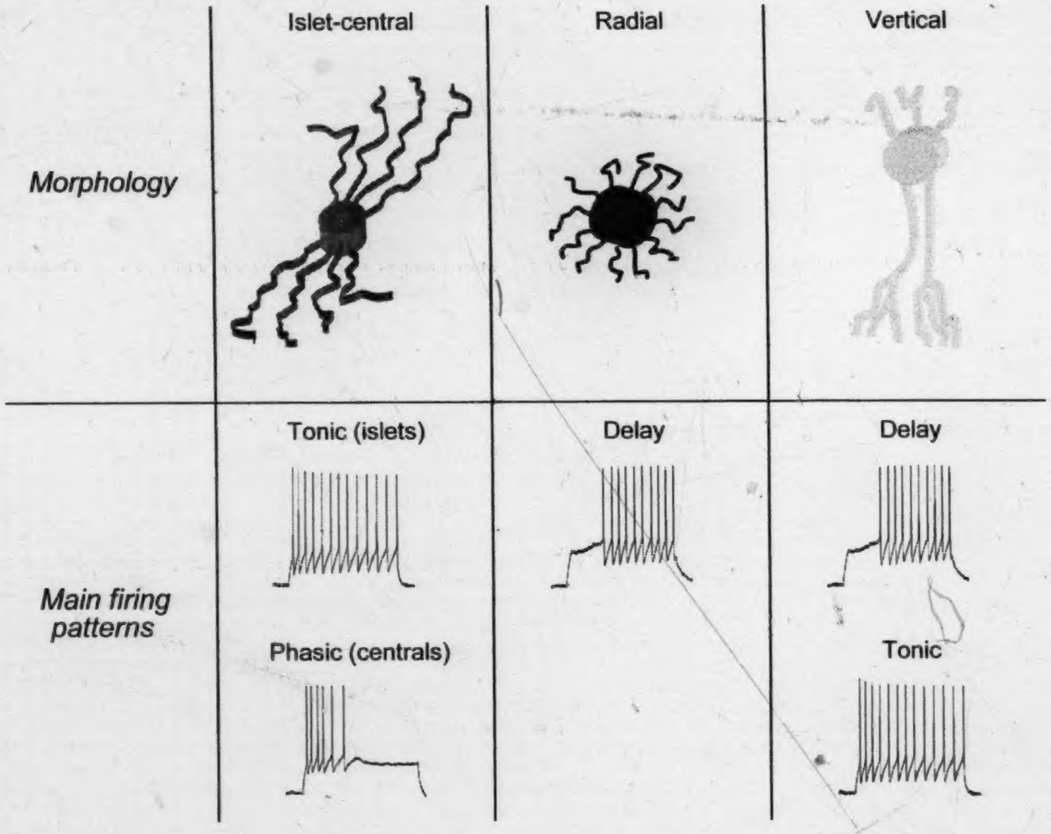
Islet-central
Radial
Vertical
Morphology
Tonic (islets)
Delay
Delay
Main firing patterns
Phasic (centrals)
Tonic

Figure 1-3: Summary of changes in nociceptive signalling following peripheral nerve injury in animal models of neuropathic pain.

This diagram shows the basic nociceptive signalling pathway: primary afferent fibre with both peripheral and central terminals, the dorsal root ganglion which houses the cell bodies of primary afferents, and the dorsal horn of the spinal cord. There are some major changes reported in neurons along this pathway following peripheral nerve injury. In addition, there is a progressive enhancement of neuronal excitability from peripheral to central neurons and this process is termed 'central sensitization'.

References:

1. Abdulla and Smith (2001).
2. Wall and Devor (1983).
3. Dalal et al. (1999), Kohno et al. (2003) and Laird and Bennett (1993).
4. Baba et al. (2003) and Moore et al. (2002).
5. Coull et al. (2003).

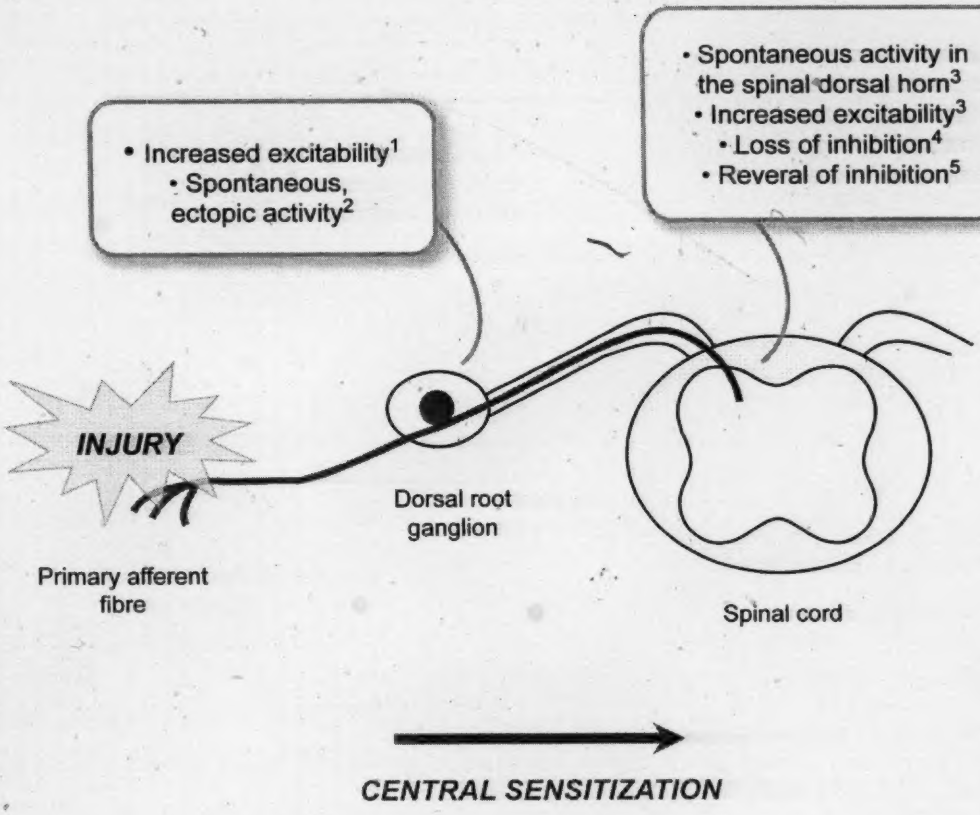
• Increased excitability[1]
• Spontaneous, ectopic activity[2]
• Spontaneous activity in the spinal dorsal horn[3]
• Increased excitability[3]
• Loss of inhibition[4]
• Reveral of inhibition[5]
INJURY
Primary afferent fibre
Dorsal root ganglion
Spinal cord
CENTRAL SENSITIZATION

Figure 1-4: Neuropeptides may instigate long-lasting changes in dorsal horn neurons during chronic neuropathic pain states.

Illustrated in this figure is a close up view of the synapse between a primary afferent fibre and a dorsal horn neuron. The main neurotransmitter in the primary afferent nerve terminal is glutamate, and there are also stores of neuropeptides in large dense-core vesicles.

During normal nociceptive signalling, the activity in primary afferents is sufficient to trigger the release of readily-releasable pools of glutamate located near release sites. Activation of postsynaptic glutamate receptors on the membrane of dorsal horn neurons will initiate and continue the transmission of the nociceptive signal to second-order neurons.

On the other hand, during neuropathic pain signalling, there is an abundance of activity in primary afferents leading to bombardment of the nerve terminal with action potentials. High-frequency activity can trigger the release of neuropeptides which can initiate neuropeptide receptor-coupled signalling cascades not normally activated during normal nociceptive signalling. The alterations in nociceptive signalling mediated by neuropeptides may lead to abnormal nociceptive processing which is commonly observed in diseases such as chronic, neuropathic pain.

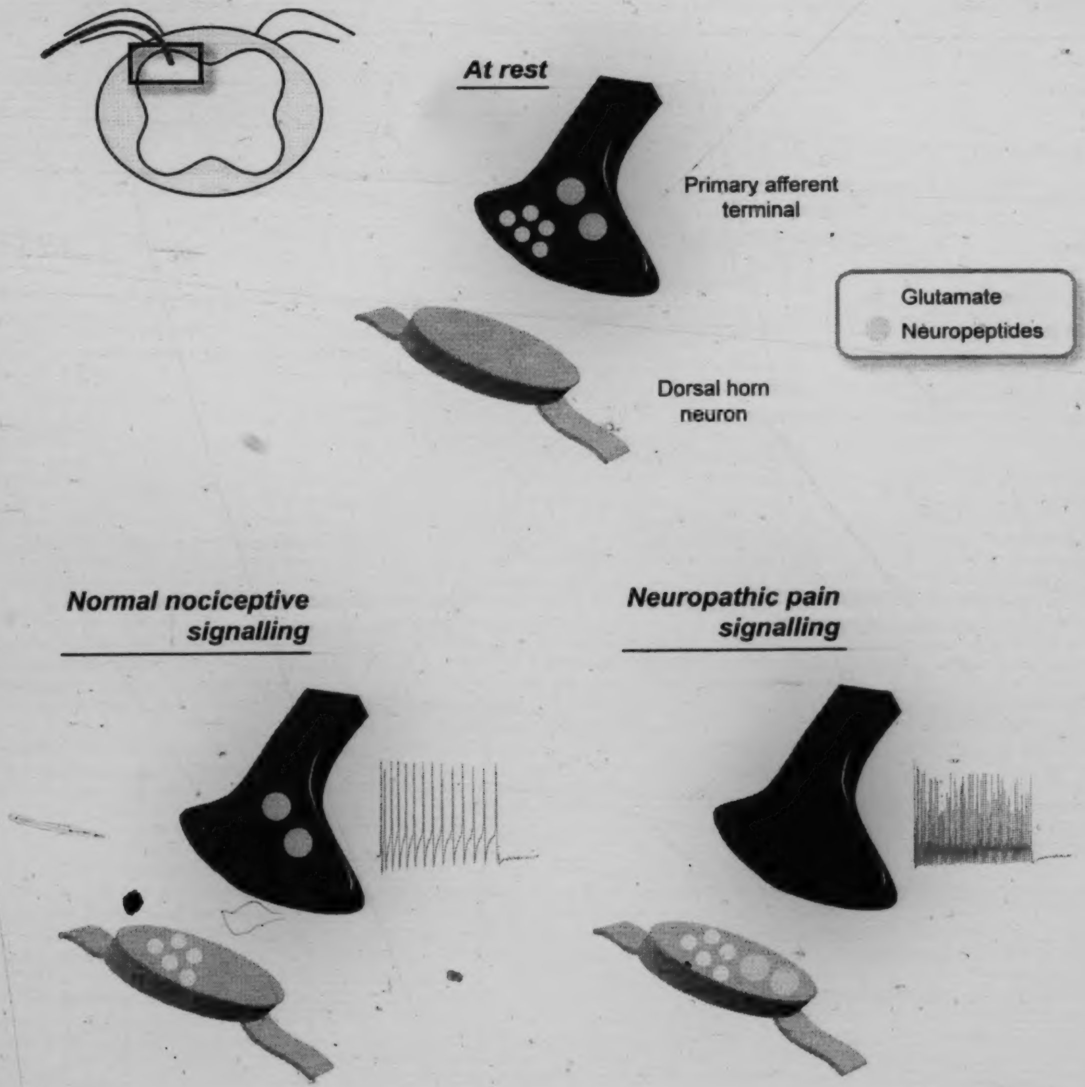
At rest
Primary afferent terminal
Glutamate
Neuropeptides
Dorsal horn neuron
Normal nociceptive signalling
Neuropathic pain signalling

1.10 References

Abdulla FA, Smith PA (2001a) Axotomy- and autotomy-induced changes in Ca2+ and K+ channel currents of rat dorsal root ganglion neurons. J Neurophysiol 85: 644-658.

Abdulla FA, Smith PA (2001b) Axotomy- and autotomy-induced changes in the excitability of rat dorsal root ganglion neurons. J Neurophysiol 85: 630-643.

Abdulla FA, Smith PA (2002) Changes in Na(+) channel currents of rat dorsal root ganglion neurons following axotomy and axotomy-induced autotomy. J Neurophysiol 88: 2518-2529.

American Pain Foundation. Pain Facts & Figures. http://www.painfoundation.org/page.asp?file=Newsroom/PainFacts.htm. Accessed June 2007.

Amir R, Devor M (2003) Extra spike formation in sensory neurons and the disruption of afferent spike patterning. Biophys J 84: 2700-2708.

Apfel SC, Wright DE, Wiideman AM, Dormia C, Snider WD, Kessler JA (1996) Nerve growth factor regulates the expression of brain-derived neurotrophic factor mRNA in the peripheral nervous system. Mol Cell Neurosci 7: 134-142.

Baba H, Ji RR, Kohno T, Moore KA, Ataka T, Wakai A, Okamoto M, Woolf CJ (2003) Removal of GABAergic inhibition facilitates polysynaptic A fiber-mediated excitatory transmission to the superficial spinal dorsal horn. Mol Cell Neurosci 24: 818-830.

Balasubramanyan S (2006) Changes in the properties of Substantia gelatinosa neurons induced by peripheral nerve injury. PhD Thesis Dissertation.

Balasubramanyan S, Stemkowski PL, Stebbing MJ, Smith PA (2006) Sciatic chronic constriction injury produces cell-type-specific changes in the electrophysiological properties of rat substantia gelatinosa neurons. J Neurophysiol 96: 579-590.

Bennett GJ, Abdelmoumene M, Hayashi H, Dubner R (1980) Physiology and morphology of substantia gelatinosa neurons intracellularly stained with horseradish peroxidase. J Comp Neurol 194: 809-827.

Bennett GJ, Xie YK (1988) A peripheral mononeuropathy in rat that produces disorders of pain sensation like those seen in man. Pain 33: 87-107.

Blum R, Kafitz KW, Konnerth A (2002) Neurotrophin-evoked depolarization requires the sodium channel Na(V)1.9. Nature 419: 687-693.

Bond M, Breivik H (2004) Why pain control matters in a world full of killer diseases. Pain Clinical Updates: International Association for the Study of Pain 12: 1-4.

Boyd JG, Gordon T (2001) The neurotrophin receptors, trkB and p75, differentially regulate motor axonal regeneration. J Neurobiol 49: 314-325.

Braschler UF, Iannone A, Spenger C, Streit J, Luscher HR (1989) A modified roller tube technique for organotypic cocultures of embryonic rat spinal cord, sensory ganglia and skeletal muscle. J Neurosci Methods 29: 121-129.

Brigadski T, Hartmann M, Lessmann V (2005) Differential vesicular targeting and time course of synaptic secretion of the mammalian neurotrophins. J Neurosci 25: 7601-7614.

Cahill CM, Coderre TJ (2002) Attenuation of hyperalgesia in a rat model of neuropathic pain after intrathecal pre- or post-treatment with a neurokinin-1 antagonist. Pain 95: 277-285.

Cervero F, Iggo A (1980) The substantia gelatinosa of the spinal cord: a critical review. Brain 103: 717-772.

Chen R, Cohen LG, Hallett M (2002) Nervous system reorganization following injury. Neuroscience 111: 761-773.

Chen SR, Pan HL (2002) Hypersensitivity of spinothalamic tract neurons associated with diabetic neuropathic pain in rats. J Neurophysiol 87: 2726-2733.

Cho HJ, Kim JK, Park HC, Kim JK, Kim DS, Ha SO, Hong HS (1998) Changes in brain-derived neurotrophic factor immunoreactivity in rat dorsal root ganglia, spinal cord, and gracile nuclei following cut or crush injuries. Exp Neurol 154: 224-230.

Cho HJ, Kim SY, Park MJ, Kim DS, Kim JK, Chu MY (1997) Expression of mRNA for brain-derived neurotrophic factor in the dorsal root ganglion following peripheral inflammation. Brain Res 749: 358-362.

Chronic Pain Association of Canada. Pain Facts. http://www.chronicpaincanada.com/. Accessed June 2007.

Coull JA, Beggs S, Boudreau D, Boivin D, Tsuda M, Inoue K, Gravel C, Salter MW, De Koninck Y (2005) BDNF from microglia causes the shift in neuronal anion gradient underlying neuropathic pain. Nature 438: 1017-1021.

Coull JA, Boudreau D, Bachand K, Prescott SA, Nault F, Sik A, De Koninck P, De Koninck Y (2003) Trans-synaptic shift in anion gradient in spinal lamina I neurons as a mechanism of neuropathic pain. Nature 424: 938-942.

Dalal A, Tata M, Allegre G, Gekiere F, Bons N, Albe-Fessard D (1999) Spontaneous activity of rat dorsal horn cells in spinal segments of sciatic projection following transection of sciatic nerve or of corresponding dorsal roots. Neuroscience 94: 217-228.

De Biasi S, Rustioni A (1988) Glutamate and substance P coexist in primary afferent terminals in the superficial laminae of spinal cord. Proc Natl Acad Sci U S A 85: 7820-7824.

Dechant G, Barde YA (2002) The neurotrophin receptor p75(NTR): novel functions and implications for diseases of the nervous system. Nat Neurosci 5: 1131-1136.

Delcroix JD, Patel J, Averill S, Tomlinson DR, Priestley JV, Fernyhough P (2003) Peripheral axon crush elevates transport of p75NTR in the central projection of sensory neurones of rats. Neurosci Lett 351: 181-185.

Diatchenko L, Nackley AG, Slade GD, Fillingim RB, Maixner W (2006) Idiopathic pain disorders--pathways of vulnerability. Pain 123: 226-230.

Dobrowsky RT, Carter BD (2000) p75 neurotrophin receptor signaling: mechanisms for neurotrophic modulation of cell stress? J Neurosci Res 61: 237-243.

Dougherty KD, Dreyfus CF, Black IB (2000) Brain-derived neurotrophic factor in astrocytes, oligodendrocytes, and microglia/macrophages after spinal cord injury. Neurobiol Dis 7: 574-585.

Dougherty KJ, Sawchuk MA, Hochman S (2005) Properties of mouse spinal lamina I GABAergic interneurons. J Neurophysiol 94: 3221-3227.

Ducreux D, Attal N, Parker F, Bouhassira D (2006) Mechanisms of central neuropathic pain: a combined psychophysical and fMRI study in syringomyelia. Brain 129: 963-976.

Flor H (2002) Phantom-limb pain: characteristics, causes, and treatment. Lancet Neurol 1: 182-189.

Fukuoka T, Kondo E, Dai Y, Hashimoto N, Noguchi K (2001) Brain-derived neurotrophic factor increases in the uninjured dorsal root ganglion neurons in selective spinal nerve ligation model. J Neurosci 21: 4891-4900.

Gahwiler BH (1981) Organotypic monolayer cultures of nervous tissue. J Neurosci Methods 4: 329-342.

Gahwiler BH, Capogna M, Debanne D, McKinney RA, Thompson SM (1997) Organotypic slice cultures: a technique has come of age. Trends Neurosci 20: 471-477.

Gahwiler GH, Thompson SM, McKinney RA, Debanne D, Robertson RT (1998) Organotypic Slice Cultures of Neural Tissue. In: Culturing Nerve Cells (Baker G, Goslin K, eds), pp 461-497. Cambridge, Massachusetts.

Garraway SM, Petruska JC, Mendell LM (2003) BDNF sensitizes the response of lamina II neurons to high threshold primary afferent inputs. Eur J Neurosci 18: 2467-2476.

Gilron I, Bailey JM, Tu D, Holden RR, Weaver DF, Houlden RL (2005) Morphine, gabapentin, or their combination for neuropathic pain. N Engl J Med 352: 1324-1334.

Gobel S (1975) Golgi studies in the substantia gelatinosa neurons in the spinal trigeminal nucleus. J Comp Neurol 162: 397-415.

Gobel S (1978) Golgi studies of the neurons in layer II of the dorsal horn of the medulla (trigeminal nucleus caudalis). J Comp Neurol 180: 395-413.

Groth R, Aanonsen L (2002) Spinal brain-derived neurotrophic factor (BDNF) produces hyperalgesia in normal mice while antisense directed against either BDNF or trkB, prevent inflammation-induced hyperalgesia. Pain 100: 171-181.

Grudt TJ, Perl ER (2002) Correlations between neuronal morphology and electrophysiological features in the rodent superficial dorsal horn. J Physiol 540: 189-207.

Ha SO, Kim JK, Hong HS, Kim DS, Cho HJ (2001) Expression of brain-derived neurotrophic factor in rat dorsal root ganglia, spinal cord and gracile nuclei in experimental models of neuropathic pain. Neuroscience 107: 301-309.

Hains BC, Saab CY, Waxman SG (2005) Changes in electrophysiological properties and sodium channel Nav1.3 expression in thalamic neurons after spinal cord injury. Brain 128: 2359-2371.

Hains BC, Saab CY, Waxman SG (2006) Alterations in burst firing of thalamic VPL neurons and reversal by Na(v)1.3 antisense after spinal cord injury. J Neurophysiol 95: 3343-3352.

Hains BC, Waxman SG (2006) Activated microglia contribute to the maintenance of chronic pain after spinal cord injury. J Neurosci 26: 4308-4317.

Hains BC, Willis WD, Hulsebosch CE (2002) Differential electrophysiological effects of brain-derived neurotrophic factor on dorsal horn neurons following chronic spinal cord hemisection injury in the rat. Neurosci Lett 320: 125-128.

Hantman AW, van den Pol AN, Perl ER (2004) Morphological and physiological features of a set of spinal substantia gelatinosa neurons defined by green fluorescent protein expression. J Neurosci 24: 836-842.

Harstall C, Ospina M (2003) How prevalent is chronic pain? Pain Clinical Updates 11: 1-4.

Heinke B, Ruscheweyh R, Forsthuber L, Wunderbaldinger G, Sandkuhler J (2004) Physiological, neurochemical and morphological properties of a subgroup of GABAergic spinal lamina II neurones identified by expression of green fluorescent protein in mice. J Physiol 560: 249-266.

Hill R (2000) NK1 (substance P) receptor antagonists--why are they not analgesic in humans? Trends Pharmacol Sci 21: 244-246.

Hokfelt T, Kellerth JO, Nilsson G, Pernow B (1975a) Experimental immunohistochemical studies on the localization and distribution of substance P in cat primary sensory neurons. Brain Res 100: 235-252.

Hokfelt T, Kellerth JO, Nilsson G, Pernow B (1975b) Substance p: localization in the central nervous system and in some primary sensory neurons. Science 190: 889-890.

Ikeda O, Murakami M, Ino H, Yamazaki M, Nemoto T, Koda M, Nakayama C, Moriya H (2001) Acute up-regulation of brain-derived neurotrophic factor expression resulting from experimentally induced injury in the rat spinal cord. Acta Neuropathol (Berl) 102: 239-245.

Jarvis CR, Xiong ZG, Plant JR, Churchill D, Lu WY, MacVicar BA, MacDonald JF (1997) Neurotrophin modulation of NMDA receptors in cultured murine and isolated rat neurons. J Neurophysiol 78: 2363-2371.

Karchewski LA, Gratto KA, Wetmore C, Verge VM (2002) Dynamic patterns of BDNF expression in injured sensory neurons: differential modulation by NGF and NT-3. Eur J Neurosci 16: 1449-1462.

Kerr BJ, Bradbury EJ, Bennett DL, Trivedi PM, Dassan P, French J, Shelton DB, McMahon SB, Thompson SW (1999) Brain-derived neurotrophic factor modulates nociceptive sensory inputs and NMDA-evoked responses in the rat spinal cord. J Neurosci 19: 5138-5148.

Kim KJ, Yoon YW, Chung JM (1997) Comparison of three rodent neuropathic pain models. Exp Brain Res 113: 200-206.

Kim SH, Chung JM (1992) An experimental model for peripheral neuropathy produced by segmental spinal nerve ligation in the rat. Pain 50: 355-363.

King VR, Bradbury EJ, McMahon SB, Priestley JV (2000) Changes in truncated trkB and p75 receptor expression in the rat spinal cord following spinal cord hemisection and spinal cord hemisection plus neurotrophin treatment. Exp Neurol 165: 327-341.

Kohno T, Moore KA, Baba H, Woolf CJ (2003) Peripheral nerve injury alters excitatory synaptic transmission in lamina II of the rat dorsal horn. J Physiol 548: 131-138.

Laird JM, Bennett GJ (1993) An electrophysiological study of dorsal horn neurons in the spinal cord of rats with an experimental peripheral neuropathy. J Neurophysiol 69: 2072-2085.

Laird MA, Gidal BE (2000) Use of gabapentin in the treatment of neuropathic pain. Ann Pharmacother 34: 802-807.

Lenz FA, Kwan HC, Dostrovsky JO, Tasker RR (1989) Characteristics of the bursting pattern of action potentials that occurs in the thalamus of patients with central pain. Brain Res 496: 357-360.

Lenz FA, Kwan HC, Martin R, Tasker R, Richardson RT, Dostrovsky JO (1994) Characteristics of somatotopic organization and spontaneous neuronal activity in the region of the thalamic principal sensory nucleus in patients with spinal cord transection. J Neurophysiol 72: 1570-1587.

Lever I, Cunningham J, Grist J, Yip PK, Malcangio M (2003a) Release of BDNF and GABA in the dorsal horn of neuropathic rats. Eur J Neurosci 18: 1169-1174.

Lever IJ, Bradbury EJ, Cunningham JR, Adelson DW, Jones MG, McMahon SB, Marvizon JC, Malcangio M (2001) Brain-derived neurotrophic factor is released in the dorsal horn by distinctive patterns of afferent fiber stimulation. J Neurosci 21: 4469-4477.

Lever IJ, Pezet S, McMahon SB, Malcangio M (2003b) The signaling components of sensory fiber transmission involved in the activation of ERK MAP kinase in the mouse dorsal horn. Mol Cell Neurosci 24: 259-270.

Levine JD, Fields HL, Basbaum AI (1993) Peptides and the primary afferent nociceptor. J Neurosci 13: 2273-2286.

Liebl DJ, Huang W, Young W, Parada LF (2001) Regulation of Trk receptors following contusion of the rat spinal cord. Exp Neurol 167: 15-26.

Light AR, Perl ER (1979a) Reexamination of the dorsal root projection to the spinal dorsal horn including observations on the differential termination of coarse and fine fibers. J Comp Neurol 186: 117-131.

Light AR, Perl ER (1979b) Spinal termination of functionally identified primary afferent neurons with slowly conducting myelinated fibers. J Comp Neurol 186: 133-150.

Lohof AM, Ip NY, Poo MM (1993) Potentiation of developing neuromuscular synapses by the neurotrophins NT-3 and BDNF. Nature 363: 350-353.

Lu Y, Perl ER (2003) A specific inhibitory pathway between substantia gelatinosa neurons receiving direct C-fiber input. J Neurosci 23: 8752-8758.

Lu Y, Perl ER (2005) Modular organization of excitatory circuits between neurons of the spinal superficial dorsal horn (laminae I and II). J Neurosci 25: 3900-3907.

Luo XG, Rush RA, Zhou XF (2001) Ultrastructural localization of brain-derived neurotrophic factor in rat primary sensory neurons. Neurosci Res 39: 377-384.

Mackie M, Hughes DI, Maxwell DJ, Tillakaratne NJ, Todd AJ (2003) Distribution and colocalisation of glutamate decarboxylase isoforms in the rat spinal cord. Neuroscience 119: 461-472.

Maihofner C, Handwerker HO, Neundorfer B, Birklein F (2004) Cortical reorganization during recovery from complex regional pain syndrome. Neurology 63: 693-701.

Manfredi M, Bini G, Cruccu G, Accornero N, Berardelli A, Medolago L (1981) Congenital absence of pain. Arch Neurol 38: 507-511.

Mannion RJ, Costigan M, Decosterd I, Amaya F, Ma QP, Holstege JC, Ji RR, Acheson A, Lindsay RM, Wilkinson GA, Woolf CJ (1999) Neurotrophins: peripherally and centrally acting modulators of tactile stimulus-induced inflammatory pain hypersensitivity. Proc Natl Acad Sci U S A 96: 9385-9390.

Mantyh PW, Hunt SP (2004) Mechanisms that generate and maintain bone cancer pain. Novartis Found Symp 260: 221-238.

Matayoshi S, Jiang N, Katafuchi T, Koga K, Furue H, Yasaka T, Nakatsuka T, Zhou XF, Kawasaki Y, Tanaka N, Yoshimura M (2005) Actions of brain-derived neurotrophic factor on spinal nociceptive transmission during inflammation in the rat. J Physiol 569: 685-695.

McCaffery M (1972) Nursing management of the patient in pain. Philadelphia, PA: JB Lippincott.

Melzack R (1975) The McGill Pain Questionnaire: major properties and scoring methods. Pain 1: 277-299.

Michael GJ, Averill S, Nitkunan A, Rattray M, Bennett DL, Yan Q, Priestley JV (1997) Nerve growth factor treatment increases brain-derived neurotrophic factor selectively in TrkA-expressing dorsal root ganglion cells and in their central terminations within the spinal cord. J Neurosci 17: 8476-8490.

Michael GJ, Averill S, Shortland PJ, Yan Q, Priestley JV (1999) Axotomy results in major changes in BDNF expression by dorsal root ganglion cells: BDNF expression in large trkB and trkC cells, in pericellular baskets, and in projections to deep dorsal horn and dorsal column nuclei. Eur J Neurosci 11: 3539-3551.

Miletic G, Miletic V (2002) Increases in the concentration of brain derived neurotrophic factor in the lumbar spinal dorsal horn are associated with pain behavior following chronic constriction injury in rats. Neurosci Lett 319: 137-140.

Moore KA, Kohno T, Karchewski LA, Scholz J, Baba H, Woolf CJ (2002) Partial peripheral nerve injury promotes a selective loss of GABAergic inhibition in the superficial dorsal horn of the spinal cord. J Neurosci 22: 6724-6731.

Mosconi T, Kruger L (1996) Fixed-diameter polyethylene cuffs applied to the rat sciatic nerve induce a painful neuropathy: ultrastructural morphometric analysis of axonal alterations. Pain 64: 37-57.

Nagasako EM, Oaklander AL, Dworkin RH (2003) Congenital insensitivity to pain: an update. Pain 101: 213-219.

Narita M, Yoshida T, Nakajima M, Narita M, Miyatake M, Takagi T, Yajima Y, Suzuki T (2006) Direct evidence for spinal cord microglia in the development of a neuropathic pain-like state in mice. J Neurochem 97: 1337-1348.

Nestler EJ, Hyman SE, Malenka RC (2001) Pain. In: Molecular Neuropharmacology (Foltin J, Lebowitz H, eds), pp 433-452. Toronto: McGraw-Hill.

Obata K, Yamanaka H, Fukuoka T, Yi D, Tokunaga A, Hashimoto N, Yoshikawa H, Noguchi K (2003) Contribution of injured and uninjured dorsal root ganglion neurons to pain behavior and the changes in gene expression following chronic constriction injury of the sciatic nerve in rats. Pain 101: 65-77.

Peyron R, Schneider F, Faillenot I, Convers P, Barral FG, Garcia-Larrea L, Laurent B (2004) An fMRI study of cortical representation of mechanical allodynia in patients with neuropathic pain. Neurology 63: 1838-1846.

Pezet S, Cunningham J, Patel J, Grist J, Gavazzi I, Lever IJ, Malcangio M (2002a) BDNF modulates sensory neuron synaptic activity by a facilitation of GABA transmission in the dorsal horn. Mol Cell Neurosci 21: 51-62.

Pezet S, Malcangio M, Lever IJ, Perkinton MS, Thompson SW, Williams RJ, McMahon SB (2002b) Noxious stimulation induces Trk receptor and downstream ERK phosphorylation in spinal dorsal horn. Mol Cell Neurosci 21: 684-695.

Polgar E, Fowler JH, McGill MM, Todd AJ (1999) The types of neuron which contain protein kinase C gamma in rat spinal cord. Brain Res 833: 71-80.

Poo MM (2001) Neurotrophins as synaptic modulators. Nat Rev Neurosci 2: 24-32.

Prescott SA, De Koninck Y (2002) Four cell types with distinctive membrane properties and morphologies in lamina I of the spinal dorsal horn of the adult rat. J Physiol 539: 817-836.

Raja SN, Haythornthwaite JA, Pappagallo M, Clark MR, Travison TG, Sabeen S, Royall RM, Max MB (2002) Opioids versus antidepressants in postherpetic neuralgia: a randomized, placebo-controlled trial. Neurology 59: 1015-1021.

Rose CR, Blum R, Kafitz KW, Kovalchuk Y, Konnerth A (2004) From modulator to mediator: rapid effects of BDNF on ion channels. Bioessays 26: 1185-1194.

Salio C, Averill S, Priestley JV, Merighi A (2007) Costorage of BDNF and neuropeptides within individual dense-core vesicles in central and peripheral neurons. Dev Neurobiol 67: 326-338.

Salio C, Lossi L, Ferrini F, Merighi A (2005) Ultrastructural evidence for a pre- and postsynaptic localization of full-length trkB receptors in substantia gelatinosa (lamina II) of rat and mouse spinal cord. Eur J Neurosci 22: 1951-1966.

Sen D, Christie D (2006) Chronic idiopathic pain syndromes. Best Pract Res Clin Rheumatol 20: 369-386.

Sindrup SH, Otto M, Finnerup NB, Jensen TS (2005) Antidepressants in the treatment of neuropathic pain. Basic Clin Pharmacol Toxicol 96: 399-409.

Sivilotti L, Woolf CJ (1994) The contribution of GABAA and glycine receptors to central sensitization: disinhibition and touch-evoked allodynia in the spinal cord. J Neurophysiol 72: 169-179.

Slack SE, Pezet S, McMahon SB, Thompson SW, Malcangio M (2004) Brain-derived neurotrophic factor induces NMDA receptor subunit one phosphorylation via ERK and PKC in the rat spinal cord. Eur J Neurosci 20: 1769-1778.

Slack SE, Thompson SW (2002) Brain-derived neurotrophic factor induces NMDA receptor 1 phosphorylation in rat spinal cord. Neuroreport 13: 1967-1970.

Stoppini L, Buchs PA, Muller D (1991) A simple method for organotypic cultures of nervous tissue. J Neurosci Methods 37: 173-182.

Sugiura Y, Lee CL, Perl ER (1986) Central projections of identified, unmyelinated (C) afferent fibers innervating mammalian skin. Science 234: 358-361.

Teng KK, Hempstead BL (2004) Neurotrophins and their receptors: signaling trios in complex biological systems. Cell Mol Life Sci 61: 35-48.

Thomas RJ, McEwen J, Asbury AJ (1996) The Glasgow Pain Questionnaire: a new generic measure of pain; development and testing. Int J Epidemiol 25: 1060-1067.

Thompson SW, Bennett DL, Kerr BJ, Bradbury EJ, McMahon SB (1999) Brain-derived neurotrophic factor is an endogenous modulator of nociceptive responses in the spinal cord. Proc Natl Acad Sci U S A 96: 7714-7718.

Todd AJ, Hughes DI, Polgar E, Nagy GG, Mackie M, Ottersen OP, Maxwell DJ (2003) The expression of vesicular glutamate transporters VGLUT1 and VGLUT2 in neurochemically defined axonal populations in the rat spinal cord with emphasis on the dorsal horn. Eur J Neurosci 17: 13-27.

Todd AJ, Lewis SG (1986) The morphology of Golgi-stained neurons in lamina II of the rat spinal cord. J Anat 149: 113-119.

Todd AJ, McKenzie J (1989) GABA-immunoreactive neurons in the dorsal horn of the rat spinal cord. Neuroscience 31: 799-806.

Tsuda M, Inoue K, Salter MW (2005) Neuropathic pain and spinal microglia: a big problem from molecules in "small" glia. Trends Neurosci 28: 101-107.

Walker SM, Mitchell VA, White DM, Rush RA, Duggan AW (2001) Release of immunoreactive brain-derived neurotrophic factor in the spinal cord of the rat following sciatic nerve transection. Brain Res 899: 240-247.

Wall PD, Devor M (1983) Sensory afferent impulses originate from dorsal root ganglia as well as from the periphery in normal and nerve injured rats. Pain 17: 321-339.

Waxman SG, Kocsis JD, Black JA (1994) Type III sodium channel mRNA is expressed in embryonic but not adult spinal sensory neurons, and is reexpressed following axotomy. J Neurophysiol 72: 466-470.

Wiesmann C, de Vos AM (2001) Nerve growth factor: structure and function. Cell Mol Life Sci 58: 748-759.

Woolf CJ (1983) Evidence for a central component of post-injury pain hypersensitivity. Nature 306: 686-688.

Woolf CJ, Chong MS (1993) Preemptive analgesia--treating postoperative pain by preventing the establishment of central sensitization. Anesth Analg 77: 362-379.

World Health Organization. The World Health Report 2003. Geneva, WHO.

Xu B, Michalski B, Racine RJ, Fahnestock M (2004) The effects of brain-derived neurotrophic factor (BDNF) administration on kindling induction, Trk expression and seizure-related morphological changes. Neuroscience 126: 521-531.

Yajima Y, Narita M, Narita M, Matsumoto N, Suzuki T (2002) Involvement of a spinal brain-derived neurotrophic factor/full-length TrkB pathway in the development of nerve injury-induced thermal hyperalgesia in mice. Brain Res 958: 338-346.

Yajima Y, Narita M, Usui A, Kaneko C, Miyatake M, Narita M, Yamaguchi T, Tamaki H, Wachi H, Seyama Y, Suzuki T (2005) Direct evidence for the involvement of brain-derived neurotrophic factor in the development of a neuropathic pain-like state in mice. J Neurochem 93: 584-594.

Yasaka T, Kato G, Furue H, Rashid MH, Sonohata M, Tamae A, Murata Y, Masuko S, Yoshimura M (2007) Cell-type-specific excitatory and inhibitory circuits involving primary afferents in the substantia gelatinosa of the rat spinal dorsal horn in vitro. J Physiol 581: 603-618.

Zhou XF, Chie ET, Deng YS, Zhong JH, Xue Q, Rush RA, Xian CJ (1999) Injured primary sensory neurons switch phenotype for brain-derived neurotrophic factor in the rat. Neuroscience 92: 841-853.

Zhou XF, Li WP, Zhou FH, Zhong JH, Mi JX, Wu LL, Xian CJ (2005) Differential effects of endogenous brain-derived neurotrophic factor on the survival of axotomized sensory neurons in dorsal root ganglia: a possible role for the p75 neurotrophin receptor. Neuroscience 132: 591-603.

CHAPTER 2

GENERAL METHODS:

Preparation of organotypic slice cultures and whole-cell recordings from visually identified dorsal horn neurons.

2.1 Preparation of Organotypic Slice Cultures

All procedures were carried out in compliance with the guidelines of the Canadian Council for Animal Care and with the approval of the University of Alberta Health Sciences Laboratory Animal Services Welfare Committee.

The prenatal rat spinal cord slice culture technique was adapted from previously published methods (Ballerini and Galante, 1998; Braschler et al., 1989; Gahwiler, 1981; Gahwiler et al., 1998; Spenger et al., 1991). Embryonic day 13-14 rat fetuses were delivered by caesarean section from timed-pregnant female Sprague-Dawley rats (Charles River, Saint-Constant, QC, Canada) under deep isoflurane anaesthesia (Figure 2-1A, left and middle panel). The dam was subsequently euthanized with an overdose of intracardial chloral hydrate (10.5%) (Figure 2-1A, right panel). The entire embryonic sac was placed in chilled Hanks' balanced salt solution (HBSS; Figure 2-1C) containing (in mM): 138 NaCl, 5.33 KCl, 0.44 KH_2PO_4, 0.5 $MgCl_2$-$6H_2O$, 0.41 $MgSO_4$-$7H_2O$, 4 $NaHCO_3$, 0.3 Na_2HPO_4, 5.6 D-glucose and 1.26 $CaCl_2$. The rest of the procedure was performed in a laminar flow tissue culture hood, and proper sterile and aseptic techniques were employed. Individual rat fetuses were removed from their embryonic sacs by cutting a slit along the embryonic sac and exposing the amniotic sac (Figure 2-1D, upper left and middle panel). The sac was punctured and the fetus removed into a new dish filled with chilled HBSS (Figure 2-1D, right panel). Afterwards, the backs of each fetus were isolated with three cuts: one to decapitate the fetus, one to cut the hind limbs and tail, and one to trim internal organs ventral to the spinal cord (Figure 2-2A). Then spinal cords were placed dorsal side up on a plastic cover on the chopping stage of the tissue chopper (McIlwain, St. Louis, MO, USA; Figure 2-2B, left panel). Excess solution was removed around the spinal cord to prevent sliding during the chopping procedure (Figure 2-2B, middle left panel), and then the spinal cords were sliced into 300 ± 25 μm transverse slices (Figure 2-2B, middle right panel). The slices on the plastic cover were removed into a new dish filled with HBSS (Figure 2-2B, right panel) and trimmed of excess ventral tissue. Only lumbar spinal cord slices with an intact spinal cord and two attached dorsal root ganglia (DRGs) were chosen (Figure 2-4A). Newly trimmed slices were transferred to a new dish filled with HBSS and chilled for 1 hour at 4°C to allow recovery from the slicing procedure.

Each embryonic spinal cord slice, with attached DRGs, was plated on to clean glass coverslips (Karl Hecht, Sondheim, Germany) with a clot of reconstituted chicken plasma (lyophilized, 0.2mg% heparin; Cocalico Biologicals Inc., Stevens, PA, USA or SIGMA, St. Louis, MO, USA) and thrombin (200 units/ml; SIGMA, St. Louis, MO, USA) (Figure 2-2C, left) and allowed to dry for 1 hour at room temperature (20-22°C). Coverslips were then inserted into flat-sided tissue culture tubes (Nunc-Nalgene International, Mississauga, ON, Canada) filled with 1 ml of medium, and then placed into a roller drum (Model # TC-8, New Brunswick Scientific, Edison, NJ, USA) (Figure 2-2C, right) rotating at 120 rotations per hour in a dry heat (regular air-atmospheric CO_2) incubator at 36°C. The medium in tubes was composed of 82% Dulbecco's Modified Eagle Medium (DMEM), 10% fetal bovine serum, and 8% sterile water to adjust the osmolarity (all from Gibco, Grand Island, NY, USA). The medium was supplemented with 20 ng/ml NGF (Alomone Laboratories, Jerusalem, Israel) for the first 4 days, and then omitted subsequently thereafter. Antibacterial and antimycotic drugs (5 units/ml penicillin G, 5 units/ml streptomycin and 12.5 ng/ml amphotericin B; Gibco) were also included in the medium during the first 4 days of culture. After 4 days in culture, OTC slices were treated with a 10 μM antimitotic drug cocktail consisting of uridine, cytosine-β-D-arabino-furanoside (AraC), and 5-fluorodeoxyuridine (all from SIGMA) for 24 hours to prevent the overgrowth of glial cells.

The medium for exchanges was freshly prepared prior to use and warmed up to 37°C before the exchange. The old medium from flat-bottom tubes was completely aspirated and then replaced with 1 ml of new medium. Only ten tubes were exchanged at a time to prevent excess cooling of slices while removed from the incubator. All media preparations and exchanges took place in a tissue culture hood and proper sterile and aseptic techniques were used to minimize contamination of cultures.

2.1.1 Serum-free culture conditions

Fetal bovine serum (FBS) is useful for buffering the acidity of culture medium and also provides non-specific trophic support for the survival of cells. The undefined factors and mediators present in FBS could confound the interpretation of effects induced by long-term application of BDNF. So in order to control for these variables, the medium composition was altered to a medium absent of serum in order to remove the reliance of cultures on FBS. During the anti-mitotic treatment, the serum medium was progressively switched (first diluted 50:50 after 4 days, then completely exchanged after 5 days) to a defined, serum-free medium consisting of Neurobasal medium with N-2 supplement and 5 mM Glutamax-1 (all from Gibco). The medium within these tubes was exchanged regularly with freshly prepared medium every 3-4 days. The medium schedule is summarized in Figure 2-3A.

Also for reasons stated earlier, the NGF applied initially to support neurons in culture was removed prior to applying BDNF. After the first 4 days in culture, NGF was completely removed from the culture medium applied to OTC slices. Therefore, the medium applied to cultured slices was a defined, neurotrophin- and serum-free medium.

2.2 Treatment Protocol of Defined Medium OTCs (DMOTCs) with BDNF

DMOTC slices were maintained *in vitro* 3-4 weeks before experiments to allow cultures to stabilize. Also, the BDNF treatment schedule was chosen to parallel previous whole animal studies (Balasubramanyan et al., 2006) so exposure of dorsal horn neurons to BDNF would match the time-course of BDNF elevation following nerve injury (Figure 2-3B). Slices were treated after 15-21 days *in vitro* for a period of 5-6 days with 200 ng/ml BDNF (Alomone Laboratories) in the serum-free medium described above. The BDNF medium was exchanged on the 3rd treatment day. Age-matched untreated DMOTC slices served as controls.

In addition, the effects of heat-inactivated BDNF were tested on DMOTC slices. BDNF was inactivated by fully thawing pre-aliquoted vials of BDNF to 37°C then immersing the vial in a hot (56°C) water bath for 30 min, mixing the vial every 5-10 minutes. Immediately following, the vial was cooled by immersing in an ice bath. Heat-inactivated BDNF was applied to DMOTCs in a manner similar to active BDNF.

2.3 Electrophysiology

DMOTC spinal cord slices were viewed with a Zeiss Axioskop FS upright microscope equipped with infrared differential interference contrast (IR-DIC) optics. The glass coverslip with the OTC slice was removed from the flat-bottomed tube and placed in a chamber perfused with 95% O_2-5% CO_2-saturated, external recording solution containing (in mM): 127 NaCl, 2.5 KCl, 1.2 NaH_2PO_4, 1.3 $MgSO_4$, 26 $NaHCO_3$, 25 D-glucose, 2.5 $CaCl_2$, exchanging at a rate of 1 ml/min. All experiments were carried out at room temperature (20-22°C). Slices were positioned with visible light under the 10X objective before viewing dorsal horn neurons under IR-DIC optics using the 40X water immersion objective. An IR-sensitive video camera (NC-70, Dage-MTI, Michigan City, IN, USA) was used to capture the image of neurons which was viewed on a video monitor. Typical markers such as the ventral fissure and DRG on the lateral sides of the spinal cord were utilized to determine orientation of the slice and locate the dorsal half of the slice (Figure 2-4B). Dorsal neurons were selected from the dorsal half of the spinal cord 0.5-2 mm from the edge of the slice (Figure 2-4B). Healthy neurons possessed a round cell body with a flat appearance (Figure 2-4C). Large (> 80 μm soma diameter) and 'bloated' neurons were avoided for recordings.

Electrophysiological recordings were made using a NPI SEC-05L amplifier (npi Electronic Gmbh, Tamm, Germany) in whole-cell discontinuous single-electrode voltage-clamp or current-clamp mode. Patch pipettes were pulled from thin-walled borosilicate glass (1.5/1.12 mm OD/ID, Cat. No. TW140F-4; WPI, Sarasota, FL, USA) to 5-10 MΩ resistances and filled with an internal recording solution containing (in mM): 130 potassium gluconate, 1 $MgCl_2$, 2 $CaCl_2$, 10 HEPES, 10 EGTA, 4 Mg-ATP, 0.3 Na-GTP, pH 7.2, 280-310 mOsm. In some synaptic recordings, a Cs^+-based internal solution containing (in mM): 140 CsCl, 5 HEPES, 10 EGTA, 2 $CaCl_2$, 2 Mg-ATP, 0.3 Na-GTP, pH 7.2, was used. Biocytin (0.2%) was also added to the internal solution for subsequent *post-hoc* morphological analysis. Recordings were obtained using Axon Instruments pCLAMP 9.0 acquisition software (Molecular Devices, Burlingame, CA, USA), and protocols were designed to test the electrical properties of the cell.

2.4 Histology and Immunohistochemistry

At the end of recordings, the recording pipette was slowly withdrawn from the cell and the slice was placed in cold (4°C) 4% paraformaldehyde in phosphate buffer solution (PBS) for 2-3 days before proceeding with staining. If DMOTC slices were being stored for longer than a month, slices were transferred to PBS containing 0.1% sodium azide.

For cell identification and morphological characterization, DMOTC slices were rinsed three times with PBS before staining with a Texas red-streptavidin conjugate (1:50; Molecular Probes, Eugene, OR, USA) made in 0.3% Triton X-100 (VWR International, West Chester, PA, USA) for 45 minutes on a 3D rotator (Labline Instruments, Melrose Park, IL, USA). Slices were washed thoroughly with distilled water before mounting on to microscope slides. Slices were allowed to dry sufficiently before a coverslip (thickness 1; Fisher Scientific, Edmonton, AB, Canada) was applied using low viscosity mounting medium (Cytoseal™-60, Richard-Allan Scientific, Kalamazoo, MI, USA).

For immunohistochemistry experiments, fixed DMOTC slices were rinsed three times with PBS before incubating with primary antibodies (1:8000), made up with 2% normal goat serum (NGS; Rockland, Gilbertsville, PA, USA) and 0.3% Triton X-100 in PBS. The primary antibody used was anti-glutamic acid decarboxylase (anti-GAD, rabbit; Chemicon, Temecula, CA, USA). The primary antibody incubation was in a sealed, light-protected container at 4°C for 48 hours. DMOTC slices were then rinsed three times with PBS before incubating with Alexa-488 fluorescently-tagged secondary antibodies (1:300, anti-rabbit; Molecular Probes), made up with 2% NGS and 0.3% Triton X-100 in PBS for 2.5 hours. During incubation, slices were rocked on the 3D rotator. To label biocytin-filled neurons, a Texas red-streptavidin conjugate was added after two hours of the start of incubation with the secondary antibody solution. Slices were washed thoroughly with distilled water before mounting on to microscope slides. Stained slices were allowed to dry sufficiently before a coverslip was applied using the anti-fading mounting reagent Prolong Gold (Molecular Probes).

The concentration of antibodies was optimized using control DMOTC slices to produce sufficient staining and reduce background. The fluorescent dyes used, Texas Red and Alexa-488, did not produce spectral crossover in staining controls (data not shown).

Fluorescent confocal images were captured by a mounted AxioCam HR camera (Zeiss) and displayed on a computer using proprietary software (Zeiss LSM image browser, v. 3, 2, 70). Confocal z-stacks and 3D reconstructions were also acquired using Zeiss LSM 510 imaging software. Some pictures are shown in black and white to increase contrast and clarity.

2.5 Fluorescent Calcium Imaging

A single DMOTC slice was incubated for 1 hour prior to imaging with 5 µM of the membrane-permeable acetoxy-methyl form of the fluorescent Ca^{2+}-indicator dye Fluo-4 (TEF Labs Inc., Austin, Texas, USA). The conditions for incubating the dye were standardized across different slices to avoid uneven dye loading. After dye loading, the DMOTC slice was transferred to a recording chamber and perfused with external recording solution described above, at room temperature (20-22°C), and at a flow rate of 4 ml/min. Changes in Ca^{2+}-fluorescence intensity evoked by a high K^+ solution (20, 35, or 50 mM, 90 s application) or other pharmacological agents, were measured in dorsal horn neurons with a confocal microscope equipped with an argon (488 nm) laser and filters (20X XLUMPlanF1-NA-0.95 objective; Olympus FV300, Markham, Ontario, Canada). Full frame images (512 x 512 pixels) in a fixed xy plane were acquired at a scanning time of 1.08 s/frame (Ruangkittisakul et al., 2006). In some experiments, images were cropped to accommodate faster scan rates. Selected regions of interest were drawn around distinct cell bodies and fluorescence intensity traces were generated with FluoView v.4.3 software (Olympus).

2.6 Analysis and Statistical Tests

All electrophysiological data, except spontaneous postsynaptic currents, were analyzed using pCLAMP 9.0 software. Statistical comparisons were made with paired or unpaired t-tests, chi-squared (χ^2) tests, or analysis of variance (ANOVA) with the Student Newman-Keuls (SNK) multiple comparisons test as specified and appropriate. *P values* from these statistical tests were generated using GraphPad InStat 3.05 (GraphPad Software, San Diego, CA, USA). Statistical significance was taken as $p<0.05$.

To analyze spontaneous and miniature synaptic events, the Mini Analysis™ software program (Synaptosoft, Decatur, GA, USA) was used. Peaks of events were first automatically detected by the software according to a set of threshold criteria, and then all detected events were visually re-examined and accepted or rejected subjectively (Moran et al., 2004). To generate cumulative probability plots for both amplitude and inter-event time interval, the same number of events (50-200 events acquired after an initial 1 min of recording) from each neuron was pooled for each neuronal class, and input into the Mini Analysis program. The Kolmogorov-Smirnov two-sample statistical test (KS-test) was used to compare the distribution of events between two populations, i.e. control and BDNF-treated groups.

All dendritic length measurements were made using Zeiss LSM 510 image browser software. The longest visible projection from the cell soma on the confocal reconstruction of the transverse plane was measured.

All graphs were plotted using Origin 7 (Origin Lab, Northampton, MA, USA) and figures were produced with Adobe Illustrator 10 (Adobe Software, San Jose, CA, USA).

2.7 Drugs

Unless otherwise stated, all chemicals were from SIGMA (St. Louis, MO, USA). Chicken plasma (Cocalico Biologicals Inc. or SIGMA) was reconstituted with HBSS and centrifuged for 30 minutes at 3500 r.p.m. at 4°C to separate excess fat from the plasma. Thrombin was prepared with HBSS as well.

TTX (Alomone Laboratories) was dissolved in distilled water as a 1 mM stock solution and stored at -20°C until use. Strychnine was prepared in a similar manner to TTX, and bicuculline (Tocris, Ballwin, MO, USA) was dissolved in dimethyl sulfoxide (DMSO) as a 10 mM stock solution. 6-cyano-7-nitroquinoxaline-2,3-dione (CNQX, Tocris) and 2,3-dihydroxy-6-nitro-7-sulfamoyl-benzo[f]quinoxaline-2,3-dione (NBQX, Tocris) were prepared as 10 mM stocks dissolved in distilled water, and D(-)-2-Amino-5-phosphonopentanoic acid (D-AP5, Tocris) was prepared as a 50 mM stocks dissolved in 30% 1 M NaOH. Riluzole was prepared as 10 or 50 mM stocks, kyneurinic acid and GABA as 1 M stocks, baclofen (Tocris) as a 15 mM stock, and nitrendipine as a 1 mM stock made up in distilled water. These drugs were used at a 1:1000 dilution prepared freshly with external recording solution immediately prior to the start of experiments.

Fluo-4 AM dye was dissolved in a mixture of DMSO and 20% pluronic acid (Invitrogen, Burlington, Ontario, Canada) to a 0.5 mM stock solution and kept frozen until used. The dye was thawed and sonicated thoroughly before incubating with a DMOTC slice.

Figure 2-1: Removal of fetuses during preparation of OTC spinal cord slices.

A: Photos of the caesarean dissection performed while the dam is under deep anesthesia. First the abdominal cavity is opened up from just above the urethra (left panel) up to the diaphragm (middle panel). Then an overdose of chloral hydrate (10.5%) is administered directly into the heart to euthanize the female rat (right panel).

B: Photo of the exposed abdominal cavity with major organs labelled. The embryonic sac is visible in the lower abdomen below the intestines of pregnant female rats.

C: Removal of the embryonic sac. The entire embryonic sac is removed by cutting it away from the uterus (left panel) and mesenteric wall (middle panel) before placing in a dish filled with chilled (4°C) Hanks' balanced salt solution (HBSS) (right panel). The embryonic sac is a chain of approximately 6-12 embryos attached together.

D: Removal of fetuses from their embryonic sac. The amniotic sac surrounding each fetus is first exposed by cutting a slit along the embryonic sac to widen the opening (upper left panel) for the amniotic sac containing the fetus to protrude out (middle panel). Then the segment of the embryonic sac including the amniotic sac is removed from the rest of the chain. The amniotic sac is then punctured to allow the fetus to separate (right panel) and is placed in a new dish filled with HBSS. The lower left panel shows a single fetus.

A. Caesarean dissection

B. Abdominal cavity

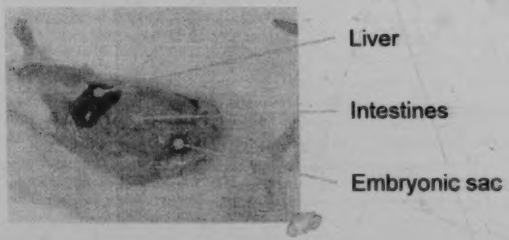

C. Removal of embryonic sac

D. Removal of fetus

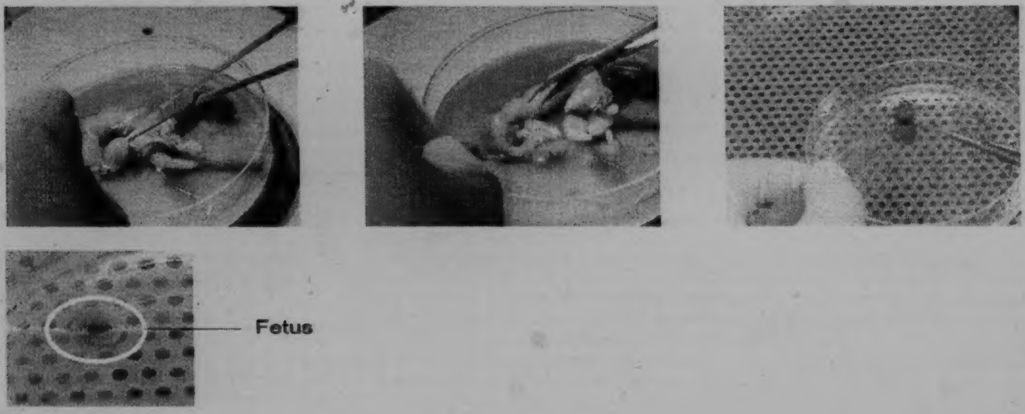

Figure 2-2: Preparation of spinal cord slices for roller-tube organotypic cultures (OTCs).

A: Illustration of the cuts required to isolate the spinal cords of each fetus. The first cut is to decapitate the fetus, the second cut is to remove the tail and hindlimbs, and the final cut is the trim internal organs ventral to the spinal cord, which is drawn as a thick grey line.

B: Chopping procedure for isolated spinal cords. Each isolated spinal cord slice is placed on a plastic cover on the chopping stage of a tissue chopper (left panel). Spinal cords are oriented dorsal side up and the rostrocaudal axis is perpendicular to the blade in order to produce transverse spinal cord slices. Excess fluid around the spinal cord is removed (middle left panel) to prevent movement during the chopping procedure (middle right panel). The chopped spinal cords are removed by immersing the plastic cover in a new dish filled with HBSS (right panel).

C: Slice plating procedure. The trimmed spinal cord slice is placed in 20 µl of reconstituted chicken plasma on a glass coverslip. The spinal cord slice is attached to the glass coverslip by mixing 30 µl of thrombin to form a plasma clot (left panel). The glass coverslip with a spinal cord slice attached (middle left panel) is then placed into a flat-sided tube filled with serum medium and tightly sealed before placing on a roller drum rotating at 120 rotations per hour in a dry heat (36°) incubator, as illustrated on the right.

A. Isolation of spinal cord

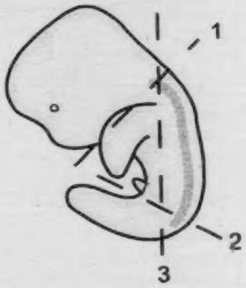

B. Spinal cord chopping

C. Slice plating

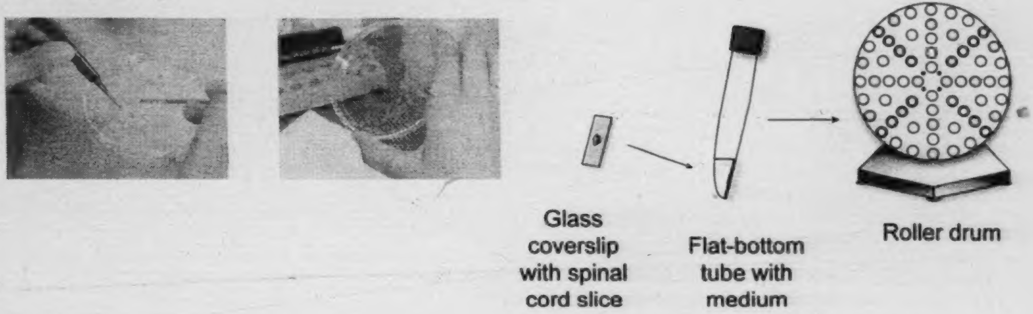
Glass coverslip with spinal cord slice
Flat-bottom tube with medium
Roller drum

Figure 2-3: Proposed schedule for medium exchanges of OTC slices and justification for timeline.

A: Medium exchange schedule for OTC slices. Day 0 marks the start of cultures. Pen/Strep/Amp are the antibiotics used at the start of culturing: 5 units/ml penicillin G, 5 units/ml streptomycin and 12.5 ng/ml amphotericin B. Ara-C/U/5FDU are the antimitotics applied for 24 hours to prevent the overgrowth of glial cells: cytosine-β-D-arabino-furanoside (AraC), uridine (U) and 5-fluorodeoxyuridine (5FDU), all at 10 μM. NGF (20 ng/ml) was applied for the first 4 days of culture and then completely removed once serum-free conditions were established. DMEM with fetal bovine serum (FBS) was progressively removed, first diluted 50% then completely switched to a serum- and neurotrophin-free medium of Neurobasal and N2-supplement. BDNF-treated OTC slices were treated for 5-6 days at a concentration of 200 ng/ml. Controls were time-matched, untreated OTC slices.

B: Timeline comparison of proposed experiments, the long-term treatment of dorsal horn neurons with BDNF, in pink and previous experiments using a chronic constriction nerve injury model (CCI) in animals, in purple. The treatment period for BDNF was chosen to parallel the increase in BDNF observed following peripheral nerve injury in animal models of neuropathic pain.

A. Medium exchange schedule

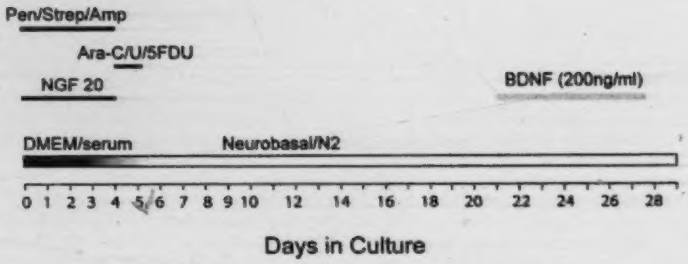

B. Comparison between defined-medium OTCs and previous nerve injury studies

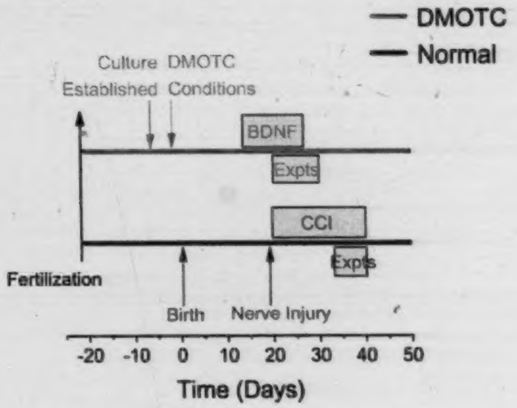

Figure 2-4: Pictures of OTC slices.

A: An acutely isolated transverse slice of the embryonic spinal cord. Dorsal side is along the top of the picture. The slice has been trimmed of excess ventral tissue and is ready for plating on a glass coverslip with a plasma clot as described. Asterisks indicate the dorsal root ganglia (DRGs) located on either side of the cord. At this stage of gestation (E13-14) the DRGs have not migrated out. White scale bar is 500 µm.

B: An OTC slice after 10 days *in vitro*. Dorsal side is along the top of the picture and the white scale bar is 500 µm. The white semi-circle on the dorsal half of the OTC slice indicates the region where electrophysiological recordings were obtained from. Labelled are the dorsal root ganglion (DRG) attached to the cultured spinal cord and the ventral fissure. Picture to the right of each is a higher magnification view of the DRG and ventral section, respectively. Black scale bar is 50 µm.

C: Higher magnification view of the dorsal region of an OTC slice under infrared differential interference contrast (IR-DIC) optics. Healthy neurons are visible as flat, rounded cells and a few are marked by white bullets (○). Black scale bar is 50 µm.

A. Acutely isolated embryonic spinal cord slice

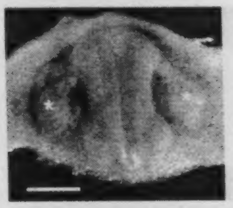

B. OTC slice in culture for 10 days

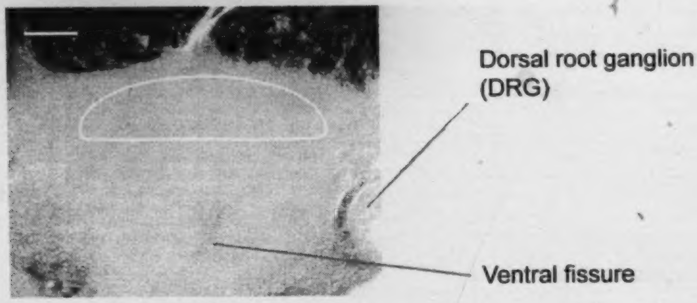

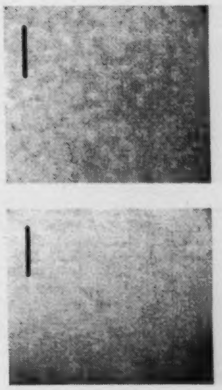

C. High power (40X) view of dorsal region

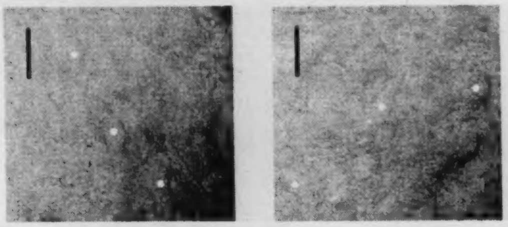

2.8 References

Balasubramanyan S, Stemkowski PL, Stebbing MJ, Smith PA (2006) Sciatic chronic constriction injury produces cell-type-specific changes in the electrophysiological properties of rat substantia gelatinosa neurons. J Neurophysiol 96: 579-590.

Ballerini L, Galante M (1998) Network bursting by organotypic spinal slice cultures in the presence of bicuculline and/or strychnine is developmentally regulated. Eur J Neurosci 10: 2871-2879.

Braschler UF, Iannone A, Spenger C, Streit J, Luscher HR (1989) A modified roller tube technique for organotypic cocultures of embryonic rat spinal cord, sensory ganglia and skeletal muscle. J Neurosci Methods 29: 121-129.

Gahwiler BH (1981) Organotypic monolayer cultures of nervous tissue. J Neurosci Methods 4: 329-342.

Gahwiler GH, Thompson SM, McKinney RA, Debanne D, Robertson RT (1998) Organotypic Slice Cultures of Neural Tissue. In: Culturing Nerve Cells (Baker G, Goslin K, eds), pp 461-497. Cambridge, Massachusetts.

Moran TD, Colmers WF, Smith PA (2004) Opioid-like actions of neuropeptide Y in rat substantia gelatinosa: Y1 suppression of inhibition and Y2 suppression of excitation. J Neurophysiol 92: 3266-3275.

Ruangkittisakul A, Schwarzacher SW, Secchia L, Poon BY, Ma Y, Funk GD, Ballanyi K (2006) High sensitivity to neuromodulator-activated signaling pathways at physiological [K+] of confocally imaged respiratory center neurons in on-line-calibrated newborn rat brainstem slices. J Neurosci 26: 11870-11880.

Spenger C, Braschler UF, Streit J, Luscher HR (1991) An Organotypic Spinal Cord - Dorsal Root Ganglion - Skeletal Muscle Coculture of Embryonic Rat. I. The Morphological Correlates of the Spinal Reflex Arc. Eur J Neurosci 3: 1037-1053.

CHAPTER 3

CHARACTERIZATION OF DORSAL NEURONS IN DEFINED-MEDIUM ORGANOTYPIC CULTURES OF RAT SPINAL CORDS.

* A version of this chapter has been published.

3.1 Introduction

The defined-medium, organotypic culture (DMOTC) of rat spinal cords is a unique system which enables the long-term application of a mediator, in our case BDNF, and the study of its effects on neurons in the dorsal horn. The medium incubating these cultures have been optimized to remove undefined trophic factors and neurotrophins that could interact or compete for the same receptors as BDNF, which would complicate interpretation of results. Thus, these experiments allow for the specific study of BDNF action under controlled experimental conditions. This system also offers the opportunity to isolate the effects of BDNF on nociceptive signalling from other mediators released during nerve injury in animal models of neuropathic pain. From these studies I can determine the role of BDNF in altering the excitability of dorsal horn neurons which can consequently lead to central sensitization and long-lasting changes in nociceptive signalling; a hallmark feature of neuropathic pain.

Neurons in OTC preparations have been studied in extensive detail, especially neurons in hippocampal OTC slices. Hippocampal pyramidal and granule cells within OTC slices have similar morphologies and dendritic spine formations as neurons found in acute slice preparations (Gahwiler, 1984; Gahwiler et al., 1998; Stoppini et al., 1991). The differentiation and development of functional synapses of hippocampal neurons in slice culture closely resembles the time course of neuronal development *in vivo* (Buchs et al., 1993; Gahwiler, 1984; Muller et al., 1993); though, some report a slower rate of maturation of neurons in OTC slices (De Simoni et al., 2003).

In OTCs of spinal cord tissue, the maturation of neurons in culture was tested biochemically by examining the expression of developmentally regulated protein markers

(Avossa et al., 2003). The spatial and temporal expression pattern of enzymes such as glutamic acid decarboxylase-67 (GAD67) has been well characterized in developmental studies and has been shown to progress along a similar time course in neurons from OTC spinal cord preparations. Even markers of mature glial cells are expressed at the same time points in organotypic slice cultures as in whole animal studies. Therefore, cells in OTC slices mature accordingly and develop at a parallel rate to similarly aged cells from the intact animal.

Nevertheless, there have been reports of dedifferentiation of mature motoneurons in long-term (>4 weeks) OTCs (Perrier et al., 2000). Although cultures from these studies were prepared from adult spinal cords, it is not known if similar changes occur in OTC slices derived from an embryonic source. In fact, the phenotype and identity of dorsal horn neurons in OTCs has not been characterized yet, nor have they been compared to dorsal horn neurons described extensively in acute spinal cord preparations. Comparative studies between dorsal horn neurons in DMOTC and acute slices are needed to demonstrate that the same neuronal phenotypes are maintained in long-term cultures. These studies can also validate the use of this technique in the study of nociceptive signalling and demonstrate that dorsal horn neurons present in our DMOTCs are indeed comparable to dorsal horn neurons affected in neuropathic pain states.

This chapter presents a characterization of dorsal horn neurons in DMOTC slices and compares neuronal phenotypes to those described in acutely isolated spinal cords. Some of this work has already been published (Lu et al., 2003; Lu et al., 2006).

3.2 Methods

3.2.1 Defined-medium organotypic cultures (DMOTCs) of spinal cord slices

DMOTC slices were prepared as previously described (see Chapter 2: General methods). Very briefly, spinal cords were isolated from embryonic (E13-14) rat pups and transverse slices (300 ± 25 μm) were cultured using the roller-tube technique. Serum-free conditions were established after 5 days *in vitro* following the medium exchange schedule outlined in Figure 2-3A. Medium was exchanged with freshly prepared medium every 3-4 days. DMOTC slices were studied after 1, 2, 3 and 4 weeks in culture with day 0 as the day cultures were established.

3.2.2 Electrophysiology

Dorsal horn neurons in DMOTCs were viewed with a Zeiss Axioskop FS upright microscope and neurons were patched under the guidance of infrared differential interference contrast (IR-DIC) optics. Whole-cell recordings were obtained using a NPI SEC-05L amplifier (npi Electronic Gmbh, Tamm, Germany) in discontinuous current- or voltage-clamp mode. Patch pipettes were pulled from thin-walled borosilicate glass (1.5/1.12 mm OD/ID, Cat. No. TW140F-4, WPI, Sarasota, FL, USA) to 5-10 MΩ resistances and filled with either K^+ gluconate- or CsCl-based internal solution described in Chapter 2. Dorsal neurons were selected for recordings from the dorsal half of the spinal cord, 0.5-2 mm from the dorsal edge of the slice (Figure 2-4B).

Neurons were categorized on the basis of their action potential firing pattern from a preset membrane potential of -60 mV (Grudt and Perl, 2002). A series of 2 pA incremental depolarizing current steps beginning from rheobase was applied to characterize each neuron's discharge firing pattern. The rheobase was determined as the minimum amount of current required to initiate firing of an action potential from a membrane potential adjusted to -60 mV. Classification of neurons was based on previously described action potential firing patterns in dorsal horn neurons from acute spinal cord preparations (Balasubramanyan et al., 2006; Grudt and Perl, 2002). Briefly, 'tonic' neurons exhibit continuous action potential discharges in response to depolarizing current pulses, 'delay' neurons have a sustained pause before the onset of action potential firing, 'phasic' neurons display an initial burst of action potentials before accommodation or cessation of firing, 'transient' or single-spike neurons fire only a single action potential regardless of the intensity of current stimulation, and 'irregular' neurons which do not exhibit any clear relationship between action potential discharge pattern and intensity of depolarization stimulus (Figure 3-1A).

Current-voltage (I-V) relationships were determined in voltage-clamp mode using a range (-20 to -140 mV) of 800 ms voltage commands steps. "Pseudo-steady state" current was measured just prior to the termination of each voltage pulse. The input resistance (R_{input}) of each cell was calculated from the inverse slope of the I-V curve, from the voltage range of -130 to -100 mV, generated for each individual neuron.

Membrane excitability was quantified by examining discharge rates in response to 1.5 s current ramps from a preset membrane potential of -60 mV. The time to elicit the first action potential spike was measured from current ramp rates of 20, 33.3, 46.7 and 60 pA/s and plotted against ramp rates.

Excitatory postsynaptic currents were evoked (eEPSCs) at 0.05 Hz with a teflon-coated nichrome stimulating electrode. It was made from two twisted strands of nichrome wire (7620, A-M Systems, Carlsborg, WA, USA) with the ends cut to expose the nichrome within the strand. Stimulating electrodes were placed directly on the DRG to activate primary afferent fibres. Evoked inhibitory postsynaptic currents (eIPSCs) were generated at 0.05 Hz by focal stimulation (positioned 50-100 μm from the cell body) with a patch pipette containing 2 M NaCl. The stimulating electrode was repositioned until a reliable synaptic input to the cell was found. The orientation of the stimulating electrode, relative to the cell body, varied in the dorsoventral and mediolateral axes. Stimulus intensity was between 2-30 V for both eEPSCs and eIPSCs and stimulus duration was 100 or 400 μs. Monosynaptic eEPSCs and eIPSCs were identified by their ability to follow high frequency stimulation (10-20 Hz) with constant latency and the absence of failures.

A CsCl-based internal solution was used for recording all evoked synaptic responses except evoked responses to baclofen and eEPSC concentration-inhibition experiments where a K^+-gluconate-based internal solution was used. Membrane potential was clamped at -70 mV for recording eIPSCs when a CsCl-based internal solution was used. The E_{Cl} for the CsCl-based internal was ~0 mV so eIPSCs appeared as inward currents at a negative holding potential. When a K^+-gluconate-based internal solution was used, the membrane potential was clamped at -40 mV for recording eIPSCs. The E_{Cl} for the K^+ gluconate-based internal was ~-80 mV so eIPSCs appeared as outward currents at more positive holding potentials. The voltage-gated Na^+ channel blocker QX-314 (5 mM) was included in the internal solution during the recording of eEPSCs to prevent action potential discharges. Evoked responses were averaged from 6-10 successive sweeps with a similar rise time and baseline.

The concentration-inhibition curves of eEPSCs to CNQX was determined by isolating CNQX-sensitive responses with the application of bicuculline (10 μM), strychnine (1 μM) and D-AP5 (50 μM) while stimulating the DRG of DMOTCs. When a stable response was obtained, increasing doses of CNQX were applied (0.1, 0.3, 1, 3 and 10 μM) with washout periods in between each dose. The washout period was terminated when a test pulse produced an eEPSC response similar in amplitude to a control response obtained at the start of the experiment. The concentration-inhibition curve of eEPSCs to 0.3, 1, 3, 10 and 30 μM doses of AP5 was obtained in a similar manner to CNQX described above, except CNQX (10 μM) replaced AP5 in the initial blocking solution and evoked responses were obtained from a membrane potential of -40 mV to remove depolarization-dependent Mg^{2+}-block of NMDA receptors.

A K^+-gluconate-based internal solution was used to record spontaneous excitatory and inhibitory postsynaptic currents (sEPSCs and sIPSCs). Spontaneous currents were recorded for 3 minutes with the neuron clamped at -70 mV for sEPSCs and 0 mV for sIPSCs. Recordings were digitized at 5 kHz and filtered at 1 kHz.

3.2.3 Histology and immunohistochemistry

When possible, biocytin (0.2%) was added to the internal solution for subsequent *post-hoc* morphological analysis as described in detail in Chapter 2. Also, an immunohistochemical marker of inhibitory dorsal horn neurons was probed using procedures also outlined in Chapter 2.

All dendritic length measurements were made using Zeiss LSM 510 image browser software. The longest visible projection from the cell soma on the confocal reconstruction of the transverse plane was measured.

3.3 Results

3.3.1 Observation of living neurons under IR-DIC optics

'Healthy' neurons in DMOTC slices had a 'smooth' appearance, whereas 'unhealthy' cells typically appeared 'bloated' or had a 'wrinkled' appearance. The DMOTC slices thinned considerably from the initial ~300 μm thick slices at the start of cultures. Thus, neurons in culture could be visualized easily up to a depth of 100 μm. Stable, whole-cell recordings could be obtained from neurons in DMOTCs for up to 8 hours.

3.3.2 Populations of dorsal horn neurons

All five main populations of dorsal horn neurons, identified by their action potential firing pattern, are found in DMOTC slices (Figure 3-1A and B). The most common neuronal phenotypes were the tonic and 'delay' neurons which comprised 25% and 38% of total dorsal horn neurons recorded, respectively. The least common cell type encountered were the phasic neurons as these only comprised 6% of total dorsal horn population. There were a small group of neurons that could not be identified because recording conditions were not ideal. Action potential shape could be obscured by leaky cells and other voltage recording errors. Therefore, cells with leak currents greater than 150 pA were omitted from further study.

Although the discharge pattern of individual neurons did not change appreciably during the course of recordings, some cells can display different discharge patterns when depolarizing current was applied from different initial membrane potentials. This has been previously noted in lamina I neurons by Prescott and de Koninck (2005). Therefore, all cell identifications are based on responses to current commands from a preset membrane potential of -60mV.

Compared to dorsal horn neurons identified in acutely prepared spinal cord slices (Figure 3-1C) the proportion of each cell type was very similar to that found in DMOTC slices. In fact, there was no significant difference in the proportion of each cell type compared to acute slices (χ^2-test, $p>0.05$).

In addition to demonstrating that dorsal horn neurons in DMOTCs are similar to those found in acute slices, I also wanted to examine any alteration in their relative proportions over four weeks in culture. To test this, the proportion of each cell type recorded after 1, 2, 3, and 4 weeks in culture was calculated and plotted as a time course of development as shown in Figure 3-1D. After 3 weeks in culture, the proportions of each cell type stabilized and similar levels were found after 4 weeks in culture. There was a decline in the proportion of phasic and transient neurons as the cultures aged, and a converse increase in the percentage of 'delay' and 'irregular' neurons recorded from older DMOTCs (Figure 3-1D).

3.3.3 Morphology and immunohistochemical staining

Biocytin-filled neurons in DMOTCs exhibit a variety of different cell morphologies. Those shown in Figure 3-2A to C display the main phenotypic groups identified in DMOTCs. Although cultured slices thinned considerably and reduced the rostrocaudal spread of dendrites, the neuronal phenotypes described in acutely prepared sections of rodent dorsal horn (Balasubramanyan et al., 2006; Grudt and Perl, 2002) could still be identified in DMOTCs. Islet-central (IC) cells have thin, moderately long dendrites that mainly exit the soma in a bipolar fashion. On occasion, dendrites of IC neurons turn back towards the cell soma as observed in Figure 3-2A. The longest putative dendrite of IC neurons averaged 184.1 ± 15.6 μm (n = 14). Radial cells have the shortest dendrites which averaged 115.1 ± 12.9 μm (n = 26). Their dendrites extended in all directions and the dendritic tree tended to have a bushy appearance. Vertical cells typically have long, thick dendrites extending mainly along the dorsoventral plane. The longest dendritic process averaged 242.4 ± 19 μm (n = 7) in length. The longest putative dendrite of all three cell morphologies described differed significantly from one another (ANOVA-SNK test, $p<0.001$).

Correlating the morphology of recorded neurons with their firing pattern revealed three distinct classes of dorsal horn neurons. The tonic firing IC cells, the 'delay' firing radial cells and the 'delay' firing vertical cells were the largest correlated groups (Figure 3-2D). These groups of cells have been identified by Lu and Perl (2003 and 2005) in the dorsal horn of acute spinal cord slices. Transient firing radial cells was another well correlated group, and this may represent a group of transient firing border cells within Lamina I which have been reported (Prescott and De Koninck, 2002).

Immunohistochemical staining in DMOTCs revealed the presence of the enzyme glutamic acid decarboxylase (GAD) in over 50% of recorded cells tested (11/19 GAD-positive neurons). Colocalization of biocytin-filled cells and GAD was best observed within axonal boutons and within the cell soma (labelled as i and ii respectively in Figure 3-2E). Co-localization was confirmed using confocal z-stacks and examining orthogonal views, both top and side views, to ensure GAD-stained boutons were completely enclosed within biocytin-filled neurons (Figure 3-2F).

3.3.4 Passive membrane properties

The resting membrane potential (RMP) was taken as the voltage the cell rested at with no measurable current across the membrane. The RMP did not differ significantly across all pairs of cell types of dorsal horn neurons in DMOTCs (Table 3-1, ANOVA-SNK test, $p>0.3$). Also, similar values were found in dorsal horn neurons of acutely prepared spinal cord slices (Table 3-1, unpaired t-test, $p>0.05$).

The rheobase, or the minimum amount of current required to trigger an action potential from a neuron, was measured and there were significant differences in rheobase across different cell types of dorsal horn neurons in DMOTCs (Table 3-1). In particular, the rheobase of tonic and phasic neurons were significantly lower than 'delay', transient and 'irregular' neurons (ANOVA-SNK test, $p<0.001$ for all comparisons). Tonic neurons had the lowest rheobase of all cell types and transient neurons had the highest rheobase recorded. Interestingly, a similar pattern of rheobase values was found in acute slice preparations: tonic neurons had the lowest rheobase and transient neurons had the highest rheobase. Rheobase values were similar between cell types in acute and DMOTC slices except for 'irregular' neurons where 'irregular' neurons in DMOTCs had significantly lower rheobase values than those in acutely prepared spinal cord slices (unpaired t-test, $p<0.05$).

Input resistance (R_{input}) was taken as the inverse slope of the current-voltage (I-V) relationship for individual neurons from a voltage range of -130 to -100 mV. There were no significant differences between R_{input} values between different cell types of dorsal horn neurons in DMOTCs (Table 3-1, ANOVA-SNK test, $p>0.1$). Compared to corresponding cell types in acute slices, there was a significant difference between R_{input} values of 'delay', 'irregular' and transient cell groups (unpaired t-test, $p<0.05$ for 'irregular', $p<0.01$ for transient and $p<0.001$ for 'delay').

The I-V relationship for all five cell types in both acute slices and DMOTCs is shown in Figure 3-3. I-V curves were typically linear over a negative voltage range, -140 to -60 mV, and outward rectification was present at more positive potentials. Significant differences were found at various points along the I-V curves between neurons from DMOTCs and acute slices in all cell types (unpaired t-test, *p-values* ranged from $p<0.05$ to $p<0.001$). But in general, the membrane resistance was always lower in DMOTCs compared to acute slices.

3.3.5 Membrane excitability

As more current is injected into a neuron during current ramp stimulation, membrane excitability increases and the neuron fires more action potentials; except when accommodation occurs. Also, the time or latency for a neuron to fire the first action potential spike decreases as the current ramp rate increases (Figure 3-4, left side). This measure of membrane excitability depends on a variety of factors, including the rate of activation and inactivation of sodium channel conductance, as well as the rate of activation of various potassium conductances. It therefore provides a 'snap shot' which can be used to compare membrane excitability between different neurons or between different populations of neurons.

Similar to the pattern observed with rheobase, tonic neurons fired the first action potential spike more readily than the other cell types (Figure 3-4A); whereas transient neurons only began firing action potentials at higher ramp rates (Figure 3-4E).

Compared to neurons in acutely prepared slices, neurons in DMOTCs accommodated more easily at faster ramp rates than acute slices. Therefore, the ramp rates used to evaluate membrane excitability in DMOTCs were much lower than those applied and tolerated well by dorsal horn neurons in acute slices. However, upon comparison between neurons in both preparations, surprisingly membrane excitability did not differ appreciably between similar cell types (Figure 3-4).

3.3.6 Synaptic pharmacology

Evoked responses could be generated and measured from neurons in DMOTCs. eEPSCs generated in the presence of bicuculline (10 μM) and strychnine (1 μM) were abolished by CNQX (10 μM) plus APV (50 μM) (Figure 3-5A). A concentration-inhibition curve for eEPSCs by CNQX is shown if Figure 3-5F and a similar inhibition curve for eEPSCs and APV is shown in Figure 3-5G. Compared to dorsal horn neurons in acutely prepared slices, the average amplitude and decay time constant (τ) of eEPSCs were significantly greater in DMOTC neurons than in acute slices (Table 3-2, unpaired t-test, $p<0.001$).

GABA-mediated eIPSCs generated in the presence of CNQX, APV and strychnine (at the same concentrations listed above) could be completely blocked by bicuculline (Figure 3-5B). Also, glycinergic eIPSCs generated in the presence of CNQX, APV and bicuculline could be abolished by strychnine (Figure 3-5C). The relative glycinergic and GABAergic contribution to the generation of inhibitory responses was assessed by measuring eIPSCs in the presence of strychnine or bicuculline alone, followed by an application of both strychnine and bicuculline. Figure 3-5H illustrates the percentage contribution of GABA versus the percentage contribution of glycine to eIPSCs in each neuron studied. Pure GABAergic, pure glycinergic and mixed responses were observed. In some cells, application of strychnine or bicuculline alone produced a slight increase in eIPSC amplitude. For the purposes of Figure 3-5H, such cells were defined as purely GABAergic or purely glycinergic, respectively. This is because the response persisting in strychnine was 100% antagonized by bicuculline and vice versa. This augmentation may have reflected attenuation of presynaptic inhibitory tone or 'run up' of the response amplitude during continued recording.

The average τ for decay and amplitude of eIPSCs are reported in Table 3-2. Glycinergic eIPSCs decayed more rapidly than GABAergic responses (unpaired t-test, $p<0.001$). Decay time constants for glycinergic eIPSCs were greater in DMOTCs than in acute slices (unpaired t-test, $p<0.001$) whereas τ for GABAergic responses were the same in both preparations (unpaired t-test, $p>0.1$). The amplitude of GABAergic eIPSCs in DMOTCs was significantly larger than acute slices (unpaired t-test, $p<0.001$), but significantly smaller glycinergic eIPSCs were encountered in DMOTCs (unpaired t-test, $p<0.001$).

It has been well documented that the $GABA_B$ receptor agonist, baclofen (15-30 μM) suppresses synaptic transmission to dorsal horn neurons (Ataka et al., 2000).

Baclofen had a similar effect on neurons recorded in DMOTCs suppressing eEPSCs 78.1 ± 3.0% (Figure 3-5D, n = 5) and GABA/glycine eIPSCs 69.0 ± 6.1% (Figure 3-5E, n = 7).

3.3.7 Time-course of development

To examine further the development of inhibitory transmission in DMOTCs, I studied the pharmacology of miniature inhibitory postsynaptic currents (mIPSCs) in the presence of 1 μM TTX. mIPSCs, which may represent action-potential independent release of single vesicles of neurotransmitter (Keller et al., 2001), are exclusively GABA-mediated at birth, with the glycinergic contribution increasing with age (Baccei and Fitzgerald, 2004). If inhibitory transmission is developing normally within the cultures, I would predict that neurons in 7d cultures, which are the same age as neurons in P0 animals *in vivo*, would not display glycinergic mIPSCs and that the number of glycinergic mIPSCs would increase as cultures aged. This was the case as shown in Figure 3-5I. At 7d in culture, mIPSCs were either pure GABAergic or mixed GABA/glycine events (see Keller et al., 2001). The percentage of neurons expressing pure, glycine-mediated mIPSCs increased with more time in culture at the expense of pure GABAergic mIPSCs. Similar to eIPSCs, the time for decay of GABAergic mIPSCs (τ = 15.0 ± 0.2 ms, n = 6144 events) was significantly larger than that of glycinergic events (τ = 10.3 ± 0.3 ms, n = 4056 events, unpaired t-test, $p<0.001$).

3.3.8 Antagonist-induced bursting activity

Neurons in DMOTCs often displayed bursts of action potentials when treated with bicuculline or bicuculline plus strychnine (Figure 3-6B). These bursts lasted for 1-2 s and the inter-burst interval was 20-30 s. Under voltage-clamp mode (held at -70mV), bursts of 'giant' spontaneous excitatory postsynaptic currents (sEPSCs) were seen in 13 out of 16 neurons treated with bicuculline with or without strychnine (Figure 3-6C). These events, which were 2-5 times the amplitude of regular sEPSCs, were likely responsible for the appearance of bursts of action potentials under current-clamp. These 'giant' sEPSCs persisted even with the Na^+-channel blocker QX-314 present in the internal recording pipette, therefore excluding the possibility of unclamped action potentials generating this phenomenon. These bursts occurred at a low frequency and resembled the antagonist-induced bursts which have been described in ventral horn interneurons in organotypic culture (Ballerini et al., 1999; Ballerini and Galante, 1998).

3.3.9 Spontaneous synaptic activity

Figures 3-7A and B illustrate cumulative probability plots of sEPSC amplitude and inter-event interval, which is an inverse measure of instantaneous frequency, for all five cell types in DMOTCs. Also included in the figures are the cumulative probability plots of sEPSC measurements recorded from the same cell types in acute slices. In all cell types, sEPSCs were statistically larger in amplitude and more frequent in DMOTCs than in acute slices (KS-test, $p<0.0001$). sEPSCs represented glutamatergic signalling since application of CNQX and AP5 at concentrations shown to completely block eEPSCs

(Figure 3-5A, F and G) could completely block spontaneous synaptic activity at -70 mV (Figure 3-7C).

Spontaneous action potentials were not seen in neurons from acute spinal cord slices (Lu et al., 2006) but occurred quite frequently in cells from DMOTCs (Figure 3-7D). These action potentials were seen using normal extracellular solution and were distinct from the bursts of action potentials seen in bicuculline + strychnine (Figure 3-6B). Thus, 4/9 neurons after one week in culture, 5/14 neurons after 2 weeks, 23/33 neurons after 3 weeks, 34/41 neurons after 4 weeks, and 4/6 neurons after 5–6 weeks exhibited spontaneous action potentials.

Large, spontaneous inhibitory postsynaptic potentials (sIPSPs) were observed in current-clamp recordings, indicating active inhibitory neurons (Figure 3-7E). sIPSPs were particularly prevalent when action potentials were elicited with depolarizing current pulses (arrows in Figure 3-7E). In some cells, sIPSPs appeared time-locked with preceding action potentials (right-side records in Figure 3-7E). sIPSPs were not seen in neurons in acutely isolated slices (Lu et al., 2006). Spontaneous inhibitory postsynaptic currents (sIPSCs) could be obtained using a K^+-gluconate-based internal solution and holding the cell at 0 mV (Figure 3-7F). sIPSCs were mediated by GABA and glycine since addition of pharmacological blockers of their receptors terminated spontaneous activity at 0 mV (Figure 3-7F). Prolonged application of bicuculline and strychnine also induced large bursts of inward current, similar to what has been described previously.

3.4 Discussion

The main finding of this chapter is that the physiological characteristics of neurons in DMOTC are remarkably similar to those in acute slices. It is particularly important to note that: 1) A variety of cell morphologies are seen in the cultures (Figure 3-2A to C) and these may correspond to morphologically-defined cell types in the *in vivo* dorsal horn (Figure 3-2D); 2) All five neuron types defined electrophysiologically in acute slices are preserved in DMOTC and all cell types are seen in similar proportions in both situations (Figure 3-1B and C). There are fewer phasic cells in DMOTCs compared to acute slices (but see discussion below); 3) with a few exceptions, the RMP, rheobase, and R_{input} of the various neuron types in culture are similar to those of corresponding neuron types in acute slices (Table 3-1); 4) inhibitory transmission is present and diverse, as GABAergic, glycinergic, and mixed eIPSCs are seen in culture (Figure 3-5H). Moreover, previous developmental studies have shown that glycinergic transmission is absent at birth *in vivo* (Baccei and Fitzgerald, 2004) but develops as animals mature (Keller et al., 2001). A similar developmental sequence appears in the cultures (Figure 3-5I) and this further attests to the persistence of normal developmental processes under these conditions. Presynaptic, $GABA_B$-mediated effects of baclofen are also maintained in neurons from DMOTC slices (Figures 3-5D and E).

Although methods for preparing organotypic cultures of embryonic spinal cord (Avossa et al., 2003; Ballerini and Galante, 1998; Braschler et al., 1989; Gahwiler, 1981; Spenger et al., 1991) have been available for some time, I believe we are the first to develop a serum-free, defined-medium culture for this tissue. This system is especially useful for examining the long-term effects of growth factors such as NGF or BDNF, cytokines or neurotransmitters that may be involved in promoting chronic increases in activity in dorsal horn neurons that lead to neuropathic pain (Garraway et al., 2005; Kerr et al., 1999; Lu et al., 2004; Lu et al., 2007). The defined-medium allows us to circumvent complications imposed by the presence of serum that contains an undefined mixture of trophic substances and/or cytokines. Any findings regarding the actions of 'pain-producing' chemical mediators in culture may therefore be related to studies of the effects of nerve injury *in vivo* which are done in adult animals.

The main difference between neurons in DMOTC and those in acute slices is that spontaneous synaptic activity is increased in the cultures. Also, slow bursting activity can be induced in cultures in the presence of bicuculline with or without strychnine. The frequency and amplitude of these bursts resemble those generated by bicuculline/strychnine in ventral horn neurons in organotypic culture. Such bursts have been attributed to the synaptic network properties of the cultures rather than to altered properties of individual cultured neurons (Ballerini and Galante, 1998).

3.4.1 Neuronal phenotypes in DMOTC slices

Recent work has refined the criteria to identify neurons in the dorsal horn of the spinal cord (Grudt and Perl, 2002; Lu and Perl, 2003; Lu and Perl, 2005; Ruscheweyh and Sandkuhler, 2002). Thus, the five electrophysiologically defined neuronal phenotypes found in the *substantia gelatinosa* of acute and DMOTC slices correspond well with previous reports. Also, discrete morphological phenotypes can be found in the cultures and the cells illustrated in Figure 3-3 (A to C) are similar to the islet-central, radial and vertical cells defined in acutely prepared sections of rodent dorsal horn (Grudt and Perl, 2002; Heinke et al., 2004). Furthermore, the correlation between firing pattern and cell morphology of neurons in DMOTCs (Figure 3-2D) fits very well with what has been described previously in acute spinal cord preparations (Lu and Perl, 2003; Lu and Perl, 2005). Therefore, the same neuronal phenotypes identified within the dorsal horn are also found and comparable to the neurons in this study using DMOTCs.

If differentiation of these morphological and electrophysiological phenotypes occurs before embryonic day 13–14 (when the cultures are prepared), their persistence in DMOTC would indicate that no de-differentiation occurs. Alternatively, if morphological and electrophysiological differentiation occurs after E13-14, these processes would appear to proceed normally in culture. The progressive loss of the 'phasic' cells in DMOTCs may reflect alterations in accommodation or enhanced spontaneous activity. For example, during electrophysiological classification, spontaneous action potential generation may interfere with the accomodation of phasic cells and appear as 'irregular' cells in DMOTCs.

3.4.2 GAD as an immunochemical marker of inhibitory dorsal horn neurons

Approximately 75% of all inhibitory neurotransmission studied utilized GABA (Figure 3-5H and I); therefore, the rate-limiting enzyme in the synthesis of GABA, GAD, is a fairly good marker of inhibitory spinal neurons. Other immunochemical markers such as vGLUT2 have been used as markers of excitatory neurons (Todd et al., 2003); however, these markers are only expressed in a small subset population of all excitatory neurons. It is more practical during *post-hoc* labelling, to utilize general markers expressed in a large population of neurons, such as GAD.

Good colocalization staining of GAD and biocytin-filled neurons was found in DMOTCs (Figure 3-2E). GAD staining was present mainly as distinct punctate within cell bodies and axonal boutons. Others have found similar punctate staining in spinal cord preparations (Eaton et al., 1998; Hughes et al., 2005; Mackie et al., 2003), therefore necessitating the use of confocal stacks to confirm positive colocalization (Figure 3-2F). Immunohistochemical labelling of recorded neurons for GAD will be useful in identifying this population of dorsal horn neurons and studying the effects of BDNF on their properties.

3.4.3 Development of inhibitory synaptic transmission

Studies of developmentally regulated markers in organotypic cultures of embryonic mouse spinal cord suggest that inhibitory transmission as well as neuronal development in general proceeds similarly in DMOTC and *in vivo*. Thus, the pattern of appearance of the GABAergic marker, glutamic acid decarboxylase (GAD), and glial fibrillary acidic protein; a marker for mature astrocytes, paralleled the situation *in vivo* (Avossa et al., 2003). In agreement with this, the absence of pure glycinergic inhibition in 7d cultures (Figure 3-5I) parallels its absence in P0 *substantia gelatinosa* neurons *in vivo* (Baccei and Fitzgerald, 2004). Although there is a downward trend in the percentage of neurons exhibiting mixed GABA/glycine mIPSCs (Figure 3-5I), they were still seen in the oldest (36d) cultures. This might reflect a slight difference between DMOTC and the *in vivo* situation where mixed mIPSCs persist into adulthood, but postjunctional detection of GABA released in mixed mIPSCs ceases (Keller et al., 2001). This developmental ‘tuning of inhibitory synapses’ does not appear to occur in DMOTCs.

3.4.4 Increased synaptic activity and spontaneous excitability in DMOTCs

Thus far, I can only speculate as to the mechanisms that underlie increased spontaneous synaptic activity in DMOTC neurons. Decreased inter-event intervals for sEPSCs (Figure 3-7B) may reflect the development of increased synaptic contacts. Also, large IPSPs appear in current-clamp recordings when neurons are made to discharge by injection of depolarizing current (Figure 3-7E). These events are not seen in acute slices where only about 11% of *substantia gelatinosa* neurons interact synaptically (Lu and Perl, 2003). They may therefore reflect the enabling or growth of local synaptic circuits. The probability that altered synaptic circuitry is present in the cultures is also reflected by the ability of bicuculline and strychnine to produce bursting activity (Ballerini and Galante, 1998). Since there is spontaneous action potential generation (Figure 3-7D) in DMOTC, this could also lead to increased synaptic activity as presynaptic action potentials would generate more spontaneous postsynaptic currents.

It should also be noted that neurons in acute slices are likely subject to acute inflammatory reactions, anoxia, and acute trauma following the preparation of slices in a vibratome. On the other hand, neurons in DMOTC have had weeks to recover following the initial establishment of a culture. It has been reported that microglia reassume their inactive, ramified morphology in 9d old organotypic hippocampal cultures. This may indicate abatement of the inflammatory response at this time (Hailer et al., 1997). The simple 'health' of long-term cultured neurons may therefore be a major determinant of their increased synaptic activity and membrane responsiveness rather than any real phenotypic or developmental difference between them and neurons in acutely prepared slices.

3.4.5 Altered I-V relationship in DMOTCs

There was an increase in inward currents in the I–V plots of neurons in DMOTC compared to those in acute slices (Figure 3-3). However, this is unlikely to reflect alterations in voltage-gated channels because there was no significant change in membrane excitability between all cell types in both preparations (Figure 3-5). In addition, ionic gradients should have been the same between neurons since identical recording solutions were used. Possibly the recovery of dendrites in DMOTCs led to better preservation of dendrites compared to acutely prepared slices and this could result in an increase in membrane surface area. The membrane resistance of neurons in DMOTCs were smaller than acute slices in all cell types (Table 3-1), thus supporting this possibility. Furthermore, the neuronal cell types which had significantly lower membrane input resistances compared to acute slices, i.e. the 'delay', 'irregular' and transient cell groups, also produced the greatest differences in the I-V plots (Figure 3-3B, C and E).

3.5 Conclusions

The many processes that underlie and/or maintain differentiation of the five distinct electrophysiological phenotypes remain intact in DMOTC. Basic synaptic pharmacology and the development of glycinergic inhibition in DMOTC proceed over a similar time course to the *in vivo* situation (Baccei and Fitzgerald, 2004; Keller et al., 2001). Lastly, neuronal morphologies corresponding to the *in vivo* situation can be found in DMOTCs. Therefore, I suggest that experimental findings in these cultures may provide new insights into the changes in dorsal horn neurons induced by BDNF which may, in turn, be relevant to the process of central sensitization.

Table 3-1: Comparison of passive membrane properties of cell types in DMOTCs with those in acutely prepared slices.

Mean values indicated with SEM. Statistical significance determined with unpaired t-tests. * = $p < 0.05$, # = $p < 0.01$, § = $p < 0.001$.

a = significant difference vs. corresponding neurons in acute slices
b = significant difference vs. tonic and phasic neurons in DMOTCs
c = significant difference vs. tonic neurons in acute slices

Data from acute slices kindly provided by S. Balasubramanyan.

	RMP (mV)	Rheobase (pA)	R_{input} (MΩ)
Tonic			
DMOTC	–49.9 ± 1.2 (n = 57)	27.2 ± 1.9 (n = 63)	554 ± 47 (n = 52)
Acute slice	–51.8 ± 1.5 (n = 46)	24.8 ± 2.6 (n = 28)	573 ± 77 (n = 22)
Delay			
DMOTC	–47.7 ± 1.2 (n = 73)	66.5 ± 4.5 (n = 89)^{b§}	456 ± 51 (n = 69)^{a§}
Acute slice	–46.6 ± 1.0 (n = 61)	60.9 ± 3.3 (n = 52)^{c§}	743 ± 37 (n = 43)
Irregular			
DMOTC	–45.4 ± 2.7 (n = 49)	66.6 ± 7.0 (n = 54)$^{a*, b\S}$	369 ± 91 (n = 46)^{a*}
Acute slice	–51.0 ± 1.3 (n = 57)	49.7 ± 3.7 (n = 42)^{c§}	581 ± 50 (n = 39)
Phasic			
DMOTC	–49.5 ± 2.6 (n = 19)	36.7 ± 3.5 (n = 24)	639 ± 160 (n = 14)
Acute slice	–49.5 ± 2.8 (n = 20)	41.0 ± 6.0 (n = 12)^{c*}	757 ± 135 (n = 13)
Transient			
DMOTC	–45.3 ± 3.3 (n = 21)	68.8 ± 8.9 (n = 30)^{b§}	365 ± 54 (n = 23)
Acute slice	–49.0 ± 2.1 (n = 29)	61.2 ± 7.2 (n = 21)^{c§}	653 ± 72 (n = 23)$^{a\#}$

Table 3-2: Properties of evoked synaptic responses from neurons in DMOTC and acute slices.

Mean values indicated with SEM. Statistical significance determined with unpaired t-tests. * = $p< 0.05$, § = $p<0.001$.

a = significant difference vs. DMOTCs
b = significant difference vs. GABAergic eIPSCs

Data from acute slices kindly provided by K. Alier and S. Balasubramanyan.

	DMOTC		*Acute slices*	
	Amplitude (pA)	τ (ms)	Amplitude (pA)	τ (ms)
eEPSC	205.8 ± 34 (n = 25)^{a§}	17.0 ± 4.0 (n = 22)^{a*}	88.0 ± 6.0 (n = 14)	8.3 ± 0.5 (n = 13)
GABAergic eIPSC	243.5 ± 31 (n = 7)^{a§}	57.5 ± 11.9 (n = 7)	66.9 ± 9.6 (n = 6)	46.7 ± 4.9 (n = 6)
Glycinergic eIPSC	126.9 ± 37 (n = 10)$^{a*, b\S}$	35.6 ± 6.2 (n = 10)$^{a\S, b\S}$	171.6 ± 16.7 (n = 9)^{b§}	13.1 ± 0.8 (n = 9)^{b§}

Figure 3-1: Electrophysiologically classified populations of dorsal horn neurons.

A: Sample current-clamp recordings from neurons in DMOTC slices. Effects of depolarizing current commands and typical recordings from a ‘tonic’, ‘delay’, ‘irregular’, ‘transient’ and ‘phasic’ neuron shown. Calibration bars refer to all traces. B and C: Bar graphs to illustrate percentage of cells in each category in DMOTC (n = 260) and acute slices (n = 149). D: Time course of changes in percentage of cells recorded in DMOTC during culture. For 7d, n = 34; for 14d, n = 64; for 21d, n = 66; for 28d, n = 80.

Data from acute slices kindly provided by S. Balasubramanyan.

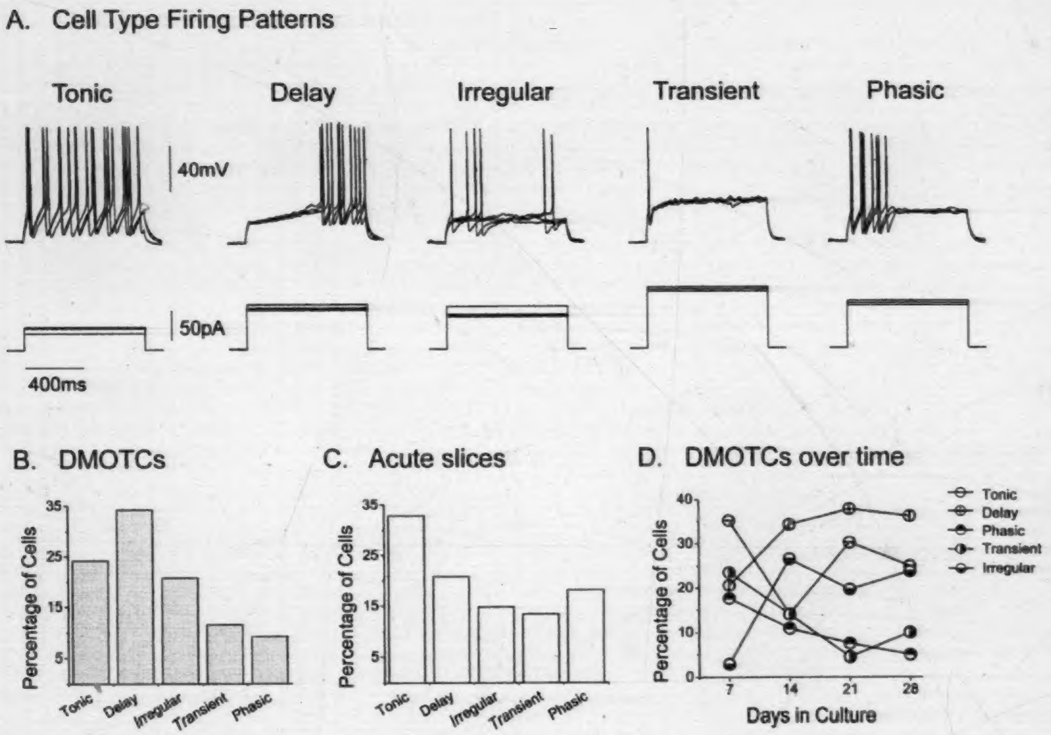
A. Cell Type Firing Patterns
Tonic
Delay
Irregular
Transient
Phasic
40mV
50pA
400ms
B. DMOTCs
C. Acute slices
D. DMOTCs over time
Percentage of Cells
35
25
15
5
Tonic
Delay
Irregular
Transient
Phasic
40
30
20
10
0
7
14
21
28
Days in Culture
Tonic
Delay
Phasic
Transient
Irregular

Figure 3-2: Morphological classification and immunohistochemical labelling of dorsal horn neurons in DMOTC slices.

A to C: Confocal images of three biocytin-filled neurons in DMOTC slices. Arrows labelled D point to dorsal surface of cultured slice. Black scale bar = 50 µm. D: Correlation of cell morphology with electrophysiological firing pattern in control DMOTC slices (n = 73). Colour coded scale bar indicating percentage of cells with the identified morphology expressing the various action potential firing patterns is shown on the right. Note the high correlation between tonic firing islet-central cells, delay firing radial cells and delay firing vertical cells. E: Staining of an islet-central cell for GAD. Top left panel shows one confocal section of the Texas-red stained biocytin-cell fill. Top right panel shows same confocal section but of the Alexa-488 GAD staining. Note GAD staining mainly present as distinct punctate. Lower left panel shows the merged image. Note good colocalization of GAD-stained punctate in an axonal bouton (labelled as i) and within the cell soma (labelled as ii). White scale bar = 20 µm. F: Orthogonal side view of GAD staining from the same neuron in (E). Same punctate labelled as i and ii in (E) shown in orthogonal profiles focused on the punctate in question. Note GAD-positive punctate completely embedded within the biocytin-filled cell indicating a GAD-positive neuron.

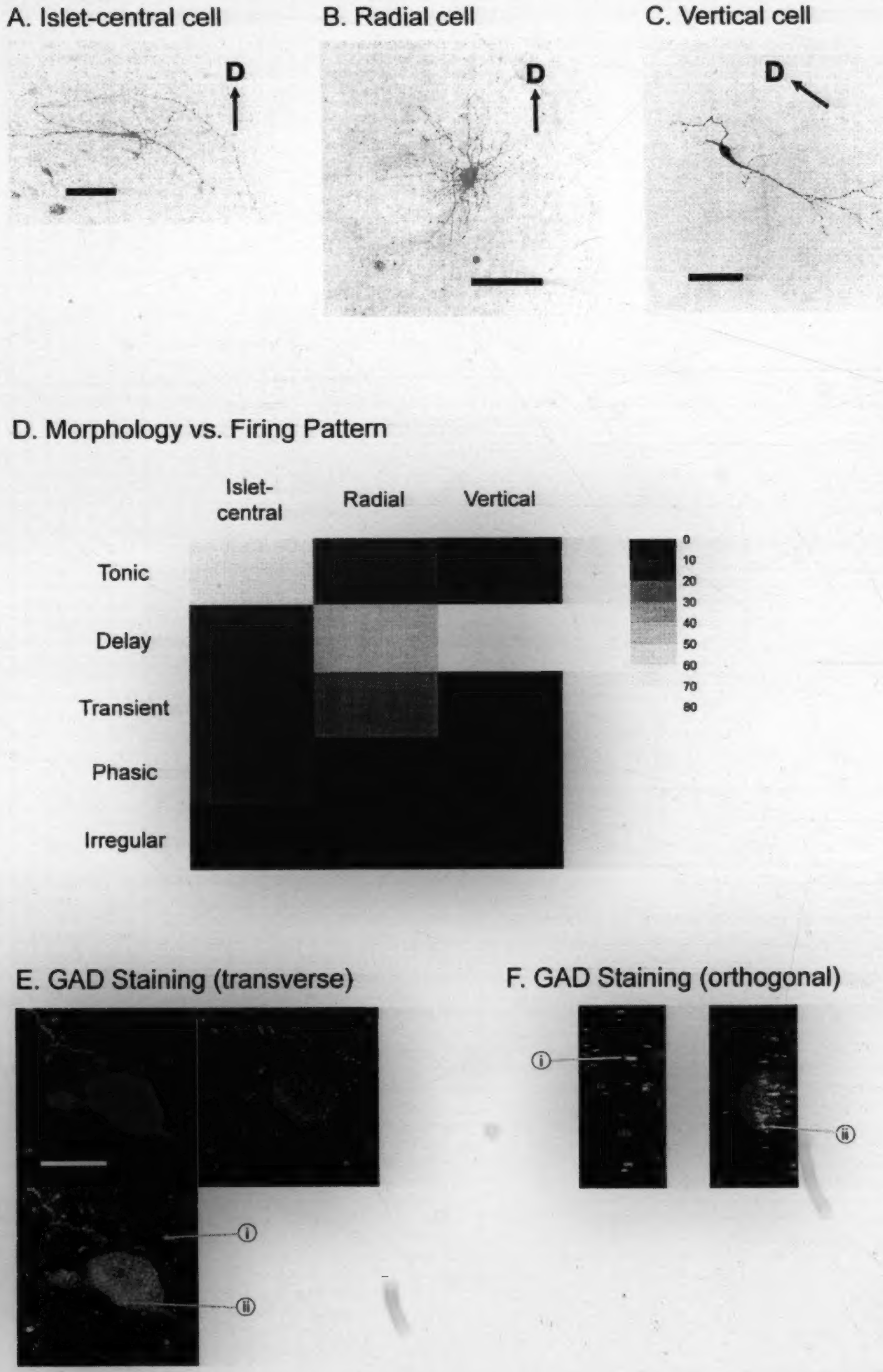
A. Islet-central cell
B. Radial cell
C. Vertical cell
D
D
D
D. Morphology vs. Firing Pattern
Islet-central
Radial
Vertical
Tonic
Delay
Transient
Phasic
Irregular
0
10
20
30
40
50
60
70
80
E. GAD Staining (transverse)
F. GAD Staining (orthogonal)
i
ii
i
ii

Figure 3-3: Current-voltage (I-V) relationship of neurons in DMOTCs compared to acutely prepared spinal cord slices.

Filled circles indicate data from neurons in DMOTC slices and open circles represent data from neurons in acutely isolated slices. For some values, error bars indicating SEM are smaller than symbols used to designate data points. Statistical significance determined with unpaired t-tests. * = $p < 0.05$, # = $p < 0.01$, § = $p < 0.001$.

Data from acute slices kindly provided by S. Balasubramanyan.

A. Tonic

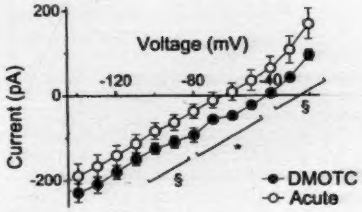

B. Delay

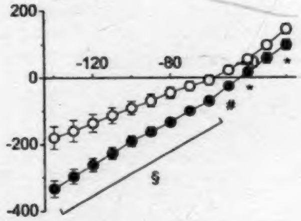

C. Irregular

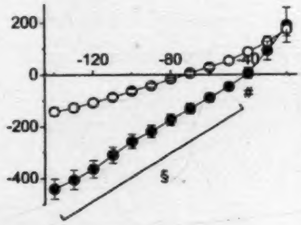

D. Phasic

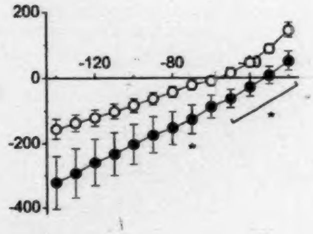

E. Transient

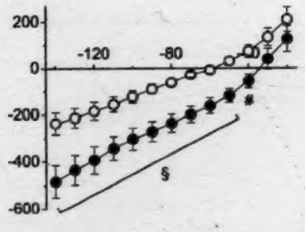

Figure 3-4: Comparison of membrane excitability of neuronal cell types in DMOTCs with acute slices.

Left panels show sample recordings of responses to current ramp protocols used for quantitative assessment of membrane excitability. * indicates first action potential spike used for measurements. Note the decrease in latency to first spike as the current ramp rate increases. A to E: Plots of latency to first spike versus current ramp rate for each cell type. Filled circles indicate data from neurons in DMOTC slices and open circles represent data from neurons in acutely isolated slices. For some values, error bars indicating SEM are smaller than symbols used to designate data points. Transient neurons in acute slices did not fire action potentials regularly at the current ramp rates tested and are therefore not shown in (E).

Data from acute slices kindly provided by S. Balasubramanyan.

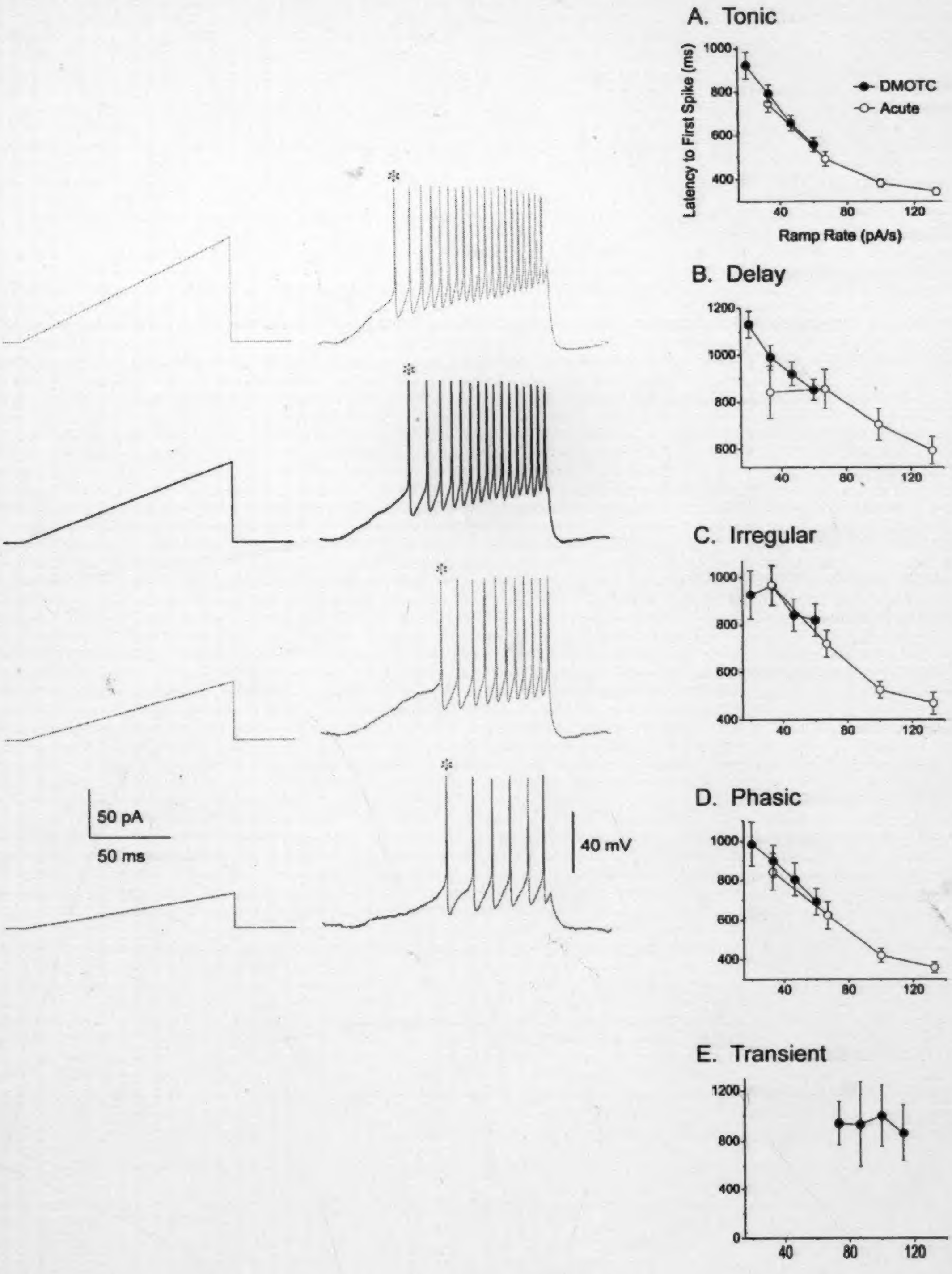A. Tonic
Latency to First Spike (ms)
1000
800
600
400
40
80
120
Ramp Rate (pA/s)
DMOTC
Acute
B. Delay
1200
1000
800
600
40
80
120
C. Irregular
1000
800
600
400
40
80
120
D. Phasic
1000
800
600
400
40
80
120
E. Transient
1200
800
400
0
40
80
120
50 pA
50 ms
40 mV

Figure 3-5: Pharmacology of synaptic responses in DMOTCs.

A: Stimulation of DRG in the presence of bicuculline (10 μM) and strychnine (1 μM) generates an AMPA and NMDA-mediated eEPSC. Current traces show sample responses before, during and after application of CNQX (10 μM) and AP5 (50 μM). V_h = -70 mV, CsCl-based internal solution. B: GABA-mediated eIPSCs generated by focal stimulation in the presence of CNQX (10 μM), AP5 (50 μM) and strychnine (1 μM). Averaged current traces of eIPSCs before, during and after application of bicuculline (10 μM). V_h = -70 mV, CsCl-based internal solution. C: Glycine-mediated eIPSCs generated by focal stimulation in the presence of CNQX (10 μM), AP5 (50 μM) and bicuculline (10 μM). Averaged current traces of eIPSCs before, during and after application of strychnine (1 μM). V_h = -70 mV, CsCl-based internal solution. D: eEPSCs generated by stimulation of DRG in the presence of bicuculline (10 μM) and strychnine (1 μM). Averaged current traces of eEPSCs before, during and after application of baclofen (15 μM). V_h = -70 mV, K^+-gluconate-based internal solution. E: GABA/glycine-mediated eIPSCs generated by focal stimulation in the presence of CNQX (10 μM) and AP5 (50 μM). Averaged current traces of eIPSCs before, during and after application of baclofen (15 μM). V_h = -40 mV, K^+-gluconate-based internal solution. F: Concentration-inhibition curve of eEPSCs to CNQX. Responses obtained in the presence of bicuculline (10 μM), strychnine (1 μM) and AP5 (50 μM). V_h = -70 mV, K^+-gluconate-based internal solution. Error bars represent SEM. (n = 4) G: Concentration-inhibition curve of eEPSCs to AP5. Responses obtained in the presence of bicuculline (10 μM), strychnine (1 μM) and CNQX (10 μM). V_h = -40 mV, K^+-gluconate-based internal solution. Error bars represent SEM. (n = 5) H: Plots of percentage contributions of GABA versus percentage contribution of glycine to eIPSCs in neurons studied in DMOTCs. I: Developmental pharmacology of mIPSCs. Percentage of cells in DMOTC exhibiting GABAergic, glycinergic and mixed mIPSCs in three time periods in culture: 7d *in vitro* (n = 9), 14d *in vitro* (n = 17), and 28d *in vitro* (n = 17). Note the absence of pure glycinergic mIPSCs at 7d *in vitro* which is equivalent to P0 *in vivo*.

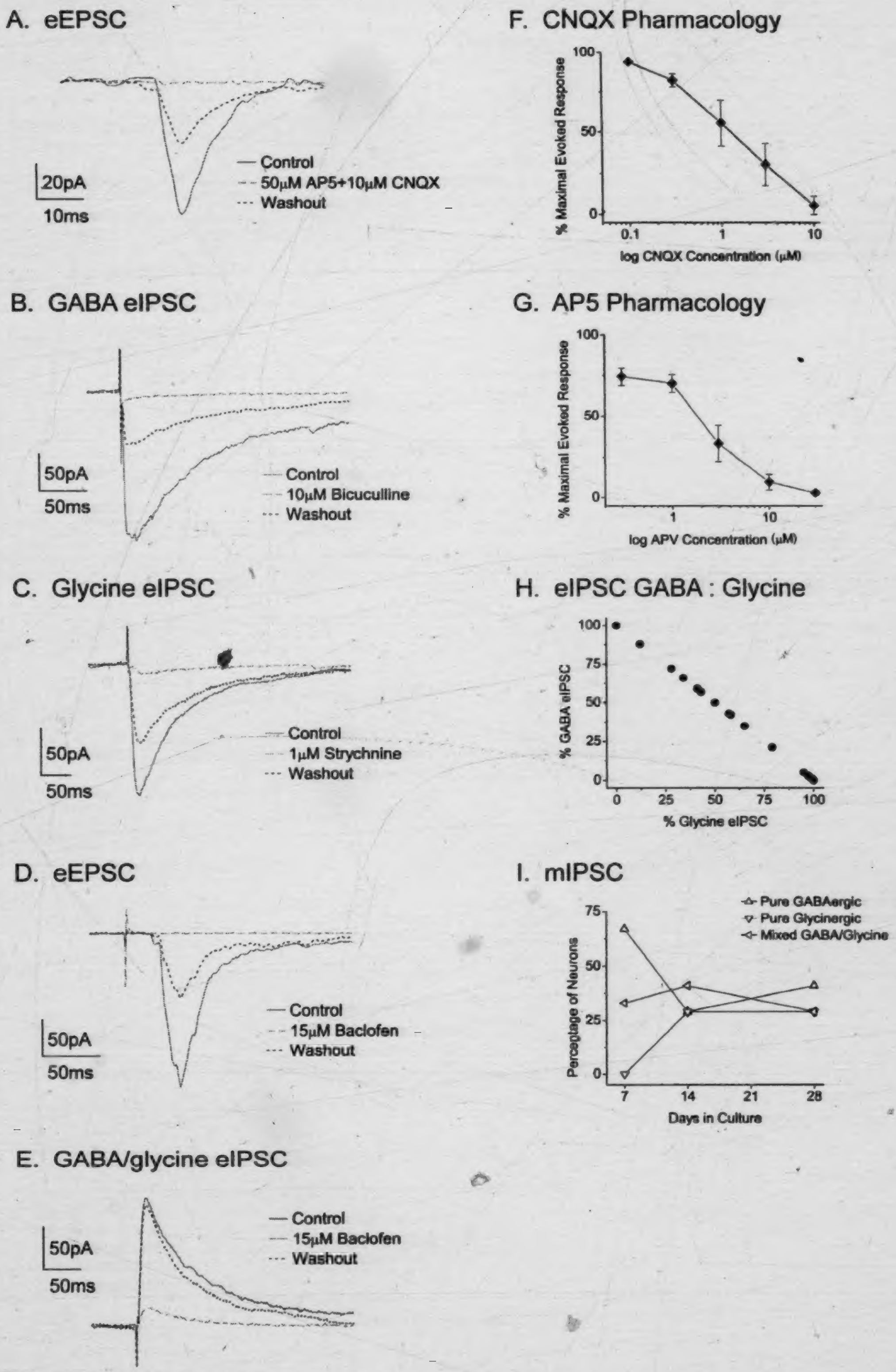
A. eEPSC
20pA
10ms
Control
50μM AP5+10μM CNQX
Washout
B. GABA eIPSC
50pA
50ms
Control
10μM Bicuculline
Washout
C. Glycine eIPSC
50pA
50ms
Control
1μM Strychnine
Washout
D. eEPSC
50pA
50ms
Control
15μM Baclofen
Washout
E. GABA/glycine eIPSC
50pA
50ms
Control
15μM Baclofen
Washout
F. CNQX Pharmacology
% Maximal Evoked Response
100
50
0
0.1
1
10
log CNQX Concentration (μM)
G. AP5 Pharmacology
% Maximal Evoked Response
100
50
0
1
10
log APV Concentration (μM)
H. eIPSC GABA : Glycine
% GABA eIPSC
100
75
50
25
0
0
25
50
75
100
% Glycine eIPSC
I. mIPSC
Pure GABAergic
Pure Glycinergic
Mixed GABA/Glycine
Percentage of Neurons
75
50
25
0
7
14
21
28
Days in Culture

Figure 3-6: Antagonist-induced bursting in DMOTCs.

A: Current-clamp recording prior to administration of bicuculline (10 µM) and strychnine (1 µM). B: Spontaneous bursts of action potentials seen in the presence of antagonists. *Below*: Action potential burst at a faster time scale. Section of current-clamp trace expanded indicated by the grey bar above. C: Long bursts of spontaneous excitatory synaptic activity seen in another neuron at -70 mV in the presence of antagonists. *Below*: 'Giant' sEPSC at a faster time scale. Section of voltage-clamp trace expanded indicated by the grey bar above.

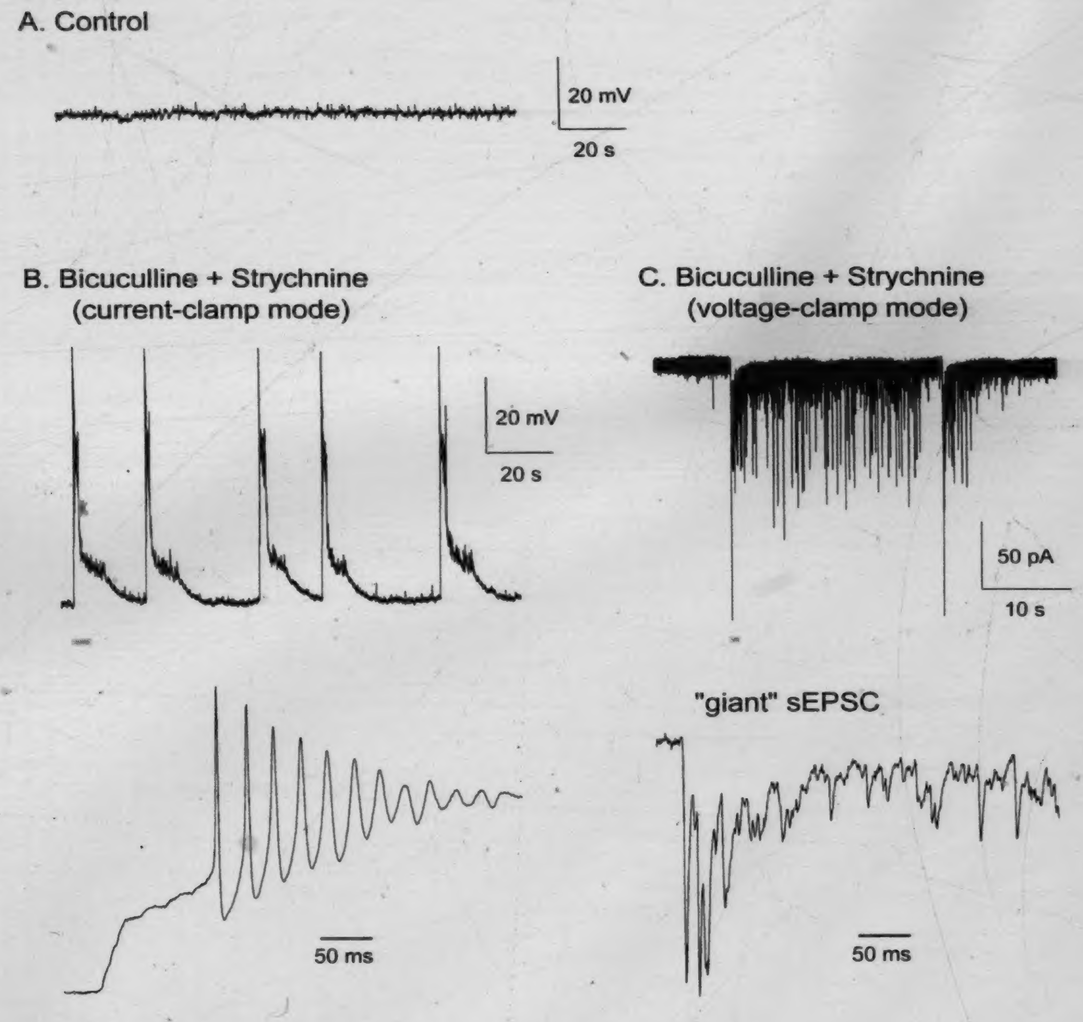
A. Control

B. Bicuculline + Strychnine (current-clamp mode)

C. Bicuculline + Strychnine (voltage-clamp mode)

"giant" sEPSC

Figure 3-7: Enhanced synaptic activity in DMOTCs compared to acute slices.

Cumulative probability plots of sEPSC amplitude (A) and inter-event intervals (B) for all five cell groups from DMOTC and acute spinal cord slices. Note sEPSC amplitude was significantly larger (KS test, $p<0.001$) and sEPSC inter-event interval was significantly smaller (KS test, $p<0.001$) in all cell types in DMOTCs compared to acute slices. C: Example of spontaneous excitatory synaptic activity. Sample 3 minute voltage-clamp recording trace of sEPSCs obtained at -70 mV with a K^+-gluconate-based internal solution. sEPSC activity is abolished following 1 min application of CNQX (10 μM) and AP5 (50 μM). D: Spontaneous action potential generation from a tonic neuron in DMOTC. Neuronal excitability was being studied by passing increasing depolarizing current pulses into the cell. The arrows indicate persistence of discharges between the current pulses. E: Sample current-clamp recordings from two neurons in DMOTC illustrating large spontaneous and action potential-related IPSPs (marked by arrows). F: Example of spontaneous inhibitory synaptic activity. Sample 3 minute voltage-clamp recording trace of sIPSCs obtained at 0 mV with a K^+-gluconate-based internal solution. sIPSC activity is abolished following application of bicuculline (10 μM) and strychnine (1 μM). Prolonged application of antagonists also induces large bursts of inward current as shown previously (Figure 3-6).

Data from acute slices in (A) and (B) kindly provided by S. Balasubramanyan.

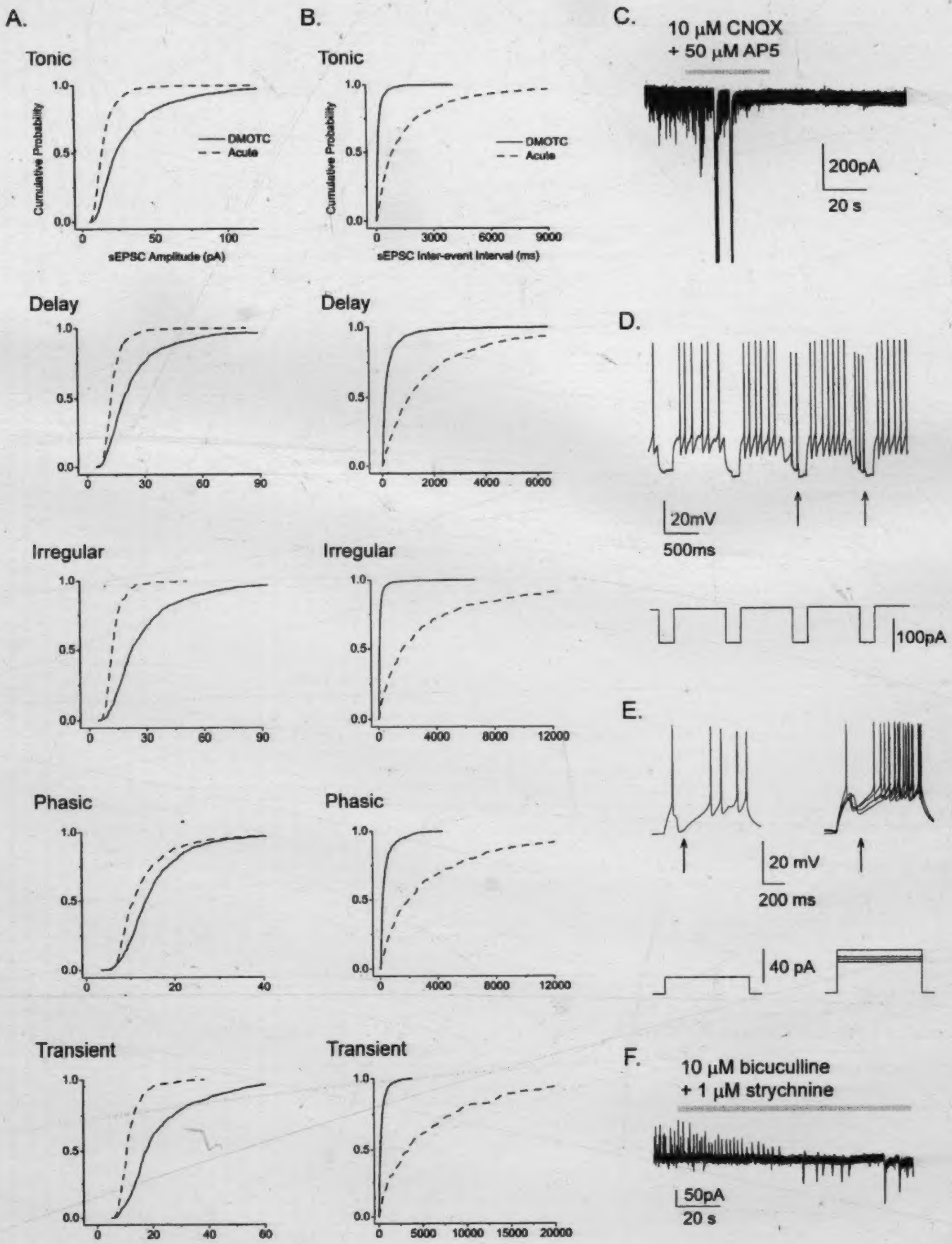
A.
Tonic
Cumulative Probability
DMOTC
Acute
sEPSC Amplitude (pA)
Delay
Irregular
Phasic
Transient
B.
Tonic
Cumulative Probability
DMOTC
Acute
sEPSC Inter-event Interval (ms)
Delay
Irregular
Phasic
Transient
C.
10 μM CNQX
+ 50 μM AP5
200pA
20 s
D.
20mV
500ms
100pA
E.
20 mV
200 ms
40 pA
F.
10 μM bicuculline
+ 1 μM strychnine
50pA
20 s

3.6 References

Ataka T, Kumamoto E, Shimoji K, Yoshimura M (2000) Baclofen inhibits more effectively C-afferent than Adelta-afferent glutamatergic transmission in substantia gelatinosa neurons of adult rat spinal cord slices. Pain 86: 273-282.

Avossa D, Rosato-Siri MD, Mazzarol F, Ballerini L (2003) Spinal circuits formation: a study of developmentally regulated markers in organotypic cultures of embryonic mouse spinal cord. Neuroscience 122: 391-405.

Baccei ML, Fitzgerald M (2004) Development of GABAergic and glycinergic transmission in the neonatal rat dorsal horn. J Neurosci 24: 4749-4757.

Balasubramanyan S, Stemkowski PL, Stebbing MJ, Smith PA (2006) Sciatic chronic constriction injury produces cell-type-specific changes in the electrophysiological properties of rat substantia gelatinosa neurons. J Neurophysiol 96: 579-590.

Ballerini L, Galante M (1998) Network bursting by organotypic spinal slice cultures in the presence of bicuculline and/or strychnine is developmentally regulated. Eur J Neurosci 10: 2871-2879.

Ballerini L, Galante M, Grandolfo M, Nistri A (1999) Generation of rhythmic patterns of activity by ventral interneurones in rat organotypic spinal slice culture. J Physiol 517 (Pt 2): 459-475.

Braschler UF, Iannone A, Spenger C, Streit J, Luscher HR (1989) A modified roller tube technique for organotypic cocultures of embryonic rat spinal cord, sensory ganglia and skeletal muscle. J Neurosci Methods 29: 121-129.

Buchs PA, Stoppini L, Muller D (1993) Structural modifications associated with synaptic development in area CA1 of rat hippocampal organotypic cultures. Brain Res Dev Brain Res 71: 81-91.

De Simoni A, Griesinger CB, Edwards FA (2003) Development of rat CA1 neurones in acute versus organotypic slices: role of experience in synaptic morphology and activity. J Physiol 550: 135-147.

Eaton MJ, Plunkett JA, Karmally S, Martinez MA, Montanez K (1998) Changes in GAD- and GABA- immunoreactivity in the spinal dorsal horn after peripheral nerve injury and promotion of recovery by lumbar transplant of immortalized serotonergic precursors. J Chem Neuroanat 16: 57-72.

Gahwiler BH (1981) Organotypic monolayer cultures of nervous tissue. J Neurosci Methods 4: 329-342.

Gahwiler BH (1984) Development of the hippocampus in vitro: cell types, synapses and receptors. Neuroscience 11: 751-760.

Gahwiler GH, Thompson SM, McKinney RA, Debanne D, Robertson RT (1998) Organotypic Slice Cultures of Neural Tissue. In: Culturing Nerve Cells (Baker G, Goslin K, eds), pp 461-497. Cambridge, Massachusetts.

Garraway SM, Anderson AJ, Mendell LM (2005) BDNF-induced facilitation of afferent-evoked responses in lamina II neurons is reduced after neonatal spinal cord contusion injury. J Neurophysiol 94: 1798-1804.

Grudt TJ, Perl ER (2002) Correlations between neuronal morphology and electrophysiological features in the rodent superficial dorsal horn. J Physiol 540: 189-207.

Hailer NP, Heppner FL, Haas D, Nitsch R (1997) Fluorescent dye prelabelled microglial cells migrate into organotypic hippocampal slice cultures and ramify. Eur J Neurosci 9: 863-866.

Heinke B, Ruscheweyh R, Forsthuber L, Wunderbaldinger G, Sandkuhler J (2004) Physiological, neurochemical and morphological properties of a subgroup of GABAergic spinal lamina II neurones identified by expression of green fluorescent protein in mice. J Physiol 560: 249-266.

Hughes DI, Mackie M, Nagy GG, Riddell JS, Maxwell DJ, Szabo G, Erdelyi F, Veress G, Szucs P, Antal M, Todd AJ (2005) P boutons in lamina IX of the rodent spinal cord express high levels of glutamic acid decarboxylase-65 and originate from cells in deep medial dorsal horn. Proc Natl Acad Sci U S A 102: 9038-9043.

Keller AF, Coull JA, Chery N, Poisbeau P, De Koninck Y (2001) Region-specific developmental specialization of GABA-glycine cosynapses in laminas I-II of the rat spinal dorsal horn. J Neurosci 21: 7871-7880.

Kerr BJ, Bradbury EJ, Bennett DL, Trivedi PM, Dassan P, French J, Shelton DB, McMahon SB, Thompson SW (1999) Brain-derived neurotrophic factor modulates nociceptive sensory inputs and NMDA-evoked responses in the rat spinal cord. J Neurosci 19: 5138-5148.

Lu VB, Balasubramanyan S, Dryden WF, Colmers WF, Smith PA (2003) Identification of different cell types in the dorsal region of organotypic embryonic spinal cord cultures. 2003 Abstract Viewer and Itinerary Planner Washington, D C : Society for Neuroscience Online.

Lu VB, Colmers W.F, Dryden W.F., Smith P.A. (2004) Brain - derived neurotrophic factor alters the synaptic activity of dorsal horn neurons in long - term organotypic spinal cord slice cultures. Program No 289,15 2004 Abstract Viewer/Itinerary Planner Washington, DC: Society for Neuroscience Online.

Lu VB, Colmers WF, Smith PA (2007) Long-term exposure to brain-derived neurotrophic factor induces specific changes in inhibitory synaptic transmission in rat dorsal horn neurons. The Canadian Journal of Neurological Sciences 34: S86.

Lu VB, Moran TD, Balasubramanyan S, Alier KA, Dryden WF, Colmers WF, Smith PA (2006) Substantia Gelatinosa neurons in defined-medium organotypic slice culture are similar to those in acute slices from young adult rats. Pain 121: 261-275.

Lu Y, Perl ER (2003) A specific inhibitory pathway between substantia gelatinosa neurons receiving direct C-fiber input. J Neurosci 23: 8752-8758.

Lu Y, Perl ER (2005) Modular organization of excitatory circuits between neurons of the spinal superficial dorsal horn (laminae I and II). J Neurosci 25: 3900-3907.

Mackie M, Hughes DI, Maxwell DJ, Tillakaratne NJ, Todd AJ (2003) Distribution and colocalisation of glutamate decarboxylase isoforms in the rat spinal cord. Neuroscience 119: 461-472.

Muller D, Buchs PA, Stoppini L (1993) Time course of synaptic development in hippocampal organotypic cultures. Brain Res Dev Brain Res 71: 93-100.

Perrier JF, Noraberg J, Simon M, Hounsgaard J (2000) Dedifferentiation of intrinsic response properties of motoneurons in organotypic cultures of the spinal cord of the adult turtle. Eur J Neurosci 12: 2397-2404.

Prescott SA, De Koninck Y (2002) Four cell types with distinctive membrane properties and morphologies in lamina I of the spinal dorsal horn of the adult rat. J Physiol 539: 817-836.

Ruscheweyh R, Sandkuhler J (2002) Lamina-specific membrane and discharge properties of rat spinal dorsal horn neurones in vitro. J Physiol 541: 231-244.

Spenger C, Braschler UF, Streit J, Luscher HR (1991) An Organotypic Spinal Cord - Dorsal Root Ganglion - Skeletal Muscle Coculture of Embryonic Rat. I. The Morphological Correlates of the Spinal Reflex Arc. Eur J Neurosci 3: 1037-1053.

Stoppini L, Buchs PA, Muller D (1991) A simple method for organotypic cultures of nervous tissue. J Neurosci Methods 37: 173-182.

Todd AJ, Hughes DI, Polgar E, Nagy GG, Mackie M, Ottersen OP, Maxwell DJ (2003) The expression of vesicular glutamate transporters VGLUT1 and VGLUT2 in neurochemically defined axonal populations in the rat spinal cord with emphasis on the dorsal horn. Eur J Neurosci 17: 13-27.

CHAPTER 4

BDNF AND NEURONAL EXCITATION:*

Neuron type-specific effects of brain-derived neurotrophic factor on excitatory synaptic transmission of dorsal horn neurons in defined medium organotypic slice cultures.

---

* A version of this chapter has been published.

4.1 Introduction

Neuropathic pain, which is characteristically chronic and frequently intractable, is a major clinical problem. It can be initiated by nerve, brain or spinal cord injury (Kim et al., 1997; Kim and Chung, 1992) or by complications associated with diseases such as post-herpetic neuralgia, stroke or diabetes (Chen and Pan, 2002).

Much of our understanding of neuropathic pain mechanisms comes from animal models in which experimentally-induced peripheral nerve damage is used to initiate behaviours analogous to the signs of human neuropathic pain. It has been shown that injury to primary afferents can give rise to a global increase in excitability of the dorsal horn (Dalal et al., 1999; Kohno et al., 2003; Laird and Bennett, 1993; Woolf, 1983). Activation of microglia has also been implicated in this process of 'central sensitization' (Hains and Waxman, 2006; Tsuda et al., 2003; Zhuang et al., 2005). Our work, using chronic constriction injury (CCI) of the sciatic nerve revealed a distinct pattern of altered synaptic drive to electrophysiologically-defined populations of neurons in the *substantia gelatinosa* of the rat dorsal horn; putative excitatory 'delay' firing neurons received more excitation whereas putative inhibitory tonic firing neurons received less (Balasubramanyan et al., 2006).

It has been postulated that substances released from damaged primary afferents and/or activated microglia (Coull et al., 2005) signal changes in the properties of dorsal horn neurons. Thus, any chemical instigator of central sensitization should affect the dorsal horn in the same way as CCI.

The neurotrophin, brain-derived neurotrophic factor (BDNF), may be one such instigator. It is found in the central nerve terminals of primary afferents fibres (Apfel et al., 1996), and neuropathic pain-related behaviours, such as allodynia, are attenuated by blocking or sequestering BDNF (Coull et al., 2005; Matayoshi et al., 2005; Zhou et al., 2000). Also, following nerve injury, the expression of BDNF and its high-affinity receptor, TrkB, are upregulated in the superficial dorsal horn (Cho et al., 1998; Dougherty et al., 2000; Fukuoka et al., 2001; Ha et al., 2001; Michael et al., 1999; Miletic and Miletic, 2002). Although elevated levels of BDNF have been shown to persist for several days following nerve injury (Cho et al., 1997; Dougherty et al., 2000; Fukuoka et al., 2001; Zhou et al., 1999), most studies examining its action on dorsal horn neurons have used acute, short-term exposures (Garraway et al., 2003; Kerr et al., 1999; Slack et al., 2004). It is yet to be determined whether long-term exposure of dorsal horn neurons to BDNF instigates the same enduring neuron type-specific changes as CCI, which would be expected if it contributes to central sensitization.

To test this, I used a defined-medium organotypic culture (DMOTC) of rat spinal cords that allowed us to expose neurons to elevated levels of BDNF for durations that would mimic the levels found during CCI *in vivo* (Lu et al., 2006). Reports of some of our findings have appeared in abstract form (Lu et al., 2004; Smith et al., 2005).

4.2 Methods

4.2.1 Defined-medium organotypic cultures (DMOTCs) of spinal cord slices

DMOTC slices were prepared as previously described (see Chapter 2: General methods). Very briefly, spinal cords were isolated from embryonic (E13-14) rat pups and transverse slices (300 ± 25 μm) were cultured using the roller-tube technique. Serum-free conditions were established after 5 days *in vitro* following the medium exchange schedule outlined in Figure 2-3A. The medium was exchanged with freshly prepared medium every 3-4 days.

Slices were treated after 15-21 days *in vitro* for a period of 5-6 days with 200 ng/ml BDNF (Alomone Laboratories, Jerusalem, Israel) in serum-free medium, or heat-inactivated BDNF as described in Chapter 2. Age-matched, untreated DMOTC slices served as controls.

4.2.2 Electrophysiology

Dorsal horn neurons in DMOTCs were viewed with a Zeiss Axioskop FS upright microscope and neurons were patched under the guidance of infrared differential interference contrast (IR-DIC) optics. Whole-cell recordings were obtained using a NPI SEC-05L amplifier (npi Electronic Gmbh, Tamm, Germany) in discontinuous current- or voltage-clamp mode. Patch pipettes were pulled from thin-walled borosilicate glass (1.5/1.12 mm OD/ID, Cat. No. TW140F-4, WPI, Sarasota, FL, USA) to 5-10 MΩ resistances and filled with a K^+ gluconate-based internal solution described in Chapter 2.

Current-voltage (I-V) relationships were determined in voltage-clamp mode using a range (-20 to -140 mV) of 800 ms voltage commands steps. "Pseudo-steady state" current was measured just prior to the termination of each voltage pulse. The input resistance (R_{input}) of each cell was calculated from the inverse slope of the I-V curve, from the voltage range of -130 to -100 mV, generated for each individual neuron.

Membrane excitability was quantified by examining action potential discharges in response to a series of 1.5 s current ramps from a preset membrane potential of -60 mV. The time to elicit the first action potential spike was measured from current ramp rates of

20, 33.3, 46.7 and 60 pA/s and plotted against ramp rates. In addition, the cumulative latencies for the first, second, third and subsequent action potentials from a current ramp of 60 pA/s were plotted. The rheobase was determined as the minimum amount of current required to initiate firing of an action potential from a membrane potential adjusted to -60 mV.

Spontaneous excitatory postsynaptic currents (sEPSCs) were recorded for 3 minutes with the neuron clamped at -70 mV. At this voltage, Cl^- mediated inhibitory events would be small outward currents generated by a 10 mV driving force from the estimated E_{Cl} of -80mV. Miniature excitatory postsynaptic currents (mEPSCs) were recorded in a similar manner but in the presence of 1 μM tetrodotoxin (TTX, Alomone Laboratories, Jerusalem, Israel) to block action potential-dependent neurotransmitter release. Blockade of action potential generation was confirmed by the cessation of action potential discharges in response to depolarizing current pulses. Also, the percentage of TTX-sensitive sEPSCs in each neuron (i.e. action potential-dependent events) was calculated from two 3 min recording periods in the absence and presence of TTX using the following equation:

$$\text{\% TTX-sensitive sEPSCs} = \frac{\text{total \# of sEPSCs} - \text{total \# of mEPSCs}}{\text{total \# of sEPSCs}}$$

Spontaneous excitatory postsynaptic potentials (sEPSPs) and action potentials were recorded at resting membrane potential in current-clamp mode. All data were acquired using Axon Instruments pCLAMP 9.0 software (Molecular Devices, Burlingame, CA, USA).

4.2.3 Data analysis, modeling and statistical testing

All data, except sEPSCs, mEPSCs and sEPSPs, were analyzed using pCLAMP 9.0 software. Excitatory synaptic events were analyzed using Mini Analysis™ software (Synaptosoft, Decatur, GA, USA). Peaks of events were first automatically detected by the software according to a set of threshold criteria, and then all detected events were visually re-examined and accepted or rejected subjectively (refer to Moran et al., 2004 for complete details). To generate cumulative probability plots for both amplitude and inter-event time interval, the same number of events (50-200 events acquired after an initial 1 min of recording) from each neuron was pooled for each neuron type, and input into the Mini Analysis program. The Kolmogorov-Smirnov two-sample statistical test (KS-test) was used to compare the distribution of events between control and BDNF-treated groups.

All graphs were plotted and fitted using Origin 7.0 (Origin Lab, Northampton, MA, USA) and statistical significance was taken as $p<0.05$. Statistical comparisons were made with unpaired t-tests or Chi-squared (χ^2) tests as specified and appropriate, using GraphPad InStat 3.05 (GraphPad Software, San Diego, CA, USA).

Rise times and decay times of individual mEPSCs were fit with a double exponential equation of the form

$$y = y0 + A*(1-\exp(-(x-x0)/\tau1))^{\wedge}P * \exp(-(x-x0)/\tau2)$$

Where y0 and x0 determine the position of the fit relative to the x and y axes, A is an amplitude term, $\tau1$ and $\tau2$ are time constants for the rise and decay of the mEPSC respectively and P is a value determining the relative importance of the two parts of the equation; this was set to 1 for all fits and simulations. Fitting was carried out by repeated iterations until the χ^2 value was unchanged for successive fits, this consistently yielded r^2 values >0.99. Manipulation of the decay time constant, $\tau2$, to assess its contribution to response amplitude (Figure 4-7H to J) was done using with a subroutine written in Microsoft Excel by Dr. Gerda de Vries (Department of Mathematics and Statistics, University of Alberta).

Analysis of mEPSC amplitude also involved redistributing event lists into 1 pA bins to produce histograms such as those illustrated in Figures 4-7E, F, and 4-8E, F. Gaussian curve fitting protocols available in Origin 7.0 were used to identify peaks within the data. Fitting was carried out by repeating iterations until the χ^2 value was not further reduced. For most experimental situations, best fits were obtained by fitting to 3 peak amplitudes as changing from 2 to 3 Gaussian fits produced large increases in χ^2 values but adding a fourth component produced very little change (see insets to Figures 4-7E and F, 4-8E and F).

4.2.4 Drugs and chemicals

Unless otherwise stated, all chemicals were from SIGMA (St. Louis, MO, USA). TTX was dissolved in distilled water as a 1 mM stock solution and stored at -20ºC until use. TTX was diluted to a final desired concentration of 1 μM in external recording solution on the day of the experiment.

4.3 Results

4.3.1 Classification of neurons in the superficial dorsal horn of the cultures

Previous studies have classified dorsal horn neurons on the basis of their action potential discharge pattern in response to depolarizing current steps from a preset membrane potential of -60 mV as tonic, 'delay', phasic, transient or 'irregular' (Balasubramanyan et al., 2006; Figure 4-1A). Because all five neuron types were also encountered in recordings made 0.5 to 2 mm from the dorsal edge of DMOTCs, this region corresponded well with the *substantia gelatinosa* of acute slices. As was seen with acute slices (Balasubramanyan et al., 2006) 'delay' and tonic cells, which are putative excitatory and inhibitory interneurons respectively, made up about 60% of the total population in the cultures (Figure 4-1B).

There was no significant change in the contribution of each neuronal cell type (χ^2 test, *p-values* ranged from 0.18 to 0.88) to the total population following BDNF treatment (Figure 4-1C, n = 142 for controls, n = 143 for BDNF).

4.3.2 No effect of BDNF on passive membrane properties

Long-term treatment of DMOTCs with BDNF did not affect resting membrane potential (RMP), input resistance (R_{input}), or rheobase of any neuronal cell type (Table 4-1, unpaired t-test, *p-values* ranged from 0.15 to 0.83 for RMP, 0.23 to 0.97 for R_{input} and 0.06 to 0.97 for rheobase). There was also no change in the I-V relationship in the -140 to -20 mV range across all neuron types with BDNF treatment (Figure 4-2).

4.3.3 Minimal effects of BDNF on active membrane properties

The threshold for membrane excitability was measured as the time to fire the first action potential spike during a series of current ramps injections. There was no significant difference observed in excitability threshold between control and BDNF-treated neurons in any cell type (Figure 4-3B, unpaired t-test, $p>0.05$).

Excitability was evaluated further by examining the firing rate in response to a 60 pA/s depolarizing current ramp. Firing rate was expressed as the cumulative latency to each action potential spike (Figure 4-3C). Under these conditions, only 'delay' neurons appeared to show a slight increase in excitability following prolonged BDNF exposure (Figure 4-3C). Although the data only attained statistical significance at the most positive excursions of the current ramps, its possible importance cannot be ignored as 'delay' neurons tended to display bursts of spontaneous action potentials following BDNF treatment (see Figure 4-9).

4.3.4 Effects of BDNF on sEPSCs

Since long-term BDNF exposure had minimal effects on various aspects of the intrinsic excitability of single dorsal horn neurons, I next examined possible changes in network excitatory synaptic transmission.

The effects of BDNF on sEPSC amplitude are illustrated in Figure 4-4A to E, and effects on inter-event interval (the reciprocal of instantaneous frequency) are illustrated in Figure 4-4F to J. As shown, BDNF reduced the amplitude and frequency of sEPSCs in tonic neurons (Figure 4-4A and F). Sample recordings illustrating BDNF's effects on sEPSCs of tonic neurons are shown in Figure 4-6D. By contrast, BDNF increased the frequency of sEPSCs in 'delay' neurons but did not affect their amplitude (Figure 4-4B and G). Sample recordings illustrating the effect of BDNF on sEPSCs of 'delay' neurons are shown in Figure 4-6E.

BDNF also increased the amplitude and frequency of sEPSCs in 'irregular' (Figure 4-4C and H), phasic (Figure 4-4D and I) and transient (Figure 4-4E and J) neurons. All changes were significant according to the Kolmogorov-Smirnoff two-sample test (KS-test, *p-values* presented in figures).

A simpler, but more rigorous, unpaired t-test of all data sets was also applied (Figure 4-4K and L). The trends of changes of sEPSC amplitude and inter-event interval identified in the KS-test were also apparent from the t-test.

Disrupting BDNF protein activity with heat-inactivation, prevented the effect of BDNF on sEPSC amplitude (Figure 4-4M) and inter-event interval (Figure 4-4N) of tonic and 'delay' neurons. The mean values from neurons treated with heat-inactivated BDNF were similar to untreated control values (unpaired t-test, $p>0.5$), except for the mean sEPSC amplitude of heat-inactivated BDNF-treated 'delay' neurons where a significant decrease was observed compared to controls and even BDNF-treated neurons (unpaired t-test, $p<0.001$).

Thus, BDNF did not produce identical changes in the synaptic excitation of all neuron groups, but rather induced neuron type-specific effects. Tonic neurons received reduced spontaneous excitatory synaptic activity and all other neuron types: 'delay', 'irregular', phasic and transient neurons, generally displayed increased synaptic activity. This pattern of BDNF-induced changes in sEPSCs across all cell types was quite similar to that produced by CCI *in vivo* (Table 4-2). The correlation was particularly clear for sEPSC frequency; CCI and BDNF increased frequency in all cell types except tonic cells where both produced a decrease.

4.3.5 Effects of BDNF on mEPSCs

Miniature excitatory postsynaptic currents (mEPSCs) represent the action potential independent release of neurotransmitter (Colomo and Erulkar, 1968). To further characterize the changes in synaptic excitation induced by BDNF, mEPSCs were recorded in the presence of 1 μM TTX and analyzed in a similar manner to sEPSC events.

The effects of BDNF on mEPSC amplitude are illustrated in Figure 4-5A- to E, and its effects on inter-event interval are illustrated in Figure 4-5F to J. Similar to its action on sEPSCs, BDNF reduced the amplitude and frequency of mEPSCs in tonic neurons (Figure 4-5A and F). Sample recordings illustrating BDNF-induced decreases in mEPSCs on tonic neurons are shown in Figure 4-6D. Conversely, long-term BDNF exposure increased the amplitude and frequency of mEPSCs in 'delay' neurons (Figure 4-5B and G). Sample recordings illustrating BDNF-induced increases in mEPSCs on 'delay' neurons are shown in Figure 4-6E.

In addition, BDNF reduced the amplitude and frequency of mEPSCs in 'irregular' neurons (Figure 4-5C and H), reduced the amplitude but increased the frequency of mEPSCs in phasic neurons (Figure 4-5D and I) and increased both the frequency and amplitude in transient neurons (Figure 4-5E and J). All changes mentioned were significant and the *p-values* from KS-tests are presented in figures. The results from unpaired t-tests on the same data sets are in agreement with the conclusions from the KS-test (Figure 4-5K and L). As was seen with sEPSCs, heat-inactivation of BDNF attenuated the changes induced by BDNF on mEPSCs (Figure 4-5M and N). Furthermore, the pattern of activity of BDNF on mEPSCs across all cell types was similar to that seen with CCI *in vivo* (Table 4-2).

4.3.6 BDNF-induced alterations in the frequency of presynaptic action potentials does not account for changes in sEPSCs of tonic and delay neurons

The sEPSC population is composed of synaptic events generated in response to presynaptic action potentials, as well as mEPSCs resulting from action potential-independent release. TTX significantly reduced the mean sEPSC amplitude (Figure 4-6A, unpaired t-test, $p<0.001$) and produced the expected increase in inter-event interval (Figure 4-6B, unpaired t-test, $p<0.001$) in all neuron types.

BDNF-induced changes in the mEPSC population (Figure 4-5) may not be solely responsible for the changes in sEPSCs (Figure 4-4). I cannot exclude the possible contribution of changes in presynaptic action potential activity. This would alter the proportion of action potential-dependent synaptic events that are removed by the addition of TTX.

The decrease in sEPSC frequency observed in tonic neurons with chronic BDNF treatment (Figure 4-4F), could not be accounted for by a decrease in action potential-dependent events as the percentage of TTX-sensitive sEPSCs was increased (Figure 4-6C, unpaired t-test, $p<0.05$). Sample recordings illustrating this effect of BDNF on relative sEPSC and mEPSC frequency are shown in Figure 4-6D.

In 'delay' neurons, an increase in action potential-dependent release is unlikely to contribute to the observed increase in sEPSC frequency (Figure 4-4G) since the percentage of TTX-sensitive sEPSCs decreased significantly with BDNF treatment (Figure 4-6C, unpaired t-test, $p<0.05$). Sample recordings illustrating this effect of BDNF on relative sEPSC and mEPSC frequency are shown in Figure 4-6E. Thus, the increased frequency of sEPSCs in 'delay' neurons (Figure 4-4G) is most likely attributed to an increase in mEPSC frequency (Figure 4-5G) and thus perhaps to changes in the release process.

In the case of 'irregular' neurons, BDNF increased the frequency of sEPSCs but decreased the frequency of their corresponding mEPSCs. Thus, an increase in the action potential-dependent events is mainly responsible for the increase in synaptic activity in these neuron cell types.

Lastly for phasic and transient neurons, there was no change in the percentage of TTX-sensitive sEPSCs with BDNF treatment (Figure 4-6C, unpaired t-test, $p>0.1$). Since mEPSC frequency increased (Figure 4-5I and J), it is possible that this, as well as an increase in action potential-dependent events, occurred in both cell types.

4.3.7 Further analysis of the mechanism of action of BDNF on tonic cells

Since tonic and 'delay' cells comprise ~60% of the neurons studied, and they likely represent inhibitory and excitatory neurons respectively, mEPSC data from these two cell types were analyzed more thoroughly.

Besides the reduction in mEPSC amplitude and frequency (Figure 4-5A and F), BDNF reduced the time constant for mEPSC decay ($\tau2$) by 35%. $\tau2 = 10.5 \pm 0.43$ ms, (n

= 1151) for control and 6.8 ± 0.28 ms (n = 631) for mEPSCs recorded after BDNF treatment (unpaired t-test, $p<0.001$). Superimposed events from a typical control tonic neuron and from another neuron from a BDNF-treated culture are shown in Figure 4-7A and B. The white traces show the averaged data from the two cells and these are compared in Figure 4-7C. The scaled averages presented in Figure 4-7D emphasize the increased rate of mEPSC decay in tonic neurons from BDNF-treated cultures.

Three populations of mEPSC amplitudes of 12.1 ± 0.28, 19.7 ± 2.22 and 35.7 ± 7.38 pA were seen in control tonic cells (Figure 4-7E). These may reflect three different populations of vesicles in presynaptic terminals, different sizes of vesicles in different types of afferents, *i.e.* various intraspinal inputs such as primary afferents or local interneurons, or different populations of terminals at different distances from the site of recording. Three populations of mEPSC amplitude were also seen in BDNF-treated neurons (Figure 4-7F) but these had smaller peak amplitudes at 7.3 ± 0.19, 10.9 ± 1.19 and 19.4 ± 2.35 pA. The insets to Figure 4-7E and F show that fitting with 3 Gaussian peaks produced the optimal reduction in χ^2 (see methods). Figure 4-7G shows a replot of the three Gaussian distributions of mEPSC amplitude from control and BDNF-treated tonic cells for comparison.

The apparent leftward shift in the three distributions raised the possibility that the reduction in time constant for mEPSC recovery contributed to the observed decrease in amplitude. To test this, I modelled three different populations of mEPSCs using two exponential equations (Figure 4-7H to J; see methods). I used the mean value of $\tau 2$ as 10.5 ms and modelled the event amplitudes to represent the three peak mEPSC amplitudes seen in control neurons (Figure 4-7E and G). I next modelled mEPSCs based on the three peak amplitudes for events in BDNF-treated neurons using the reduced mean value of 6.8 ms for $\tau 2$. Lastly, I remodelled the control events using the $\tau 2$ value of 6.8 ms from events acquired in BDNF. Since this increase in decay rate produced only slight reductions in the calculated amplitudes of peaks 1, 2 and 3, a decrease in the decay time constant $\tau 2$ for mEPSC decay cannot account for the substantially reduced peak amplitudes seen in BDNF-treated cells; other pre- or postsynaptic mechanisms must contribute to this effect.

4.3.8 Further analysis of the mechanism of action of BDNF on delay cells

Unlike tonic cells, the overall τ for recovery of mEPSC amplitude was unchanged in 'delay' cells (control $\tau = 10.73 \pm 0.55$ ms, n = 766; BDNF $\tau = 9.5 \pm 0.82$ ms, n = 1177; unpaired t-test, $p>0.2$). Superimposed events from a typical control and BDNF-treated 'delay' neuron are shown in Figure 4-8A and B. Figure 4-8C shows superimposed average data from these cells and scaled averages are presented in Figure 4-8D.

As with tonic cells, three populations of mEPSC amplitude were identified in control 'delay' cells by fitting Gaussian curves to binned histogram data. These appeared at 9.26 ± 1.51, 12.7 ± 9.0 and 19.0 ± 12.3 pA in control 'delay' cells (Figure 4-8E) and at very similar amplitudes (8.14 ± 0.24, 12.5 ± 1.38 and 20.5 ± 4.3 pA) in BDNF-treated cells (Figure 4-8F). Insets to Figure 4-8E and F show optimized χ^2 values when using 3 peaks to fit the data. Figure 4-8G is a replot of the distributions for comparison between control and BDNF-treated cells. Since overall mEPSC amplitude is increased in 'delay' cells (Figure 4-5B), I tested whether changes in the number of events contributing to each of the three distributions could explain this increase. This was done by measuring the area under the Gaussian curves in Figure 4-8G and expressing the results as percentage of the total area (Figure 4-8G inset). Surprisingly, similar proportions of the total events made up each of the three peaks under control and BDNF-treated conditions. However, further inspection of the histogram data obtained from BDNF-treated cells revealed a new population of very large events (indicated by arrow in Figure 4-8F). The appearance of this new population of large events is emphasized by the presentation of data for mEPSCs larger than 30 pA in Figure 4-8H and I. Whereas only 30 events in the control data had amplitudes larger than 30 pA, 106 events in data from BDNF-treated cells fell into this category. Although few events appear in this group, those that do, have large amplitudes. Thus, the emergence of a new group of large mEPSC amplitude events in BDNF may have a noticeable effect on overall mEPSC amplitude.

4.3.9 Alterations in synaptic activity can affect spontaneous action potential activity of dorsal horn neurons

If BDNF-induced changes in spontaneous synaptic activity are responsible for the overall increased excitability of the dorsal horn observed in neuropathic animals (Dalal et al., 1999; Laird and Bennett, 1992), one might expect to observe changes in spontaneous action potential activity in neurotrophin-treated cultures. I evaluated this possibility by counting the number of spontaneous action potentials and spontaneous excitatory postsynaptic potentials (sEPSPs) generated at resting membrane potential during recordings of neurons in control and BDNF-treated cultures.

As predicted from the sEPSC data (Figure 4-4A and F), long-term BDNF treatment significantly reduced the mean number of sEPSPs/min in tonic neurons (Figure

4-9A, unpaired t-test, $p<0.05$). More importantly however, the mean number of spontaneous action potentials generated from these sEPSPs significantly decreased following BDNF treatment (Figure 4-9B, unpaired t-test, $p<0.01$). Therefore, long-term BDNF treatment significantly reduced the spontaneous firing of tonic neurons.

There was also the anticipated significant increase in the number of sEPSPs/min in 'delay' neurons following BDNF treatment (Figure 4-9C, unpaired t-test, $p<0.05$). The mean number of spontaneous action potentials observed during the recording period also increased but did not reach statistical significance (Figure 4-9D, unpaired t-test, $p>0.1$). However, there was a change in the pattern of spontaneous action potential activity following BDNF treatment. A typical sEPSP triggering a single action potential in a control 'delay' neuron is illustrated in Figure 4-9E. However in BDNF-treated cultures, sEPSPs often produced bursts of 3-4 action potentials in 'delay' neurons (Figure 4-9F). There was a 15% increase in the number of 'delay' neurons that displayed such bursts following long-term BDNF exposure (Figure 4-9G). A low percentage of control tonic neurons displayed bursting behaviour but the percentage did not change following BDNF treatment. Therefore, long-term BDNF treatment selectively increased the spontaneous bursting activity of 'delay' neurons.

4.4 Discussion

The main findings of this chapter are that 1) BDNF produces a pattern of neuron type-specific changes that resembled those seen with CCI *in vivo*. This suggests that the actions of BDNF in DMOTCs are not a general neurotrophic effect but are instead more relevant to its putative role as a harbinger of neuropathic pain (Coull et al., 2005; Yajima et al., 2005). 2) BDNF increases excitatory synaptic drive to most neuron types except putative inhibitory tonic cells, where synaptic drive decreases. 3) Effects of BDNF on putative excitatory 'delay' cells may be exclusively presynaptic whereas both pre- and postsynaptic components are involved in its action on putative inhibitory tonic neurons (discussed below). 4) BDNF does not increase the sensitivity of 'delay' cells to glutamate (discussed below). 5) There are minimal changes to passive and active membrane properties of individual neurons following long-term BDNF exposure. However, changes in network activity gives rise to alterations in spontaneous action potential activity in DMOTC slices. 6) Abolishing BDNF protein activity with heat attenuates most of the BDNF-induced changes in sEPSCs in tonic and 'delay' neurons.

Most studies of injury-induced increases in spinal BDNF levels have relied on immunological or immunohistochemical techniques (Cho et al., 1997; Cho et al., 1998; Ha et al., 2001) and this has precluded measurements of exact neurotrophin concentration. The nature of our study dictated the use of a relatively high concentration of BDNF to assure that a robust effect would be reproducibly observed. Extensive data analysis from large numbers of neurons was required to document the actions of BDNF. Had a lower concentration been used, considerable effort may have been wasted in attempting to statistically distinguish some potentially small effects. Also, because it was not feasible to routinely maintain sterile viable cultures for more than 40 days, the age of neurons used in the BDNF experiments only approximates that of the *in vivo* neurones used in the CCI study (Figure 2-3B). Neuronal age in the *in vivo* studies is dictated by the need to use animals >20d old to produce behavioural manifestations of neuropathic pain (Balasubramanyan et al., 2006). Although there are inevitable physiological differences between age-matched *substantia gelatinosa* neurons *in vivo* and in DMOTCs, these are surprisingly minor (Chapter 3 and Lu et al., 2006). Therefore, comparison of BDNF's effects in DMOTCs with the effects induced by CCI *in vivo* is the best feasible methodology given the constraints imposed by the two experimental systems.

4.4.1 Neuronal type-specific effects of BDNF on excitatory synaptic transmission

Long-term BDNF exposure produced no changes in RMP, input resistance, rheobase and firing latency in all neuronal cell types (Table 4-1, Figures 4-2 and 4-3). An exception is the increased firing rate of 'delay' neurons (Figure 4-3C) as these tended to display bursts of action potentials in response to spontaneously occurring EPSPs (Figure 4-9D to G).

Thus, the actions of BDNF are dominated by its effects on synaptic activity (Figures 4-4 to 4-9). Spontaneous excitatory synaptic activity increased in all neuron types except tonic cells where a decrease was observed (Figure 4-4A, F, K and L). Interestingly, similar changes in excitatory synaptic activity were observed following sciatic nerve CCI (Balasubramanyan et al., 2006). Table 4-2 compares the changes seen in the five defined types of *substantia gelatinosa* neurons in CCI with those seen with long-term BDNF exposure. The degree of similarity, which is especially clear for tonic, 'delay' and transient neurons and for sEPSC frequency in all cell types, supports the role of BDNF in instigating changes in dorsal horn neurons which can lead to neuropathic pain.

It could be argued that any potentially traumatic manipulation of the cultures would produce a similar pattern of changes, so that the similarity between the actions of

CCI and BDNF is of little significance. However, in other experiments we have maintained DMOTC in the presence of interleukin-1β (IL-1β) (Lu et al., 2005). This cytokine has been implicated in various types of chronic inflammatory pain (Ledeboer et al., 2005; Watkins et al., 1995), but it is probably not responsible for the allodynia associated with neuropathic pain (Ledeboer et al., 2006). Consistent with this, we found that the pattern of changes produced by IL-1β, was quite dissimilar to that produced by BDNF and CCI (Lu et al., 2005). This underlines the significance of the similarity between the actions of BDNF and CCI which produces neuropathic pain.

4.4.2 Effect of BDNF on tonic neurons

Several lines of evidence are consistent with the possibility that tonic neurons are inhibitory. Specifically, tonic neurons often exhibit the morphology of dorsal horn islet cells (Grudt and Perl, 2002), and many islet cells express markers for GABAergic neurons (Heinke et al., 2004; Todd and McKenzie, 1989). Moreover, simultaneous paired whole-cell recordings of Lamina II neurons have revealed the generation of inhibitory postsynaptic potentials following stimulation of tonic neurons (Lu and Perl, 2003).

Our finding that BDNF reduced excitatory synaptic transmission to tonic neurons would predict decreased release of inhibitory neurotransmitters and a reduction in inhibitory tone within the dorsal horn network. Loss of inhibition has been implicated in the generation of pain-like behaviours in nerve injury models of neuropathic pain (Baba et al., 2003; Moore et al., 2002; Sivilotti and Woolf, 1994) and as shown in Table 4-2, a reduction in synaptic drive to tonic neurons also occurs following CCI (Balasubramanyan et al., 2006).

The decrease in sEPSC and mEPSC frequency of tonic neurons implicates a presynaptic site of action for BDNF. A loss of vesicular glutamate transporter 1 (VGLUT1), which has been observed following nerve injury (Alvarez et al., 2004; Oliveira et al., 2003), could account for the observed decrease in sEPSC and mEPSC frequency, but other mechanisms such as loss of presynaptic release sites may also be involved (Bailey and Ribeiro-da-Silva, 2006). Reduced sEPSC frequency is unlikely to reflect a decrease in the frequency of presynaptic action potentials because a greater percentage of TTX-sensitive spontaneous events appeared in tonic neurons after BDNF treatment (Figure 4-9C).

Since the decrease in the time constant for mEPSC decay ($\tau 2$) had little effect on event amplitude (Figure 4-7H to J), other pre- or postsynaptic mechanisms must be invoked to explain the BDNF-induced decrease in mEPSC amplitude. One possibility is increased dendritic shunting, as this would reduce the amplitude as well as increasing the rate of decay of mEPSCs. This could occur, for example, as a result of BDNF-induced increases in dendritic K^+ conductance(s).

Thus, effects of BDNF on mEPSC in tonic cells include a presynaptic component, which accounts for their decrease in frequency, a postsynaptic component which accounts for their increased rate of decay and a third component that may be either pre- or postsynaptic which accounts for much of their reduction in amplitude.

4.4.3 Effect of BDNF on delay neurons

Less than 1% of GAD-positive neurons in the *substantia gelatinosa* display a 'delay' firing pattern (Dougherty et al., 2005; Hantman et al., 2004; Heinke et al., 2004), and since simultaneous paired recordings show the production of an excitatory postsynaptic potential following stimulation of 'delay' neurons (Lu and Perl, 2005), these likely represent a population of excitatory neurons.

In contrast to tonic neurons, long-term BDNF exposure produced a significant increase in excitatory synaptic drive to 'delay' neurons. As illustrated in Table 4-2, a similar effect was seen following CCI (Balasubramanyan et al., 2006). Lu and Perl (2005) have suggested Lamina II 'delay' neurons form excitatory connections with Lamina I neurons which may include projection neurons that signal to higher pain centres. Therefore, enhanced activation of 'delay' neurons following BDNF treatment could lead to increased transmission of nociceptive information at the spinal level.

The increased frequency of sEPSCs in 'delay' neurons following BDNF treatment (Figure 4-5G) implies a presynaptic site of action. However, the proportion of TTX-sensitive sEPSC events decreased (Figure 4-6C), indicating a smaller proportion of spontaneous synaptic events were action potential-dependent. This argues against an increase in presynaptic action potential activity as a mechanism of BDNF action. Noxious stimulation induces phosphorylation of the GluR1 subunit of AMPA receptors and subsequently enhances recruitment and surface expression of functional AMPA receptors (Galan et al., 2004; Nagy et al., 2004). Interestingly, BDNF has also been shown to enhance phosphorylation of the GluR1 subunit (Wu et al., 2004), and GluR1 is strongly associated with nociceptive primary afferents and its distribution in the dorsal horn is restricted to Lamina II (Lee et al., 2002; Nagy et al., 2004). Possible recruitment of Ca^{2+}-permeable AMPA receptors presynaptically could increase intracellular Ca^{2+} levels in the terminal and thereby enhance action potential-independent glutamate release. This could explain the action of BDNF on mEPSC amplitude and frequency. If expression of GluR1 is specific to primary afferent terminals that contact 'delay' neurons, this could represent a possible mechanism by which BDNF can differentially affect one neuron type in the dorsal horn and not another.

Increased insertion of postsynaptic AMPA receptors is unlikely to occur as the mean amplitudes of the three populations of mEPSCs in 'delay' neurons were unchanged (Figure 4-8E to G) and a new population of events appeared in BDNF-treated neurons. These large events may reflect co-incident release of two or more vesicles from terminals contacting 'delay' cells. Mechanistically, this could reflect increased levels of ambient Ca^{2+} in the presynaptic terminal as described above, or perhaps BDNF-induced sprouting of presynaptic terminals such that co-incidental release of vesicles occurs more frequently.

These observations are important as they imply that BDNF treatment does not change the postsynaptic sensitivity of 'delay' cells to glutamate (Figure 4-8G). This further suggests that its actions do not invoke an LTP-type phenomenon involving the insertion of new postsynaptic AMPA receptors (Hayashi et al., 2000). Therefore, all actions of BDNF on synaptic activity in 'delay' cells are attributed to presynaptic mechanisms.

4.4.4 Effect of BDNF on irregular, phasic and transient neurons

There is currently no consensus as to the transmitter phenotype of neurons that exhibit an 'irregular', phasic or transient firing pattern. Rather, evidence has been found to support these neurons as both excitatory or inhibitory (Dougherty et al., 2005;

Hantman et al., 2004; Heinke et al., 2004). Regardless, the magnitude and frequency of spontaneous excitatory neurotransmission to all three neuron types increased significantly following BDNF treatment (Figure 4-5C to E and H to J). Because of the ambiguity of these neuronal populations, it is unclear if an increase in the excitatory drive to any of them would enhance excitation in the dorsal horn. Nevertheless, it would appear that the action potential-dependent population of synaptic events mainly contributed to the increase in synaptic events for 'irregular' neurons. There may have also been an accompanying increase in the action potential-dependent population of synaptic events with an increase in mEPSC frequency in phasic and transient neurons since there was no change in the proportion of TTX-sensitive events following BDNF treatment (Figure 4-6C). This implicates BDNF in increasing the activity of presynaptic excitatory neurons, either primary afferents or excitatory spinal interneurons such as 'delay' neurons.

Several underlying mechanisms may produce the differential actions of BDNF on the various cell types in the dorsal horn. First, as already mentioned, GluR1 receptors which are phosphorylated following BDNF exposure (Wu et al., 2004) are strongly associated with nociceptive primary afferents that terminate primarily in Lamina I and II (Lee et al., 2002; Nagy et al., 2004). This implies that BDNF may not affect terminals that do not express this receptor subunit. Second, BDNF exerts its actions both by TrkB and via the p75 neurotrophin receptor (p75^{NTR}). Whereas TrkB activation generally produces positive actions on neuronal growth and sprouting, activation of p75^{NTR} can produce deleterious effects that include apoptosis (Huang and Reichardt, 2003). Thus, in order to determine how the differential effects of BDNF on various neuronal terminals and cell bodies in the dorsal horn are generated, it will be necessary to determine which

AMPA receptor subtypes and which BDNF receptors are expressed on the afferent terminals and cell bodies of various types of electrophysiologically-defined dorsal horn neurons. Such information is not yet available.

4.4.5 BDNF-induced increase in overall dorsal horn excitability?

Long-term treatment of dorsal horn neurons to BDNF failed to produce any changes in intrinsic membrane excitability in the neuronal cell types studied (Figure 4-3B and C). This finding argues against BDNF-induced changes in voltage-gated channels which can govern action potential activity and excitability of neurons (Rose et al., 2004). Yet one of the characteristic changes observed in neuropathic animals is a long-lasting increase in dorsal horn excitability (Dalal et al., 1999; Laird and Bennett, 1992). Changes in spinal inhibitory tone have been implicated in neuropathic pain states (Baba et al., 2003; Coull et al., 2003; Moore et al., 2002; Sivilotti and Woolf, 1994), and the reduction of excitatory synaptic drive to tonic neurons following BDNF treatment (Figures 4-4A, F and 4-5A, F) suggests loss of inhibition may play a large role in dictating dorsal horn excitability. This will be the focus of the next chapter.

There were alterations in the occurrence of spontaneous action potentials and bursts (Figure 4-9B and D) which reflect the changes observed in spontaneous synaptic activity following BDNF treatment (Figure 4-4A, F, and G). However, the consequences of altered spontaneous action potential activity to overall dorsal horn excitability are not clear. These interpretations rely upon the role each electrophysiologically-classified population of neurons play in nociceptive signalling, which is still unclear. Also, the techniques used to study the properties of individual neurons limit the extrapolation of results to changes in overall dorsal horn circuitry. To assess the possible changes in overall dorsal horn excitability induced by long-term BDNF exposure, techniques which are amendable to observation of overall network activity must be considered.

4.5 Conclusions

BDNF induced significant changes in excitatory neurotransmission that reflected both pre- and postsynaptic mechanisms. The pattern of changes was specific to different neuronal populations and was not uniform across the entire dorsal horn. Moreover, the similarity between this pattern of changes and that seen in CCI are consistent with a role for BDNF in the induction of neuropathic pain.

Table 4-1: Comparison of membrane properties between control, BDNF-treated and heat-inactivated BDNF-treated DMOTC slices.

Values expressed as mean ± SEM. N values in brackets, *nd* indicates not determined because n values were too low. For unpaired t-test, * = $p<0.05$.

a = significant difference vs. irregular neurons in control slices

	RMP (mV)	R_{input} (MΩ)	Rheobase (pA)
Tonic			
Control	–50.9 ± 1.5 (40)	457.7 ± 35.5 (38)	29.3 ± 2.4 (40)
BDNF	–51.4 ± 1.6 (33)	422.6 ± 45.8 (33)	32.5 ± 3.7 (34)
Heat-inact BDNF	–59.2 ± 5.4 (6)	532.9 ± 125.4 (6)	36.7 ± 7.6 (6)
Delay			
Control	–48.0 ± 1.6 (46)	329.8 ± 27.1 (45)	76.3 ± 5.7 (54)
BDNF	–51.1 ± 1.4 (48)	361.5 ± 32.4 (52)	76.6 ± 7.6 (52)
Heat-inact BDNF	–52.0 ± 2.1 (15)	414.5 ± 82.4 (14)	63.7 ± 11.9 (14)
Irregular			
Control	–47.7 ± 1.9 (31)	270.0 ± 45.1 (31)	73.9 ± 8.9 (33)
BDNF	–46.9 ± 2.5 (25)	334.7 ± 30.1 (25)	53.7 ± 5.8 (26)
Heat-inact BDNF	–42.3 ± 1.5 (3)[a]*	289.4 ± 84.1 (3)	100.0 ± 25.7 (3)
Phasic			
Control	–47.1 ± 5.5 (8)	409.4 ± 98.5 (8)	44.1 ± 5.9 (9)
BDNF	–49.9 ± 2.9 (8)	391.7 ± 68.3 (10)	48.0 ± 5.5 (10)
Heat-inact BDNF	*nd*	*nd*	*nd*
Transient			
Control	–47.7 ± 5.5 (8)	277.9 ± 71.8 (11)	98.2 ± 17.1 (11)
BDNF	–52.8 ± 2.9 (18)	275.1 ± 38.5 (19)	95.9 ± 9.2 (22)
Heat-inact BDNF	–48.3 ± 7.3 (3)	324.5 ± 134.2 (3)	111.7 ± 15.9 (3)

Table 4-2: Summary of comparison between sEPSCs and mEPSCs following chronic constriction nerve injury (CCI) and long-term BDNF exposure.

Data for changes induced by CCI from *Balasubramanyan et al., 2006*. Table Legend: ↑ indicates a significant increase compared to control; ↓ indicates a significant decrease compared to control; ↔ indicates no change compared to control and *nd* indicates not determined because n values were too low.

Data from acute slices kindly provided by S. Balasubramanyan.

	Tonic	Delay	Irregular	Phasic	Transient
sEPSC amplitude					
CCI	↓	↑	↑	↓	↑
BDNF	↓	↔	↑	↑	↑
sEPSC frequency					
CCI	↓	↑	↑	↑	↑
BDNF	↓	↑	↑	↑	↑
mEPSC amplitude					
CCI	↓	↑	↑	*nd*	↑
BDNF	↓	↑	↓	↓	↑
mEPSC frequency					
CCI	↓	↑	↔	*nd*	↑
BDNF	↓	↑	↓	↑	↑

Figure 4-1: No changes in the proportion of each characterized neuronal cell type within the dorsal horn following BDNF treatment.

A: Sample current-clamp recordings displaying different discharge firing patterns used to classify neurons within the dorsal horn. Three different recording traces at different current intensities are overlapped for each cell type. Membrane potential was set to -60 mV prior to injection of current pulses. Refer to text for details of characteristic features of each cell type. Calibration bars apply to all traces. B and C: Bar graphs showing percentage of each neuronal cell type identified in recordings from control DMOTC slices (blue bars, n = 142) and BDNF-treated DMOTC slices (orange bars, n = 143). There were no significant differences between percentage of cells in control and BDNF-treated DMOTCs of any neuronal cell type group (χ^2 test, $p>0.15$ for all comparisons).

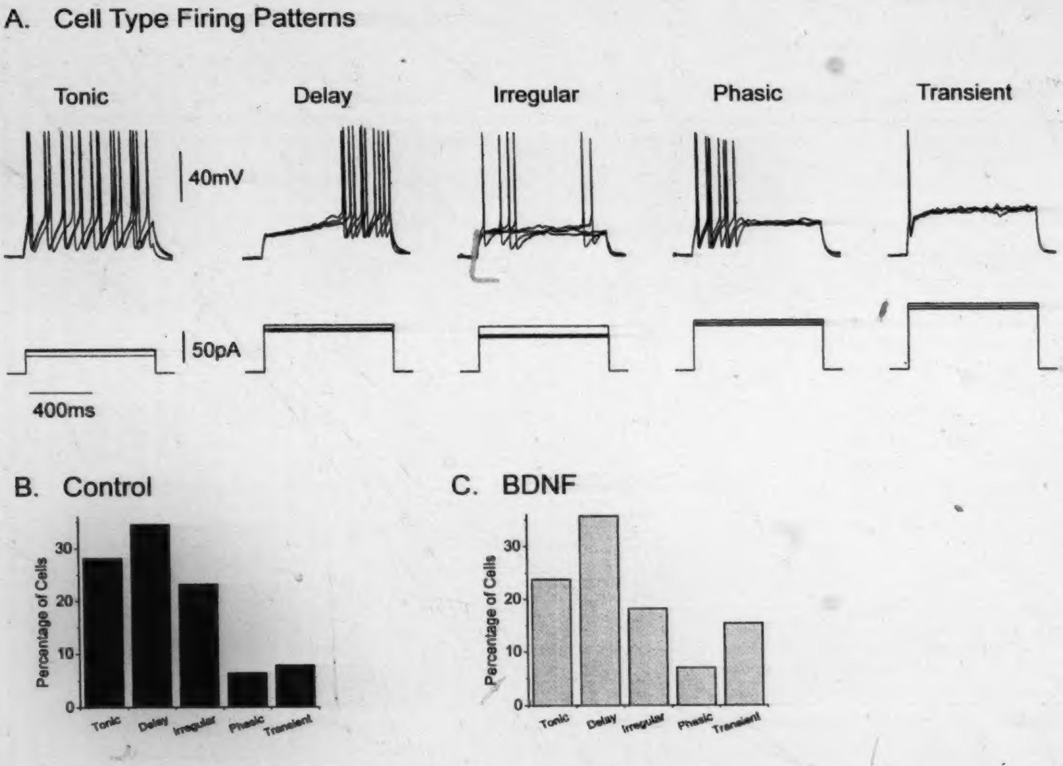

A. Cell Type Firing Patterns

B. Control

C. BDNF

Figure 4-2: Current-voltage (I-V) relationship of neurons in control slices compared to BDNF-treated slices.

Open blue circles indicate data from neurons in control DMOTC slices and filled orange circles represent data from neurons in BDNF-treated DMOTC slices. A: Tonic neurons, n = 35 for controls, n = 33 for BDNF-treated group. B: Delay neurons, n = 45 for controls, n = 51 for BDNF-treated group. C: Irregular neurons, n = 27 for controls, n = 26 for BDNF-treated group. D: Phasic neurons, n = 7 for controls, n = 10 for BDNF-treated group. E: Transient neurons, n = 10 for controls, n = 19 for BDNF-treated group. For some values, error bars indicating SEM are smaller than symbols used to designate data points. No statistical difference was observed along any points in the current-voltage relationship between control and BDNF-treated neurons (unpaired t-test, *p>0.2* for all comparisons).

A. Tonic

B. Delay

C. Irregular

D. Phasic

E. Transient

Figure 4-3: Minimal effects of BDNF membrane excitability.

Membrane excitability was measured as the cumulative latency of action potential discharges in response to depolarizing current ramps from -60 mV. A: Lower panels show one current ramp, a 60 pA/s current ramp injection for 1.5 s, used to test the excitability of neurons in DMOTC. Top panels show sample voltage records of a typical response of tonic, delay, irregular, phasic and transient cells. With the exception of transient cells, all cell types discharged ≥3 spikes in response to the current ramp. B: Plots of latency to first action potential spike for each cell type. Open blue circles denote controls and filled orange circles denote BDNF-treated DMOTCs. In some cases, error bars indicating SEM are smaller than the symbols used to plot the data. C: Plots of cumulative latency against spike number for each cell type. Not all cells produced the same number of action potential spikes during ramps. For example, of the 27 tonic cells examined only 5 of them fired 15 action potentials. The mean cumulative latencies for each spike number therefore have different sample sizes. For tonic cells (n = 5-27 for controls, n = 11-22 for BDNF). For delay cells (n = 6-27 for controls, n = 10-32 for BDNF). For irregular cells (n = 5-18 for controls, n = 5-19 for BDNF). For phasic cells (n = 5-7 for controls, n = 5-9 for BDNF). For transient cells (n = 3 for controls, n = 4 for BDNF). The only increase in excitability after BDNF treatment was observed in delay cells (unpaired t-test, * = $p<0.05$).

A. Sample Traces

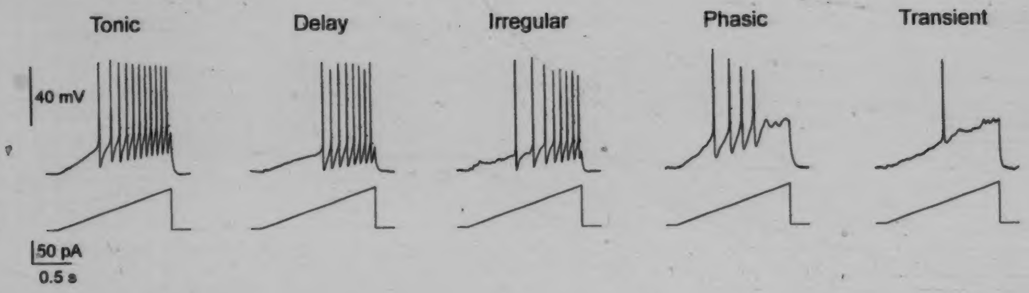

B. Latency to First Action Potential Spike

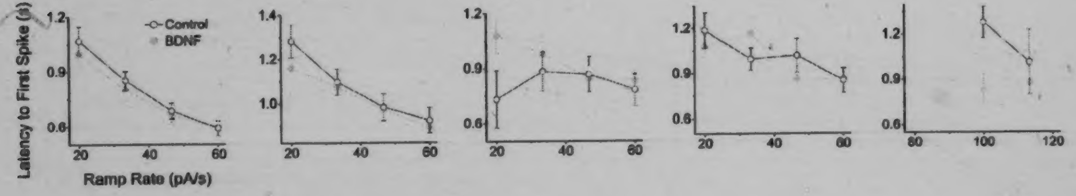

C. Cumulative Latency of Spikes at 60pA/s

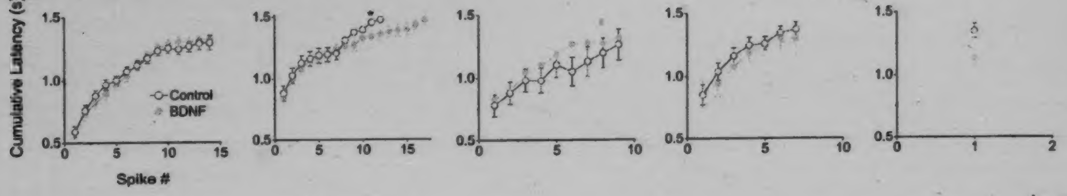

Figure 4-4: Effects of BDNF on amplitude and inter-event interval of spontaneous excitatory postsynaptic currents (sEPSCs).

A to E: Cumulative probability plots for sEPSC amplitude. The first 50 events following the 1st minute of recordings from each cell were pooled in order to construct cumulative distribution plots, except for phasic and transient cells where the first 200 or 100 events following the 1st minute of recording were taken, respectively. A: Tonic cells; 1450 events from control DMOTC slices, 1950 events from BDNF-treated DMOTC slices. B: Delay cells; 1900 events for controls, 1100 events for BDNF. C: Irregular cells; 1350 events for controls, 1100 events for BDNF. D: Phasic cells; 1356 events for controls, 1670 events for BDNF. E: Transient cells; 800 events for controls, 800 events for BDNF. An equal number of BDNF-treated transient cells as controls were chosen at random to analyze sEPSC events. *P values* derived from the KS test indicated on graphs. F to J: Cumulative probability plots for sEPSC inter-event interval (IEI). *P values* derived from the KS test indicated on graphs. K and L: Effects of BDNF on mean amplitude (K) and IEI (L) of sEPSC events. The same events used to construct cumulative probability plots were used, so the same n values apply. M and N: Comparison of the mean amplitude (M) and mean inter-event interval (N) of sEPSC events to heat-inactivated BDNF controls. The same mean values for control and BDNF-treated tonic and delay cells in (K) and (L) are shown. For tonic cells treated with heat-inactivated BDNF, 300 events were averaged; for delay cells treated with heat-inactivated BDNF, 700 events were averaged. Error bars indicate SEM. For Student's unpaired t-test, * = $p<0.05$, § = $p< 0.001$.

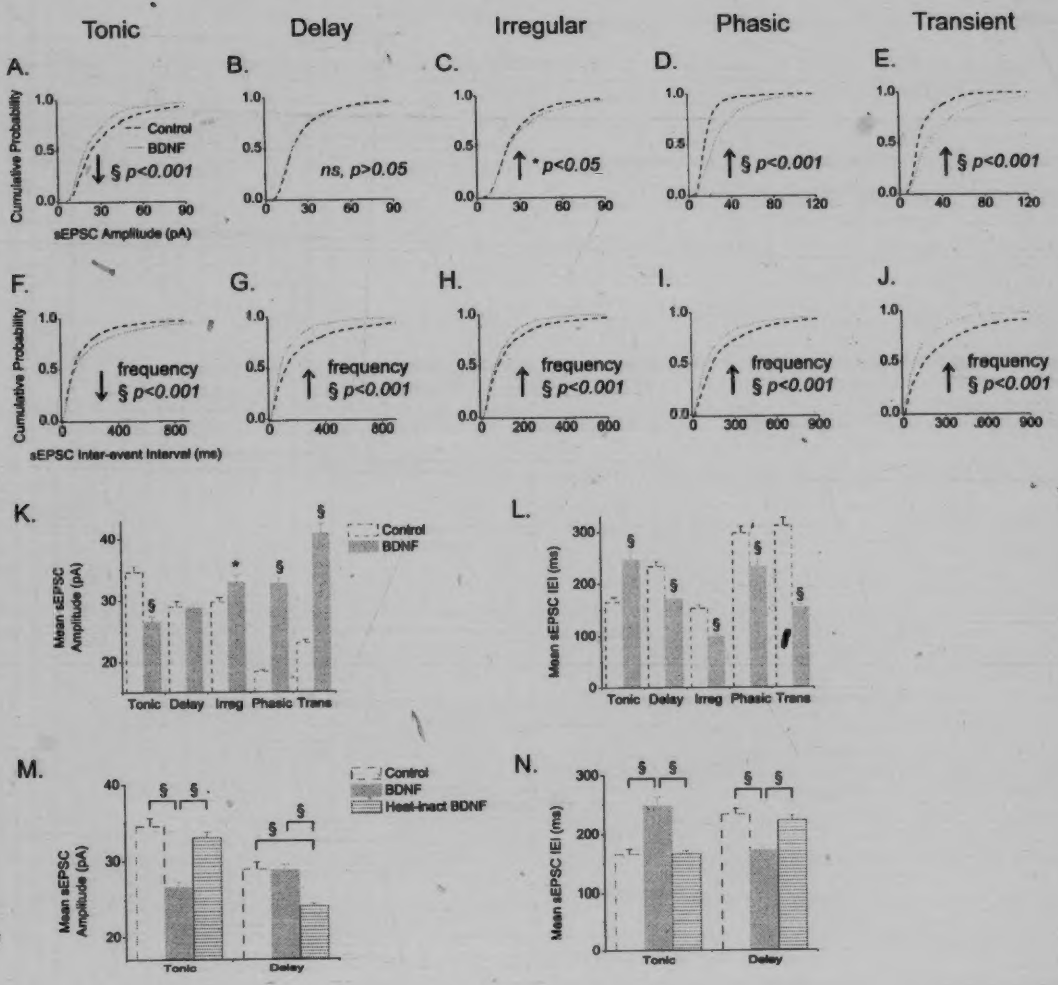
Tonic
Delay
Irregular
Phasic
Transient
A.
B.
C.
D.
E.
Cumulative Probability
sEPSC Amplitude (pA)
Control
BDNF
↓ § p<0.001
ns, p>0.05
↑ * p<0.05
↑ § p<0.001
↑ § p<0.001
F.
G.
H.
I.
J.
sEPSC Inter-event Interval (ms)
↓ frequency § p<0.001
↑ frequency § p<0.001
↑ frequency § p<0.001
↑ frequency § p<0.001
↑ frequency § p<0.001
K.
Mean sEPSC Amplitude (pA)
Tonic Delay Irreg Phasic Trans
L.
Mean sEPSC IEI (ms)
Tonic Delay Irreg Phasic Trans
M.
Control
BDNF
Heat-inact BDNF
Tonic
Delay
N.
Mean sEPSC IEI (ms)
Tonic
Delay

Figure 4-5: Effects of BDNF on amplitude and inter-event interval of miniature excitatory postsynaptic currents (mEPSCs).

A to E: Cumulative probability plots for mEPSC amplitude. The first 50 events following the 1st minute of recordings from each cell were pooled in order to construct cumulative distribution plots. A: Tonic cells; 1100 events from control DMOTC slices, 877 events from BDNF-treated DMOTC slices. B: Delay cells; 1074 events for controls, 1554 events for BDNF. C: Irregular cells; 700 events for controls, 800 events for BDNF. D: Phasic cells; 303 events for controls, 300 events for BDNF. E: Transient cells; 300 events for controls, 300 events for BDNF. An equal number of BDNF-treated transient cells as controls were chosen at random to analyze mEPSC events. *P values* derived from the KS test indicated on graphs. F to J: Cumulative probability plots for mEPSC inter-event interval (IEI). *P values* derived from the KS test indicated on graphs. K and L: Effects of BDNF on mean amplitude (K) and IEI (L) of mEPSC events. The same events used to construct cumulative probability plots were used, so the same n values apply. M and N: Comparison of the mean amplitude (M) and mean inter-event interval (N) of mEPSC events to heat-inactivated BDNF controls. The same mean values for control and BDNF-treated tonic and delay cells in (K) and (L) are shown. For tonic cells treated with heat-inactivated BDNF, 300 events were averaged; for delay cells treated with heat-inactivated BDNF, 700 events were averaged. Error bars indicate SEM. For Student's unpaired t-test, * = $p<0.05$, § = $p< 0.001$.

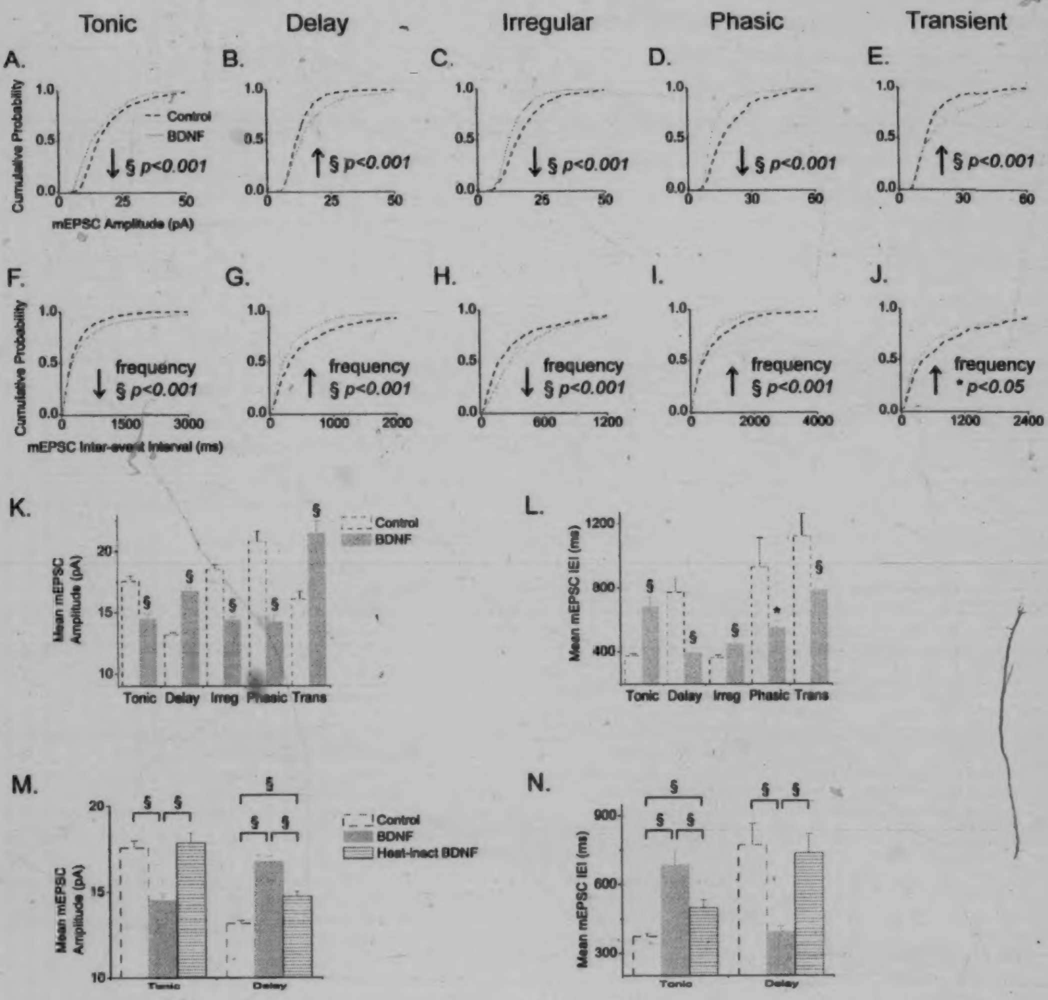
Tonic
Delay
Irregular
Phasic
Transient
A.
B.
C.
D.
E.
Cumulative Probability
mEPSC Amplitude (pA)
Control
BDNF
↓ § p<0.001
↑ § p<0.001
↓ § p<0.001
↓ § p<0.001
↑ § p<0.001
F.
G.
H.
I.
J.
mEPSC Inter-event Interval (ms)
↓ frequency § p<0.001
↑ frequency § p<0.001
↓ frequency § p<0.001
↑ frequency § p<0.001
↑ frequency * p<0.05
K.
Mean mEPSC Amplitude (pA)
Tonic
Delay
Irreg
Phasic
Trans
L.
Mean mEPSC IEI (ms)
M.
Control
BDNF
Heat-inact BDNF
N.

Figure 4-6: Effects of BDNF on the action potential-dependent (TTX-sensitive) sEPSC population.

A and B: Comparison of sEPSCs to mEPSCs for controls. Comparison of mean amplitudes (A) and mean inter-event intervals, IEI, (B) are shown. Cross-hatched bars indicate values for sEPSCs and vertical lined bars indicate values for mEPSCs. C: The percentage of TTX-sensitive sEPSCs was calculated as the number of mEPSCs subtracted from the total number of sEPSCs over the total sEPSCs for each cell. The mean percentages are shown for controls, blue dashed bars, and the BDNF-treated group, orange bars. Error bars indicate SEM. For Student's unpaired t-test, * = $p<0.05$, § = $p<0.001$. D and E: Sample recording traces from tonic (D) and delay (E) cells under control and long-term BDNF exposure conditions. Sample mEPSC recording traces were from the same cell represented in the above sample sEPSC recording trace.

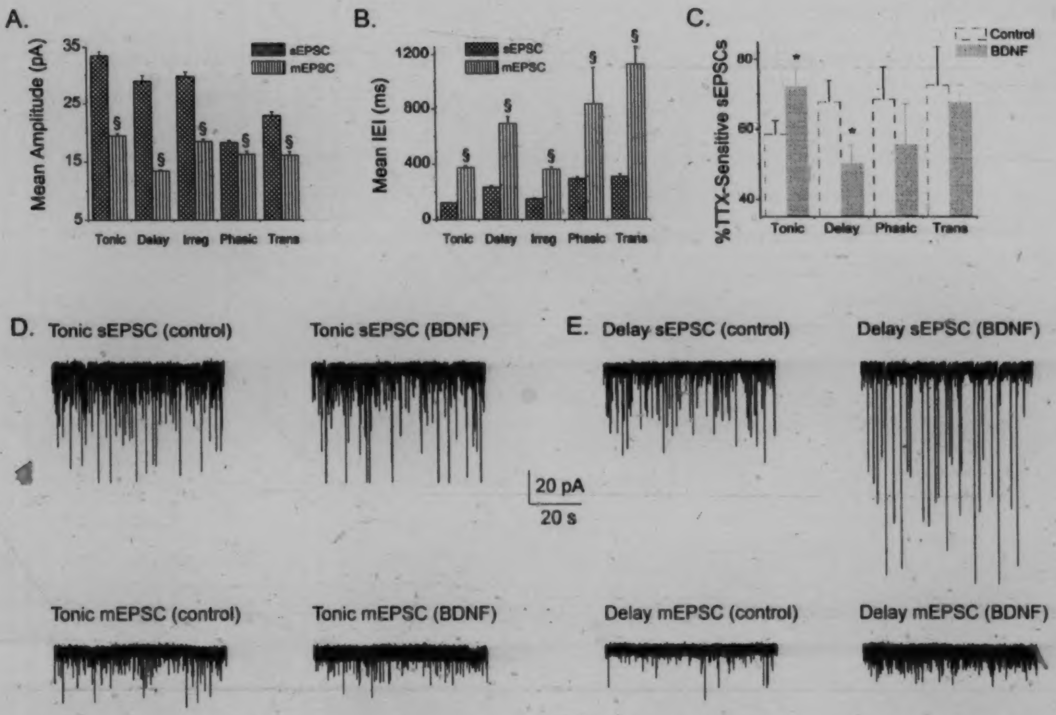
A.
Mean Amplitude (pA)
35
25
15
5
sEPSC
mEPSC
§
Tonic
Delay
Irreg
Phasic
Trans
B.
Mean IEI (ms)
1200
800
400
0
sEPSC
mEPSC
§
Tonic
Delay
Irreg
Phasic
Trans
C.
%TTX-Sensitive sEPSCs
80
60
40
Control
BDNF
*
Tonic
Delay
Phasic
Trans
D.
Tonic sEPSC (control)
Tonic sEPSC (BDNF)
E.
Delay sEPSC (control)
Delay sEPSC (BDNF)
20 pA
20 s
Tonic mEPSC (control)
Tonic mEPSC (BDNF)
Delay mEPSC (control)
Delay mEPSC (BDNF)

Figure 4-7: Analysis of the effects of BDNF on mEPSCs of tonic neurons.

A: Superimposed recordings of 3 min of mEPSC activity in a control tonic neuron, average of events presented as superimposed white trace. B: Similar superimposed recordings from a tonic neuron in a BDNF-treated culture. C: Averaged events from the neurons illustrated in (A) and (B). D: Averaged events normalized to control size. Note marked increased rate of decay of current. E: Distribution histogram (1 pA bins) for amplitudes of 1100 mEPSCs from control tonic neurons. Fit of the data to three Gaussian distributions represented by blue dashed lines. F: Similar histogram and fit to three Gaussian functions for 877 mEPSCs from BDNF-treated neurons: *Insets* in E and F: Graphs to show effect of number of Gaussian fits (peaks) on the value of χ^2 divided by the number of degrees of freedom. G: Superimposition of the three Gaussian peaks obtained in (E) with those obtained in (F). H to J: Modelled mEPSCs to represent the three peak Gaussian amplitudes obtained in (E) and (F). Dashed blue lines are for control events (from E), orange lines are for events in BDNF (from F) and dotted lines illustrate effect of a 35% reduction of $\tau 2$ on the control events.

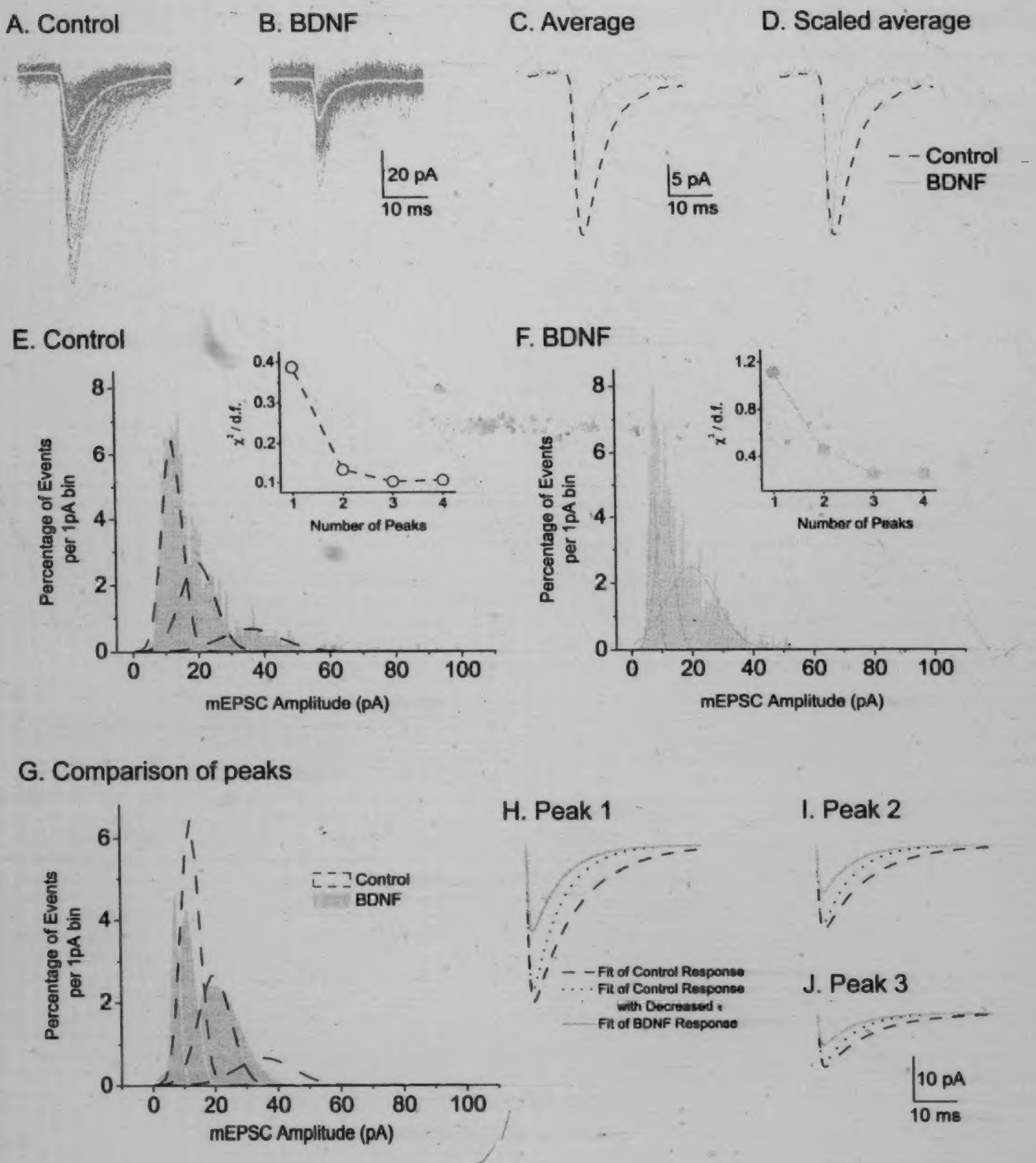
A. Control
B. BDNF
C. Average
D. Scaled average
20 pA
10 ms
5 pA
10 ms
Control
BDNF
E. Control
F. BDNF
Percentage of Events per 1pA bin
mEPSC Amplitude (pA)
χ² / d.f.
Number of Peaks
G. Comparison of peaks
Control
BDNF
H. Peak 1
I. Peak 2
J. Peak 3
Fit of Control Response
Fit of Control Response with Decreased ε
Fit of BDNF Response
10 pA
10 ms

Figure 4-8: Analysis of the effects of BDNF on mEPSCs of delay neurons.

A: Superimposed recordings of 3 min of mEPSC activity in a control delay neuron, average of events presented as superimposed white trace. B: Similar superimposed recordings from a delay neuron in a BDNF-treated culture. C: Averaged events from the neurons illustrated in (A) and (B). D: Averaged events normalized to control size. Note no change in the rate of decay of current. E: Distribution histogram (1 pA bins) for amplitudes of 1074 mEPSCs from control delay neurons. Fit of the data to three Gaussian distributions represented by blue dashed lines. F: Similar histogram and fit to three Gaussian functions for 1554 mEPSCs from BDNF-treated neurons, arrow points out small number of very large events that appear in BDNF: *Insets in* E and F: Graphs to show effect of number of Gaussian fits (peaks) on the value of χ^2 divided by the number of degrees of freedom. G: Superimposition of the three Gaussian peaks obtained in (E) with those obtained in (F). *Inset*: Comparison of area under curves for the three peaks (normalized to total area under peaks). H: Data for control and BDNF mEPSCs >30 pA replotted and compared on the same axes. *Inset*: Number of mEPSC events larger than 30 pA.

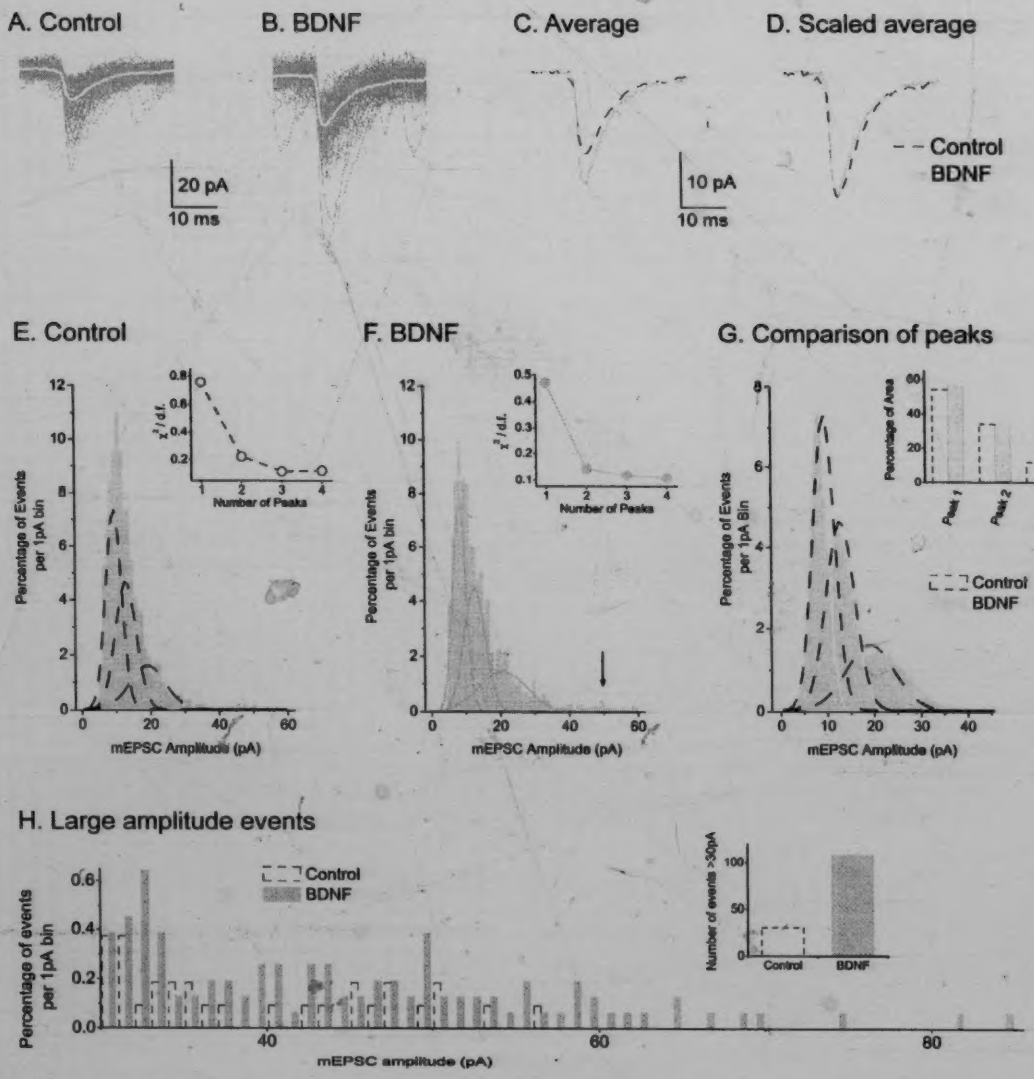
A. Control
B. BDNF
C. Average
D. Scaled average
20 pA
10 ms
10 pA
10 ms
- - Control
BDNF
E. Control
F. BDNF
G. Comparison of peaks
Percentage of Events per 1pA bin
mEPSC Amplitude (pA)
χ^2 / d.f.
Number of Peaks
Percentage of Events per 1pA Bin
Percentage of Area
Peak 1
Peak 2
Peak 3
Control
BDNF
H. Large amplitude events
Percentage of events per 1pA bin
mEPSC amplitude (pA)
Control
BDNF
Number of events >30pA
Control
BDNF

Figure 4-9: Effect of BDNF on spontaneous activity of tonic and delay neurons.

Spontaneous activity was measured as the number of depolarizations or action potential discharges at resting membrane potential in current-clamp mode. The mean number of spontaneous excitatory postsynaptic potentials (sEPSPs) and spontaneous action potentials generated from sEPSPs are shown for tonic (A and B, respectively) and delay neurons (C and D, respectively). For tonic neurons (n = 36 for controls, n = 15 for BDNF). For delay neurons (n = 35 for controls, n = 27 for BDNF). Error bars indicate SEM. For Student's unpaired t-test, * = $p<0.05$, # = $p< 0.01$. E and F: Sample 2 min recording of spontaneous activity from a control (E) and BDNF-treated (F) delay neuron. Lower panels show an expanded time scale of a large sEPSP generating an action potential. Note under long-term BDNF treatment conditions, the probability of a large sEPSP generating a burst of action potentials is greater. G: Percentage of cells in the tonic and delay group firing a burst of action potentials. Blue dashed bars indicate controls and orange filled bars indicate BDNF-treated neurons.

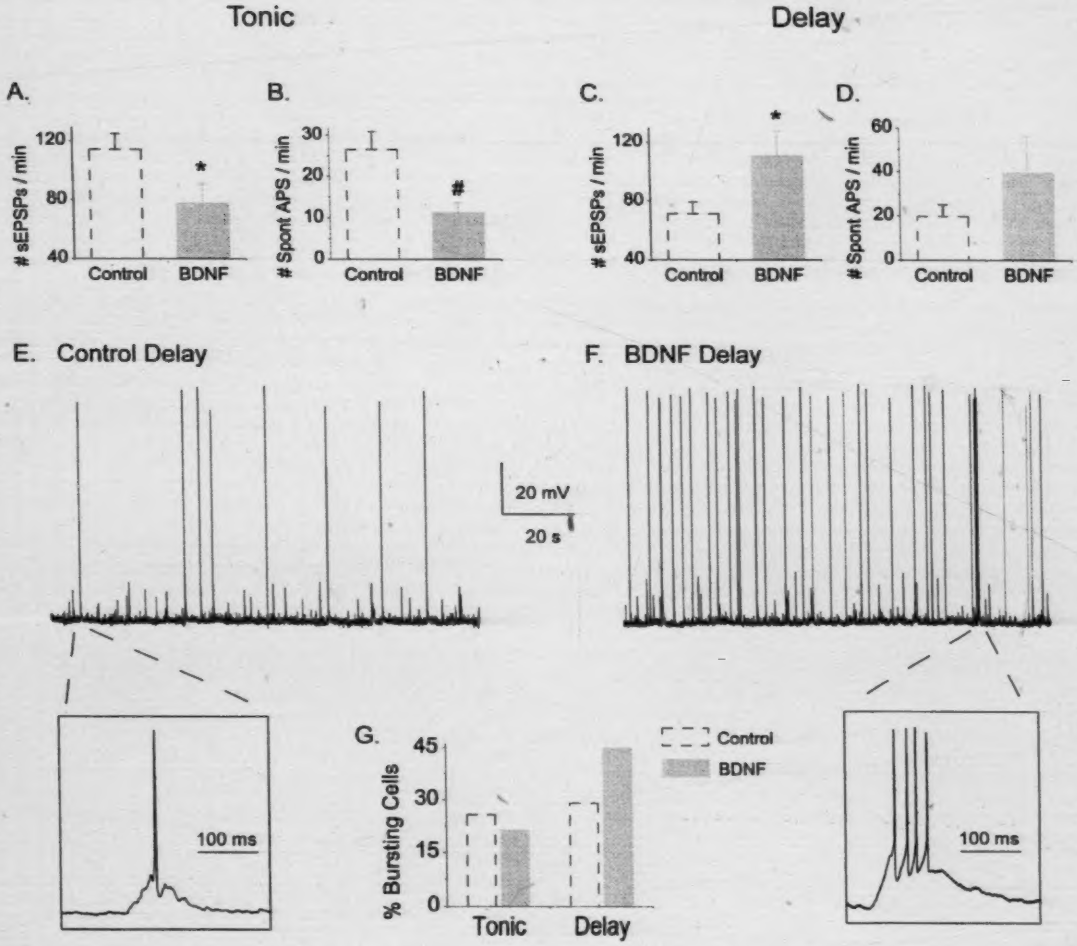
Tonic
Delay
A.
# sEPSPs / min
120
80
40
Control
BDNF
*
B.
# Spont APS / min
30
20
10
0
Control
BDNF
#
C.
# sEPSPs / min
120
80
40
Control
BDNF
*
D.
# Spont APS / min
60
40
20
0
Control
BDNF
E. Control Delay
20 mV
20 s
F. BDNF Delay
100 ms
G.
% Bursting Cells
45
30
15
0
Tonic
Delay
Control
BDNF
100 ms

4.6 References

Alvarez FJ, Villalba RM, Zerda R, Schneider SP (2004) Vesicular glutamate transporters in the spinal cord, with special reference to sensory primary afferent synapses. J Comp Neurol 472: 257-280.

Apfel SC, Wright DE, Wiideman AM, Dormia C, Snider WD, Kessler JA (1996) Nerve growth factor regulates the expression of brain-derived neurotrophic factor mRNA in the peripheral nervous system. Mol Cell Neurosci 7: 134-142.

Baba H, Ji RR, Kohno T, Moore KA, Ataka T, Wakai A, Okamoto M, Woolf CJ (2003) Removal of GABAergic inhibition facilitates polysynaptic A fiber-mediated excitatory transmission to the superficial spinal dorsal horn. Mol Cell Neurosci 24: 818-830.

Bailey AL, Ribeiro-da-Silva A (2006) Transient loss of terminals from non-peptidergic nociceptive fibers in the substantia gelatinosa of spinal cord following chronic constriction injury of the sciatic nerve. Neuroscience 138: 675-690.

Balasubramanyan S, Stemkowski PL, Stebbing MJ, Smith PA (2006) Sciatic chronic constriction injury produces cell-type-specific changes in the electrophysiological properties of rat substantia gelatinosa neurons. J Neurophysiol 96: 579-590.

Chen SR, Pan HL (2002) Hypersensitivity of spinothalamic tract neurons associated with diabetic neuropathic pain in rats. J Neurophysiol 87: 2726-2733.

Cho HJ, Kim JK, Park HC, Kim JK, Kim DS, Ha SO, Hong HS (1998) Changes in brain-derived neurotrophic factor immunoreactivity in rat dorsal root ganglia, spinal cord, and gracile nuclei following cut or crush injuries. Exp Neurol 154: 224-230.

Cho HJ, Kim JK, Zhou XF, Rush RA (1997) Increased brain-derived neurotrophic factor immunoreactivity in rat dorsal root ganglia and spinal cord following peripheral inflammation. Brain Res 764: 269-272.

Colomo F, Erulkar SD (1968) Miniature synaptic potentials at frog spinal neurones in the presence of tertodotoxin. J Physiol 199: 205-221.

Coull JA, Beggs S, Boudreau D, Boivin D, Tsuda M, Inoue K, Gravel C, Salter MW, De Koninck Y (2005) BDNF from microglia causes the shift in neuronal anion gradient underlying neuropathic pain. Nature 438: 1017-1021.

Coull JA, Boudreau D, Bachand K, Prescott SA, Nault F, Sik A, De Koninck P, De Koninck Y (2003) Trans-synaptic shift in anion gradient in spinal lamina I neurons as a mechanism of neuropathic pain. Nature 424: 938-942.

Dalal A, Tata M, Allegre G, Gekiere F, Bons N, Albe-Fessard D (1999) Spontaneous activity of rat dorsal horn cells in spinal segments of sciatic projection following transection of sciatic nerve or of corresponding dorsal roots. Neuroscience 94: 217-228.

Dougherty KD, Dreyfus CF, Black IB (2000) Brain-derived neurotrophic factor in astrocytes, oligodendrocytes, and microglia/macrophages after spinal cord injury. Neurobiol Dis 7: 574-585.

Dougherty KJ, Sawchuk MA, Hochman S (2005) Properties of mouse spinal lamina I GABAergic interneurons. J Neurophysiol 94: 3221-3227.

Fukuoka T, Kondo E, Dai Y, Hashimoto N, Noguchi K (2001) Brain-derived neurotrophic factor increases in the uninjured dorsal root ganglion neurons in selective spinal nerve ligation model. J Neurosci 21: 4891-4900.

Galan A, Laird JM, Cervero F (2004) In vivo recruitment by painful stimuli of AMPA receptor subunits to the plasma membrane of spinal cord neurons. Pain 112: 315-323.

Garraway SM, Petruska JC, Mendell LM (2003) BDNF sensitizes the response of lamina II neurons to high threshold primary afferent inputs. Eur J Neurosci 18: 2467-2476.

Grudt TJ, Perl ER (2002) Correlations between neuronal morphology and electrophysiological features in the rodent superficial dorsal horn. J Physiol 540: 189-207.

Ha SO, Kim JK, Hong HS, Kim DS, Cho HJ (2001) Expression of brain-derived neurotrophic factor in rat dorsal root ganglia, spinal cord and gracile nuclei in experimental models of neuropathic pain. Neuroscience 107: 301-309.

Hains BC, Waxman SG (2006) Activated microglia contribute to the maintenance of chronic pain after spinal cord injury. J Neurosci 26: 4308-4317.

Hantman AW, van den Pol AN, Perl ER (2004) Morphological and physiological features of a set of spinal substantia gelatinosa neurons defined by green fluorescent protein expression. J Neurosci 24: 836-842.

Hayashi Y, Shi SH, Esteban JA, Piccini A, Poncer JC, Malinow R (2000) Driving AMPA receptors into synapses by LTP and CaMKII: requirement for GluR1 and PDZ domain interaction. Science 287: 2262-2267.

Heinke B, Ruscheweyh R, Forsthuber L, Wunderbaldinger G, Sandkuhler J (2004) Physiological, neurochemical and morphological properties of a subgroup of GABAergic spinal lamina II neurones identified by expression of green fluorescent protein in mice. J Physiol 560: 249-266.

Huang EJ, Reichardt LF (2003) Trk receptors: roles in neuronal signal transduction. Annu Rev Biochem 72: 609-642.

Kerr BJ, Bradbury EJ, Bennett DL, Trivedi PM, Dassan P, French J, Shelton DB, McMahon SB, Thompson SW (1999) Brain-derived neurotrophic factor modulates nociceptive sensory inputs and NMDA-evoked responses in the rat spinal cord. J Neurosci 19: 5138-5148.

Kim KJ, Yoon YW, Chung JM (1997) Comparison of three rodent neuropathic pain models. Exp Brain Res 113: 200-206.

Kim SH, Chung JM (1992) An experimental model for peripheral neuropathy produced by segmental spinal nerve ligation in the rat. Pain 50: 355-363.

Kohno T, Moore KA, Baba H, Woolf CJ (2003) Peripheral nerve injury alters excitatory synaptic transmission in lamina II of the rat dorsal horn. J Physiol 548: 131-138.

Laird JM, Bennett GJ (1992) Dorsal root potentials and afferent input to the spinal cord in rats with an experimental peripheral neuropathy. Brain Res 584: 181-190.

Laird JM, Bennett GJ (1993) An electrophysiological study of dorsal horn neurons in the spinal cord of rats with an experimental peripheral neuropathy. J Neurophysiol 69: 2072-2085.

√

Ledeboer A, Mahoney JH, Milligan ED, Martin D, Maier SF, Watkins LR (2006) Spinal cord glia and interleukin-1 do not appear to mediate persistent allodynia induced by intramuscular acidic saline in rats. J Pain 7: 757-767.

Ledeboer A, Sloane EM, Milligan ED, Frank MG, Mahony JH, Maier SF, Watkins LR (2005) Minocycline attenuates mechanical allodynia and proinflammatory cytokine expression in rat models of pain facilitation. Pain 115: 71-83.

Lee CJ, Bardoni R, Tong CK, Engelman HS, Joseph DJ, Magherini PC, MacDermott AB (2002) Functional expression of AMPA receptors on central terminals of rat dorsal root ganglion neurons and presynaptic inhibition of glutamate release. Neuron 35: 135-146.

Lu VB, Chee MJS, Gustafson SL, Colmers WF, Smith PA (2005) Concentration-dependent effects of long-term interleukin-1 treatment on spinal dorsal horn neurons in organotypic slice cultures. Abstract Viewer/Itinerary Planner Washington, DC: Society for Neuroscience, Online 292.3.

Lu VB, Colmers W.F, Dryden W.F., Smith P.A. (2004) Brain - derived neurotrophic factor alters the synaptic activity of dorsal horn neurons in long - term organotypic spinal cord slice cultures. Program No 289,15 2004 Abstract Viewer/Itinerary Planner Washington, DC: Society for Neuroscience Online.

Lu VB, Moran TD, Balasubramanyan S, Alier KA, Dryden WF, Colmers WF, Smith PA (2006) Substantia Gelatinosa neurons in defined-medium organotypic slice culture are similar to those in acute slices from young adult rats. Pain 121: 261-275.

Lu Y, Perl ER (2003) A specific inhibitory pathway between substantia gelatinosa neurons receiving direct C-fiber input. J Neurosci 23: 8752-8758.

Lu Y, Perl ER (2005) Modular organization of excitatory circuits between neurons of the spinal superficial dorsal horn (laminae I and II). J Neurosci 25: 3900-3907.

Matayoshi S, Jiang N, Katafuchi T, Koga K, Furue H, Yasaka T, Nakatsuka T, Zhou XF, Kawasaki Y, Tanaka N, Yoshimura M (2005) Actions of brain-derived neurotrophic factor on spinal nociceptive transmission during inflammation in the rat. J Physiol 569: 685-695.

Michael GJ, Averill S, Shortland PJ, Yan Q, Priestley JV (1999) Axotomy results in major changes in BDNF expression by dorsal root ganglion cells: BDNF expression in large trkB and trkC cells, in pericellular baskets, and in projections to deep dorsal horn and dorsal column nuclei. Eur J Neurosci 11: 3539-3551.

Miletic G, Miletic V (2002) Increases in the concentration of brain derived neurotrophic factor in the lumbar spinal dorsal horn are associated with pain behavior following chronic constriction injury in rats. Neurosci Lett 319: 137-140.

Moore KA, Kohno T, Karchewski LA, Scholz J, Baba H, Woolf CJ (2002) Partial peripheral nerve injury promotes a selective loss of GABAergic inhibition in the superficial dorsal horn of the spinal cord. J Neurosci 22: 6724-6731.

Moran TD, Colmers WF, Smith PA (2004) Opioid-like actions of neuropeptide Y in rat substantia gelatinosa: Y1 suppression of inhibition and Y2 suppression of excitation. J Neurophysiol 92: 3266-3275.

Nagy GG, Al Ayyan M, Andrew D, Fukaya M, Watanabe M, Todd AJ (2004) Widespread expression of the AMPA receptor GluR2 subunit at glutamatergic synapses in the rat spinal cord and phosphorylation of GluR1 in response to noxious stimulation revealed with an antigen-unmasking method. J Neurosci 24: 5766-5777.

Oliveira AL, Hydling F, Olsson E, Shi T, Edwards RH, Fujiyama F, Kaneko T, Hokfelt T, Cullheim S, Meister B (2003) Cellular localization of three vesicular glutamate transporter mRNAs and proteins in rat spinal cord and dorsal root ganglia. Synapse 50: 117-129.

Rose CR, Blum R, Kafitz KW, Kovalchuk Y, Konnerth A (2004) From modulator to mediator: rapid effects of BDNF on ion channels. Bioessays 26: 1185-1194.

Sivilotti L, Woolf CJ (1994) The contribution of GABAA and glycine receptors to central sensitization: disinhibition and touch-evoked allodynia in the spinal cord. J Neurophysiol 72: 169-179.

Slack SE, Pezet S, McMahon SB, Thompson SW, Malcangio M (2004) Brain-derived neurotrophic factor induces NMDA receptor subunit one phosphorylation via ERK and PKC in the rat spinal cord. Eur J Neurosci 20: 1769-1778.

Smith PA, Lu V.B., Balasubramanyan S (2005) Chronic constriction injury and brain-derived neurotrophic factor (BDNF) generate similar "pain footprints" in dorsal horn neurons. Program No 748,2 2005 Abstract Viewer/Itinerary Planner Washington, DC: Society for Neuroscience, 2005 Online.

Todd AJ, McKenzie J (1989) GABA-immunoreactive neurons in the dorsal horn of the rat spinal cord. Neuroscience 31: 799-806.

Tsuda M, Shigemoto-Mogami Y, Koizumi S, Mizokoshi A, Kohsaka S, Salter MW, Inoue K (2003) P2X4 receptors induced in spinal microglia gate tactile allodynia after nerve injury. Nature 424: 778-783.

Watkins LR, Maier SF, Goehler LE (1995) Immune activation: the role of pro-inflammatory cytokines in inflammation, illness responses and pathological pain states. Pain 63: 289-302.

Woolf CJ (1983) Evidence for a central component of post-injury pain hypersensitivity. Nature 306: 686-688.

Wu K, Len GW, McAuliffe G, Ma C, Tai JP, Xu F, Black IB (2004) Brain-derived neurotrophic factor acutely enhances tyrosine phosphorylation of the AMPA receptor subunit GluR1 via NMDA receptor-dependent mechanisms. Brain Res Mol Brain Res 130: 178-186.

Yajima Y, Narita M, Usui A, Kaneko C, Miyatake M, Narita M, Yamaguchi T, Tamaki H, Wachi H, Seyama Y, Suzuki T (2005) Direct evidence for the involvement of brain-derived neurotrophic factor in the development of a neuropathic pain-like state in mice. J Neurochem 93: 584-594.

Zhou XF, Chie ET, Deng YS, Zhong JH, Xue Q, Rush RA, Xian CJ (1999) Injured primary sensory neurons switch phenotype for brain-derived neurotrophic factor in the rat. Neuroscience 92: 841-853.

Zhou XF, Deng YS, Xian CJ, Zhong JH (2000) Neurotrophins from dorsal root ganglia trigger allodynia after spinal nerve injury in rats. Eur J Neurosci 12: 100-105.

Zhuang ZY, Gerner P, Woolf CJ, Ji RR (2005) ERK is sequentially activated in neurons, microglia, and astrocytes by spinal nerve ligation and contributes to mechanical allodynia in this neuropathic pain model. Pain 114: 149-159.

CHAPTER 5

BDNF AND NEURONAL INHIBITION:

Neuron type-specific effects of brain-derived neurotrophic factor on inhibitory synaptic transmission of dorsal horn neurons in defined medium organotypic slice cultures.

5.1 Introduction

In the previous chapter it was demonstrated that long-term exposure of dorsal horn neurons to BDNF, similar to the conditions present in neuropathic pain models *in vivo*, produces a distinct pattern of changes in populations of excitatory and inhibitory dorsal horn neurons. Excitatory synaptic drive and spontaneous bursting activity of putative excitatory 'delay' firing neurons (Heinke et al., 2004; Lu and Perl, 2005) increases following BDNF treatment; whilst the synaptic activity to presumed inhibitory tonic firing neurons (Heinke et al., 2004; Lu and Perl, 2003) decreases. Since a similar pattern of changes is also produced in a model of chronic constriction injury (CCI, Table 4-2) (Balasubramanyan et al., 2006), this may represent the mechanism by which prolonged release of BDNF can instigate chronic neuropathic pain.

However, changes in dorsal horn inhibition can also lead to neuropathic pain (Baba et al., 2003; Coull et al., 2003; Moore et al., 2002; Sivilotti and Woolf, 1994). A loss of inhibitory tone can offset the balance in the dorsal horn network regardless of any changes in excitation. Reduced synaptic drive to tonic firing neurons following long-term BDNF exposure shown previously (Chapter 4) suggests that there may be reduced output from these putative inhibitory dorsal horn neurons. Furthermore, BDNF has been proposed to alter the inhibitory actions of GABA (Coull et al., 2005; Prescott et al., 2006) which could also have implications on inhibitory tone in the dorsal horn.

But recent reports suggest that BDNF can enhance release of GABA into the dorsal horn (Bardoni et al., 2007; Pezet et al., 2002). Such changes could oppose the increase in excitatory synaptic activity induced by BDNF on the majority of neuronal cell types in the dorsal horn: 'delay', 'irregular', phasic, and transient neurons (Chapter 4).

To aid in determining the effects of BDNF on overall dorsal horn inhibition, identification of the inhibitory neurons in the dorsal horn might prove useful. BDNF has selective and sometimes opposite actions on electrophysiologically-identified populations of dorsal horn neurons. The consequences of these effects will vary greatly depending on whether excitatory or inhibitory populations are affected. Immunohistochemical techniques are available for the positive identification of GAD-expressing inhibitory neurons. This identification will allow the examination of changes to this specific population of neurons following long-term BDNF treatment.

Thus, changes in inhibition can impact dorsal horn excitability and can play a key role in 'central sensitization' and the initiation of neuropathic pain. Therefore, this chapter will focus on examining the effects of long-term BDNF exposure on dorsal horn inhibition.

5.2 Methods

5.2.1 Defined-medium organotypic cultures (DMOTCs) of spinal cord slices

DMOTC slices were prepared as previously described (see Chapter 2: General methods). Very briefly, spinal cords were isolated from embryonic (E13-14) rat pups and transverse slices (300 ± 25 μm) were cultured using the roller-tube technique. Serum-free conditions were established after 5 days *in vitro* following the medium exchange schedule outlined in Figure 2-3A. The medium was exchanged with freshly prepared medium every 3-4 days.

Slices were treated after 15-21 days *in vitro* for a period of 5-6 days with 200 ng/ml BDNF (Alomone Laboratories, Jerusalem, Israel) in serum-free medium, or heat-inactivated BDNF as described in Chapter 2. Age-matched, untreated DMOTC slices served as controls.

5.2.2 Electrophysiology

Dorsal horn neurons in DMOTCs were viewed with a Zeiss Axioskop FS upright microscope and neurons were patched under the guidance of infrared differential interference contrast (IR-DIC) optics. Whole-cell recordings were obtained using a NPI SEC-05L amplifier (npi Electronic Gmbh, Tamm, Germany) in discontinuous current- or voltage-clamp mode. Patch pipettes were pulled from thin-walled borosilicate glass (1.5/1.12 mm OD/ID, Cat. No. TW140F-4, WPI, Sarasota, FL, USA) to 5-10 MΩ resistances and filled with a K$^+$ gluconate-based internal solution described in Chapter 2.

Spontaneous inhibitory postsynaptic currents (sIPSCs) were recorded for 3 minutes with the neuron clamped at 0 mV. At this voltage, Cl$^-$ mediated inhibitory events would be outward currents and excitatory currents would be inward, but of small amplitude as they would occur close to their reversal potential. Miniature inhibitory postsynaptic currents (mIPSCs) were recorded in a similar manner but in the presence of 1 μM tetrodotoxin (TTX, Alomone Laboratories, Jerusalem, Israel) to block action potential-dependent neurotransmitter release. Blockade of action potential generation was confirmed by the cessation of action potential discharges in response to depolarizing current pulses. Also, the percentage of TTX-sensitive sIPSCs in each neuron (i.e. action potential-dependent events) was calculated from two 3 min recording periods in the absence and presence of TTX using the following equation:

$$\% \text{ TTX-sensitive sIPSCs} = \frac{\text{total \# of sIPSCs} - \text{total \# of mIPSCs}}{\text{total \# of sIPSCs}}$$

The involvement of presynaptic inhibition in regulating dorsal horn transmission was evaluated by measuring the change in spontaneous excitatory postsynaptic currents (sEPSCs) following removal of inhibition by addition of bicuculline (10 μM) and strychnine (1 μM) (Figure 5-7). sEPSCs were recorded in a similar manner to sIPSCs, but with the neuron clamped at -70 mV (see Chapter 4 for details), and comparisons were made from two 3 min recordings before and after application of inhibitory receptor antagonists. 'Tonic' conductances were measured as the change in holding current following application of bicuculline (10 μM) and strychnine (1 μM).

All data were acquired using Axon Instruments pCLAMP 9.0 software (Molecular Devices, Burlingame, CA, USA).

5.2.3 GAD staining

To identify populations of dorsal horn neurons expressing GAD, a marker of inhibitory neurons, cells in recorded DMOTC slices were probed using immunohistochemical procedures outlined in Chapter 2. Briefly, primary GAD antibodies (1:8000, anti-GAD, rabbit; Chemicon, Temecula, CA, USA) in 2% normal goat serum (NGS; Rockland, Gilbertsville, PA, USA) and 0.3% Triton X-100 solution in PBS were incubated with DMOTC slices for 48 hours at 4°C. Secondary antibodies (1:300, anti-rabbit Alexa-488; Molecular Probes, Eugene, OR, USA) in 2% NGS and 0.3% Triton X-100 in PBS, were applied for 2.5 hours. A Texas red-streptavidin conjugate used to stain biocytin-filled cells was added after two hours of the start of incubation with the secondary antibody solution. Slices were washed thoroughly with distilled water before mounting on to microscope slides. Stained slices were allowed to dry sufficiently before a coverslip was applied using Prolong Gold (Molecular Probes). The concentration of antibodies was optimized using control DMOTC slices to produce sufficient staining and reduce background. Fluorescent dyes used, Texas Red and Alexa-488, did not produce spectral crossover in staining controls (data not shown).

To visualize staining, a Zeiss inverted confocal laser scanning microscope (LSM 510; Zeiss, Toronto, ON, Canada) equipped with appropriate lasers (HeNe1, 543 nm; Argon, 488 nm) and filters was used to examine the tissue. Fluorescent confocal images and 3D reconstructions were acquired using Zeiss LSM 510 imaging software (Zeiss LSM image browser, v. 3, 2, 70).

5.2.4 Data analysis and statistical testing

Excitatory and inhibitory synaptic events were analyzed using Mini Analysis™ software (Synaptosoft, Decatur, GA, USA). Peaks of events were first automatically detected by the software according to a set of threshold criteria, and then all detected events were visually re-examined and accepted or rejected subjectively (refer to Moran et al., 2004 for complete details). To generate cumulative probability plots for both amplitude and inter-event time interval, the same number of events (100-200 events acquired after an initial 1 min of recording) from each neuron was pooled for each cell type, and input into the Mini Analysis program. The Kolmogorov-Smirnov two-sample statistical test (KS-test) was used to compare the distribution of events between control and BDNF-treated groups.

Analysis of mIPSC amplitude also involved redistributing event lists into 1 pA bins to produce histograms such as those illustrated in Figures 5-4H, I and 5-5E, F. Gaussian curve fitting protocols available in Origin 7.0 were used to identify peaks within the data. Fitting was carried out by repeating iterations until the χ^2 value was not further reduced. For most experimental situations, best fits were obtained by fitting to 2-3 peak amplitudes as changing to a higher number of Gaussian fits produced little change in χ^2 values (see insets to Figures 5-4H, I and 5-5E, F).

All graphs were plotted and fitted using Origin 7.0 (Origin Lab, Northampton, MA, USA) and statistical significance was taken as $p<0.05$. Statistical comparisons were made with unpaired t-tests or Chi-squared (χ^2) tests as specified and appropriate, using GraphPad InStat 3.05 (GraphPad Software, San Diego, CA, USA).

5.2.5 Drugs and chemicals

Unless otherwise stated, all chemicals were from SIGMA (St. Louis, MO, USA). TTX was dissolved in distilled water as a 1 mM stock solution and stored at -20°C until use. TTX was diluted to a final desired concentration of 1 μM in external recording solution on the day of the experiment. Strychnine was prepared in a similar manner to TTX, and bicuculline (Tocris, Ballwin, MO, USA) was dissolved in DMSO as a 10 mM stock solution and then diluted to 10 μM in external recording solution immediately prior to use.

5.3 Results

5.3.1 Effect of BDNF on sIPSCs

The effects of BDNF on sIPSC amplitude are illustrated in Figure 5-1A to E, and effects on inter-event interval (IEI, or the reciprocal of instantaneous frequency) are illustrated in Figure 5-1F to J. As shown, BDNF reduced the frequency of sIPSCs in tonic neurons (Figure 5-1F) but had no effect on amplitude (Figure 5-1A). Sample recordings illustrating BDNF's effects on sIPSCs of tonic neurons are shown in Figure 5-3D. By contrast, BDNF increased the amplitude and frequency of sIPSCs in 'delay' neurons (Figure 5-1B and G). Sample recordings illustrating the effect of BDNF on sIPSCs of 'delay' neurons are shown in Figure 5-3E. BDNF also decreased the amplitude and frequency of sIPSCs in 'irregular' neurons (Figure 5-1C and H), and reduced the amplitude of sIPSCs in phasic (Figure 5-1D) and transient (Figure 5-1E) neurons. There was no change in the frequency of sIPSCs in both phasic and transient neurons (Figure 5-1I and J). All changes were significant according to the Kolmogorov-Smirnoff two-sample test (KS-test, *p-values* presented in figures).

An unpaired t-test of all data sets was also applied (Figure 5-1K and L), and the trends of changes of sIPSC amplitude and inter-event interval identified in the KS-test were also apparent from the t-test.

Disrupting BDNF protein activity with heat-inactivation, prevented the effect of BDNF on sIPSC amplitude of 'delay' neurons and produced similar mean sIPSC amplitude values as controls of tonic neurons (Figure 5-1M). The mean IEI values for heat-inactivated BDNF were statistically different from BDNF-treated tonic and 'delay' neurons (Figure 5-1N, unpaired t-test, $p<0.001$) and produced similar values to untreated control values (unpaired t-test, *$p>0.05$*), except for 'delay' neurons (unpaired t-test, *$p<0.01$*).

Thus, BDNF did not produce identical changes in inhibitory synaptic transmission in all neuron groups, but rather induced neuron type-specific effects. 'Delay' neurons received more spontaneous inhibitory synaptic activity and all other neuron types: tonic, 'irregular', phasic and transient neurons, displayed decreased inhibitory synaptic activity following BDNF treatment. This pattern of BDNF-induced changes in sIPSCs is different from the neuron type-specific changes in sEPSCs seen in the previous chapter where all cell types except tonic neurons received more excitatory synaptic drive following BDNF treatment.

5.3.2 Effect of BDNF on mIPSCs

To further characterize the changes in inhibitory synaptic activity induced by BDNF, mIPSCs were recorded in the presence of 1 μM TTX and analyzed in a similar manner to sIPSC events. A large percentage of spontaneous inhibitory currents were removed upon application of TTX (Figure 5-3C to E). Consequently, there were insufficient events obtained from the smallest cell type group, the phasic neurons, to conduct adequate analysis of mIPSCs.

The effects of BDNF on mIPSC amplitude are illustrated in Figure 5-2A to D, and its effects on IEI are illustrated in Figure 5-2E to H. Opposite to its action on sIPSCs, BDNF increased the amplitude of mIPSCs in tonic neurons (Figure 5-2A) and had no effect on mIPSC frequency (Figure 5-2E). Sample recordings illustrating BDNF-induced effect in mIPSCs on tonic neurons are shown in Figure 5-3D. However, similar to its action on sIPSCs, long-term BDNF exposure increased the amplitude and frequency of mIPSCs in 'delay' neurons (Figure 5-2B and F). Sample recordings illustrating BDNF-induced increases in mIPSCs on 'delay' neurons are shown in Figure 5-3E. In addition, BDNF reduced the amplitude and frequency of mIPSCs in 'irregular' neurons (Figure 5-2C and G) and reduced the amplitude but had no effect on the frequency of mIPSCs in transient neurons (Figure 5-2D and H). All changes mentioned were significant and the *p-values* from KS-tests are presented in figures. The results from unpaired t-tests on the same data sets are in agreement with the conclusions from the KS-test (Figure 5-2I and J). As was seen with sIPSCs, heat-inactivation of BDNF attenuated the changes induced by BDNF on mIPSCs (Figure 5-2K and L).

5.3.3 BDNF-induced alterations in presynaptic action potential activity of inhibitory neurons can account for some of the changes in sIPSC population

TTX significantly reduced the mean sIPSC amplitude (Figure 5-3A, unpaired t-test, $p<0.001$) and produced the expected increase in inter-event interval (Figure 5-3B, unpaired t-test, $p<0.001$) in all neuron types. As mentioned, the application of TTX removed the majority of spontaneous inhibitory currents (Figure 5-3D and E) indicating that a large percentage of sIPSCs are TTX-sensitive or driven by presynaptic action potential-dependent mechanisms. Therefore, changes in action potential activity of presynaptic inhibitory neurons could play a significant role in modulating the sIPSC population. This possibility was assessed by examining the proportion of action potential-dependent synaptic events that are removed by the addition of TTX (Figure 5-3C).

In the case of tonic neurons, BDNF decreased the frequency of sIPSCs but had no effect on the frequency of their corresponding mIPSCs. Thus, a decrease in the action potential-dependent events is mainly responsible for the decrease in inhibitory synaptic activity in tonic neurons. This is represented in Figure 5-3C where a significant decrease in TTX-sensitive events was observed (unpaired t-test, $p<0.05$). Sample recordings illustrating the effect of BDNF on relative sIPSC and mIPSC frequency of tonic neurons are shown in Figure 5-3D.

For 'delay' neurons, there was no change in the percentage of TTX-sensitive sIPSCs with BDNF treatment (Figure 5-3C, unpaired t-test, $p>0.1$). Since mIPSC frequency increased (Figure 5-2F), it is possible that this, as well as an increase in action potential-dependent events, occurred in this cell type. Sample recordings illustrating the effect of BDNF on relative sIPSC and mIPSC frequency of 'delay' neurons are shown in Figure 5-3E.

For 'irregular' neurons, there was a decrease in sIPSC and mIPSC frequency (Figures 5-1H and 5-2G). The lack of change in the percentage of TTX-sensitive sIPSCs (Figure 5-3C) indicates that there was an accompanying reduction in presynaptic action potential activity which contributed to the reduction in sIPSC population observed following BDNF treatment.

Lastly for transient neurons, there was no change in the frequency of sIPSCs (Figure 5-1J) or mIPSCs (Figure 5-2H); and so, no significant difference in the percentage of TTX-sensitive sIPSCs with BDNF treatment was observed (Figure 5-3C, unpaired t-test, $p>0.2$).

5.3.4 Further analysis of the mechanism of BDNF action on tonic cells

Since tonic neurons comprise 25% of the neurons studied and likely represent the main population of inhibitory neurons in the dorsal horn, mIPSC data from this cell type group were analyzed more thoroughly.

Besides the increase in mIPSC amplitude (Figure 5-2A), BDNF increased the time constant for mIPSC decay (τ) by 35%. The $\tau = 13.3 \pm 0.37$ ms ($n = 1063$) for control and 17.9 ± 0.66 ms ($n = 720$) for mIPSCs recorded from BDNF-treated tonic neurons (unpaired t-test, $p<0.001$). Superimposed events from a typical control tonic neuron and from another neuron from a BDNF-treated culture are shown in Figure 5-4A and B. The white traces show the averaged data from the two cells and these are compared in Figure 5-4C. The scaled averages presented in Figure 5-4D emphasize the decreased rate of mIPSC decay in tonic neurons from BDNF-treated cultures.

As shown in Chapter 3, three main populations of mIPSCs are present in DMOTC slices (see Figure 3-5I) and each population differs in their inhibitory neurotransmitter content: pure GABA, pure glycine or a mix of GABA and glycine neurotransmitters. Each population of mIPSCs gives rise to its own τ of decay which is evident in the three peaks fitted from the distribution of mIPSC τ (Figure 5-4E and F). For control tonic cells, the mean τ values for decay were 5.6 ± 0.10, 16.9 ± 0.78 and 39.4 ± 3.0 ms, and similar values were obtained from BDNF-treated tonic control cells ($\tau = 6.23 \pm 0.11$, 17.6 ± 0.82 and 41.4 ± 6.1 ms). A comparison of the peaks (Figure 5-4G) reveals no shift in the mean τ for decays of each population following BDNF treatment. There was however an increase in the proportion of events under the largest peak (Figure 5-4G inset). This likely contributes to the increase in the decay time constant in the overall mIPSC population.

Three populations of mIPSC amplitudes of 13.5 ± 0.23, 18.8 ± 0.33 and 22.0 ± 2.6 pA were seen in control tonic cells (Figure 5-4H). These may reflect three different populations of vesicles in presynaptic terminals, different sizes of vesicles in different types of afferents, *i.e.* various local inhibitory interneurons, or different populations of terminals at different distances from the site of recording. Three populations of mIPSC amplitude were also seen in BDNF-treated neurons (Figure 5-4I) but these had larger peak amplitudes at 16.3 ± 10.4, 20.8 ± 2.1 and 30.7 ± 2.3 pA. The insets to Figure 5-4H and I show that fitting with three Gaussian peaks produced the optimal reduction in χ^2 (see methods). Figure 5-4J shows a replot of the three Gaussian distributions of mIPSC amplitude from control and BDNF-treated tonic cells for comparison.

5.3.5 Further analysis of the mechanism of BDNF action on delay cells

Unlike tonic cells, the τ for decay of mIPSCs was unchanged in 'delay' cells (control $\tau = 15.6 \pm 0.66$ ms, n = 564; BDNF $\tau = 15.8 \pm 0.54$ ms, n = 1322; unpaired t-test, $p>0.5$). Superimposed events from a typical control and BDNF-treated 'delay' neuron are shown in Figure 5-5A and B. Figure 5-5C shows the averages of superimposed data from these cells and scaled averages are presented in Figure 5-5D.

Two populations of mIPSC amplitude were identified in control and BDNF-treated 'delay' cells by fitting Gaussian curves to binned histogram data. Insets to Figure 5-5E and F show optimized χ^2 values when using two peaks to fit the data. The peaks of these mIPSC populations appeared at 11.5 ± 0.11 and 15.0 ± 0.26 pA in control 'delay' cells (Figure 5-5E), and at 16.8 ± 0.48 and 25.3 ± 4.9 pA in BDNF-treated 'delay' cells (Figure 5-5F). Figure 5-5G is a replot of the distributions for comparison between control and BDNF-treated cells. There was an increase in the amplitude of both mIPSC populations in BDNF-treated 'delay' neurons as indicated by the rightward shift of both peaks.

5.3.6 Effect of BDNF on postsynaptic receptors mediating 'tonic' inhibitory conductances

The inhibitory postsynaptic currents examined thus far are governed by inhibitory receptors located within the synaptic cleft. However, there are inhibitory receptors present extrasynaptically which are activated by ambient levels of inhibitory neurotransmitters. This 'tonic' conductance has been postulated to play a role in disorders of hyperexcitability (Bai et al., 2001) and appears as a decrease in holding current upon application of bicuculline (10 μM) and strychnine (1 μM) (Brickley et al., 1996).

Pharmacological removal of inhibition blocked all outward spontaneous inhibitory currents as well as reduced the holding current in neurons held at -70 mV (Figure 5-6A to D). Quantification of the change in holding current, or 'tonic' conductance, reveals a significant increase in BDNF-treated 'delay' neurons compared to controls (Figure 5-6E). No change in 'tonic' conductance was observed in tonic neurons following BDNF treatment (Figure 5-6E). A BDNF-induced increase in 'tonic' conductance could represent an increase in extrasynaptic receptor numbers or enhanced single channel conductance through these receptors; both of these possibilities involve postsynaptic modulation of 'delay' neurons. An increase in 'tonic' conductance could also arise from an increase in the ambient levels of GABA in the synapse, but this would also increase the decay time constant of mIPSCs which was not observed in 'delay' neurons (Figure 5-5D).

5.3.7 Effect of BDNF on presynaptic inhibition of excitatory transmission

Thus far, the effect of long-term BDNF exposure on dorsal horn inhibition has been examined by analyzing inhibitory currents generated by inhibitory neurotransmitter release from synapses that form direct contacts with recorded neurons. However, primary afferent and local excitatory inputs are also subject to presynaptic modulation by the action of inhibitory neurotransmitters (Baba et al., 2003). Moreover, the increased synaptic drive to 'delay' neurons observed in the previous chapter could involve BDNF-induced alterations in presynaptic inhibition. Therefore to assess this, changes in sEPSCs were measured following removal of inhibition with $GABA_A$ and glycine receptor antagonists, bicuculline (10μM) and strychnine (1μM) respectively.

As illustrated in a 'delay' control neuron in Figure 5-7A, addition of bicuculline and strychnine increased the frequency of sEPSCs (Figure 5-7C). Any BDNF-induced alteration in presynaptic inhibition would be reflected as a change in the percent increase of sEPSC frequency observed during bicuculline and strychnine application. However, there was no significant change in the effectiveness of removal of inhibition in BDNF-treated 'delay' or tonic neurons compared to controls (Figure 5-7C, unpaired t-test, $p>0.1$). Figure 5-7B illustrates a similar increase in sEPSC frequency in a BDNF-treated 'delay' neuron as observed in control (Figure 5-7A).

There was also an increase in sEPSC amplitude in controls after addition of bicuculline and strychnine (Figure 5-7A and D). This increase in amplitude could reflect the removal of inhibition of presynaptic neurotransmitter release or alleviation of postsynaptic inhibition. If BDNF enhances inhibition of either one of these processes, then a change in the percent increase in sEPSC amplitude would be apparent following addition of antagonists. This was the case in BDNF-treated 'delay' neurons where there was a significant increase in sEPSC amplitude following application of bicuculline and strychnine compared to controls (Figure 5-7D, unpaired t-test, $p<0.01$) but not for BDNF-treated tonic neurons (Figure 5-7D, unpaired t-test, $p>0.8$). Increased inhibition on 'delay' neurons by BDNF is in agreement with increased inhibitory currents, sIPSCs and mIPSCs, recorded following BDNF treatment in 'delay' neurons (Figures 5-1B, G, K, L and 5-2B, F, I, J).

5.3.8 Changes in network excitability cannot be attributed to BDNF-induced reversal of inhibition

BDNF has been reported to decrease expression of the K^+/Cl^- cotransporter (KCC2) in the dorsal horn (Coull *et al.*, 2005). This increases the intracellular concentration of Cl^- so that GABA and/or glycine produce depolarizing excitatory responses rather than hyperpolarizing inhibitory responses. It has been argued that the ability of GABA to reduce the membrane time constant during membrane depolarization may overcome its shunting effect on the membrane (Prescott et al., 2006).

If GABA/glycine are excitatory modulators of excitatory synaptic input in BDNF-treated cultures, superfusion of bicuculline or strychnine under these conditions would be expected to reduce network excitability and hence excitatory synaptic drive. Figure 5-7B shows this was not the case, as bicuculline and strychnine increased synaptic drive to a 'delay' cell in a BDNF-treated slice. Addition of bicuculline and strychnine increased sEPSC frequency by 88 ± 34.4% (n = 10) in control 'delay' neurons and actually produced a larger but non-significant increase in frequency (132 ± 40.9%, n = 15, $p>0.5$) in BDNF-treated 'delay' neurons (Fig 5-7C). A similar increase in sEPSC frequency following application of antagonists was also observed in tonic neurons as well (86 ± 31.2%, n = 11 for controls; 159 ± 31.0%, n = 11 for BDNF-treated). To further demonstrate GABAergic activity remains inhibitory, in Chapter 7, addition of GABA on to a BDNF-treated DMOTC slice suppressed neuronal excitability and did not induce a rise in intracellular Ca^{2+} concentration (Figure 7-7C).

Therefore, the actions of GABA/glycine transmission remain inhibitory in tonic and 'delay' neurons following treatment with BDNF. The reversal of the chloride gradient following exposure to BDNF was described in Lamina I neurons (Coull et al., 2005), whereas the neurons in this study are mainly Lamina II neurons, which could explain this difference in findings.

5.3.9 GAD-positive neurons correlate well with tonic firing neurons

BDNF induces a number of selective effects on excitatory and inhibitory synaptic transmission in identified populations of dorsal horn neurons. However, its effects on inhibitory neurons have been assumed. There is good evidence to suggest tonic firing neurons are inhibitory (Heinke et al., 2004; Lu and Perl, 2003), though a mixed population of inhibitory neurons which exhibit different firing patterns might exist in the dorsal horn. Immunohistochemical techniques allow for the identification of GAD-expressing inhibitory neurons (Figure 3-2E and F) and thus the specific changes BDNF induces on this select population of dorsal horn neurons can be studied in more detail.

Loss of inhibitory neurons to apoptotic mechanisms has been suggested to play a role in the development of neuropathic pain (Moore et al., 2002; Scholz et al., 2005) but others have argued against this mechanism (Polgar et al., 2003; Polgar et al., 2004; Polgar et al., 2005). In our experiments, the proportion of GAD-positive neurons recorded from DMOTC control and BDNF-treated slices did not significantly differ (χ^2 test, $p>0.8$; 11/19 controls were GAD-positive, 11/18 BDNF-treated neurons were GAD-positive), suggesting BDNF did not alter the survival of this population of neurons.

To characterize further the effects of long-term BDNF exposure on identified inhibitory dorsal horn neurons, excitatory and inhibitory synaptic transmission to GAD-positive and GAD-negative neurons was examined. Analysis of GAD-positive neurons revealed a reduction in both excitatory and inhibitory synaptic activity with BDNF treatment. BDNF significantly decreased the amplitude and frequency of sEPSCs (Figure 5-8A, B and I) and significantly decreased the amplitude and frequency of sIPSCs (Figure 5-8E, F and I). Since these BDNF-induced changes in GAD-positive neurons are reminiscent of the BDNF-induced changes in tonic neurons (Figures 4-4A, F and 5-1A, F), it is likely that they may belong to the same population of inhibitory neurons.

The BDNF-induced changes in GAD-negative neurons were slightly different producing a significant increase in sEPSC amplitude (Figure 5-8C) but no change in frequency (Figure 5-8D), and a decrease in sIPSC amplitude (Figure 5-8G) but no change in frequency (Figure 5-8H). This population of GAD-negative neurons may include excitatory neurons as well as inhibitory glycinergic neurons which do not co-release or co-synthesize GABA at synaptic release sites where GAD staining was mainly probed (Baccei and Fitzgerald, 2004; Keller et al., 2001). This mixed population of neurons limits further interpretation of BDNF-induced changes in GAD-negative neurons.

5.4 Discussion

The main findings of this chapter are that 1) BDNF induces cell type-specific changes in inhibitory synaptic activity. In all cell types except 'delay' neurons, BDNF decreased spontaneous inhibitory synaptic transmission. 2) The effect of BDNF on putative excitatory 'delay' neurons and putative inhibitory tonic neurons involve both pre- and postsynaptic components (discussed below). 3) BDNF-induced reversal of inhibitory activity, described in Lamina I neurons, does not appear to play a role in modulating excitation in the dorsal horn neurons in this study. Neurons studied in DMOTC slices display characteristics similar to Lamina II neurons described in acute spinal cord slices (see Chapter 3 and Lu et al., 2006) and this may explain the discrepancy in findings. Also, the gramicidin-perforated patch recordings utilized by Coull et al. (2005) were not performed in this study. However, the high Cl^- extrusion capacity of mature dorsal horn neurons has been shown to preserve Cl^- concentration gradients adequately regardless of the patch configuration used (Cordero-Erausquin et al., 2005). 4) Approximately the same percentage of GAD-positive neurons is found without and following BDNF treatment, suggesting that the reduction in inhibitory synaptic activity does not involve a loss of inhibitory neurons. 5) BDNF-induced alterations in GAD-positive neurons closely resemble the effect of BDNF on tonic neurons. Since BDNF produces a distinct pattern of cell type-specific effects on dorsal horn neurons and

BDNF reduces excitatory synaptic drive exclusively to tonic neurons, tonic firing neurons may constitute a large component of the inhibitory population in the dorsal horn.

In previous measurements of inhibitory synaptic activity (Chapter 3), a CsCl-based internal solution was used. Although a better signal to noise ratio is gained, the blockade of potassium conductances precludes the identification of neurons based on action potential firing pattern. Previous studies have shown classifying dorsal horn neurons according to their firing patterns was essential in elucidating the changes in excitatory synaptic transmission following peripheral nerve injury (Balasubramanyan, 2006) and long-term BDNF treatment (Chapter 4). Moreover, populations of inhibitory and excitatory dorsal horn neurons have been correlated with distinct firing patterns (Heinke et al., 2004; Lu and Perl, 2003; Lu and Perl, 2005). The similarity of BDNF's effects on GAD-positive (Figure 5-8) and tonic firing neurons (Figures 4-4A and F, and 5-1A and F) further strengthens the argument that tonic neurons represent inhibitory interneurons in the dorsal horn. Therefore, recorded dorsal horn neurons were classified according to its action potential firing pattern prior to examining the effects of BDNF on inhibitory synaptic transmission.

5.4.1 Neuronal type-specific effects of BDNF on inhibitory synaptic transmission

Similar to its selectivity of action on excitatory synaptic transmission, BDNF induced specific effects on identified populations of dorsal horn neurons. All cell types, except for 'delay' neurons, received less inhibitory synaptic activity following BDNF treatment (Figure 5-1). The selectivity of BDNF's actions argues against an overall apoptotic loss of inhibitory neurons. Furthermore, loss of inhibitory neurons does not appear to play a role in the decrease in inhibitory synaptic activity observed in most cell types since the percentage of GAD-positive neurons recorded from did not significantly change in the BDNF-treated group.

Inhibitory modulation of excitatory inputs was also neuronal type-specific, as the magnitude or amplitude of inhibitory suppression of excitatory inputs was enhanced in 'delay' neurons by BDNF treatment but not in tonic neurons (Figure 5-7D). Also, addition of bicuculline and strychnine revealed a larger 'tonic' conductance in BDNF-treated 'delay' neurons compared to controls (Figure 5-6C to E).

5.4.2 Effect of BDNF on inhibition of tonic neurons

Long-term BDNF treatment decreased the frequency of sIPSCs (Figure 5-1F) but produced no change in the frequency of mIPSCs (Figure 5-2E). Therefore decreased sIPSC frequency is attributed to a reduction in action potential activity in presynaptic inhibitory neurons. This is consistent with the reduced spontaneous action potential activity of putative inhibitory tonic neurons reported in Chapter 4 following BDNF treatment (Figure 4-9B).

The amplitude of mIPSCs in tonic neurons increased with BDNF treatment (Figure 5-2A) and there was a rightward shift in all three populations of amplitudes fitted under the mIPSC amplitude distribution (Figure 5-4H and I). Compensatory mechanisms such as 'synaptic scaling' (Turrigiano et al., 1998) could account for this increase in mIPSC amplitude. Loss of synaptic inputs, similar to the reduction in frequency of sIPSCs with BDNF treatment (Figure 5-1F), can prompt an upregulation of postsynaptic receptors to maintain the levels of synaptic currents in a homeostatic balance.

There was also an increase in the time constant for decay (τ) in mIPSCs from BDNF-treated tonic neurons (Figure 5-4D). This increase in τ reflected an increase in the number of events with larger τ values as the mean peak values of mIPSC τ populations did not shift following BDNF treatment (Figure 5-4G). The population of larger mIPSC τ events could represent mIPSCs mediated by GABA which has been shown to have slower kinetics compared to glycine-mediated mIPSCs (Baccei and Fitzgerald, 2004; Lu et al., 2006), and its release can be enhanced by BDNF (Pezet et al., 2002). Other mechanisms such as reduction in receptor desensitization rates, which may involve altered receptor subunit expression, may also be involved.

5.4.3 Effect of BDNF on inhibition of delay neurons

Inhibitory synaptic activity, both sIPSC and mIPSC populations, increased in 'delay' neurons (Figures 5-1B, G, and 5-2B, F). Frequency of inhibitory events increased, indicating a presynaptic mechanism of action. BDNF has been shown to promote release of GABA (Pezet et al., 2002) as well as glycine (Bardoni et al., 2007) on to dorsal horn neurons. An increase in presynaptic action potential activity also contributed to the observed increase in sIPSC frequency since there was no change in the percentage of TTX-sensitive sIPSCs (Figure 5-3C). However, according to studies in Chapter 4, there was a decrease in spontaneous action potential activity in putative inhibitory tonic neurons (Figure 4-9B). There is no obvious explanation for these disparate observations.

Unlike tonic neurons, there was no change in the mIPSC decay time constant in BDNF-treated 'delay' neurons (Figure 5-5D). There was however, a similar rightward shift in amplitude distribution following BDNF treatment (Figure 5-5G). This BDNF-induced increase in mIPSC amplitude could be mediated by an increase in inhibitory receptors postsynaptically since BDNF augmented the percent increase in sEPSC amplitude following pharmacological removal of inhibition (Figure 5-7B and D). Furthermore, there was an increase in the 'tonic' conductance of BDNF-treated 'delay' neurons (Figure 5-6C to E) which are mediated by extra-postsynaptic inhibitory receptors.

5.4.4 Effect of BDNF on inhibition of irregular, phasic and transient neurons

The neurotransmitter present in 'irregular', phasic or transient firing neurons is not known. However, spontaneous inhibitory synaptic activity is significantly reduced in all three cell types following long-term BDNF treatment (Figure 5-1C to E, and H to J). A reduction in action potential activity of presynaptic inhibitory neurons was partly responsible for the reduction of inhibitory activity in 'irregular' neurons since there was no change in the proportion of TTX-sensitive sIPSCs (Figure 5-3C). This decrease could arise from the loss of spontaneous action potential activity in tonic neurons observed previously (Figure 4-9B).

The uncertainty of neurotransmitter content of these neuronal populations and their respective role in nociceptive signalling make it unclear as to whether a loss of inhibitory synaptic drive to these neuronal populations results in increased excitation or inhibition in the dorsal horn.

5.4.5 Effect of BDNF on GAD-positive neurons

Immunohistochemical staining allowed for the identification of neurons which expressed GAD, the rate-limiting enzyme in the synthesis of GABA. GAD is a good marker of inhibitory neurons because its staining has been well correlated with GABA (Eaton et al., 1998) and glycine-containing neurons (Mackie et al., 2003), and is distributed throughout the spinal cord (Eaton et al., 1998; Hughes et al., 2005; Mackie et al., 2003).

Although a reduction in GAD expression have been reported following nerve injury (Eaton et al., 1998; Hughes et al., 2005; Moore et al., 2002), its levels were not quantified in this study. Only one isoform of the enzyme, GAD65, appears to be affected in these animal models but I utilized an antibody for GAD that was not isoform-selective. In addition, the loss of GABAergic neurons has been suggested to contribute to neuropathic pain generation (Moore et al., 2002), but I did not observe a significant change in the occurrence of GAD-positive neurons.

The effect of BDNF on synaptic activity of GAD-positive neurons (Figure 5-8A, B, E and F) closely resembles the effects of BDNF on tonic firing neurons. Since the effects of BDNF on tonic neurons are distinct from its effects on 'delay' and other neuronal cell types, tonic neurons most likely represent GAD-positive, inhibitory neurons. Conversely, since the effect of BDNF on 'delay' neurons is opposite to the effects on GAD-positive neurons, it is strongly unlikely that 'delay' neurons are GAD-positive or inhibitory neurons. GAD-negative neurons represent a mixed population of excitatory and non-GAD expressing inhibitory neurons; therefore, negative GAD staining cannot be used as an indicator of excitatory neurons.

Excitatory synaptic activity to GAD-positive neurons was decreased with BDNF treatment (Figure 5-8A and B). This reduced excitatory drive to inhibitory neurons could lead to a decreased release of inhibitory neurotransmitters and a reduction in inhibitory tone within the dorsal horn network. Loss of inhibitory tone can offset the balance of excitability in the dorsal horn and has been implicated in the generation of neuropathic pain-like behaviours in animals (Baba et al., 2003; Moore et al., 2002; Sivilotti and Woolf, 1994).

5.5 Conclusions

BDNF induced significant changes in inhibitory neurotransmission which were specific to different neuronal populations. Mostly postsynaptic mechanisms played a role in altered inhibitory synaptic transmission but reduced frequency of spontaneous action potential discharges in presynaptic inhibitory tonic neurons could account for some of the changes in inhibitory signalling. Reversal of the inhibitory actions of GABA does not appear to play a role in BDNF-induced changes in network excitability in the Lamina II neurons in this study. Finally, the similarity of BDNF's effects on identified inhibitory GAD-positive neurons and tonic firing neurons strongly suggest this is an inhibitory class of neurons. Since BDNF has an effect on this class of inhibitory dorsal horn neurons, BDNF may instigate central changes which are indicative of 'central sensitization'.

Figure 5-1: Effects of BDNF on amplitude and inter-event interval of spontaneous inhibitory postsynaptic currents (sIPSCs).

A to E: Cumulative probability plots for sIPSC amplitude. The first 100 events following the 1st minute of recordings from each cell were pooled in order to construct cumulative distribution plots, except for phasic cells where the first 200 events following the 1st minute of recording were taken. A: Tonic cells; 1195 events from control DMOTC slices, 1056 events from BDNF-treated DMOTC slices. B: Delay cells; 1013 events for controls, 1827 events for BDNF. C: Irregular cells; 1000 events for controls, 1078 events for BDNF. D: Phasic cells; 776 events for controls, 746 events for BDNF. E: Transient cells; 1019 events for controls, 935 events for BDNF. *P values* derived from the KS test indicated on graphs. F to J: Cumulative probability plots for sIPSC inter-event interval (IEI). *P values* derived from the KS test indicated on graphs. K and L: Effects of BDNF on mean amplitude (K) and IEI (L) of sIPSC events. The same events used to construct cumulative probability plots were used, so the same n values apply. M and N: Comparison of the mean amplitude (M) and mean inter-event interval (N) of sIPSC events to heat-inactivated BDNF controls. The same mean values for control and BDNF-treated tonic and delay cells in (K) and (L) are shown. For tonic cells treated with heat-inactivated BDNF, 500 events were averaged; for delay cells treated with heat-inactivated BDNF, 700 events were averaged. Error bars indicate SEM. For Student's unpaired t-test, # = $p<0.01$, § = $p< 0.001$.

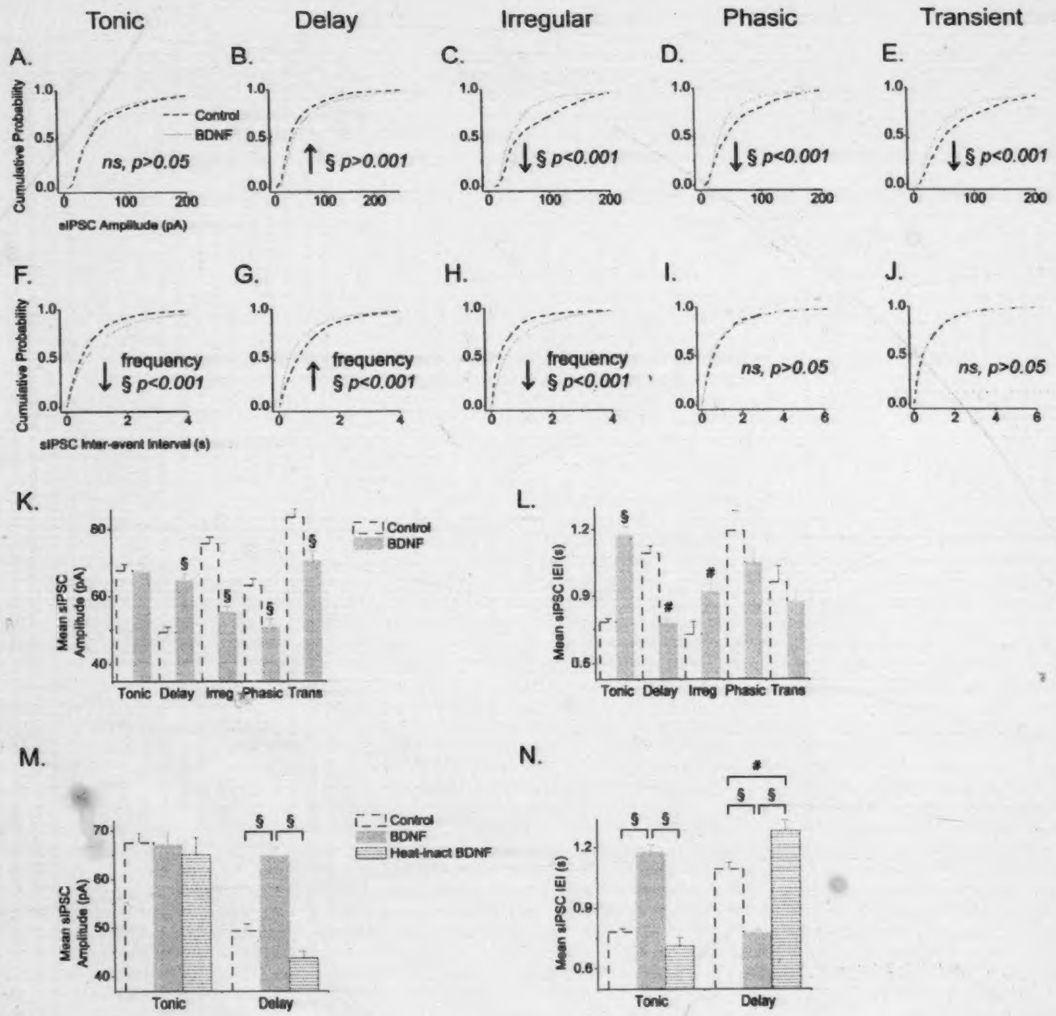
Tonic
Delay
Irregular
Phasic
Transient
A.
B.
C.
D.
E.
Cumulative Probability
sIPSC Amplitude (pA)
Control
BDNF
ns, p>0.05
↑ § p>0.001
↓ § p<0.001
↓ § p<0.001
↓ § p<0.001
F.
G.
H.
I.
J.
sIPSC Inter-event Interval (s)
↓ frequency § p<0.001
↑ frequency § p<0.001
↓ frequency § p<0.001
ns, p>0.05
ns, p>0.05
K.
Mean sIPSC Amplitude (pA)
Tonic
Delay
Irreg
Phasic
Trans
L.
Mean sIPSC IEI (s)
M.
Heat-inact BDNF
N.
§
#

Figure 5-2: Effects of BDNF on amplitude and inter-event interval of miniature inhibitory postsynaptic currents (mIPSCs).

A to D: Cumulative probability plots for mIPSC amplitude. The first 100 events following the 1st minute of recordings from each cell were pooled in order to construct cumulative distribution plots. There were insufficient numbers of events from phasic cells to conduct further mIPSC analysis. A: Tonic cells; 1014 events from control DMOTC slices, 555 events from BDNF-treated DMOTC slices. B: Delay cells; 606 events for controls, 1322 events for BDNF. C: Irregular cells; 509 events for controls, 401 events for BDNF. D: Transient cells; 260 events for controls, 559 events for BDNF. *P values* derived from the KS test indicated on graphs. E to H: Cumulative probability plots for mIPSC inter-event interval (IEI). *P values* derived from the KS test indicated on graphs. I and J: Effects of BDNF on mean amplitude (K) and IEI (L) of mIPSC events. The same events used to construct cumulative probability plots were used, so the same n values apply. K and L: Comparison of the mean amplitude (M) and mean inter-event interval (N) of mIPSC events to heat-inactivated BDNF controls. The same mean values for control and BDNF-treated tonic and delay cells in (K) and (L) are shown. For tonic cells treated with heat-inactivated BDNF, 224 events were averaged; for delay cells treated with heat-inactivated BDNF, 300 events were averaged. Error bars indicate SEM. For Student's unpaired t-test, * = $p<0.05$, § = $p< 0.001$.

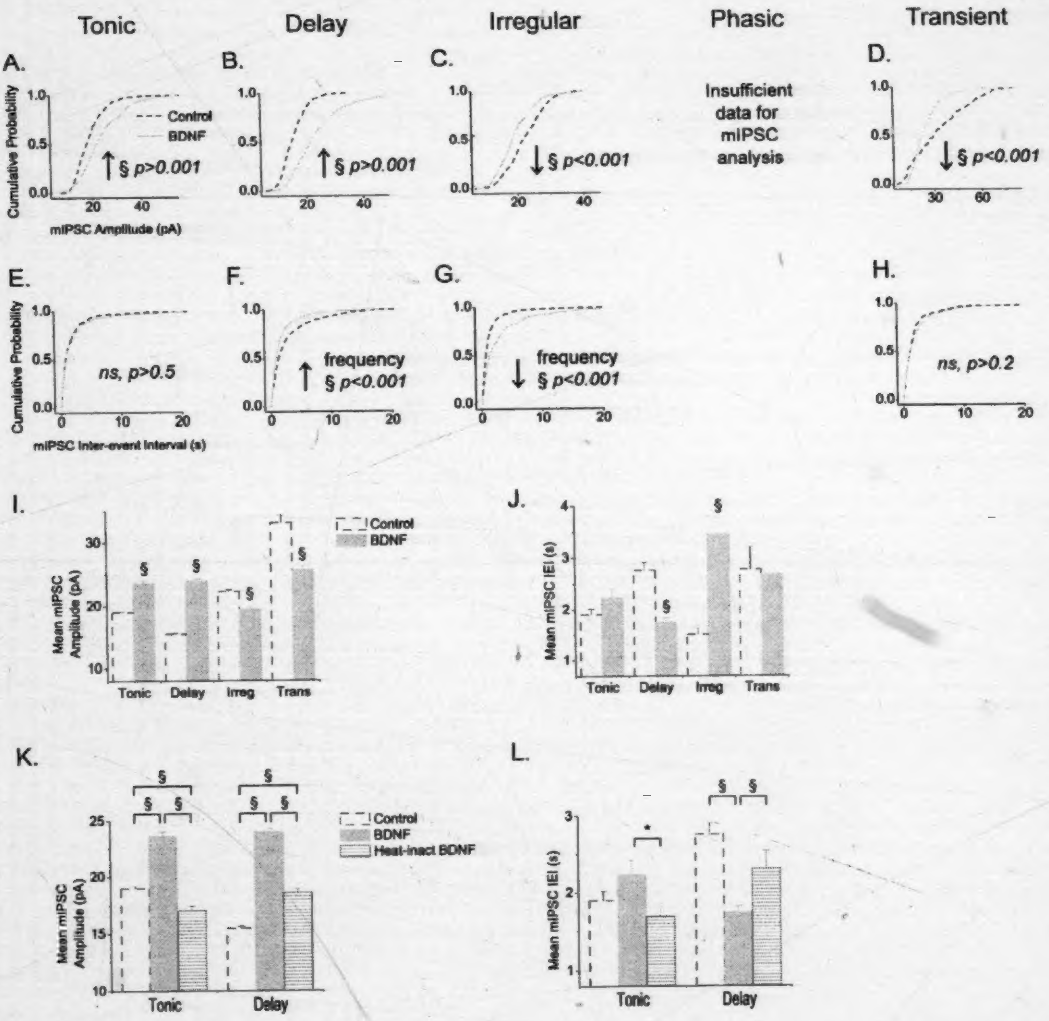

Tonic
Delay
Irregular
Phasic
Transient
A.
B.
C.
D.
Cumulative Probability
1.0
0.5
0.0
20
40
60
30
Control
BDNF
↑ § p>0.001
↑ § p>0.001
↓ § p<0.001
↓ § p<0.001
mIPSC Amplitude (pA)
Insufficient data for mIPSC analysis
E.
F.
G.
H.
0
10
20
ns, p>0.5
↑ frequency § p<0.001
↓ frequency § p<0.001
ns, p>0.2
mIPSC Inter-event Interval (s)
I.
J.
Mean mIPSC Amplitude (pA)
Mean mIPSC IEI (s)
§
Tonic
Delay
Irreg
Trans
K.
L.
Heat-inact BDNF
*

Figure 5-3: Effects of BDNF on the action potential-dependent (TTX-sensitive) sIPSC population.

A and B: Comparison of sIPSCs to mIPSCs for controls. Comparison of mean amplitudes (A) and mean inter-event intervals, IEI, (B) are shown. Cross-hatched bars indicate values for sIPSCs and vertical lined bars indicate values for mIPSCs. C: The percentage of TTX-sensitive sIPSCs was calculated as the number of mIPSCs subtracted from the total number of sIPSCs over the total sIPSCs for each cell. The mean percentages are shown for controls, blue dashed bars, and the BDNF-treated group, orange bars. Error bars indicate SEM. For Student's unpaired t-test, § = $p< 0.001$. D and E: Sample recording traces from tonic (D) and delay (E) cells under control and long-term BDNF exposure conditions. Sample mIPSC recording traces were from the same cell represented in the above sample sIPSC recording trace.

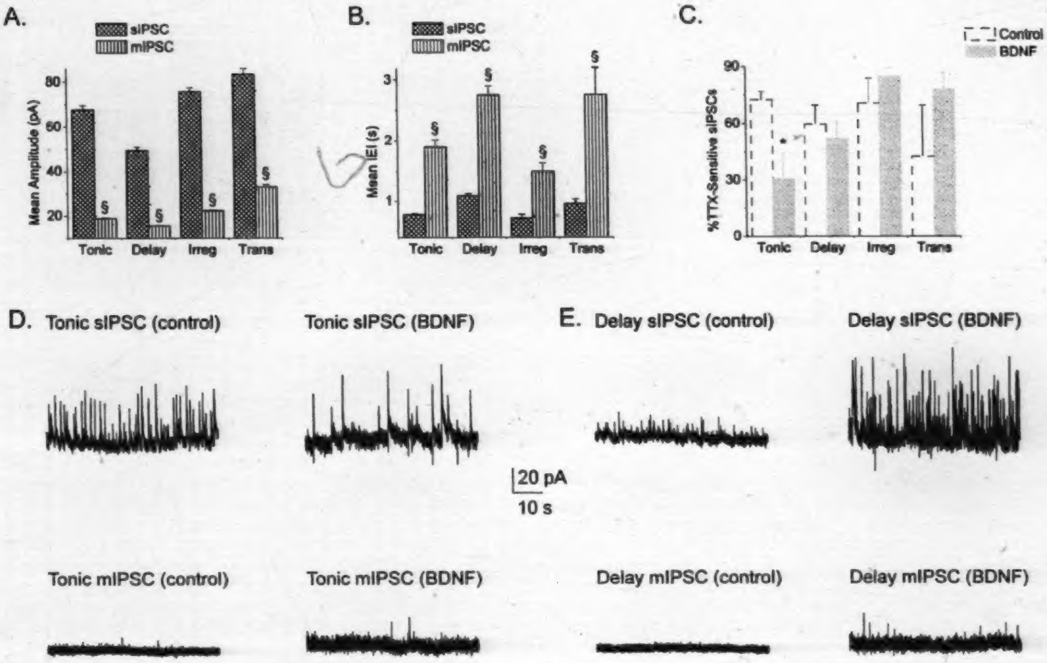

D. Tonic sIPSC (control) Tonic sIPSC (BDNF)

E. Delay sIPSC (control) Delay sIPSC (BDNF)

Tonic mIPSC (control) Tonic mIPSC (BDNF) Delay mIPSC (control) Delay mIPSC (BDNF)

Figure 5-4: Analysis of the effects of BDNF on mIPSCs of tonic neurons.

A: Superimposed recordings of 3 min of mIPSC activity in a control tonic neuron, average of events presented as superimposed white trace. B: Similar superimposed recordings from a tonic neuron in a BDNF-treated culture. C: Averaged events from the neurons illustrated in (A) and (B). D: Averaged events normalized to control size. Note decreased rate of decay of current. E: Distribution histogram (1 ms bins) for mIPSC decay time constant (τ) from control tonic neurons. Fit of the data to three Gaussian distributions represented by blue dashed lines. F: Similar histogram and fit to three Gaussian distributions from BDNF-treated tonic neurons. G: Superimposition of the three Gaussian peaks obtained in (E) and (F). *Inset* in G: Comparison of area under curves for the three peaks (normalized to total area under peaks). H: Distribution histogram (1 pA bins) for amplitudes of 1014 mIPSCs from control tonic neurons. Fit of the data to three Gaussian distributions represented by blue dashed lines. I: Similar histogram and fit to three Gaussian functions for 555 mIPSCs from BDNF-treated neurons: *Insets* in H and I: Graphs to show effect of number of Gaussian fits (peaks) on the value of χ^2 divided by the number of degrees of freedom. J: Superimposition of the three Gaussian peaks obtained in (H) with those obtained in (I).

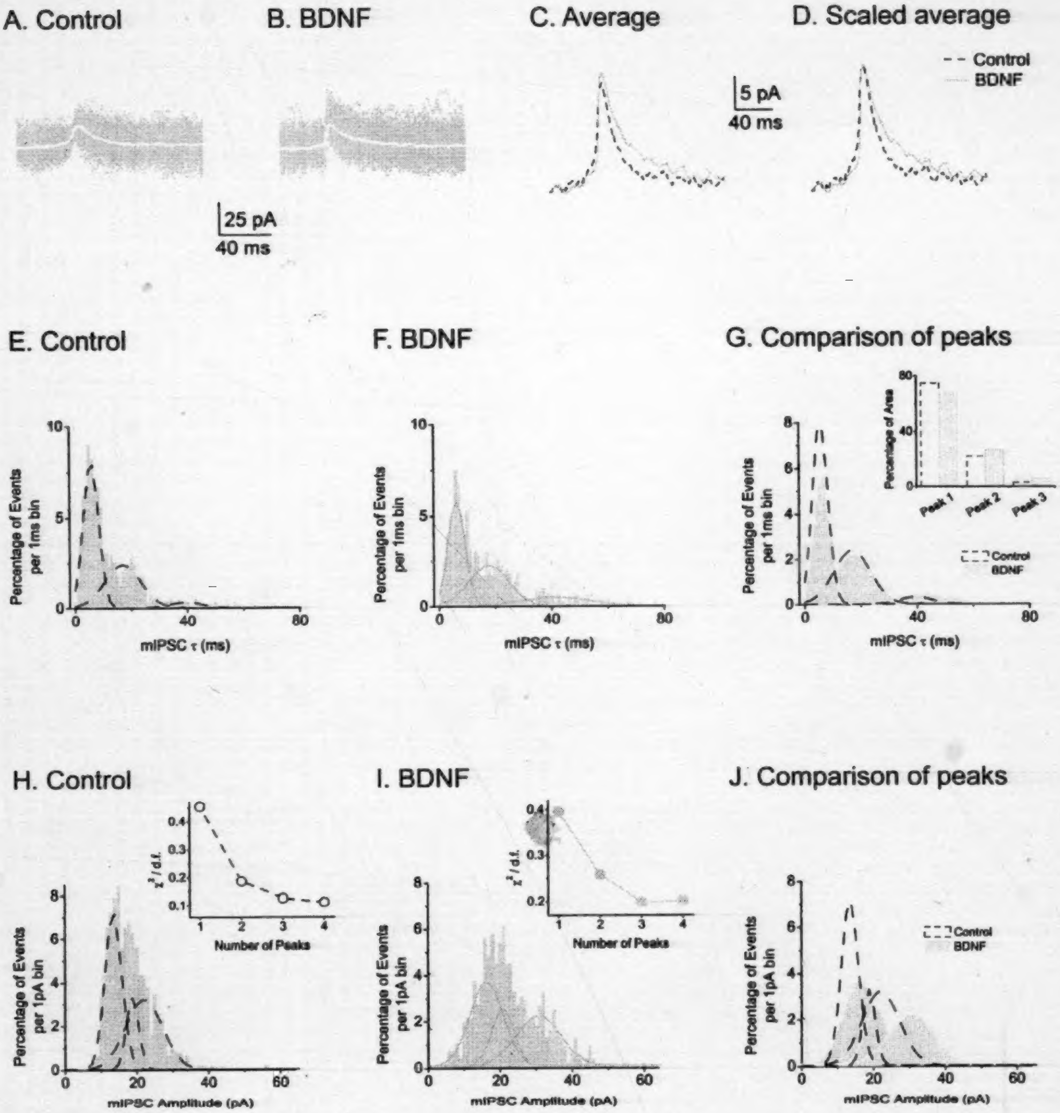
A. Control
B. BDNF
C. Average
D. Scaled average
25 pA
40 ms
5 pA
40 ms
Control
BDNF
E. Control
F. BDNF
G. Comparison of peaks
Percentage of Events per 1ms bin
mIPSC τ (ms)
Percentage of Area
Peak 1
Peak 2
Peak 3
Control
BDNF
H. Control
I. BDNF
J. Comparison of peaks
Percentage of Events per 1pA bin
mIPSC Amplitude (pA)
χ^2 / d.f.
Number of Peaks

Figure 5-5: Analysis of the effects of BDNF on mIPSCs of delay neurons.

A: Superimposed recordings of 3 min of mIPSC activity in a control delay neuron, average of events presented as superimposed white trace. B: Similar superimposed recordings from a delay neuron in a BDNF-treated culture. C: Averaged events from the neurons illustrated in (A) and (B). D: Averaged events normalized to control size. Note no change in the rate of decay of current. E: Distribution histogram (1 pA bins) for amplitudes of 606 mIPSCs from control delay neurons. Fit of the data to two Gaussian distributions represented by blue dashed lines. F: Similar histogram and fit to two Gaussian functions for 1322 mIPSCs from BDNF-treated neurons. *Insets in* E and F: Graphs to show effect of number of Gaussian fits (peaks) on the value of χ^2 divided by the number of degrees of freedom. G: Superimposition of the two Gaussian peaks obtained in (E) with those obtained in (F).

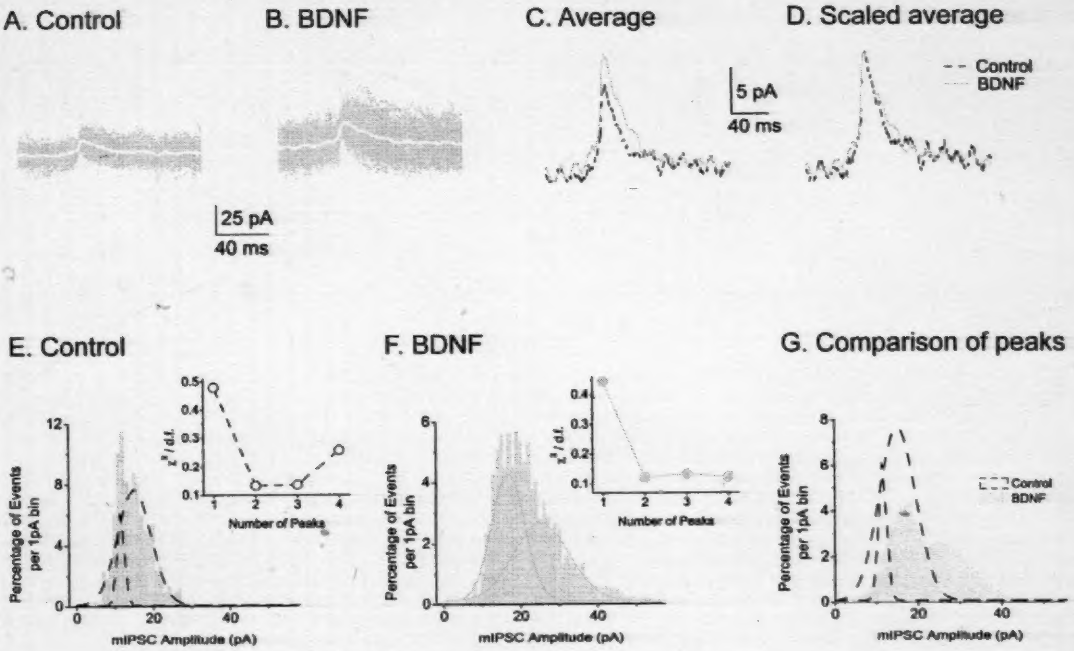
A. Control
B. BDNF
C. Average
D. Scaled average
25 pA
40 ms
5 pA
40 ms
Control
BDNF
E. Control
F. BDNF
G. Comparison of peaks
Percentage of Events per 1pA bin
mIPSC Amplitude (pA)
0
20
40
0
4
8
12
0
2
4
6
8
χ^2 / d.f.
0.1
0.2
0.3
0.4
0.5
Number of Peaks
1
2
3
4

Figure 5-6: Effect of BDNF treatment on the 'tonic' conductance of tonic and delay neurons.

A to D: Sample 3 min recordings of sEPSCs from a tonic control neuron (A), a tonic BDNF-treated neuron (B), a delay control neuron (C) and a delay BDNF-treated neuron (D). Application of 10 µM bicuculline and 1 µM strychnine (B+S) shown as grey bar. Note the decrease in holding current following blockade of inhibitory receptors. The change in holding current was measured, marked on the left of traces by the "I" bar, and represented in (E). Controls (n = 6 for tonic, n = 8 for delay) in blue dashed bars, and BDNF-treated groups (n = 10 for tonic, n = 13 for delay) in orange bars are shown. Error bars indicate SEM. For Student's unpaired t-test, * = $p<0.05$.

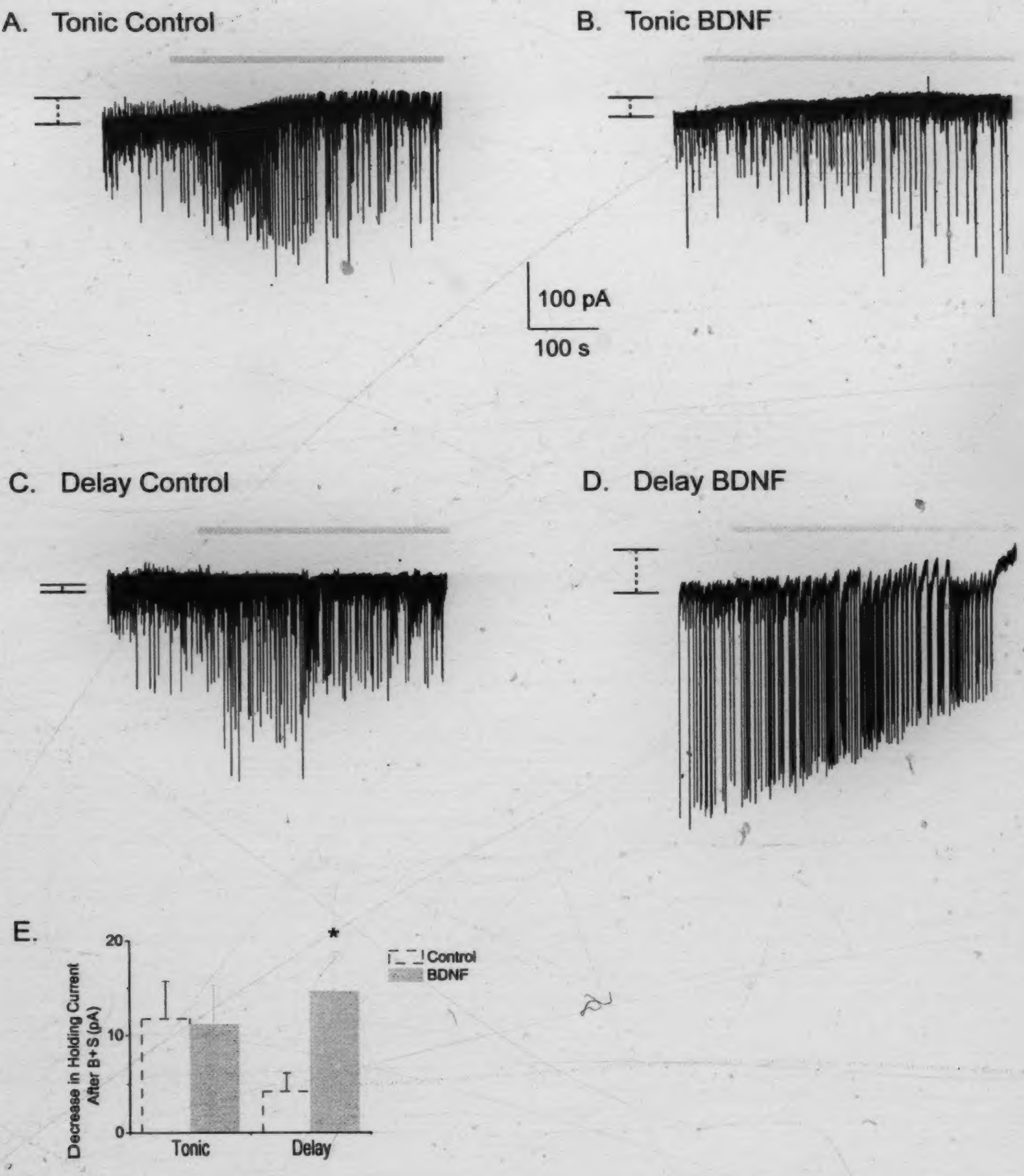
A. Tonic Control
B. Tonic BDNF
100 pA
100 s
C. Delay Control
D. Delay BDNF
E.
Decrease in Holding Current After B+S (pA)
20
10
0
Tonic
Delay
*
Control
BDNF

Figure 5-7: Effect of BDNF treatment on presynaptic inhibition of tonic and delay neurons.

A: Left is a sample 1 min recording trace of sEPSCs recorded from a delay neuron in a control DMOTC slice. Right trace shows another 1 min sEPSC recording from the same delay cell following application of 10 μM bicuculline and 1 μM strychnine (B+S). Lower insets shows a faster time scale for 1s of recording in the above trace indicated by the grey line. B: Left is a sample 1 min recording trace of sEPSCs recorded from a delay neuron in a BDNF-treated DMOTC slice. Right trace shows another 1 min sEPSC recording from the same delay cell following application of B+S. Lower insets shows a faster time scale for 1s of recording in the above trace indicated by the grey line. Note the increase in the frequency of sEPSCs following addition of B+S, similar to controls. C and D: The percent increase in mean sEPSC frequency (C) and sEPSC amplitude (D) following application of B+S. The percent increase was calculated from the mean value from BDNF-treated neurons subtracted from the mean value from control neurons normalized to the control value. Controls (n = 11 for tonic, n = 10 for delay) in blue dashed bars, and BDNF-treated groups (n = 11 for tonic, n = 15 for delay) in orange bars are shown. Error bars indicate SEM. For Student's unpaired t-test, # = $p<0.01$.

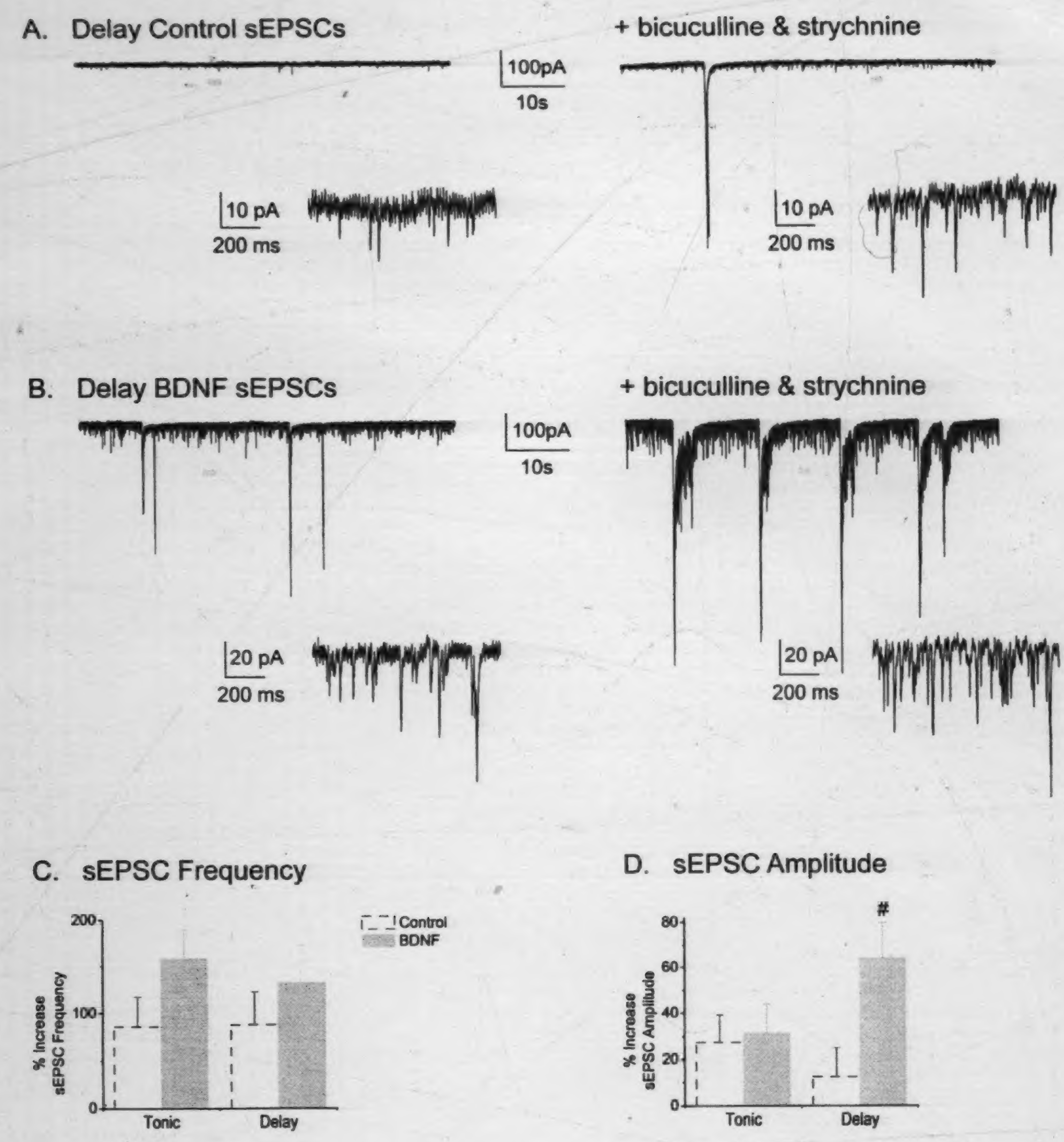
A. Delay Control sEPSCs
100pA
10s
10 pA
200 ms
+ bicuculline & strychnine
10 pA
200 ms
B. Delay BDNF sEPSCs
100pA
10s
20 pA
200 ms
+ bicuculline & strychnine
20 pA
200 ms
C. sEPSC Frequency
Control
BDNF
% Increase sEPSC Frequency
200
100
0
Tonic
Delay
D. sEPSC Amplitude
#
% Increase sEPSC Amplitude
80
60
40
20
0
Tonic
Delay

Figure 5-8: Effect of BDNF on immunohistochemically identified populations of GAD-positive and GAD-negative neurons.

A to D: Cumulative probability plots of sEPSCs amplitude (A and C) and inter-event intervals (B and D). E to H: Cumulative probability plots of sIPSCs amplitude (E and G) and inter-event intervals (F and H). The first 100 sEPSC or sIPSC events following the 1st minute of recordings from each cell were pooled in order to construct cumulative distribution plots. For GAD-positive neurons, 1100 events from control DMOTC slices and 1100 events from BDNF-treated neurons were taken. For GAD-negative neurons, 800 events from control DMOTC slices and 700 events from BDNF-treated neurons were taken. *P values* derived from the KS test indicated on graphs. I and J: Effects of BDNF on mean amplitude and IEI of sEPSC (left) and sIPSC (right) events of GAD-positive (I) and GAD-negative (J) populations of neurons. The same events used to construct cumulative probability plots were used, so the same n values apply. Controls are shown in blue dashed bars and the BDNF-treated group shown in orange bars. Error bars indicate SEM. For Student's unpaired t-test, * = $p<0.05$, # = $p<0.01$, § = $p< 0.001$.

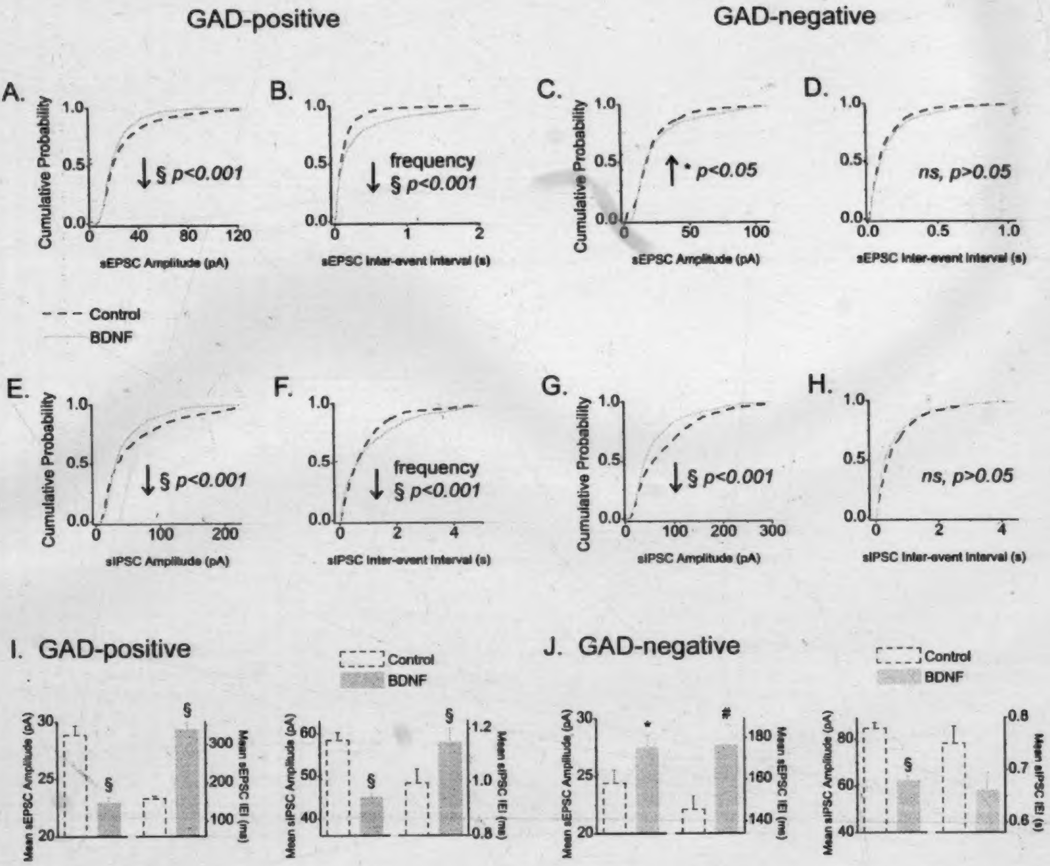
GAD-positive
GAD-negative
A.
Cumulative Probability
1.0
0.5
0.0
0
40
80
120
↓ § p<0.001
sEPSC Amplitude (pA)
B.
frequency
↓ § p<0.001
sEPSC Inter-event Interval (s)
C.
↑ * p<0.05
0
50
100
sEPSC Amplitude (pA)
D.
ns, p>0.05
0.0
0.5
1.0
sEPSC Inter-event Interval (s)
Control
BDNF
E.
↓ § p<0.001
0
100
200
sIPSC Amplitude (pA)
F.
frequency
↓ § p<0.001
0
2
4
sIPSC Inter-event Interval (s)
G.
↓ § p<0.001
0
100
200
300
sIPSC Amplitude (pA)
H.
ns, p>0.05
sIPSC Inter-event Interval (s)
I. GAD-positive
Control
BDNF
Mean sEPSC Amplitude (pA)
30
25
20
§
§
Mean sEPSC IEI (ms)
300
200
100
Mean sIPSC Amplitude (pA)
60
50
40
§
§
Mean sIPSC IEI (ms)
1.2
1.0
0.8
J. GAD-negative
Control
BDNF
Mean sEPSC Amplitude (pA)
30
25
20
*
#
Mean sEPSC IEI (ms)
180
160
140
Mean sIPSC Amplitude (pA)
80
60
40
§
Mean sIPSC IEI (s)
0.8
0.7
0.6

5.6 References

Baba H, Ji RR, Kohno T, Moore KA, Ataka T, Wakai A, Okamoto M, Woolf CJ (2003) Removal of GABAergic inhibition facilitates polysynaptic A fiber-mediated excitatory transmission to the superficial spinal dorsal horn. Mol Cell Neurosci 24: 818-830.

Baccei ML, Fitzgerald M (2004) Development of GABAergic and glycinergic transmission in the neonatal rat dorsal horn. J Neurosci 24: 4749-4757.

Bai D, Zhu G, Pennefather P, Jackson MF, MacDonald JF, Orser BA (2001) Distinct functional and pharmacological properties of tonic and quantal inhibitory postsynaptic currents mediated by gamma-aminobutyric acid(A) receptors in hippocampal neurons. Mol Pharmacol 59: 814-824.

Balasubramanyan S (2006) Changes in the properties of Substantia gelatinosa neurons induced by peripheral nerve injury. PhD Thesis Dissertation.

Balasubramanyan S, Stemkowski PL, Stebbing MJ, Smith PA (2006) Sciatic chronic constriction injury produces cell-type-specific changes in the electrophysiological properties of rat substantia gelatinosa neurons. J Neurophysiol 96: 579-590.

Bardoni R, Ghirri A, Salio C, Prandini M, Merighi A (2007) BDNF-mediated modulation of GABA and glycine release in dorsal horn lamina II from postnatal rats. Dev Neurobiol 67: 960-975.

Brickley SG, Cull-Candy SG, Farrant M (1996) Development of a tonic form of synaptic inhibition in rat cerebellar granule cells resulting from persistent activation of GABAA receptors. J Physiol 497 (Pt 3): 753-759.

Cordero-Erausquin M, Coull JA, Boudreau D, Rolland M, De Koninck Y (2005) Differential maturation of GABA action and anion reversal potential in spinal lamina I neurons: impact of chloride extrusion capacity. J Neurosci 25: 9613-9623.

Coull JA, Beggs S, Boudreau D, Boivin D, Tsuda M, Inoue K, Gravel C, Salter MW, De Koninck Y (2005) BDNF from microglia causes the shift in neuronal anion gradient underlying neuropathic pain. Nature 438: 1017-1021.

Coull JA, Boudreau D, Bachand K, Prescott SA, Nault F, Sik A, De Koninck P, De Koninck Y (2003) Trans-synaptic shift in anion gradient in spinal lamina I neurons as a mechanism of neuropathic pain. Nature 424: 938-942.

Eaton MJ, Plunkett JA, Karmally S, Martinez MA, Montanez K (1998) Changes in GAD- and GABA- immunoreactivity in the spinal dorsal horn after peripheral nerve injury and promotion of recovery by lumbar transplant of immortalized serotonergic precursors. J Chem Neuroanat 16: 57-72.

Heinke B, Ruscheweyh R, Forsthuber L, Wunderbaldinger G, Sandkuhler J (2004) Physiological, neurochemical and morphological properties of a subgroup of GABAergic spinal lamina II neurones identified by expression of green fluorescent protein in mice. J Physiol 560: 249-266.

Hughes DI, Mackie M, Nagy GG, Riddell JS, Maxwell DJ, Szabo G, Erdelyi F, Veress G, Szucs P, Antal M, Todd AJ (2005) P boutons in lamina IX of the rodent spinal cord express high levels of glutamic acid decarboxylase-65 and originate from cells in deep medial dorsal horn. Proc Natl Acad Sci U S A 102: 9038-9043.

Keller AF, Coull JA, Chery N, Poisbeau P, De Koninck Y (2001) Region-specific developmental specialization of GABA-glycine cosynapses in laminas I-II of the rat spinal dorsal horn. J Neurosci 21: 7871-7880.

Lu VB, Moran TD, Balasubramanyan S, Alier KA, Dryden WF, Colmers WF, Smith PA (2006) Substantia Gelatinosa neurons in defined-medium organotypic slice culture are similar to those in acute slices from young adult rats. Pain 121: 261-275.

Lu Y, Perl ER (2003) A specific inhibitory pathway between substantia gelatinosa neurons receiving direct C-fiber input. J Neurosci 23: 8752-8758.

Lu Y, Perl ER (2005) Modular organization of excitatory circuits between neurons of the spinal superficial dorsal horn (laminae I and II). J Neurosci 25: 3900-3907.

Mackie M, Hughes DI, Maxwell DJ, Tillakaratne NJ, Todd AJ (2003) Distribution and colocalisation of glutamate decarboxylase isoforms in the rat spinal cord. Neuroscience 119: 461-472.

Moore KA, Kohno T, Karchewski LA, Scholz J, Baba H, Woolf CJ (2002) Partial peripheral nerve injury promotes a selective loss of GABAergic inhibition in the superficial dorsal horn of the spinal cord. J Neurosci 22: 6724-6731.

Moran TD, Colmers WF, Smith PA (2004) Opioid-like actions of neuropeptide Y in rat substantia gelatinosa: Y1 suppression of inhibition and Y2 suppression of excitation. J Neurophysiol 92: 3266-3275.

Pezet S, Cunningham J, Patel J, Grist J, Gavazzi I, Lever IJ, Malcangio M (2002) BDNF modulates sensory neuron synaptic activity by a facilitation of GABA transmission in the dorsal horn. Mol Cell Neurosci 21: 51-62.

Polgar E, Gray S, Riddell JS, Todd AJ (2004) Lack of evidence for significant neuronal loss in laminae I-III of the spinal dorsal horn of the rat in the chronic constriction injury model. Pain 111: 144-150.

Polgar E, Hughes DI, Arham AZ, Todd AJ (2005) Loss of neurons from laminas I-III of the spinal dorsal horn is not required for development of tactile allodynia in the spared nerve injury model of neuropathic pain. J Neurosci 25: 6658-6666.

Polgar E, Hughes DI, Riddell JS, Maxwell DJ, Puskar Z, Todd AJ (2003) Selective loss of spinal GABAergic or glycinergic neurons is not necessary for development of thermal hyperalgesia in the chronic constriction injury model of neuropathic pain. Pain 104: 229-239.

Prescott SA, Sejnowski TJ, De Koninck Y (2006) Reduction of anion reversal potential subverts the inhibitory control of firing rate in spinal lamina I neurons: towards a biophysical basis for neuropathic pain. Mol Pain 2: 32.

Scholz J, Broom DC, Youn DH, Mills CD, Kohno T, Suter MR, Moore KA, Decosterd I, Coggeshall RE, Woolf CJ (2005) Blocking caspase activity prevents transsynaptic neuronal apoptosis and the loss of inhibition in lamina II of the dorsal horn after peripheral nerve injury. J Neurosci 25: 7317-7323.

Sivilotti L, Woolf CJ (1994) The contribution of GABAA and glycine receptors to central sensitization: disinhibition and touch-evoked allodynia in the spinal cord. J Neurophysiol 72: 169-179.

Turrigiano GG, Leslie KR, Desai NS, Rutherford LC, Nelson SB (1998) Activity-dependent scaling of quantal amplitude in neocortical neurons. Nature 391: 892-896.

CHAPTER 6

BDNF AND MORPHOLOGICAL CLASSES OF NEURONS:

Neuron type-specific effects of brain-derived neurotrophic factor on morphologically-identified populations of dorsal horn neurons.

6.1 Introduction

Recent studies have unveiled the identity of several different neuronal phenotypes within dorsal horn neurons of the spinal cord (Grudt and Perl, 2002; Heinke et al., 2004; Lu and Perl, 2003; Lu and Perl, 2005). Diverse populations of dorsal horn neurons is not a surprising finding, but nonetheless very important considering both inhibitory and excitatory neurons in the CNS play very different roles in neuronal communication. Moreover, there was a correlation between cell morphology and action potential firing pattern (Figure 1-2) providing some clues as to the anatomical organization and functionality of neurons in this region.

Preliminary examination of control neurons in DMOTC slices revealed populations of neurons corresponding to the dorsal horn phenotypes described in these studies (Figure 3-2A-D). I wanted to investigate the effect of long-term BDNF exposure on these populations of neurons in order to gain a better understanding of BDNF's effects on nociceptive signalling in the dorsal horn. Also, I was interested if the selectivity of BDNF action observed thus far applied to these identified populations of nociceptive signalling neurons. So, results from electrophysiologically classified neurons were subdivided according to cell morphology and findings from the main populations of dorsal horn neurons are described in this chapter.

Some of these findings have appeared in abstract form (Smith et al., 2005).

6.2 Methods

Refer to Chapter 2: General methods, for description of methods and techniques employed in this chapter.

6.3 Results

6.3.1 No effect of BDNF on distribution of morphologically and electrophysiologically classified populations of dorsal horn neurons

As was previously shown, a variety of different cell mophologies are exhibited by biocytin-filled neurons in DMOTCs (Figure 3-2A to C, see Chapter 3 for details on criteria for morphological classification). Correlating cell morphology of recorded neurons with their action potential firing pattern revealed three distinct classes of dorsal horn neurons. The tonic firing, islet-central cells (TIC), the 'delay' firing radial cells (DR) and the 'delay' firing vertical cells (DV) were the largest correlated groups (Figure 6-1A). These groups of cells are the same neuronal phenotypes identified by Lu and Perl (2003 and 2005) in the dorsal horn of acute spinal cord slices. Following BDNF treatment, the same correlations patterns between cell morphology and firing pattern appeared (Figure 6-1B). No significant difference in the occurrence of these populations compared to controls was observed (χ^2 test, $p>0.2$ for all comparisons). Thus, BDNF does not induce alterations in neuronal phenotype nor shift the prevalence of any neuronal population.

6.3.2 Minimal neuronal sprouting induced by BDNF

BDNF is a neurotrophin capable of inducing neuronal sprouting in spinal neurons (Koda et al., 2004; Scott et al., 2005). To examine this possible effect of BDNF, the longest putative dendrite was compared between morphologically classified control and BDNF-treated neurons.

The mean of the longest dendrite in all three cell morphologies described differed significantly from one another (Table 6-1, ANOVA-SNK test, $p<0.05$ for both controls and BDNF-treated groups). Vertical neurons on average have the longest dendrites and radial neurons possess the shortest dendrites. This pattern did not change following BDNF treatment (Table 6-1). Moreover, the mean length of the longest dendrite in islet-central and vertical neurons did not change following BDNF treatment (unpaired t-test, $p>0.3$). Only in radial cells was a significant difference found in the longest dendrite length (unpaired t-test, $p<0.05$). However, since radial cells often exhibit a bushy dendritic tree, the average length of these dendrites was also measured and no significant change was observed following BDNF treatment (Table 6-1, unpaired t-test, $p>0.6$). The longest projection measured from radial cells may be the axon which can be modulated by BDNF (Boyd and Gordon, 2001; Koda et al., 2004), but the dendrites within the dendritic tree appear to be unaffected by BDNF.

Therefore, there were no gross morphological changes to the length of dendrites in dorsal horn neurons following BDNF treatment.

6.3.3 Effect of BDNF on synaptic activity of TIC neurons

The effects of BDNF on the sEPSC amplitude and inter-event interval of TIC neurons are illustrated in Figure 6-2A and B, respectively, and a comparison of mean values is presented in Figure 6-2C. As shown, BDNF significantly reduced the amplitude and frequency of sEPSCs (KS-test and unpaired t-test, $p<0.001$ for sEPSC amplitude and $p<0.01$ for sEPSC frequency).

The effects of BDNF on the sIPSC amplitude and inter-event interval of TIC neurons are illustrated in Figure 6-2D and E, respectively, and a comparison of mean values is presented in Figure 6-2F. Similar to its effects on sEPSCs, BDNF significantly reduced the amplitude and frequency of sIPSCs (KS-test and unpaired t-test, $p<0.001$ for all comparisons).

These effects of BDNF are comparable to the effects of BDNF on GAD-positive neurons shown in the previous chapter (Figure 5-8A, B, E and F); suggesting TIC neurons may also include inhibitory, GAD-positive neurons.

6.3.4 Effect of BDNF on synaptic activity of DR neurons

The effects of BDNF on the sEPSC amplitude and inter-event interval of DR neurons are illustrated in Figure 6-3A and B, respectively, and a comparison of mean values is presented in Figure 6-3C. As shown, BDNF significantly increased the amplitude and frequency of sEPSCs (KS-test and unpaired t-test, $p<0.001$ for all comparisons).

The effects of BDNF on the sIPSC amplitude and inter-event interval of DR neurons are illustrated in Figure 6-3D and E, respectively, and a comparison of mean values is presented in Figure 6-3F. Similar to its effects on sEPSCs, BDNF significantly increased the amplitude and frequency of sIPSCs (KS-test and unpaired t-test, $p<0.001$ for all comparisons).

These effects of BDNF are comparable to the effects of BDNF on all 'delay' neurons shown previously (Figures 4-4B, G and 5-1B, G); suggesting a large proportion of total 'delay' firing neurons are represented by this population of neurons which possess a radial morphology.

6.3.5 Effect of BDNF on synaptic activity of DV neurons

The effects of BDNF on the sEPSC amplitude and inter-event interval of DV neurons are illustrated in Figure 6-4A and B, respectively, and a comparison of mean values is presented in Figure 6-4C. As shown, BDNF significantly reduced the amplitude and frequency of sEPSCs (KS-test and unpaired t-test, $p<0.01$ for sEPSC amplitude and $p<0.001$ for sEPSC frequency).

The effects of BDNF on the sIPSC amplitude and inter-event interval of DV neurons are illustrated in Figure 6-4D and E, respectively, and a comparison of mean values is presented in Figure 6-4F. Similar to its effects on sEPSCs, BDNF significantly decreased the amplitude and frequency of sIPSCs (KS-test and unpaired t-test, $p<0.001$ for sIPSC amplitude and $p<0.05$ for sIPSC frequency).

These effects of BDNF are comparable to the effects of BDNF on GAD-positive neurons shown in Chapter 5 (Figure 5-8A, B, E and F); suggesting DV neurons may also include inhibitory, GAD-positive neurons. Also, DV neurons probably comprise a small proportion of the total 'delay' firing neurons in the dorsal horn since synaptic activity was altered in the opposite direction by BDNF in the overall 'delay' population.

6.4 Discussion

The main findings of this chapter are 1) BDNF does not appear to induce sprouting of dorsal horn neurons nor does it promote the loss of neuronal populations.

There were minimal changes in dendritic length (Table 6-1) and no change in the proportion of each morphologically and electrophysiologically categorized cell type (Figure 6-1). Therefore, it is unlikely that the overall electrophysiological actions of BDNF are the result of gross morphological changes as a result of its 'traditional' neurotrophic action. 2) Classifying dorsal horn neurons according to cell morphology and action potential firing pattern revealed enhancement of synaptic activity in a select population of dorsal horn neurons. Only DR neurons received increased excitatory and inhibitory synaptic transmission (Figure 6-3) whereas all other cell populations, TIC and DV, received less (Figures 6-2 and 6-4). 3) Similarity of BDNF's effect on TIC and DV neurons to its effects on GAD-positive neurons strongly suggests these classes of dorsal horn neurons are inhibitory. Likewise, it is doubtful DR neurons are inhibitory, GAD expressing neurons. 4) Selectivity of BDNF action emphasizes the importance of identifying specific populations of dorsal horn neurons. The actions of BDNF have been shown to be diverse and sometimes opposite in different neuronal cell types. Thus, the identification of distinct neuronal phenotypes has been essential in assessing the effects of long-term BDNF exposure on nociceptive signalling in the dorsal horn.

6.4.1 Effect of BDNF on TIC neurons

The islet neurons described extensively within the Lamina II region of the dorsal horn (Bennett et al., 1980; Cervero and Iggo, 1980; Gobel, 1975; Gobel, 1978; Grudt and Perl, 2002; Todd and Lewis, 1986) have been shown to express markers of GABAergic neurons such as GAD (Bardoni et al., 2007; Heinke et al., 2004). The similarity of responses from TIC (Figure 6-2) and GAD-positive neurons (Figure 5-8) following long-term BDNF treatment also supports the notion of TIC neurons as inhibitory. Furthermore, islet neurons, which fire action potentials in a tonic pattern (TIC neurons), release inhibitory neurotransmitters on to postsynaptic targets (Lu and Perl, 2003). Unfortunately, our preparation of transverse slices does not permit differentiation between islet and central neurons especially since neurons with a central morphology have been implicated as excitatory neurons (Lu and Perl, 2005; Todd and McKenzie, 1989). However, the mistaken classification of a central neuron with TIC neurons will be minimal since excitatory central neurons normally display a phasic firing pattern (Lu and Perl, 2005).

Ultrastructural studies have localized full-length TrkB receptors within islet neurons in the dorsal horn (Bardoni et al., 2007). Therefore, BDNF could have a direct postsynaptic effect on TIC neurons which could account for the decrease in sEPSC amplitude (Figure 6-2A) or sIPSC amplitude (Figure 6-2D). Furthermore, since islet neurons are most likely inhibitory neurons (Heinke et al., 2004; Lu and Perl, 2003; Todd and McKenzie, 1989), localization of TrkB receptors near axonal boutons of islet neurons (Bardoni et al., 2007) suggests BDNF may modulate release of inhibitory neurotransmitters. Thus, a BDNF-induced decrease in sIPSC amplitude (Figure 6-2A) and frequency (Figure 6-2E) could be attributed to reduced inhibitory neurotransmitter release from other islet neurons. Moreover, TIC cells have been shown to synapse on to central phasic neurons in the dorsal horn (Lu and Perl, 2003), and a decrease in sIPSC amplitude was also observed in phasic neurons (Figure 5-1D) following BDNF treatment.

Reduced excitatory drive to TIC neurons (Figure 6-2A to C) combined with a possible direct suppression of inhibitory neurotransmitter release by BDNF implies reduced activity from these inhibitory neurons. A loss in overall inhibitory tone could increase excitation in the dorsal horn and this is a suggested means of instigating neuropathic pain (Baba et al., 2003; Moore et al., 2002; Sivilotti and Woolf, 1994).

6.4.2 Effect of BDNF on DR neurons

A majority of the 'delay' firing neurons expressed a radial morphology (Table 6-1, Figure 6-1). The synaptic connections DR neurons make with other dorsal horn neurons is unclear. However, based on their short dendrites, DR neurons are likely local interneurons in the dorsal horn. "Multipolar" cells along the border of Lamina I and II in the dorsal horn have similar features as DR neurons (Prescott and De Koninck, 2002) and have also been implicated as modulators of projection neurons in Lamina I.

Overall excitatory and inhibitory synaptic activity to DR neurons increased following BDNF treatment (Figure 6-3). Enhanced spontaneous excitatory activity could arise from primary afferents which express TrkB receptors (Bardoni et al., 2007; Karchewski et al., 2002; Michael et al., 1999), and alterations in postsynaptic receptor expression (Figure 4-8F to H) could account for the larger sEPSC amplitude observed following BDNF treatment. Regarding inhibitory activity, BDNF has been shown to enhance release of inhibitory neurotransmitters from central neurons (Pezet et al., 2002) which may selectively synapse on to DR neurons.

The overall effect of increased excitatory and inhibitory synaptic activity on the activation of putative excitatory dorsal horn neurons is not clear from these experiments. However, the occurrence of sEPSCs is greater than sIPSCs (compare Figure 6-3C and F) suggesting an increase in excitatory drive may have a greater impact on DR neurons than changes in inhibitory activity. Furthermore, presynaptic inhibition of excitatory inputs to 'delay' neurons (Figure 5-7C) was not affected by BDNF since the increase in frequency of sEPSCs did not change following pharmacological removal of inhibition. Increased activation of potentially excitatory dorsal horn neurons would increase excitatory communication between neurons which could lead to the enhanced excitation in the dorsal horn seen during neuropathic pain (Dalal et al., 1999; Laird and Bennett, 1993).

6.4.3 Effect of BDNF on DV neurons

DV neurons have been shown to release excitatory neurotransmitters (Lu and Perl, 2005). However, the comparable effects of BDNF on synaptic transmission to DV (Figure 6-4) and GAD-positive neurons (Figure 5-8) suggest that these neuronal groups may be similar. Furthermore, over 80% of vertical neurons in both control and BDNF groups were GAD-positive (data not shown). Other studies report similar findings (Heinke et al., 2004) where 14% of GAD-expressing neurons in Lamina II have a vertical morphology. Therefore this group may represent a small class of inhibitory neurons in the dorsal horn since inhibitory neurons mainly express the islet morphology (Heinke et al., 2004; Todd and McKenzie, 1989). Although inhibitory neurons normally do not express a 'delay' firing pattern (Dougherty et al., 2005; Hantman et al., 2004; Heinke et al., 2004), these DV neurons compose a small proportion of total 'delay' firing neurons as a majority of the 'delay' firing neurons have a radial morphology, DR neurons, which are thought to be excitatory (see above section).

Reduced excitatory synaptic activity following BDNF treatment could arise from reduced output of Aδ fibres (Kohno et al., 2003) which form contacts with DV neurons

(Yasaka et al., 2007). Medium to large diameter DRG neurons, which may correspond to Aδ and Aβ fibres, increase expression of TrkB following nerve injury (Karchewski et al., 2002; Michael et al., 1999) and thus may be modulated by the elevated levels of BDNF following nerve injury (Miletic and Miletic, 2002; Walker et al., 2001). Reduced inhibitory synaptic activity could also arise from reduced output of TIC neurons (see above); however, it is not known if these inhibitory neurons synapse on to DV neurons.

The overall result of reduced synaptic activity to presumed inhibitory DV neurons is not entirely clear; but since spontaneous inhibitory activity in central neurons is largely dependent on action potential-dependent mechanisms (Figure 5-3C), a reduction in excitatory drive likely results in less activation and spontaneous activity of DV neurons. Reduced excitation of inhibitory neurons would thus lead to less inhibition in the spinal dorsal horn which could initiate neuropathic pain (Baba et al., 2003; Moore et al., 2002; Sivilotti and Woolf, 1994).

6.5 Conclusions

The identified morphological classes of neurons found in DMOTC slices correlate well with what has been described in the literature. Long-term BDNF exposure has selective effects on excitatory and inhibitory synaptic activity on these populations of identified dorsal horn neurons. Also, these changes appear to promote an increase in overall dorsal horn excitability, a possible indication of established central sensitization mechanisms.

Table 6-1: Comparison of dendritic lengths of morphologically identified populations of dorsal horn neurons following BDNF treatment.

Mean values presented with SEM. N values in brackets. For Student's unpaired t-test, * = $p<0.05$.

	Control	***BDNF-treated***
Islet-Central	184.1 ± 15.6 µm (14)	213.7 ± 40.9 µm (10)
Vertical	242.4 ± 19.0 µm (7)	285.9 ± 41.0 µm (12)
Radial	115.1 ± 12.9 µm (26)	161.3 ± 17.4 µm (17)*
Radial (average dendritic tree)	107.7 ± 13.3 µm	118.1 ± 16.4 µm

Figure 6-1: Effect of BDNF on distribution of morphologically and electrophysiologically identified populations of dorsal horn neurons.

A: Correlation of cell morphology with electrophysiological firing pattern for neurons recorded from control DMOTC slices (n = 73). Colour coded scale bar indicating percentage of cells with the identified morphology expressing the various action potential firing patterns is shown on the right. Note the high correlation between tonic firing islet-central cells, delay firing radial cells and delay firing vertical cells. B: Correlation of cell morphology with electrophysiological firing pattern for neurons recorded from BDNF-treated DMOTC slices (n = 43). Note the same groups of well correlated neurons as controls appear in the BDNF group.

A. Control

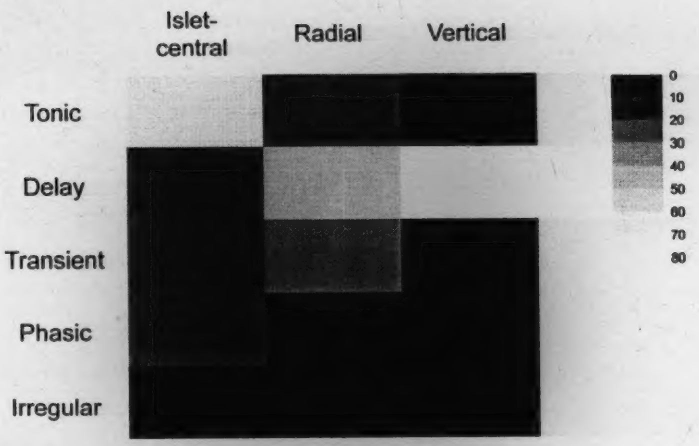

B. BDNF

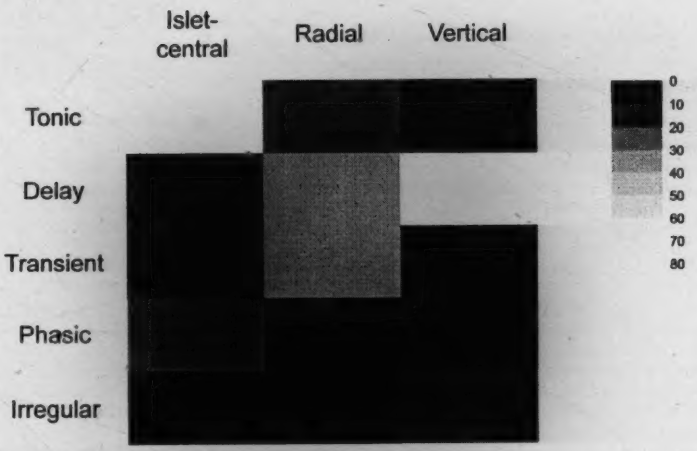

Figure 6-2: Effects of BDNF on spontaneous excitatory and inhibitory synaptic transmission in tonic firing, islet-central neurons (TIC).

A and B: Cumulative probability plots for sEPSC amplitude (A) and inter-event interval (B) for tonic firing neurons with an islet-central morphology (TIC). The first 100 events following the 1st minute of recordings from each cell were pooled in order to construct cumulative distribution plots. For sEPSCs, 1200 events from control DMOTC slices, and 1200 events from BDNF-treated DMOTC slices were analyzed. *P values* derived from the KS test indicated on graphs. C: Effects of BDNF on mean amplitude (left) and IEI (right) of sEPSC events. The same events used to construct cumulative probability plots were used, so the same n values apply. D and E: Cumulative probability plots for sIPSC amplitude (D) and inter-event interval (E) for TIC neurons. The first 100 events following the 1st minute of recordings from each cell were pooled in order to construct cumulative distribution plots. For sIPSCs, 1030 events from control DMOTC slices and 448 events from BDNF-treated DMOTC slices were analyzed. *P values* derived from the KS test indicated on graphs. F: Effects of BDNF on mean amplitude (left) and IEI (right) of sIPSC events. The same events used to construct cumulative probability plots were used, so the same n values apply. Error bars indicate SEM. For Student's unpaired t-test, # = $p<0.01$, § = $p< 0.001$.

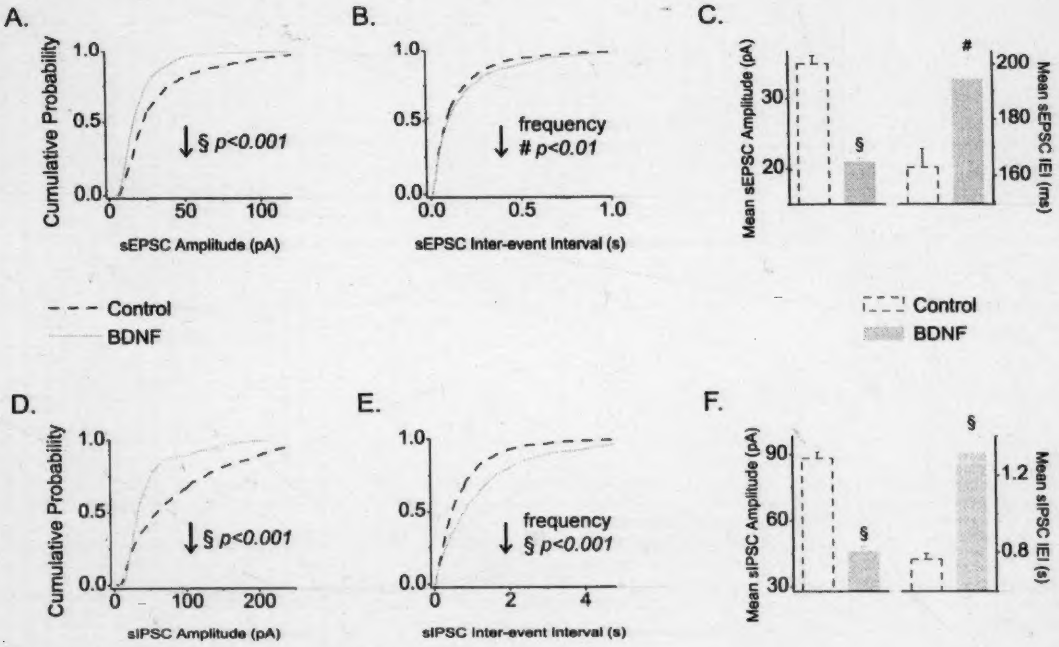
A.
Cumulative Probability
1.0
0.5
0.0
0
50
100
sEPSC Amplitude (pA)
↓ § p<0.001
B.
1.0
0.5
0.0
0.0
0.5
1.0
sEPSC Inter-event Interval (s)
↓ frequency
# p<0.01
C.
Mean sEPSC Amplitude (pA)
30
20
§
#
200
180
160
Mean sEPSC IEI (ms)
- - - Control
BDNF
Control
BDNF
D.
Cumulative Probability
1.0
0.5
0.0
0
100
200
sIPSC Amplitude (pA)
↓ § p<0.001
E.
1.0
0.5
0.0
0
2
4
sIPSC Inter-event Interval (s)
↓ frequency
§ p<0.001
F.
Mean sIPSC Amplitude (pA)
90
60
30
§
§
1.2
0.8
Mean sIPSC IEI (s)

Figure 6-3: Effects of BDNF on spontaneous excitatory and inhibitory synaptic transmission in delay firing, radial neurons (DR).

A and B: Cumulative probability plots for sEPSC amplitude (A) and inter-event interval (B) for delay firing neurons with a radial morphology (DR). The first 100 events following the 1st minute of recordings from each cell were pooled in order to construct cumulative distribution plots. For sEPSCs, 1400 events from control DMOTC slices, and 1400 events from BDNF-treated DMOTC slices were analyzed. *P values* derived from the KS test indicated on graphs. C: Effects of BDNF on mean amplitude (left) and IEI (right) of sEPSC events. The same events used to construct cumulative probability plots were used, so the same n values apply. D and E: Cumulative probability plots for sIPSC amplitude (D) and inter-event interval (E) for DR neurons. The first 100 events following the 1st minute of recordings from each cell were pooled in order to construct cumulative distribution plots. For sIPSCs, 584 events from control DMOTC slices, and 978 events from BDNF-treated DMOTC slices were analyzed. *P values* derived from the KS test indicated on graphs. F: Effects of BDNF on mean amplitude (left) and IEI (right) of sIPSC events. The same events used to construct cumulative probability plots were used, so the same n values apply. Error bars indicate SEM. For Student's unpaired t-test, § = $p < 0.001$.

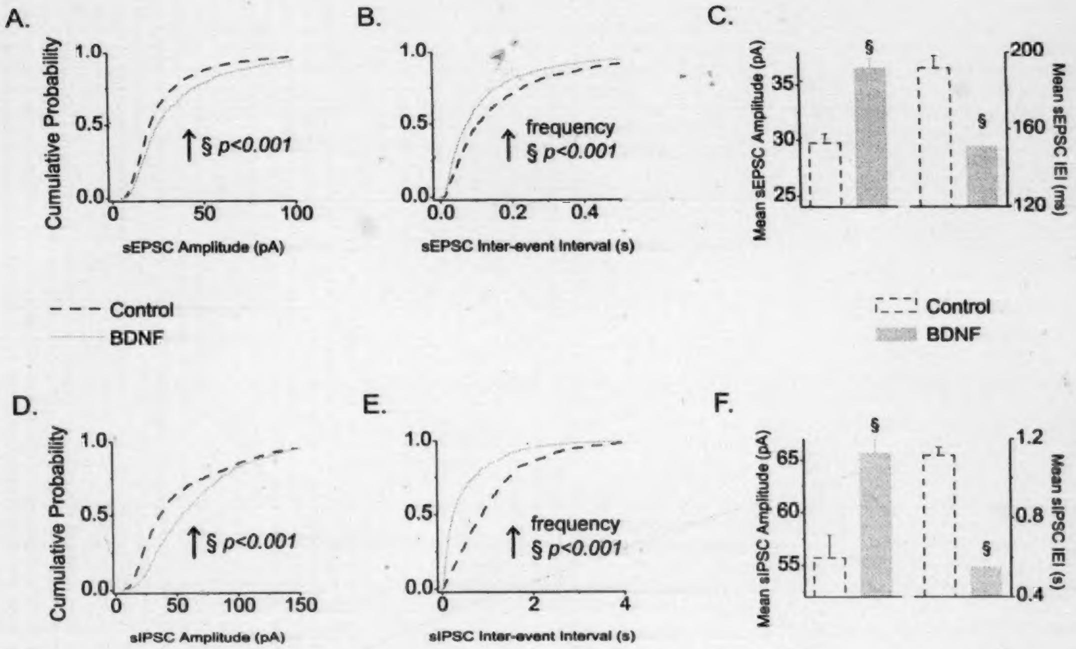
A.
Cumulative Probability
1.0
0.5
0.0
0
50
100
sEPSC Amplitude (pA)
↑ § p<0.001
B.
1.0
0.5
0.0
0.0
0.2
0.4
sEPSC Inter-event Interval (s)
↑ frequency
§ p<0.001
C.
Mean sEPSC Amplitude (pA)
35
30
25
§
§
200
160
120
Mean sEPSC IEI (ms)
Control
BDNF
Control
BDNF
D.
Cumulative Probability
1.0
0.5
0.0
0
50
100
150
sIPSC Amplitude (pA)
↑ § p<0.001
E.
1.0
0.5
0.0
0
2
4
sIPSC Inter-event Interval (s)
↑ frequency
§ p<0.001
F.
Mean sIPSC Amplitude (pA)
65
60
55
§
§
1.2
0.8
0.4
Mean sIPSC IEI (s)

Figure 6-4: Effects of BDNF on spontaneous excitatory and inhibitory synaptic transmission in delay firing, vertical neurons (DV).

A and B: Cumulative probability plots for sEPSC amplitude (A) and inter-event interval (B) for delay firing neurons with a vertical morphology (DV). The first 100 events following the 1st minute of recordings from each cell were pooled in order to construct cumulative distribution plots. For sEPSCs, 1000 events from control DMOTC slices, and 1310 events from BDNF-treated DMOTC slices were analyzed. *P values* derived from the KS test indicated on graphs. C: Effects of BDNF on mean amplitude (left) and IEI (right) of sEPSC events. The same events used to construct cumulative probability plots were used, so the same n values apply. D and E: Cumulative probability plots for sIPSC amplitude (D) and inter-event interval (E) for DV neurons. The first 100 events following the 1st minute of recordings from each cell were pooled in order to construct cumulative distribution plots. For sIPSCs, 502 events from control DMOTC slices, and 316 events from BDNF-treated DMOTC slices were analyzed. *P values* derived from the KS test indicated on graphs. F: Effects of BDNF on mean amplitude (left) and IEI (right) of sIPSC events. The same events used to construct cumulative probability plots were used, so the same n values apply. Error bars indicate SEM. For Student's unpaired t-test, * = $p<0.05$, # = $p<0.01$, § = $p<0.001$.

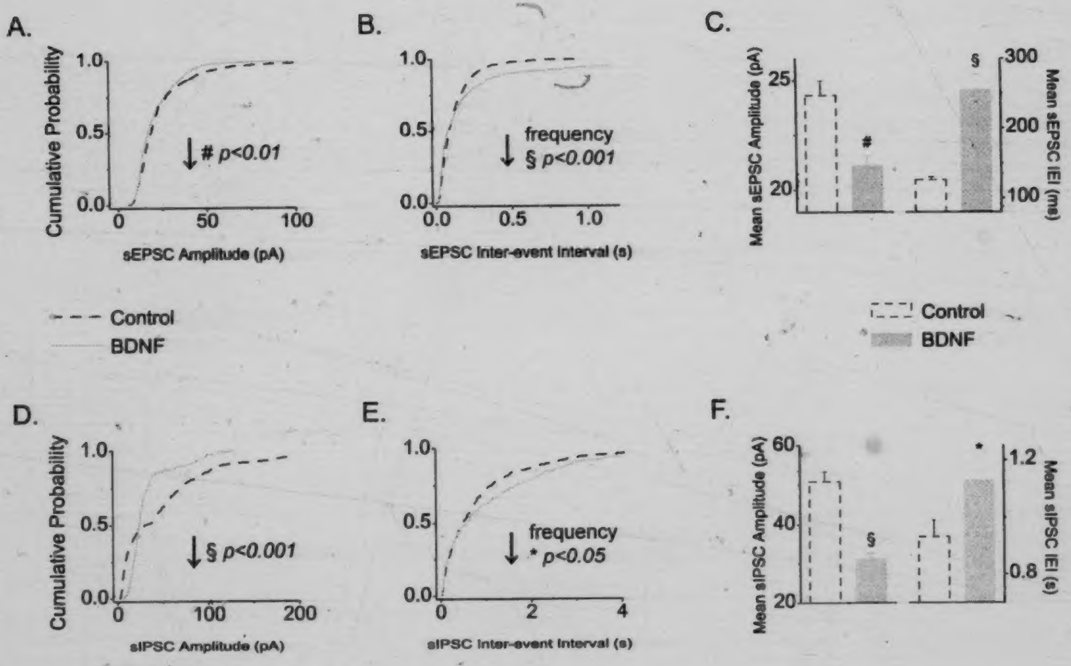
A.
Cumulative Probability
1.0
0.5
0.0
0
50
100
sEPSC Amplitude (pA)
↓ # p<0.01
B.
1.0
0.5
0.0
0.0
0.5
1.0
sEPSC Inter-event Interval (s)
↓ frequency § p<0.001
C.
Mean sEPSC Amplitude (pA)
25
20
#
§
300
200
100
Mean sEPSC IEI (ms)
Control
BDNF
D.
Cumulative Probability
1.0
0.5
0.0
0
100
200
sIPSC Amplitude (pA)
↓ § p<0.001
E.
1.0
0.5
0.0
0
2
4
sIPSC Inter-event Interval (s)
↓ frequency * p<0.05
F.
Mean sIPSC Amplitude (pA)
60
40
20
§
*
1.2
0.8
Mean sIPSC IEI (s)

6.6 References

Baba H, Ji RR, Kohno T, Moore KA, Ataka T, Wakai A, Okamoto M, Woolf CJ (2003) Removal of GABAergic inhibition facilitates polysynaptic A fiber-mediated excitatory transmission to the superficial spinal dorsal horn. Mol Cell Neurosci 24: 818-830.

Bardoni R, Ghirri A, Salio C, Prandini M, Merighi A (2007) BDNF-mediated modulation of GABA and glycine release in dorsal horn lamina II from postnatal rats. Dev Neurobiol 67: 960-975.

Bennett GJ, Abdelmoumene M, Hayashi H, Dubner R (1980) Physiology and morphology of substantia gelatinosa neurons intracellularly stained with horseradish peroxidase. J Comp Neurol 194: 809-827.

Boyd JG, Gordon T (2001) The neurotrophin receptors, trkB and p75, differentially regulate motor axonal regeneration. J Neurobiol 49: 314-325.

Cervero F, Iggo A (1980) The substantia gelatinosa of the spinal cord: a critical review. Brain 103: 717-772.

Dalal A, Tata M, Allegre G, Gekiere F, Bons N, Albe-Fessard D (1999) Spontaneous activity of rat dorsal horn cells in spinal segments of sciatic projection following transection of sciatic nerve or of corresponding dorsal roots. Neuroscience 94: 217-228.

Dougherty KJ, Sawchuk MA, Hochman S (2005) Properties of mouse spinal lamina I GABAergic interneurons. J Neurophysiol 94: 3221-3227.

Gobel S (1975) Golgi studies in the substantia gelatinosa neurons in the spinal trigeminal nucleus. J Comp Neurol 162: 397-415.

Gobel S (1978) Golgi studies of the neurons in layer II of the dorsal horn of the medulla (trigeminal nucleus caudalis). J Comp Neurol 180: 395-413.

Grudt TJ, Perl ER (2002) Correlations between neuronal morphology and electrophysiological features in the rodent superficial dorsal horn. J Physiol 540: 189-207.

Hantman AW, van den Pol AN, Perl ER (2004) Morphological and physiological features of a set of spinal substantia gelatinosa neurons defined by green fluorescent protein expression. J Neurosci 24: 836-842.

Heinke B, Ruscheweyh R, Forsthuber L, Wunderbaldinger G, Sandkuhler J (2004) Physiological, neurochemical and morphological properties of a subgroup of GABAergic spinal lamina II neurones identified by expression of green fluorescent protein in mice. J Physiol 560: 249-266.

Karchewski LA, Gratto KA, Wetmore C, Verge VM (2002) Dynamic patterns of BDNF expression in injured sensory neurons: differential modulation by NGF and NT-3. Eur J Neurosci 16: 1449-1462.

Koda M, Hashimoto M, Murakami M, Yoshinaga K, Ikeda O, Yamazaki M, Koshizuka S, Kamada T, Moriya H, Shirasawa H, Sakao S, Ino H (2004) Adenovirus vector-mediated in vivo gene transfer of brain-derived neurotrophic factor (BDNF) promotes rubrospinal axonal regeneration and functional recovery after complete transection of the adult rat spinal cord. J Neurotrauma 21: 329-337.

Kohno T, Moore KA, Baba H, Woolf CJ (2003) Peripheral nerve injury alters excitatory synaptic transmission in lamina II of the rat dorsal horn. J Physiol 548: 131-138.

Laird JM, Bennett GJ (1993) An electrophysiological study of dorsal horn neurons in the spinal cord of rats with an experimental peripheral neuropathy. J Neurophysiol 69: 2072-2085.

Lu Y, Perl ER (2003) A specific inhibitory pathway between substantia gelatinosa neurons receiving direct C-fiber input. J Neurosci 23: 8752-8758.

Lu Y, Perl ER (2005) Modular organization of excitatory circuits between neurons of the spinal superficial dorsal horn (laminae I and II). J Neurosci 25: 3900-3907.

Michael GJ, Averill S, Shortland PJ, Yan Q, Priestley JV (1999) Axotomy results in major changes in BDNF expression by dorsal root ganglion cells: BDNF expression in large trkB and trkC cells, in pericellular baskets, and in projections to deep dorsal horn and dorsal column nuclei. Eur J Neurosci 11: 3539-3551.

Miletic G, Miletic V (2002) Increases in the concentration of brain derived neurotrophic factor in the lumbar spinal dorsal horn are associated with pain behavior following chronic constriction injury in rats. Neurosci Lett 319: 137-140.

Moore KA, Kohno T, Karchewski LA, Scholz J, Baba H, Woolf CJ (2002) Partial peripheral nerve injury promotes a selective loss of GABAergic inhibition in the superficial dorsal horn of the spinal cord. J Neurosci 22: 6724-6731.

Pezet S, Cunningham J, Patel J, Grist J, Gavazzi I, Lever IJ, Malcangio M (2002) BDNF modulates sensory neuron synaptic activity by a facilitation of GABA transmission in the dorsal horn. Mol Cell Neurosci 21: 51-62.

Prescott SA, De Koninck Y (2002) Four cell types with distinctive membrane properties and morphologies in lamina I of the spinal dorsal horn of the adult rat. J Physiol 539: 817-836.

Scott AL, Borisoff JF, Ramer MS (2005) Deafferentation and neurotrophin-mediated intraspinal sprouting: a central role for the p75 neurotrophin receptor. Eur J Neurosci 21: 81-92.

Sivilotti L, Woolf CJ (1994) The contribution of GABAA and glycine receptors to central sensitization: disinhibition and touch-evoked allodynia in the spinal cord. J Neurophysiol 72: 169-179.

Smith PA, Lu V.B., Balasubramanyan S (2005) Chronic constriction injury and brain-derived neurotrophic factor (BDNF) generate similar "pain footprints" in dorsal horn neurons. Program No 748,2 2005 Abstract Viewer/Itinerary Planner Washington, DC: Society for Neuroscience, 2005 Online.

Todd AJ, Lewis SG (1986) The morphology of Golgi-stained neurons in lamina II of the rat spinal cord. J Anat 149: 113-119.

Todd AJ, McKenzie J (1989) GABA-immunoreactive neurons in the dorsal horn of the rat spinal cord. Neuroscience 31: 799-806.

Walker SM, Mitchell VA, White DM, Rush RA, Duggan AW (2001) Release of immunoreactive brain-derived neurotrophic factor in the spinal cord of the rat following sciatic nerve transection. Brain Res 899: 240-247.

Yasaka T, Kato G, Furue H, Rashid MH, Sonohata M, Tamae A, Murata Y, Masuko S, Yoshimura M (2007) Cell-type-specific excitatory and inhibitory circuits involving primary afferents in the substantia gelatinosa of the rat spinal dorsal horn in vitro. J Physiol 581: 603-618.

CHAPTER 7

BDNF AND OVERALL DORSAL HORN EXCITABILITY:

BDNF enhances dorsal horn excitability and initiates spontaneous Ca^{2+} oscillations.

* A portion of this chapter has been published.

7.1 Introduction

Brain-derived neurotrophic factor (BDNF) is a neuropeptide found in populations of nociceptive primary afferents sensitive to nerve growth factor (NGF) (Apfel et al., 1996; Michael et al., 1997). The levels of BDNF rise substantially following peripheral nerve injury (Apfel et al., 1996; Cho et al., 1997; Michael et al., 1999) as well as through enhanced primary afferent activity (Lever et al., 2001). The mechanism of BDNF action on dorsal horn neurons has been studied in extensive detail (Coull et al., 2005; Garraway et al., 2003; Kerr et al., 1999; Lever et al., 2003; Mannion et al., 1999; Matayoshi et al., 2005; Pezet et al., 2002; Thompson et al., 1999); however, these studies mainly examined the acute effects of BDNF exposure despite the fact that elevated levels can persist for up to a week (Ha et al., 2001; Ikeda et al., 2001; Miletic and Miletic, 2002). I tested and examined the effects of chronic BDNF exposure, which is analogous to the conditions found *in vivo* in models of neuropathic pain, to better understand the role of this mediator in the pathogenesis of this disease. 9

I found BDNF has selective actions on identified populations of dorsal horn neurons: excitatory and inhibitory synaptic transmission to putative excitatory dorsal horn neurons increases whereas in putative inhibitory neurons a decrease in both is observed (Chapter 4-6). Although the spontaneous excitability of individual neurons in these populations of dorsal horn neurons is affected by altered synaptic activity (Figure 4-9), the overall outcome of these alterations on dorsal horn excitability is not clear. The whole-cell recording techniques utilized thus far have been essential in identifying distinct populations of dorsal horn neurons as well as characterizing the specific changes induced by long-term BDNF exposure. However, the overall consequences of this potential mediator of neuropathic pain cannot be adequately assessed using these methods. I therefore used Ca^{2+} imaging techniques to examine the effects of BDNF on population activity in the dorsal horn.

Ca^{2+} imaging techniques are a useful means of measuring excitability in neurons. Furthermore, these methods have been effectively applied in the study of neuronal networks in tissue slices (Ruangkittisakul et al., 2006; Yuste and Konnerth, 2005). Thus, Ca^{2+} imaging techniques were applied in the assessment of dorsal horn excitability following prolonged exposure to BDNF.

7.2 Methods

7.2.1 Defined-medium organotypic cultures (DMOTCs) of spinal cord slices

DMOTC slices were prepared as previously described (see Chapter 2: General methods). Very briefly, spinal cords were isolated from embryonic (E13-14) rat pups and transverse slices (300 ± 25 μm) were cultured using the roller-tube technique. Serum-free conditions were established after 5 days *in vitro* following the medium exchange schedule outlined in Figure 2-3A. The medium was exchanged with freshly prepared medium every 3-4 days.

Slices were treated after 15-21 days *in vitro* for a period of 5-6 days with 200 ng/ml BDNF (Alomone Laboratories, Jerusalem, Israel) in serum-free medium as described in Chapter 2. Age-matched, untreated DMOTC slices served as controls.

7.2.2 Calcium imaging

A single DMOTC slice was incubated for 1 hour prior to imaging with 5 μM of the membrane-permeable acetoxy-methyl form of the fluorescent Ca^{2+}-indicator dye Fluo-4 (TEF Labs Inc., Austin, Texas, USA). The conditions for incubating the dye were standardized across different slices to avoid uneven dye loading. After dye loading, the DMOTC slice was transferred to a recording chamber and perfused with external solution containing (in mM): 131 NaCl, 2.5 KCl, 1.2 NaH_2PO_4, 1.3 $MgSO_4$, 26 $NaHCO_3$, 25 D-glucose, and 2.5 $CaCl_2$ (20°C, flow rate 4 ml/min). Changes in Ca^{2+}-fluorescence intensity evoked by a high K^+ solution (20, 35, or 50 mM, 90 s application) or other pharmacological agents, were measured in dorsal horn neurons with a confocal microscope equipped with an argon (488 nm) laser and filters (20x XLUMPlanF1-NA-0.95 objective; Olympus FV300, Markham, Ontario, Canada). Full frame images (512 x 512 pixels) in a fixed xy plane were acquired at a scanning time of 1.08 s/frame (Ruangkittisakul et al., 2006). In some experiments, images were cropped to accommodate faster scan rates. Selected regions of interest were drawn around distinct cell bodies and fluorescence intensity traces were generated with FluoView v.4.3 (Olympus).

7.2.3 Electrophysiology

Dorsal horn population activity was recorded extracellularly with a differential amplifier (DAM50, WPI, Sarasota, Florida, USA) via suction electrodes (outer diameter 80-250 μm) filled with superfusate, placed on the surface of the DMOTC slice. Signals were amplified (x10k) and band-pass filtered (0.3-1 kHz) during recordings (Powerlab/8SP, ADInstruments, Colorado Springs, Colorado, USA).

7.2.4 Drugs and chemicals

Unless otherwise stated, all chemicals were from SIGMA (St. Louis, MO, USA). Fluo-4 AM dye was dissolved in a mixture of dimethyl sulfoxide (DMSO) and 20% pluronic acid (Invitrogen, Burlington, Ontario, Canada) to a 0.5 mM stock solution and kept frozen until used. The dye was thawed and sonicated thoroughly before incubating with a DMOTC slice. TTX was dissolved in distilled water as a 1 mM stock solution and stored at -20ºC until use. TTX was diluted to a final desired concentration of 1 μM in external recording solution on the day of the experiment. Strychnine was prepared in a similar manner to TTX, and bicuculline (Tocris, Ballwin, MO, USA) was dissolved in DMSO as a 10 mM stock solution. 6-cyano-7-nitroquinoxaline-2,3-dione (CNQX, Tocris) and 2,3-dihydroxy-6-nitro-7-sulfamoyl-benzo[f]quinoxaline-2,3-dione (NBQX, Tocris) were prepared as 10 mM stocks dissolved in distilled water, and D(-)-2-Amino-5-phosphonopentanoic acid (D-AP5, Tocris) was prepared as 50 mM stocks dissolved in 30% 1 M NaOH. Riluzole was prepared as a 10 mM stock, kyneurinic acid and GABA as 1 M stocks, and nitrendipine as a 1 mM stock made up in distilled water. These drugs were used at a 1:1000 dilution prepared freshly with external recording solution immediately prior to the start of experiments.

7.2.5 Data analysis and statistical testing

Statistical comparisons were made with unpaired or paired t-tests, as specified and appropriate, using GraphPad InStat 3.05 (GraphPad Software, San Diego, CA, USA). All graphs were plotted using Origin 7 (Origin Lab, Northampton, MA, USA) and statistical significance was taken as $p<0.05$.

7.3 Results

7.3.1 Enhanced depolarization-evoked Ca^{2+} responses from BDNF-treated DMOTC slices

If BDNF is involved in generating central sensitization, then it would be expected to increase the excitability of the dorsal horn population as a whole. This possibility was evaluated using confocal Ca^{2+} imaging techniques (Ruangkittisakul et al., 2006) to monitor the responses of both control and BDNF-treated DMOTC slices to depolarizing stimuli of varying strength (20, 35, or 50 mM K^+ solution for 90 s).

With identical stimuli, presumed dorsal horn neurons in BDNF-treated DMOTC slices exhibited a larger increase in Fluo-4 fluorescence intensity compared to cells in the same region in control untreated DMOTC slices. This is clear from the images and sample traces of Fluo-4 fluorescence intensity signal for control (Figure 7-1A and C) and BDNF-treated cells (Figure 7-1B and D). Quantification of the peak amplitude revealed a significant increase in the Ca^{2+} response in the BDNF-treated group at all K^+ concentrations tested (Figure 7-1E, unpaired t-test, $p<0.001$). As well, the area under the Ca^{2+} intensity signal was significantly larger for the BDNF-treated DMOTC slices for all challenges (Figure 7-1F, unpaired t-test, $p<0.05$).

7.3.2 BDNF-induced Ca^{2+} oscillations

During the course of Ca^{2+} imaging experiments, synchronous oscillations in the Ca^{2+} signal were observed in BDNF-treated slices (Figure 7-2B) which were not usually present in control slices (Figure 7-2A). All 7/7 BDNF-treated DMOTC slices tested during high K^+ stimulation, compared to only 2/10 control DMOTC slices, displayed this phenomenon.

To ensure sufficient sampling of BDNF-induced Ca^{2+} oscillations, a range of scanning rates was applied to the same BDNF-treated slice for comparison (Figure 7-2C to E). Fluorescent signals from the same cells were acquired and shown as traces below, and no change in the frequency of oscillations was observed. Thus, these BDNF-induced oscillations were slow and occurred at a frequency of 0.143 ± 0.01 Hz (n = 7).

7.3.3 BDNF-induced Ca^{2+} oscillations parallel an increase in extracellular activity

To examine if these oscillations in BDNF-treated slices correlate to an increase in neuronal excitability, extracellular recordings were obtained simultaneously with fluorescent Ca^{2+} imaging of cells within the same dorsal region.

As shown, inhibition of Ca^{2+} oscillations by superfusion of GABA (Figure 7-3A) was accompanied by cessation of extracellular activity (Figure 7-3B). Overlays of the fluorescent intensity trace with the extracellular recording trace (Figure 7-3C) show the peaks of Ca^{2+} oscillations parallel a depolarization spike in extracellular recordings. Thus, the induction of spontaneous Ca^{2+} oscillations by BDNF also corresponds to an increase in extracellular activity in the dorsal horn, similar to what has been observed in animal models of neuropathic pain (Dalal et al., 1999; Laird and Bennett, 1993).

Since oscillatory Ca^{2+} activity is associated with dorsal horn excitability, mechanisms mediating these oscillations will be involved in enhancing overall excitability in the dorsal horn. Therefore, the effect of various pharmacological agents on the amplitude and frequency of BDNF-induced Ca^{2+} oscillations was tested to better understand these underlying mechanisms.

7.3.4 BDNF-induced Ca^{2+} oscillations depend on extracellular Ca^{2+} and voltage-gated Ca^{2+} channels

Removal of extracellular Ca^{2+}, by perfusion with a Ca^{2+}-free solution, terminated Ca^{2+} oscillations (Figure 7-4A). Therefore, Ca^{2+} entry is essential for the generation of these oscillatory signals.

To identify the route of Ca^{2+} entry, blockers of voltage-gated ion channels were applied to BDNF-treated DMOTCs. Addition of Cd^{2+}, an inorganic blocker of voltage-gated Ca^{2+} channels, completely blocked oscillations (Figure 7-4B). Other inorganic blockers such as Co^{2+} (Figure 7-4C) and Ni^{2+} (Figure 7-4D) were able to reduce the frequency of oscillations, but had no effect on amplitude. A selective blocker for L-type Ca^{2+} channels, nitrendipine, was able to reduce the frequency as well but not completely block oscillations (Figure 7-4E) and a similar effect was observed with ω-conotoxin GVIA, the selective blocker of N-type Ca^{2+} channels (Figure 7-4F). Since no effect on oscillation amplitude was observed until oscillations were completely abolished, presynaptic Ca^{2+} entry through a mixed population of voltage-gated Ca^{2+} channels is required for BDNF-induced Ca^{2+} oscillations.

7.3.5 BDNF-induced Ca^{2+} oscillations dependent on action potential generation through TTX-sensitive Na^{+} channels

The involvement of synaptic activity in the generation of BDNF-induced Ca^{2+} oscillations is emphasized by the dependence of oscillations on voltage-gated sodium channels (Figure 7-5A). The activity of presynaptic Na^{+} channels is likely involved since increasing concentrations of TTX affected oscillation frequency (Figure 7-5B) but not amplitude (Figure 7-5C) until all oscillations were abolished with TTX.

The persistent component of Na^{+} current (I_{NaP}) has been implicated in spontaneous bursting activity in cultured spinal cord slices (Darbon et al., 2004) and its possible role in generating BDNF-induced Ca^{2+} oscillations was investigated. Low dose TTX (20 nM) and riluzole (10 μM), both blockers of the I_{NaP}, significantly attenuated the frequency of oscillations (Figure 7-5B and D; paired t-test, $p<0.001$) but did not abolish them completely. Also, no effect of either drug on oscillation amplitude was observed (Figure 7-5B and D). Thus, the I_{NaP} component of total Na^{+} current may play a modulatory role in BDNF-induced Ca^{2+} oscillations, but is not essential in their generation.

Thus, depolarization of the presynaptic nerve terminal, by TTX-sensitive Na^{+} channels, activates voltage-gated Ca^{2+} channels which permit the entry of Ca^{2+}, an essential component in the propagation of BDNF-induced spontaneous Ca^{2+} oscillations.

7.3.6 BDNF-induced Ca^{2+} oscillations mediated by AMPA/kainate receptors but not NMDA receptors

Since entry of Ca^{2+} presynaptically is required for synaptic transmission, I wanted to assess the role of glutamate transmission in BDNF-induced Ca^{2+} oscillations. Kyneurinic acid (1 mM) was able to completely halt oscillations (data not shown). A selective blocker of AMPA/kainate glutamate receptors, NBQX (Bleakman and Lodge, 1998), was also able to abolish Ca^{2+} oscillations (Figure 7-6A). D-AP5, a NMDA glutamate receptor blocker, was able to significantly reduce oscillation amplitude (Figure 7-6B; paired t-test, $p<0.001$), but had no effect on frequency (paired t-test, $p>0.2$). Thus, postsynaptic NMDA receptors could play a role in modulating BDNF-induced Ca^{2+} oscillations but glutamate activity on AMPA/kainate receptors is required.

7.3.7 Large Ca^{2+} oscillations induced following removal of inhibition

Previous reports suggest BDNF decreases the anion gradient in Lamina I neurons which subsequently induces a reversal of GABA inhibition to excitation (Coull et al., 2005; Prescott et al., 2006). If BDNF-induced GABA excitation is involved in propagating these Ca^{2+} oscillations and increasing dorsal horn excitability, then blocking GABA/glycine receptors should decrease the occurrence of these events. This was not the case as shown in Figure 7-7A where addition of antagonists produced robust oscillations with larger amplitude but slower frequency than the spontaneous BDNF-induced oscillations observed prior. These oscillations resembled the large inward currents and bursts of action potentials noted previously in controls (Figure 3-6) and BDNF-treated DMOTCs (Figure 5-6). In fact, addition of bicuculline and strychnine in a control

DMOTC slice produced similar large oscillations (Figure 7-7B) as those observed in a BDNF-treated slice.

The addition of GABA on to an oscillating BDNF-treated slice suppressed all activity (Figure 7-7C) suggesting GABA actions remain inhibitory in the dorsal horn following BDNF treatment.

7.4 Discussion

The main findings in this chapter are 1) BDNF augments Ca^{2+} signals in response to a depolarization stimulus compared to time-matched control slices. 2) BDNF induces spontaneous Ca^{2+} oscillations which correspond to enhanced extracellular activity in dorsal horn neurons. Thus, prolonged BDNF exposure increases the excitability of dorsal horn neurons which support a role of BDNF in the generation of neuropathic pain.

7.4.1 Ca^{2+} imaging techniques

The essential role of calcium in neuronal activity has been exploited by fluorescent Ca^{2+}-sensitive dyes. The fluorescence of these fluorophores is altered by the presence and binding to Ca^{2+} ions and thus have been used to measure intracellular Ca^{2+} concentrations. Monitoring fluorescence allows for the real-time analysis of Ca^{2+} dynamics and neuronal excitability within dye-loaded neurons.

Various types of Ca^{2+}-sensitive dyes are commercially available. Experiments with ratiometric dyes, such as Fura-2, utilize the ratio of fluorescence from two separate emission wavelengths to measure the concentration of Ca^{2+}. Such dyes require a two-photon set-up to measure fluorescence, but allow for the measurement of exact Ca^{2+}

concentration. Non-ratiometric dyes, such as Flou-4, do not produce shifts in the emission wavelength when Ca^{2+} binds, but rather produce an increase in fluorescence intensity. These dyes are amendable to simpler microscope set-ups with a single laser source and produce less phototoxcitiy to cells. Also, these dyes can be used on confocal systems which provide high spatial resolution of fluorescence signals. So although the exact intracellular Ca^{2+} concentration was not determined, the relative increase in Fluo-4 fluorescence signal intensity still provided a good measure of a slice's excitability since Fluo-4 fluorescence intensity correlates well with Ca^{2+} concentration at physiological ranges (Gee *et al.*, 2000). Also, it is unlikely that the dye saturated since there was a progressive increase in the Ca^{2+} signal amplitude at higher K^+ concentrations.

7.4.2 BDNF enhances overall dorsal horn excitability

The Ca^{2+} responses to high K^+ stimulation were significantly larger in BDNF-treated DMOTC slices than in age-matched controls (Figure 7-1). Also, the probability of synchronous Ca^{2+} oscillations increased notably in BDNF-treated DMOTC slices. The appearance of spontaneous Ca^{2+} oscillations matched an increase in activity detected in extracellular recordings (Figure 7-3C). Therefore, BDNF increased the overall excitability of the dorsal horn.

Although other studies have examined the acute effects of BDNF on dorsal horn neurons (Garraway et al., 2003; Kerr et al., 1999; Slack et al., 2004), I am the first to show that long-term, 5-6d exposure to BDNF, which resembles the time course of nerve injury-induced BDNF elevation (Cho et al., 1997; Dougherty et al., 2000; Fukuoka et al., 2001; Zhou et al., 1999), can induce persistent, and possibly permanent, changes to the dorsal horn network.

7.4.3 The mechanism of BDNF-induced Ca^{2+} oscillations

The mechanisms mediating BDNF-induced Ca^{2+} oscillations were investigated to understand which alterations are involved in increasing dorsal horn excitability and to relate it to BDNF's selective effects on synaptic transmission across dorsal horn neurons which have been observed (Chapter 4 to 6).

The Ca^{2+} oscillations observed following BDNF treatment was dependent on activity of Na^+ channels (Figure 7-5A) and Ca^{2+} entry through voltage-gated Ca^{2+} channels (Figure 7-4). Since oscillations were blocked by TTX (1 μM) (Figure 7-5A), they likely represented oscillations in neuronal rather than glial cells. Also, the sensitivity of oscillation frequency to pharmacological blockers of Na^+ and Ca^{2+} channels suggests presynaptic action potential activity was involved in mediating this phenomenon.

Glutamatergic synaptic transmission is involved since kyneurinic acid and NBQX was able to completely block BDNF-induced Ca^{2+} oscillations (Figure 7-6A). I have previously shown that long-term exposure to BDNF increased excitatory synaptic drive to all neuronal cell types except tonic cells (Figure 4-4) and the increase in excitatory drive was partially attributed to an increase in presynaptic action potential activity in 'irregular', phasic and transient neurons (Figure 4-6C). 'Delay' neurons, which comprise a portion of excitatory dorsal horn neurons, exhibit increased spontaneous bursting activity following BDNF treatment (Figure 4-9F) which may have also contributed to production of these oscillations in intracellular Ca^{2+} concentration. NMDA receptor function in the dorsal horn has been shown to be modulated by BDNF (Garraway et al., 2003; Kerr et al., 1999; Slack et al., 2004; Slack and Thompson, 2002) and this may contribute to the magnitude of Ca^{2+} oscillations but is not essential in their generation.

The loss of inhibitory tone in the spinal cord has been implicated in neuropathic pain (Baba et al., 2003; Moore et al., 2002; Sivilotti and Woolf, 1994) and BDNF has been shown to reduce spontaneous action potential activity in tonic inhibitory neurons (Figure 4-9A and B). Although blockade of inhibitory receptors in control slices was able to induce rhythmic Ca^{2+} oscillations (Figure 7-7B), it is not clear if reduced inhibitory activity is responsible for BDNF-induced Ca^{2+} oscillations. Removal of inhibition produced an amplification of Ca^{2+} oscillation amplitude (Figure 7-7A) suggesting a fair amount of inhibitory tone remains in the dorsal horn following BDNF treatment. Perhaps, based on the selective actions of BDNF on inhibitory synaptic transmission, reduced inhibition to certain populations of neurons is involved in generating spontaneous Ca^{2+} oscillations rather than an overall reduction in dorsal horn inhibition. Also, it is more likely a reduction in inhibitory neurotransmitter release to select populations of dorsal horn neurons, but not a loss of postsynaptic receptor function, is involved since exogenous application of GABA was sufficient to suppress Ca^{2+} oscillations in a BDNF-treated slice (Figure 7-7C).

Interestingly, the phenomenon of rhythmic Ca^{2+} oscillations has been reported in the spinal cord following various pharmacological manipulations (Ruscheweyh and Sandkuhler, 2005) or during development (Fabbro *et al.*, 2007). The Ca^{2+} oscillations characterized by Fabbro et al. (2007) were insensitive to TTX, and since the oscillations I observed were completely blocked by TTX (Figure 7-5A), it is most likely different mechanisms governing these oscillations and BDNF does not promote a reversion to embryonic stages. Spontaneous, rhythmic Ca^{2+} oscillations have also been described in hippocampal slices under epileptiform conditions (Kovacs *et al.*, 2005) suggesting they may be indicative of hyperexcitable networks.

7.5 Conclusions

BDNF enhances the excitability of dorsal horn neurons by augmenting depolarization-evoked responses and generating spontaneous Ca^{2+} oscillations. BDNF-induced Ca^{2+} oscillations were mediated by synaptic glutamate transmission and corresponded to an increase in extracellular activity in the dorsal horn. Thus, BDNF is capable of enhancing excitability in the dorsal horn, similar to what has been described in animal models of neuropathic pain, and may be involved in the pathogenesis of this disease.

Figure 7-1: Enhanced high K^+-induced Ca^{2+} rise in BDNF-treated DMOTC slices.

A and B: Sample fluorescent Ca^{2+} intensity traces during a 90s, 20mM K^+ challenge for a cell in a control DMOTC slice (A), and a BDNF-treated DMOTC slice (B). C and D: Sample fluorescent images (512 x 512 pixels) of the dorsal region of a control slice (C) and a BDNF-treated DMOTC slice (D), loaded with Fluo-4AM, during a 20mM K^+ solution challenge. White scale bar is 50 μm. E: Comparison of fluorescent Ca^{2+} signal amplitude over a range of high K^+ solutions tested. Amplitude of the signal was measured from baseline to peak of each trace recorded from cells in control and BDNF-treated DMOTC slices (n = 30 cells for control, n = 41 cells for BDNF). Scaling is in arbitrary units (A.U.) F: Comparison of area under the fluorescent Ca^{2+} signal traces over a range of high K^+ solutions in control and BDNF-treated DMOTC slices. Error bars indicate SEM. At all concentrations tested, both area and amplitude of the Ca^{2+} signal were significantly larger in BDNF-treated cells (unpaired t-test; * = $p<0.05$; § = $p<0.001$).

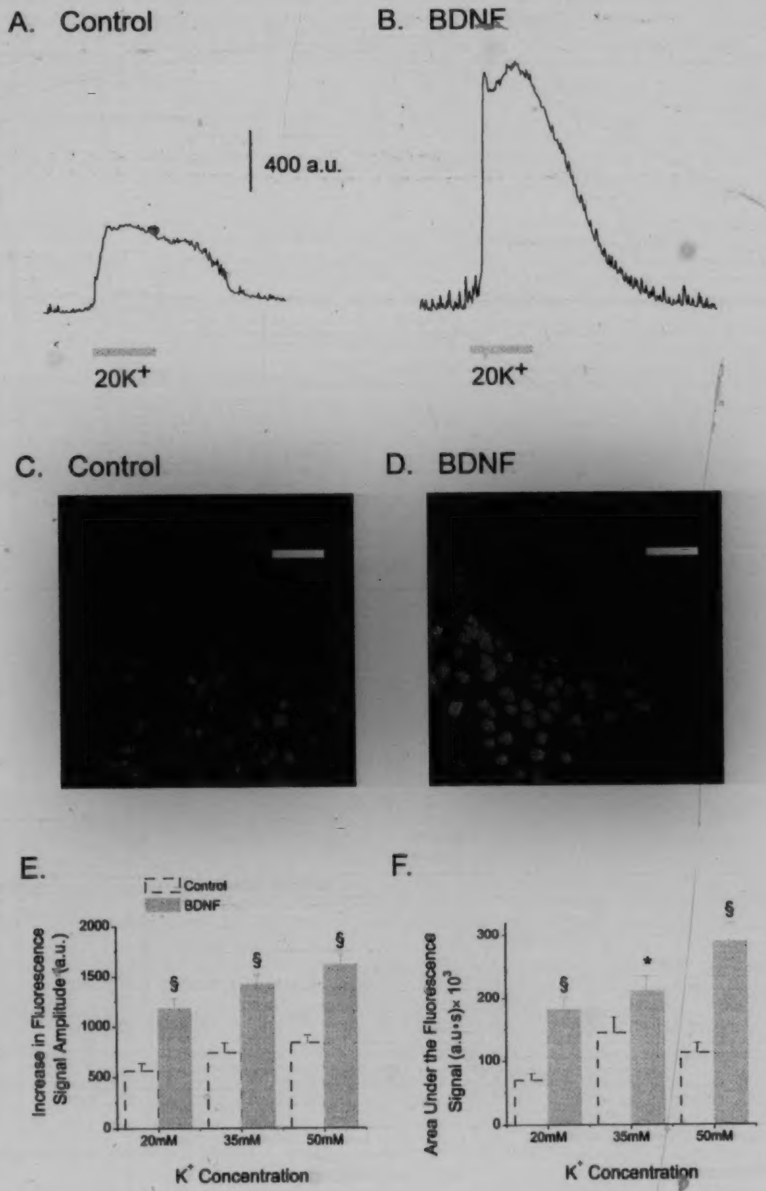
A. Control
B. BDNF
400 a.u.
20K+
20K+
C. Control
D. BDNF
E.
Control
BDNF
Increase in Fluorescence Signal Amplitude (a.u.)
2000
1500
1000
500
0
§
§
§
20mM
35mM
50mM
K+ Concentration
F.
Area Under the Fluorescence Signal (a.u•s)× 10³
300
200
100
0
§
*
§
20mM
35mM
50mM
K+ Concentration

Figure 7-2: BDNF-induced spontaneous Ca^{2+} oscillations.

A and B: Sample baseline recordings from four cells in the same control DMOTC slice (A) and a BDNF-treated DMOTC slice (B). Dots with dashed lines indicate synchronous oscillations in Ca^{2+}. C to E: Scanning of the same BDNF-treated DMOTC slice with three different scanning rates. Above images show the fluorescent images of the dorsal region imaged. Note the same cells were selected in each recording and the fluorescent intensity traces are shown below.

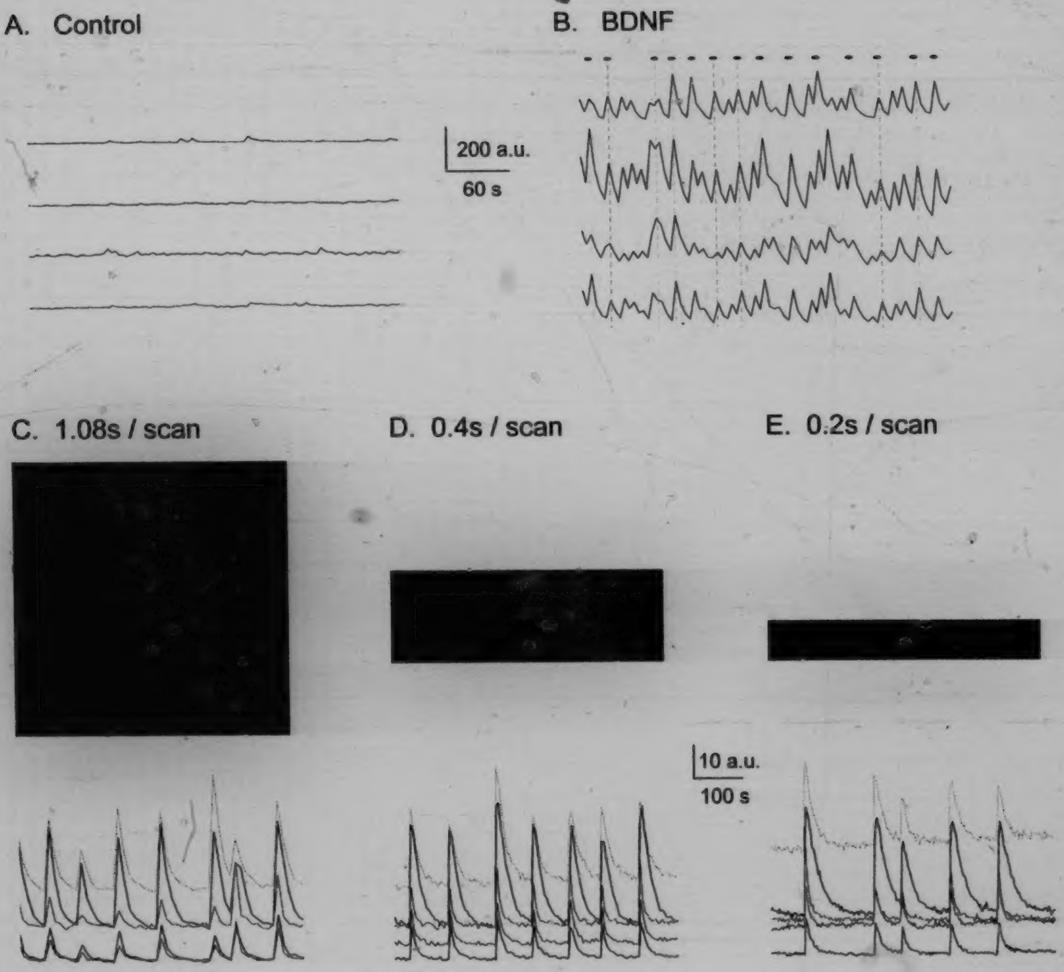
A. Control
B. BDNF
200 a.u.
60 s
C. 1.08s / scan
D. 0.4s / scan
E. 0.2s / scan
10 a.u.
100 s

Figure 7-3: Ca^{2+} oscillations correspond to an increase in extracellular activity in the dorsal horn.

A: A sample fluorescent Ca^{2+} signal trace from a BDNF-treated DMOTC slice. A blocker of Ca^{2+} oscillations (GABA, 1mM) was added at the beginning of the trace and removed after 90s, as indicated by the grey bar. Note the blockade of spontaneous Ca^{2+} oscillations which later recovered. B: The extracellular recording trace obtained simultaneously with fluorescent Ca^{2+} imaging. Note the reduction in extracellular activity at the same time Ca^{2+} oscillations stopped. C: An overlay of both recording traces at a faster time scale. Dashed lines indicate the same peaks from both recordings.

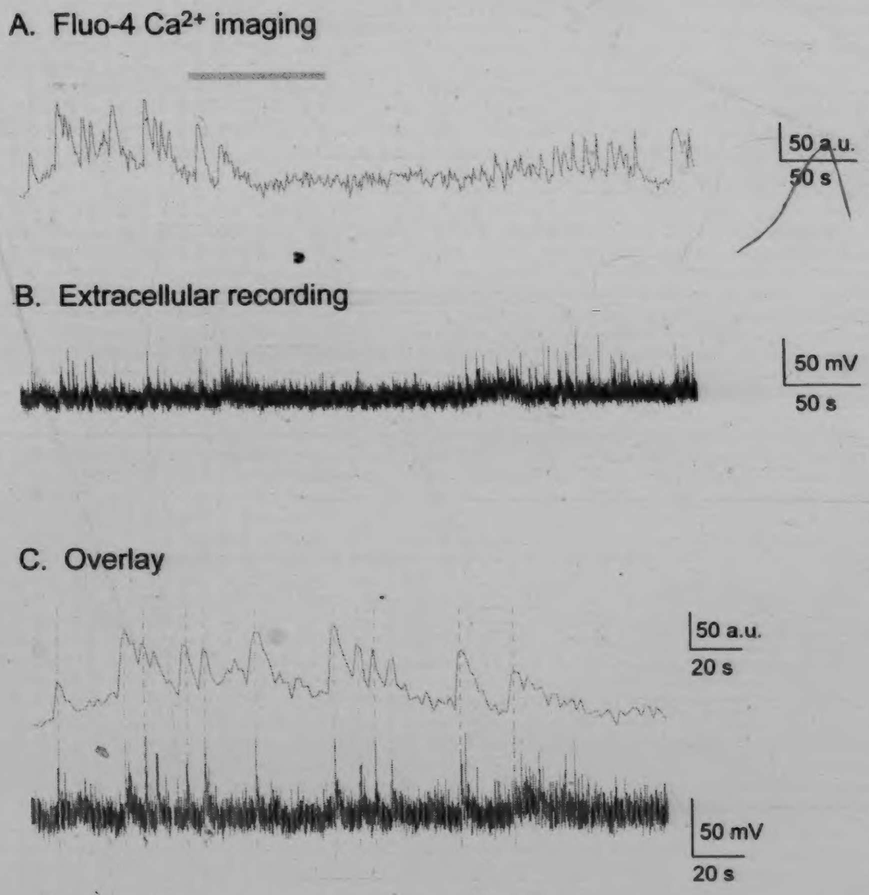

A. Fluo-4 Ca²⁺ imaging

B. Extracellular recording

C. Overlay

Figure 7-4: Dependence of BDNF-induced Ca^{2+} oscillations on extracellular Ca^{2+} entry through voltage-gated Ca^{2+} channels.

A: Perfusion of extracellular recording solution free of Ca^{2+} (0 Ca^{2+}) marked by a thick grey line. Note the complete block of oscillatory activity in recorded cells. B (left): Addition of 200 μM Cd^{2+}, marked by a thick grey line, abolished Ca^{2+} oscillations in a BDNF-treated slice. (Right): Measurement of oscillation amplitude and frequency before and after application of Cd^{2+}. Values normalized to control values obtained before addition of Cd^{2+}. C to F: Effect of 2 mM Co^{2+} (C), 100 μM Ni^{2+} (D), 1 μM nitrendipine (E) and 100 nM ω-conotoxin GVIA (F) on BDNF-induced oscillation amplitude and frequency. Average values represented. Error bars indicate SEM. For paired t-test, § = $p<0.001$.

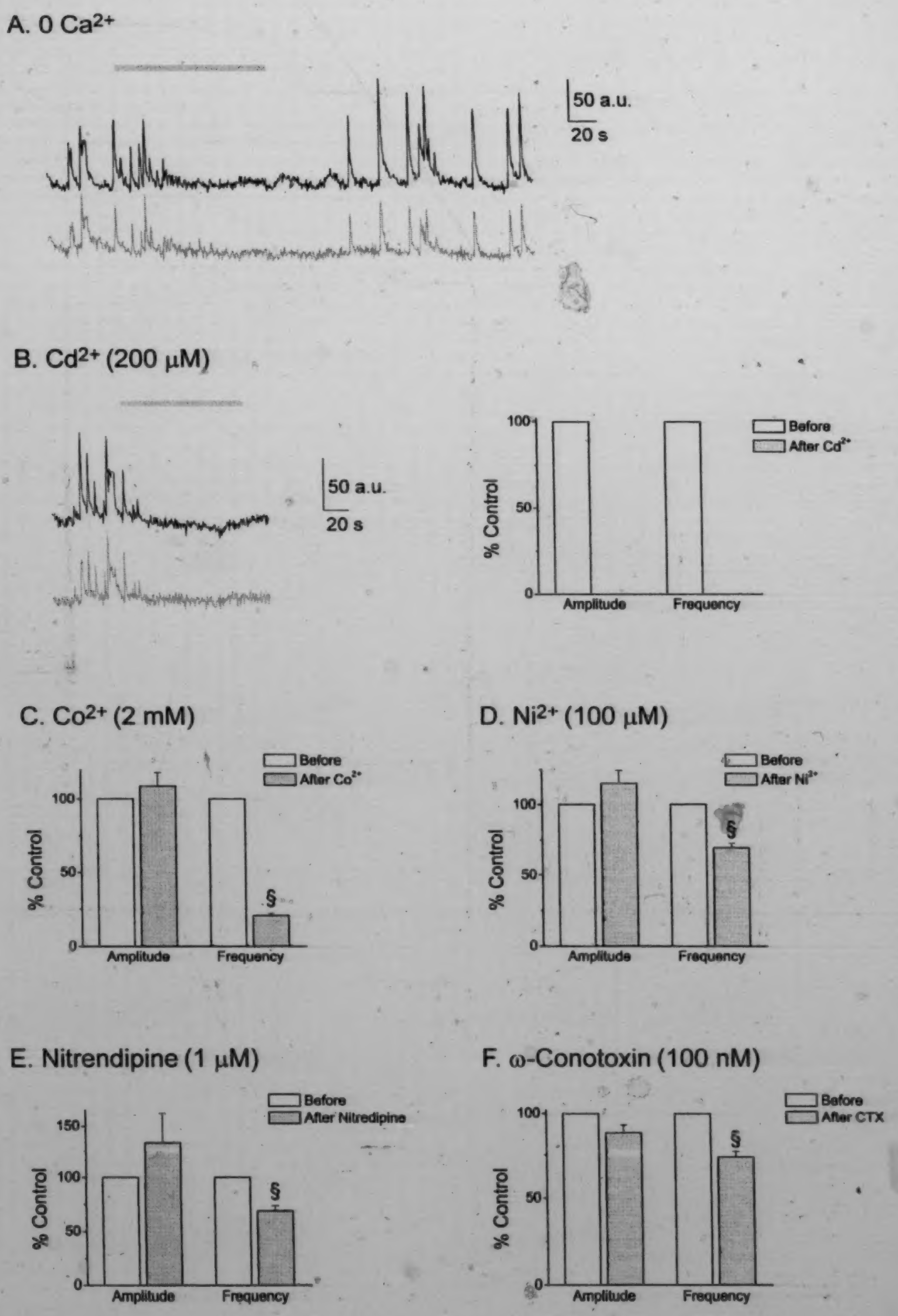

A. 0 Ca^{2+}

B. Cd^{2+} (200 μM)

C. Co^{2+} (2 mM)

D. Ni^{2+} (100 μM)

E. Nitrendipine (1 μM)

F. ω-Conotoxin (100 nM)

Figure 7-5: Dependence of BDNF-induced Ca^{2+} oscillations on TTX-sensitive voltage-gated Na^{+} current but not persistent Na^{+} current.

A: Addition of 1 μM TTX, marked by a thick grey line, abolished Ca^{2+} oscillations in a BDNF-treated slice. B: Concentration-inhibition curve for increasing concentrations of TTX on Ca^{2+} oscillation frequency. C: Concentration-inhibition curve for increasing concentrations of TTX on Ca^{2+} oscillation amplitude. Error bars indicate SEM. For paired t-test, § = $p<0.001$. D: Sample synchronous Ca^{2+} oscillation traces from a BDNF-treated slice before (left) and after (middle) application of 10 μM riluzole. (Right): Effect of riluzole on average Ca^{2+} oscillation amplitude and frequency. Error bars indicate SEM. For paired t-test, § = $p<0.001$.

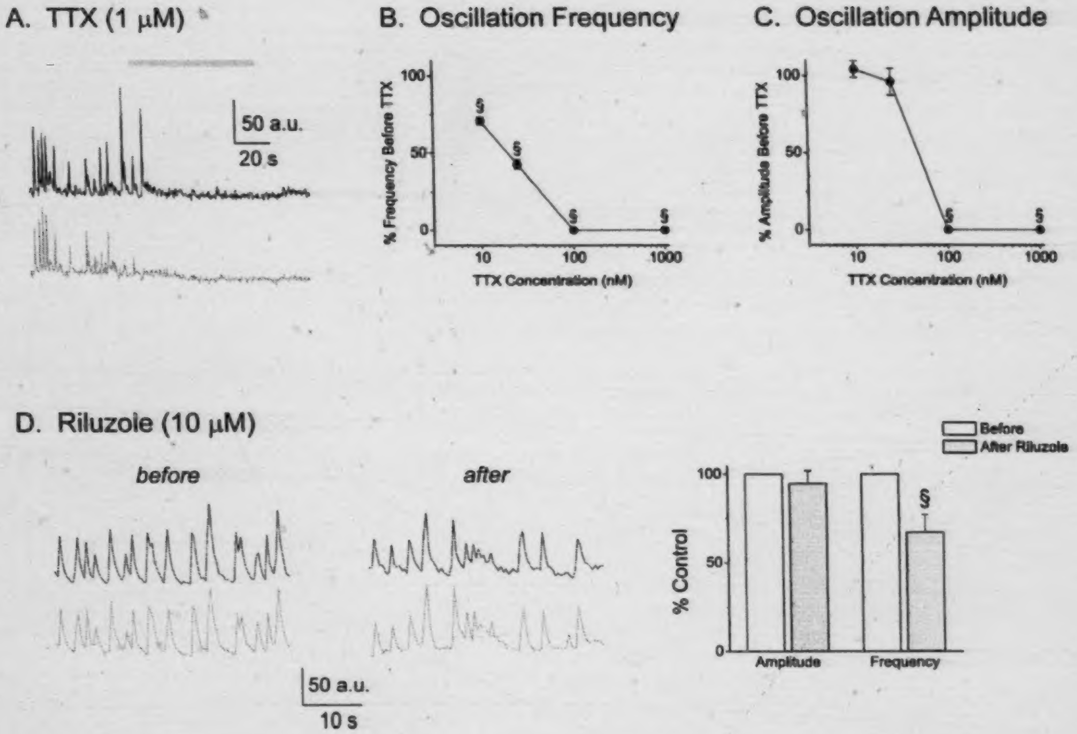
A. TTX (1 μM)
50 a.u.
20 s
B. Oscillation Frequency
% Frequency Before TTX
100
50
0
§
10
100
1000
TTX Concentration (nM)
C. Oscillation Amplitude
% Amplitude Before TTX
100
50
0
§
10
100
1000
TTX Concentration (nM)
D. Riluzole (10 μM)
before
after
50 a.u.
10 s
Before
After Riluzole
% Control
100
50
0
§
Amplitude
Frequency

Figure 7-6: BDNF-induced Ca^{2+} oscillations mediated by AMPA/kainate glutamate receptors.

A: Addition of 10 µM NBQX, marked by a thick grey line, abolished Ca^{2+} oscillations in a BDNF-treated slice. (Right): Measurement of oscillation amplitude and frequency before and after application of NBQX. B: Sample fluorescent Ca^{2+} traces from a BDNF-treated slice before (left) and after (middle) application of 50 µM AP5. (Right): Effect of AP5 on average Ca^{2+} oscillation amplitude and frequency. Error bars indicate SEM. For paired t-test, § = $p<0.001$.

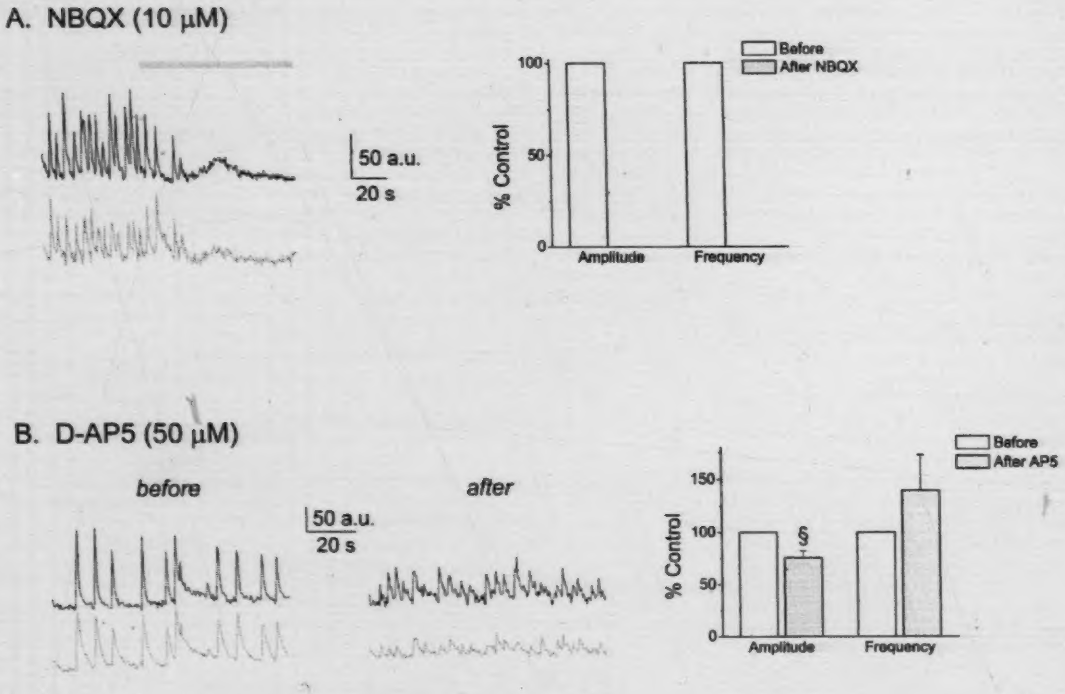
A. NBQX (10 µM)
50 a.u.
20 s
Before
After NBQX
100
50
0
% Control
Amplitude
Frequency
B. D-AP5 (50 µM)
before
after
50 a.u.
20 s
Before
After AP5
150
100
50
0
% Control
§
Amplitude
Frequency

Figure 7-7: Amplification of BDNF-induced Ca^{2+} oscillations by pharmacological removal of inhibition and suppression of oscillatory activity by GABA.

A: Addition of 10 µM bicuculline and 1 µM strychnine to a BDNF-treated slice produced robust oscillations larger in amplitude but slower in frequency than the spontaneous Ca^{2+} oscillations observed before antagonist application. B: Addition of 10 µM bicuculline and 1 µM strychnine to a control DMOTC slice produced similar robust oscillations as those observed in (A). C: Application of 1 mM GABA, marked by a thick grey line, stopped BDNF-induced Ca^{2+} oscillations.

A. BDNF: Bicuculline (10 μM) + Strychnine (1 μM)

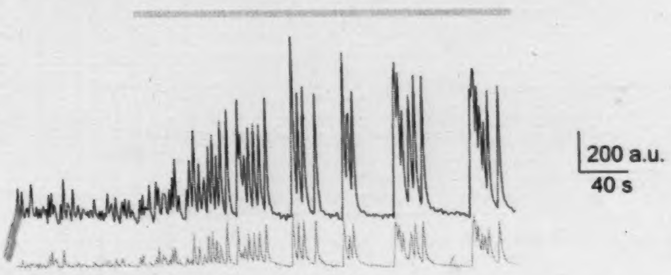

B. Control: Bicuculline (10 μM) + Strychnine (1 μM)

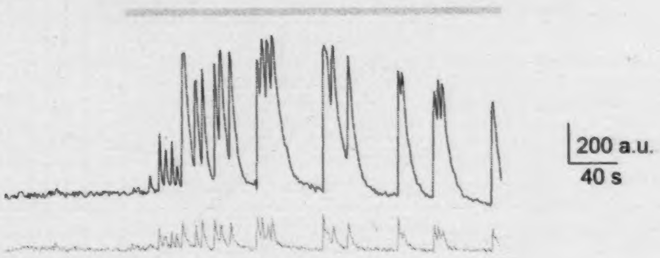

C. BDNF: GABA (1 mM)

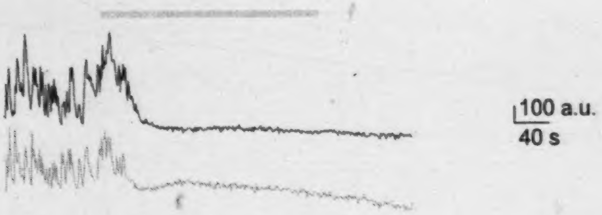

7.6 References

Apfel SC, Wright DE, Wiideman AM, Dormia C, Snider WD, Kessler JA (1996) Nerve growth factor regulates the expression of brain-derived neurotrophic factor mRNA in the peripheral nervous system. Mol Cell Neurosci 7: 134-142.

Baba H, Ji RR, Kohno T, Moore KA, Ataka T, Wakai A, Okamoto M, Woolf CJ (2003) Removal of GABAergic inhibition facilitates polysynaptic A fiber-mediated excitatory transmission to the superficial spinal dorsal horn. Mol Cell Neurosci 24: 818-830.

Bleakman D, Lodge D (1998) Neuropharmacology of AMPA and kainate receptors. Neuropharmacology 37: 1187-1204.

Cho HJ, Kim JK, Zhou XF, Rush RA (1997) Increased brain-derived neurotrophic factor immunoreactivity in rat dorsal root ganglia and spinal cord following peripheral inflammation. Brain Res 764: 269-272.

Coull JA, Beggs S, Boudreau D, Boivin D, Tsuda M, Inoue K, Gravel C, Salter MW, De Koninck Y (2005) BDNF from microglia causes the shift in neuronal anion gradient underlying neuropathic pain. Nature 438: 1017-1021.

Dalal A, Tata M, Allegre G, Gekiere F, Bons N, Albe-Fessard D (1999) Spontaneous activity of rat dorsal horn cells in spinal segments of sciatic projection following transection of sciatic nerve or of corresponding dorsal roots. Neuroscience 94: 217-228.

Darbon P, Yvon C, Legrand JC, Streit J (2004) INaP underlies intrinsic spiking and rhythm generation in networks of cultured rat spinal cord neurons. Eur J Neurosci 20: 976-988.

Dougherty KD, Dreyfus CF, Black IB (2000) Brain-derived neurotrophic factor in astrocytes, oligodendrocytes, and microglia/macrophages after spinal cord injury. Neurobiol Dis 7: 574-585.

Fabbro A, Pastore B, Nistri A, Ballerini L (2007) Activity-independent intracellular Ca(2+) oscillations are spontaneously generated by ventral spinal neurons during development in vitro. Cell Calcium 41: 317-329.

Fukuoka T, Kondo E, Dai Y, Hashimoto N, Noguchi K (2001) Brain-derived neurotrophic factor increases in the uninjured dorsal root ganglion neurons in selective spinal nerve ligation model. J Neurosci 21: 4891-4900.

Garraway SM, Petruska JC, Mendell LM (2003) BDNF sensitizes the response of lamina II neurons to high threshold primary afferent inputs. Eur J Neurosci 18: 2467-2476.

Gee KR, Brown KA, Chen WN, Bishop-Stewart J, Gray D, Johnson I (2000) Chemical and physiological characterization of fluo-4 Ca(2+)-indicator dyes. Cell Calcium 27: 97-106.

Ha SO, Kim JK, Hong HS, Kim DS, Cho HJ (2001) Expression of brain-derived neurotrophic factor in rat dorsal root ganglia, spinal cord and gracile nuclei in experimental models of neuropathic pain. Neuroscience 107: 301-309.

Ikeda O, Murakami M, Ino H, Yamazaki M, Nemoto T, Koda M, Nakayama C, Moriya H (2001) Acute up-regulation of brain-derived neurotrophic factor expression resulting from experimentally induced injury in the rat spinal cord. Acta Neuropathol (Berl) 102: 239-245.

Kerr BJ, Bradbury EJ, Bennett DL, Trivedi PM, Dassan P, French J, Shelton DB, McMahon SB, Thompson SW (1999) Brain-derived neurotrophic factor modulates nociceptive sensory inputs and NMDA-evoked responses in the rat spinal cord. J Neurosci 19: 5138-5148.

Kovacs R, Kardos J, Heinemann U, Kann O (2005) Mitochondrial calcium ion and membrane potential transients follow the pattern of epileptiform discharges in hippocampal slice cultures. J Neurosci 25: 4260-4269.

Laird JM, Bennett GJ (1993) An electrophysiological study of dorsal horn neurons in the spinal cord of rats with an experimental peripheral neuropathy. J Neurophysiol 69: 2072-2085.

Lever I, Cunningham J, Grist J, Yip PK, Malcangio M (2003) Release of BDNF and GABA in the dorsal horn of neuropathic rats. Eur J Neurosci 18: 1169-1174.

Lever IJ, Bradbury EJ, Cunningham JR, Adelson DW, Jones MG, McMahon SB, Marvizon JC, Malcangio M (2001) Brain-derived neurotrophic factor is released in the dorsal horn by distinctive patterns of afferent fiber stimulation. J Neurosci 21: 4469-4477.

Mannion RJ, Costigan M, Decosterd I, Amaya F, Ma QP, Holstege JC, Ji RR, Acheson A, Lindsay RM, Wilkinson GA, Woolf CJ (1999) Neurotrophins: peripherally and centrally acting modulators of tactile stimulus-induced inflammatory pain hypersensitivity. Proc Natl Acad Sci U S A 96: 9385-9390.

Matayoshi S, Jiang N, Katafuchi T, Koga K, Furue H, Yasaka T, Nakatsuka T, Zhou XF, Kawasaki Y, Tanaka N, Yoshimura M (2005) Actions of brain-derived neurotrophic factor on spinal nociceptive transmission during inflammation in the rat. J Physiol 569: 685-695.

Michael GJ, Averill S, Nitkunan A, Rattray M, Bennett DL, Yan Q, Priestley JV (1997) Nerve growth factor treatment increases brain-derived neurotrophic factor selectively in TrkA-expressing dorsal root ganglion cells and in their central terminations within the spinal cord. J Neurosci 17: 8476-8490.

Michael GJ, Averill S, Shortland PJ, Yan Q, Priestley JV (1999) Axotomy results in major changes in BDNF expression by dorsal root ganglion cells: BDNF expression in large trkB and trkC cells, in pericellular baskets, and in projections to deep dorsal horn and dorsal column nuclei. Eur J Neurosci 11: 3539-3551.

Miletic G, Miletic V (2002) Increases in the concentration of brain derived neurotrophic factor in the lumbar spinal dorsal horn are associated with pain behavior following chronic constriction injury in rats. Neurosci Lett 319: 137-140.

Moore KA, Kohno T, Karchewski LA, Scholz J, Baba H, Woolf CJ (2002) Partial peripheral nerve injury promotes a selective loss of GABAergic inhibition in the superficial dorsal horn of the spinal cord. J Neurosci 22: 6724-6731.

Pezet S, Cunningham J, Patel J, Grist J, Gavazzi I, Lever IJ, Malcangio M (2002) BDNF modulates sensory neuron synaptic activity by a facilitation of GABA transmission in the dorsal horn. Mol Cell Neurosci 21: 51-62.

Prescott SA, Sejnowski TJ, De Koninck Y (2006) Reduction of anion reversal potential subverts the inhibitory control of firing rate in spinal lamina I neurons: towards a biophysical basis for neuropathic pain. Mol Pain 2: 32.

Ruangkittisakul A, Schwarzacher SW, Secchia L, Poon BY, Ma Y, Funk GD, Ballanyi K (2006) High sensitivity to neuromodulator-activated signaling pathways at physiological [K+] of confocally imaged respiratory center neurons in on-line-calibrated newborn rat brainstem slices. J Neurosci 26: 11870-11880.

Ruscheweyh R, Sandkuhler J (2005) Long-range oscillatory Ca2+ waves in rat spinal dorsal horn. Eur J Neurosci 22: 1967-1976.

Sivilotti L, Woolf CJ (1994) The contribution of GABAA and glycine receptors to central sensitization: disinhibition and touch-evoked allodynia in the spinal cord. J Neurophysiol 72: 169-179.

Slack SE, Pezet S, McMahon SB, Thompson SW, Malcangio M (2004) Brain-derived neurotrophic factor induces NMDA receptor subunit one phosphorylation via ERK and PKC in the rat spinal cord. Eur J Neurosci 20: 1769-1778.

Slack SE, Thompson SW (2002) Brain-derived neurotrophic factor induces NMDA receptor 1 phosphorylation in rat spinal cord. Neuroreport 13: 1967-1970.

Thompson SW, Bennett DL, Kerr BJ, Bradbury EJ, McMahon SB (1999) Brain-derived neurotrophic factor is an endogenous modulator of nociceptive responses in the spinal cord. Proc Natl Acad Sci U S A 96: 7714-7718.

Yuste R, Konnerth A (2005) Imaging in Neuroscience and Development.

Zhou XF, Chie ET, Deng YS, Zhong JH, Xue Q, Rush RA, Xian CJ (1999) Injured primary sensory neurons switch phenotype for brain-derived neurotrophic factor in the rat. Neuroscience 92: 841-853.

CHAPTER 8

GENERAL DISCUSSION AND FINAL CONCLUSIONS

This thesis work is a thorough examination of the effects of long-term BDNF exposure on dorsal horn neurons. Prolonged BDNF release following peripheral nerve injury is thought to enhance the excitability of dorsal horn neurons in the spinal cord which can lead to central sensitization of nociceptive signalling. These alterations induced by BDNF likely reflect long-lasting, possibly even permanent changes in neuronal plasticity and may underlie the mechanisms involved in chronic, intractable neuropathic pain. Therefore, by examining the effects of BDNF on dorsal horn excitability and identifying its mechanism of action, we can better understand the progression of this disease and identify better pharmacological targets for treatment.

The main findings from this thesis work are I) BDNF can mediate central sensitization of the dorsal horn. Long-term BDNF exposure increases the excitability of the dorsal horn and initiates changes in synaptic functioning which may be responsible for the generation of neuropathic pain. II) The BDNF-induced changes observed in this population of dorsal horn neurons, which may represent mechanisms of central sensitization, probably do not involve postsynaptic alterations in glutamate receptors typically associated with LTP. III) Although changes in inhibition can drive excitability in neuronal networks, the BDNF-induced changes in inhibitory synaptic activity do not contribute to the overall increase in dorsal horn excitability observed. Furthermore, the reversal of the chloride gradient by BDNF does not appear in this neuronal population. IV) I have characterized and optimized a useful *in vitro* system that allows for the study of chronic, neuropathic pain mechanisms.

8.1 BDNF Instigates Central Sensitization

Exposure of dorsal horn neurons to BDNF, for comparable durations detected *in vivo* following nerve injury, resulted in few changes in the properties of individual neurons. No appreciable change in passive membrane properties (Table 4-1) or voltage-dependent conductances was noted in examinations of current-voltage relationships (Figure 4-2) and intrinsic membrane excitability (Figure 4-3). Moreover, there was no change in the probability of encountering each class of electrophysiologically-defined neuronal cell type (Figure 4-1) indicating no significant loss of dorsal horn neuron populations with BDNF, which has been suggested as a mechanism of neuropathic pain (Maione et al., 2002; Moore et al., 2002; Scholz et al., 2005; but see Polgar et al., 2003; Polgar et al., 2004; Polgar et al., 2005).

The lack of changes in individual neurons questions the ability of BDNF to instil long-lasting changes in central dorsal horn neurons, a hallmark feature of central sensitization. Central sensitization mechanisms are responsible for enhancing the excitability of dorsal horn neurons, irrespective of continuous input from injured primary afferents (Woolf, 1983; Woolf and Chong, 1993). It is a means of transferring increased excitability in primary afferents to dorsal horn neurons and may underlie the induction and development of intractable neuropathic pain. Therefore, if there are no changes in the properties of dorsal horn neurons, then BDNF may not participate in this process.

However, BDNF induced significant alterations in excitatory and inhibitory synaptic transmission (Chapter 4 to 6). Furthermore, BDNF exhibited selective actions on distinct populations of dorsal horn neurons, not a generic proliferative effect (Bregman et al., 1997; Deng et al., 2000). Putative inhibitory dorsal horn populations, tonic firing islet-central neurons and GAD-positive neurons, received significantly less excitatory and inhibitory synaptic activity whereas presumed excitatory dorsal horn populations, 'delay' firing radial neurons, received increased excitatory and inhibitory synaptic drive following BDNF treatment.

Still, it may be argued that these changes in synaptic transmission to identified populations of dorsal horn neurons may be too subtle to have any consequence on dorsal horn excitability. However, long-term exposure to BDNF also initiated spontaneous oscillations in intracellular Ca^{2+} concentration in the dorsal horn of treated slices (Figure 7-2) which were driven by synaptic activity (Figures 7-4 and 7-5). These BDNF-induced Ca^{2+} oscillations correlated to an increase in activity measured during extracellular recordings of the dorsal horn (Figure 7-3) similar to what has been observed in animal models of neuropathic pain (Dalal et al., 1999; Laird and Bennett, 1993). Therefore, the generation of spontaneous Ca^{2+} oscillations in the dorsal horn may represent a new mechanism which may underlie the pathogenesis of neuropathic pain. Moreover, the same depolarization stimulus evoked a larger response in BDNF-treated slices compared to controls (Figure 7-1) suggesting BDNF may also induce mechanisms responsible for the hyperalgesia observed in neuropathic pain states.

Since all BDNF-treated slices tested exhibited spontaneous Ca^{2+} oscillations, BDNF is able to alter synaptic activity reproducibly which results in a long-term increase in dorsal horn excitability. The ability of BDNF to induce long-lasting changes and promote excitability in the dorsal horn strongly supports the role of BDNF as a chemical mediator of central sensitization and possibly of chronic, neuropathic pain.

8.1.1 Similar alterations in dorsal horn neurons observed in a nerve injury model of neuropathic pain

Chronic constriction injury (CCI) of the sciatic nerve of animals induces neuropathic pain-like behaviours such as hyperalgesia and allodynia (Balasubramanyan et al., 2006). A comparison of the effects of long-term BDNF exposure and CCI on excitatory synaptic transmission to dorsal horn neurons (Table 4-2, and Figure 8-1) reveals a similar pattern of changes. The pattern of changes was specific to different neuronal populations and was not uniform across the entire dorsal horn. Excitatory synaptic drive to putative inhibitory tonic neurons decreases whereas an increase to excitatory 'delay' neurons is observed (Figure 8-1).

For tonic neurons, CCI induced a decrease in mEPSC amplitude, frequency and time constant for decay (τ) (Figures 8-1A and E, 8-2D) which paralleled the effects of long-term BDNF exposure on mEPSCs events (Figures 8-1B, F and 4-7D). Further analysis of the mechanisms underlying the decrease in excitatory synaptic activity following CCI was performed as shown in Figure 8-2. The mEPSC amplitude distribution in Figure 8-2A to C show mEPSC events fit best with two Gaussian distributions. A comparison of the population peaks reveals a leftward shift in the amplitude populations with CCI (Figure 8-2C). A similar shift in amplitude distribution was observed in mEPSC events of tonic neurons after BDNF treatment (Figure 4-7E to G). To test the reduction in mEPSC τ did not contribute to the reduction in mEPSC amplitude, two different populations of mEPSCs were modelled using a two exponential equation (Figure 8-2D and E, methods described in Chapter 4). The mean value of $\tau 2$ as 7.25 ms was used and the amplitudes peaks were modelled to represent the two mEPSC peak amplitudes seen in control sham-operated neurons (Figure 8-2D and E). Next, the two peaks of mEPSC amplitudes for events in CCI neurons were modelled based on the reduced mean value of 4.94 ms for τ2. Lastly, the control events were remodelled using the τ2 value of 4.94 ms from events acquired in CCI tonic neurons. Since this increase in decay rate produced only slight reductions in the calculated amplitudes of peaks 1 and 2, a decrease in the decay time constant τ2 for mEPSC decay cannot account for the substantially reduced peak amplitudes seen in tonic CCI neurons. A similar result was obtained following similar analysis in BDNF-treated tonic neurons (Figure 4-7H to J).

For 'delay' neurons, CCI induced an increase in mEPSC amplitude and frequency (Figure 8-1C and G) which matched the effect of long-term BDNF exposure on mEPSC events (Figure 8-1D and H). Further analysis of the mechanisms underlying the increase in excitatory synaptic activity following CCI was performed as shown in Figure 8-3. As was found in DMOTC 'delay' cells, three populations of mEPSC amplitude were identified in control sham-operated 'delay' cells by fitting Gaussian curves to binned histogram data. Insets to Figure 8-3A and B show optimized χ^2 values when using 3 peaks to fit the data. Figure 8-3C is a replot of the distributions for comparison between control (sham) and CCI cells. There was not a uniform shift in all mEPSC populations following CCI (Figure 8-3C) rather the largest population shift occurred with the third peak increasing from 16.5 ± 3.7 pA in sham-operated controls to 24.3 ± 0.9 pA in CCI. Likewise in BDNF-treated 'delay' cells, the emergence of large amplitude mEPSCs accounted for the increase in mEPSC amplitude observed following BDNF treatment (Figure 4-8G).

The similarity in the underlying mechanisms producing these specific changes in excitatory synaptic transmission following BDNF and nerve injury provide further support for the role of BDNF in the induction of neuropathic pain.

8.1.2 Blocking BDNF attenuates dorsal horn excitability

If the release of BDNF from primary afferent nerves (Michael et al., 1999; Miletic and Miletic, 2002) and microglia (Coull et al., 2005; Dougherty et al., 2000; Ikeda et al., 2001) is responsible for generating the pattern of changes in excitatory synaptic transmission produced by CCI, it should be prevented by blocking the actions of BDNF. I have already shown heat-inactivating BDNF reduces its action on excitatory and inhibitory synaptic events (Figures 4-4M, N and 5-1M, N), but this does not confirm release of BDNF from a physiological source during nerve injury is responsible for the changes in synaptic transmission I observed. To show this, fluorescent Ca^{2+} imaging techniques were used (Ruangkittisakul et al., 2006; see Chapter 7 for details) to monitor dorsal horn excitability in DMOTC slices.

Figure 8-4A and B shows typical signals from a field of neurons and the increase in signal intensity evoked by superfusion of saline containing 35 mM K^+. Figures 8-4C and D show real time recordings of fluorescent Ca^{2+} signals from three randomly selected neurons in control and BDNF-treated cultures. The latter responses are obviously larger. Quantification of data from over 30 samples of neurons confirm that 35 mM K^+ is more effective in elevating intracellular Ca^{2+} in BDNF-treated cultures (Figure 8-4E).

To demonstrate the effect of CCI on the excitability of dorsal horn neurons in DMOTC slices, Dr. James Biggs in our laboratory has exploited the response of spinal microglia to this type of injury (Coull et al., 2005; Tsuda et al., 2005). Thus, introduction of medium from activated microglia into the cultures *in vitro* was assumed to be equivalent to inducing CCI *in vivo*. The constituents released form activated microglia range from BDNF (Coull et al., 2005; Dougherty et al., 2000; Ikeda et al., 2001) to various cytokines (Hains and Waxman, 2006; Tsuda et al., 2005; Watkins and Maier, 2002). It was found that DMOTC slices maintained in the presence of activated microglial-conditioned medium, or MCM (from cortical microglia activated with lipopolysaccharide or LPS) (Lai and Todd, 2006), exhibited an overall increase in dorsal horn excitability. The Ca^{2+} responses to high K^+-induced depolarization were enhanced in cultures exposed to the MCM (Figure 8-4I). Figure 8-4F and G compare typical Ca^{2+} signals from a sampling of neurons recorded in a control DMOTC with those from cultures exposed to activated-MCM.

To test whether this increased excitability reflected the presence of BDNF in the MCM, BDNF was neutralized by using the binding protein, TrkB-d5. This recombinant protein is identical to the neurotropin binding region on the 5th extracellular domain of the high affinity TrkB receptor (Banfield et al., 2001; Naylor et al., 2002). TrkB-d5 was included at the time of activation of microglial cultures with LPS to sequester any BDNF released. It was observed that MCM, that was free of BDNF by the inclusion of TrkB-d5, was ineffective in promoting increased dorsal horn activity (Figure 8-4H) as Ca^{2+} responses were similar to those recorded from control neurons (compare Figures 8-4F and H). It is very likely therefore, that the increase in activity promoted by MCM was mediated by BDNF.

These experiments demonstrate that release of BDNF from activated microglia can enhance the excitability of dorsal horn neurons. Hence, nerve injury-induced activation of microglia and subsequent BDNF release can play a major role in the development of central sensitization in the dorsal horn which can lead to neuropathic pain.

8.1.3 BDNF is a chemical mediator of central sensitization

There are studies which suggest BDNF is a mediator of inflammatory-induced pain exclusively, and not neuropathic pain (Mannion et al., 1999; Matayoshi et al., 2005; Zhao et al., 2006). However, there are studies demonstrating attenuation of nociceptive responses in nerve injury models of neuropathic pain by prevention of BDNF signalling (Coull et al., 2005; Fukuoka et al., 2001; Yajima et al., 2002; Yajima et al., 2005). Although a level of inflammation is associated with any nerve injury model, there is a significant increase in BDNF expression and an increase in postsynaptic TrkB receptor expression that was sustained 1 week post-injury (Ha et al., 2001; Ikeda et al., 2001; Miletic and Miletic, 2002), suggesting elevated levels were sustained beyond the initial tissue inflammation associated with surgery. Therefore, prolonged release of BDNF following nerve injury supports the role of BDNF as mediator of central sensitization.

BDNF can induce acute effects on fast synaptic transmission (Blum et al., 2002; Lohof et al., 1993; Rose et al., 2004) similar to neurotransmitters. In fact, BDNF fulfills a number of criteria used to distinguish a neurotransmitter from other signalling molecules in the body.

1) *Neurotransmitters are synthesized and stored in the presynaptic nerve terminal.* BDNF is located in secretory granules or large dense-core vesicles and co-stored with other neuropeptides such as CGRP and substance P (Salio et al., 2007). Also, synthesis of BDNF rapidly increases following peripheral nerve injury (Cho et al., 1998; Michael et al., 1999).

2) *Neurotransmitters are released from the presynaptic terminal upon stimulation or depolarization.* Release of BDNF from primary afferents requires a pattern of repeated high frequency bursts (Lever et al., 2001) which may occur following peripheral nerve injury. Also, spinal microglia can release BDNF (Coull et al., 2005; Dougherty et al., 2000; Ikeda et al., 2001). Work presented in Figure 8-4 supports the release of BDNF from activated microglia is responsible for the increase in dorsal horn excitability, which is attenuated by the BDNF binding protein TrkB-d5.

3) *There is an identity of action between the putative neurotransmitter and the physiological effect it mediates.* The effect of BDNF on the excitatory synaptic transmission of dorsal horn neurons is similar to the pattern of changes observed following CCI (Figure 8-1). The actions of BDNF are unique since other potential mediators of central sensitization, such as the cytokine IL-1β, was unable to reproduce this pattern of changes (Table 8-1; Lu et al., 2005). This underlines the significance of the similarity between the actions of BDNF and CCI which produces neuropathic pain.

4) *Pharmacological manipulation of the action of the neurotransmitter has a similar effect on the physiological effect it mediates.* Conditioned medium from activated microglia was used to mimic the effect of CCI on the slice cultures (Coull et al., 2005; Tsuda et al., 2005). Antagonism of the increased excitability produced by this medium by

TrkB-d5 (Figure 8-4I) strongly implicates BDNF as a mediator of microglia-induced hyperactivity. Since microglial activation is characteristic of the spinal response to CCI, it further implicates BDNF in the development of central sensitization associated with peripheral nerve injury and the onset of neuropathic pain.

I have thus demonstrated that long-term BDNF exposure on identified populations of dorsal horn neurons induces neuronal type-specific changes in excitatory and inhibitory synaptic transmission. These modifications in neuronal communication are sufficient to increase the excitability of dorsal horn neurons. The ability of BDNF to promote excitability in this neuronal network strongly supports the role of BDNF as a chemical mediator of central sensitization.

8.2 BDNF and Synaptic Plasticity

Long-term potentiation (LTP) is an increase in synaptic strength that can last minutes to several days. The mechanisms involved in LTP are thought to represent a cellular basis for learning and memory in the nervous system. Central sensitization also involves an activity-dependent increase in the excitability of neurons. These mechanisms are responsible for instigating the long-lasting changes in dorsal horn neurons that can lead to the development of chronic, neuropathic pain syndromes.

It has been well documented that the mechanisms involved in the central sensitization of dorsal horn neurons and LTP share many characteristics (Ji et al., 2003; Woolf and Salter, 2000). For instance, the phosphorylation of postsynaptic NMDA receptors has been shown to be essential in some forms of LTP (Lynch et al., 2004) and similar receptor phosphorylation occurs in dorsal horn neurons during noxious stimulation (Guo et al., 2002). In addition, it has been shown that BDNF can induce similar phosphorylation of NMDA receptors in dorsal horn neurons (Slack and Thompson, 2002). In fact, there is growing evidence for the involvement of BDNF in LTP (Lessmann, 1998; Levine et al., 1995; Lu and Chow, 1999; Malcangio and Lessmann, 2003).

However, the increase in excitatory synaptic transmission to 'delay' neurons could not be attributed to postsynaptic mechanisms commonly associated with LTP. Insertion of AMPA receptor populations has been a proposed mechanism of LTP in central neurons (Gordon et al., 2005; Hayashi et al., 2000), but no change in the peaks of mEPSC amplitude populations (Figure 4-8G) argues against BDNF utilizing this mechanism. Other possible postsynaptic mechanisms such as phosphorylation of AMPA or NMDA receptors, or altered glutamate receptor subunit expression have been suggested to be involved in LTP and central sensitization (Ji et al., 2003; Woolf and Salter, 2000), but these mechanisms likely involve alterations in current amplitude or possibly current decay kinetics which were not observed following BDNF treatment (Figure 4-8D and G). The occurrence of a population of large amplitude mEPSCs (Figure 4-8H) probably reflects the coincident release of vesicles from the presynaptic terminal since this mechanism does not involve changes in postsynaptic receptor sensitivity to glutamate. Therefore, in the 'delay' population of dorsal horn neurons examined in this study, the postsynaptic mechanisms commonly associated with LTP do not appear to contribute to BDNF-induced enhancement of excitatory synaptic transmission.

Nevertheless, BDNF can induce long-lasting changes in postsynaptic plasticity during central sensitization. For instance, in the tonic population of dorsal horn neurons, a change in the decay kinetics (τ) was observed for both excitatory (Figure 4-7D) and inhibitory currents (Figure 5-4D). This could reflect altered receptor subunit expression and thus alterations at the genomic level of expression in dorsal horn neurons. It is unlikely a change in membrane shunting is responsible for alterations in current decay since mEPSC τ and mIPSC τ for tonic neurons were not altered the same way. Central sensitization may also involve long-lasting structural modifications such as retraction of primary afferent terminals and even loss of terminals which have been observed following nerve injury (Bailey and Ribeiro-da-Silva, 2006) and microglial activation (Beggs and Salter, 2007). Since BDNF release has been reported following both instances, these alterations in synaptic connectivity could be mediated by BDNF.

The mechanisms mediating central sensitization are diverse and may in some spinal cord regions invoke mechanisms similar to those involved in LTP. However, in the dorsal horn neurons examined in detail in this study, enhanced dorsal horn excitability by BDNF does not involve these LTP-associated mechanisms.

8.3 BDNF-induced Alterations in Inhibition is Not as Significant as Alterations in Excitation to Dorsal Horn Excitability

Following long-term BDNF exposure, there are selective changes in inhibitory synaptic activity in dorsal horn neurons. There was a decrease in spontaneous inhibitory synaptic currents to all neuronal cell types except 'delay' neurons (Figure 5-1). The increased inhibitory synaptic activity to 'delay' neurons does not reflect a reversal of GABA inhibition since addition of GABA suppressed spontaneous oscillatory activity (Figure 7-7C) and blockade of inhibitory receptors produced an increase in excitatory synaptic activity (Figure 5-7). If BDNF produces a reversal in inhibitory actions such that GABA mediates excitation, a decrease in synaptic activity would be expected after blocking inhibitory action. This mechanism of BDNF action was proposed for Lamina I neurons (Coull et al., 2005; Prescott et al., 2006) but it does seem to apply to the dorsal horn neurons in this study. Neurons in DMOTC slices resemble the neurons described in the *substantia gelatinosa* region or Lamina II of the spinal cord (Balasubramanyan et al., 2006; Grudt and Perl, 2002; Lu et al., 2006), which may explain this discrepancy.

8.3.1 Consequences of alterations in inhibitory synaptic activity to delay neurons

An increase in excitatory synaptic drive to potentially excitatory 'delay' firing neurons, which have been shown to generate bursts of spontaneous action potentials (Figure 4-9), is consistent with an increase in dorsal horn excitability. However, the parallel increase in inhibitory synaptic activity to 'delay' neurons following BDNF treatment (Figure 5-1B and G) is more difficult to interpret. Increased inhibition of excitatory neurons would be expected to reduce their excitatory output, opposing the expected action a concurrent increase in excitatory synaptic activity would produce.

However, the actions of BDNF on excitatory and inhibitory activity of 'delay' neurons do not directly counteract one another. Most of the BDNF-induced alterations in excitatory synaptic activity to 'delay' cells can be attributed to presynaptic mechanisms since there is no change in the postsynaptic sensitivity of 'delay' cells to glutamate (Figure 4-8G). The BDNF-induced increase in inhibitory activity likely involved alterations in postsynaptic receptors since a significant decrease in holding current, a measure of 'tonic' conductance (Figure 5-7D and E), and an amplification of excitatory event amplitude was observed during application of inhibitory blockers (Figure 5-6C). As well, enhanced release from inhibitory neurons on to 'delay' neurons is likely responsible for the increased frequency of inhibitory events (Figure 5-1G). But, BDNF does not alter presynaptic inhibition of excitatory inputs since the change in frequency did not differ compared to controls during removal of inhibitory activity (Figure 5-6D). So, it is possible for a simultaneous increase in both excitatory and inhibitory activity in 'delay' neurons. Though, the issue remains whether excitatory or inhibitory inputs determine the level of 'delay' neuron activity.

8.3.2 Assessing contribution of inhibition to overall neuronal activity

As noted previously, the frequency of inhibitory currents was much lower than that of excitatory synaptic currents. Moreover, the actual inhibitory currents on a neuron at membrane potentials closer to rest may actually be much smaller than the currents measured at 0 mV. Therefore, to evaluate the contribution of inhibitory and excitatory synaptic transmission to overall neuronal activity, the total charge transfer from excitatory and inhibitory synaptic events over 1 min of activity was calculated for neurons at their resting membrane potential (RMP). I wanted to approximate the charge transfer the cell would actually experience at rest to determine the net charge and thus directionality of neuronal activity. If excitatory activity is truly dominant and determines neuronal activity, the charge transfer contributed by sEPSC activity should outweigh that from sIPSC activity leaving a net positive charge transfer.

The total charge transfer was calculated from the area of sEPSCs or sIPSCs, for excitatory and inhibitory events respectively, corrected to the actual driving force of current from the cell's RMP. For instance, for a cell with a RMP of -60 mV, the actual driving force for excitatory events is 60 mV, which is 86% of the drive of sEPSCs recorded at -70 mV and 86% of the charge transfer of sEPSCs at -70 mV. For inhibitory events, the actual driving force at rest is 20 mV, which is 25% of the drive and charge transfer of sIPSCs recorded at 0 mV.

The charge transfer for a sample of tonic islet-central (TIC) cells is shown in Figure 8-5A. The sum of the integrals, or total area, for excitatory events during 1 min of recording produces a positive charge transfer which is reduced by BDNF treatment. For inhibitory events, the charge transfer is negative and BDNF also produces a slight decrease in the charge transfer. These decreases correspond to the decrease in both sEPSC and sIPSC amplitude and frequency in TIC neurons reported previously in Chapter 6 (Figure 6-2). The net charge transfer, or the sum of the excitatory and inhibitory charge transfer, produced a net positive charge which decreased with BDNF treatment (Figure 8-5A). The average charge transfer was reduced approximately 50% of the value from control TIC neurons. These BDNF-induced decreases did not reach statistical significance, though only a small sample set was tested. Nevertheless, excitatory synaptic activity outweighs inhibitory activity in TIC neurons and is the major determinant of the level of neuronal activity.

The charge transfer for a sample of 'delay' radial (DR) cells is shown in Figure 8-5B. Like TIC cells, the total area for excitatory events is positive and inhibitory events produce a negative charge transfer in DR cells. But following BDNF treatment, these values increased. The net charge transfer remained positive, supporting the importance of excitatory activity in determining neuronal activity. The net charge transfer increased over 2-fold following BDNF treatment.

In both cell types examined, the charge transfer from excitatory synaptic activity was greater than inhibitory synaptic activity at RMP. A net positive charge could depolarize and thus activate the cell. Moreover, the BDNF-induced changes to inhibitory synaptic activity are obscured by the BDNF-induced changes to excitatory synaptic activity which appears to determine neuronal activity. Therefore, spontaneous inhibitory synaptic activity may not be as important as excitatory synaptic activity in determining the spontaneous excitability of neurons.

8.3.3 Limited effect of BDNF-induced changes in inhibition on overall dorsal horn excitability

As demonstrated in the previous section, alterations in excitatory synaptic activity determine the resultant level of neuronal excitability. Thus, for 'delay' neurons, despite an increase in inhibitory transmitter signalling, enhanced excitatory activity increased the occurrence of spontaneous action potential bursting in 'delay' neurons (Figure 4-9G), which would increase the output of putative excitatory 'delay' neurons.

In all other neuronal phenotypes: tonic, 'irregular', phasic and transient firing neurons, a decrease in inhibitory synaptic transmission was observed (Figure 5-1). The disinhibition of putative inhibitory neurons, such as tonic and GAD-positive neurons would be expected to increase excitability, but this was not the case. Accompanying the loss of inhibition was reduced excitatory drive to BDNF-treated tonic neurons (Figure 4-4A and F) which would account for the reduction in spontaneous action potential generation (Figure 4-9B). In the other neuronal phenotypes, it is not clear if they represent excitatory or inhibitory neurons in the dorsal horn. But, output from these neurons is likely increased since all three of these cell types also received enhanced excitatory drive following long-term BDNF treatment (Figure 4-4C to E and H to J).

Although pharmacological removal of inhibition was sufficient to drive network oscillations and enhance dorsal horn excitability (Figure 7-7A and B), it is unlikely BDNF induces a sufficient loss of spinal inhibition since there was a marked increase in neuronal activity (Figures 5-7) and magnitude of Ca^{2+} oscillations (Figure 7-7A) following pharmacological suppression of all inhibition. Despite a decrease in inhibitory synaptic activity to most neuronal cell types, there is still substantial inhibition present in the dorsal horn following BDNF treatment. Addition of exogenous GABA was able to suppress BDNF-induced Ca^{2+} oscillations (Figure 7-7C) and excitability in the dorsal horn (Figure 7-3). Similarly, in nerve injury models, activation of inhibitory receptors alleviates neuropathic pain-like behaviours (Hwang and Yaksh, 1997).

8.4 Organotypic Culture of Spinal Cord Slices: Studying "Pain in a Dish"

Organotypic cultures of spinal cord slices offer a unique opportunity to study the effects of potential pain mediators on dorsal horn neurons. Morphological analysis of cells in DMOTC slices identified all major classes of neurons described in the dorsal horn of acutely prepared slices (Figure 6-1). Tonic firing islet-central, 'delay' firing radial and 'delay' firing vertical cells correlate well with dorsal horn neurons previously described (Heinke et al., 2004; Lu and Perl, 2003; Lu and Perl, 2005; Prescott and De Koninck, 2002). Also, the synaptic pharmacology and connectivity remain intact during culturing

(Figure 3-5) enabling the study of neuronal networks with this preparation. Furthermore, the development of inhibitory synapses in dorsal horn neurons of cultured slices progresses along normally (Figure 3-5I) and at rates similar to what has been reported in neurons from an intact animal (Baccei and Fitzgerald, 2004; Keller et al., 2001).

This preparation system was particularly useful in studying the effects of neuropeptide signalling in the dorsal horn. The expression of most TrkB receptors in dorsal horn neurons does not coincide with BDNF-expressing primary afferents (Bardoni et al., 2007; Salio et al., 2005). Even though nerve injury initiates changes in the expression of BDNF in primary afferents (Karchewski et al., 2002; Michael et al., 1999) and postsynaptic $p75^{NTR}$ and TrkB receptors (King et al., 2000), BDNF likely signals to receptors by volume transmission (Merighi, 2002). Therefore, long-term bath application of BDNF in these studies is comparable to exposure conditions present *in vivo*.

Organotypic slice cultures are easily amendable to a variety of techniques. Electrophysiological recordings and Ca^{2+} imaging experiments are done with ease through these thin cultured slices. Additionally, these cultures allow for the long-term application of chemical mediators for equivalent time-courses detected during neuropathic pain states. Therefore, this *in vitro* preparation system allows for the study of neurons involved in the nociceptive signalling pathway which can provides some insights into the mechanisms of neuropathic pain.

8.5 Final Conclusions

Prolonged exposure to elevated levels of BDNF produces an increase in dorsal horn excitability. BDNF mainly affects excitatory synaptic transmission in dorsal horn neurons which initiates spontaneous Ca^{2+} oscillations that are sufficient to generate spontaneous extracellular activity. Blockade of BDNF signalling with TrkB-d5 prevents the BDNF-induced elevation in dorsal horn excitability. Also, the pattern of synaptic changes induced by BDNF is quite similar to the changes observed in an animal model of neuropathic pain; adding to the credibility of BDNF as the instigator of central sensitization.

BDNF released following nerve injury or microglial activation, can signal rapid changes in neurons, or may induce long-lasting alterations in neuronal function. But the intended message to central nociceptive neurons is not clear. Neuropathic pain is a debilitating disease that interferes with normal functioning and reduces one's quality of life. So it is unlikely the physiological role of BDNF is to induce these detrimental changes. BDNF has been implicated in neuronal sprouting and survival which may be the intended purpose of releasing BDNF at times of nerve injury or intense inflammation. However, it may be the excess of BDNF release or other lack of compensatory changes which lead to maladaptive alterations in nociceptive signalling.

Hopefully, by identifying the mediator responsible for instigating this disease and understanding its mechanism of action, we can begin to develop new treatments and therapies for people afflicted with this disease.

Table 8-1: Summary comparisons between chronic constriction injury (CCI), BDNF-treatment and interleukin-1β (IL-1β) on excitatory synaptic transmission.

Data for changes induced by CCI from *Balasubramanyan et al., 2006* and data from IL-1β experiments from *Lu et al., 2005*. Table Legend: ↑ indicates a significant increase compared to control; ↓ indicates a significant decrease compared to control; ↔ indicates no change compared to control.

Data from acute slices kindly provided by S. Balasubramanyan and data from IL-1β (100 pM) treated DMOTCs kindly provided by S. Gustafson.

	Tonic	Delay	Irregular	Phasic	Transient
sEPSC amplitude					
CCI	↓	↑	↑	↓	↑
BDNF	↓	↔	↑	↑	↑
IL-1β	↑	↑	↓	↓	↑
sEPSC frequency					
CCI	↓	↑	↑	↑	↑
BDNF	↓	↑	↑	↑	↑
IL-1β	↔	↓	↓	↓	↑

Figure 8-1: Cumulative probability plots comparing the effects of BDNF and CCI on amplitude and frequency of sEPSCs and mEPSCs in tonic and delay cells.

A to D: Effects on sEPSC amplitude. E to H: Effects on sEPSC inter-event interval. I to L: Effects on mEPSC amplitude. M to P: Effects on mEPSC inter-event interval. With the exception of the effect on BDNF on delay neuron sEPSC amplitude (D), all data were significant according to the Kolmogorov-Smirnoff test. *P values* ranged from <0.02 to <0.001. For sEPSCs and mEPSCs in DMOTC (amplitude and IEI), the first 50 events following the 1st minute of recordings from each cell were pooled in order to construct cumulative distribution plots. The first 30 events were used for mEPSCs in CCI experiments. All comparisons were made using roughly the same number of events for the control and experimental situations. Sample sizes, which were dictated by the frequency of spontaneous events in the different cell types, ranged from 175 to 1700. Portions of the figure illustrating data from CCI experiments are modified from *Balasubramanyan et al., 2006*.

Data from acute slices kindly provided by S. Balasubramanyan.

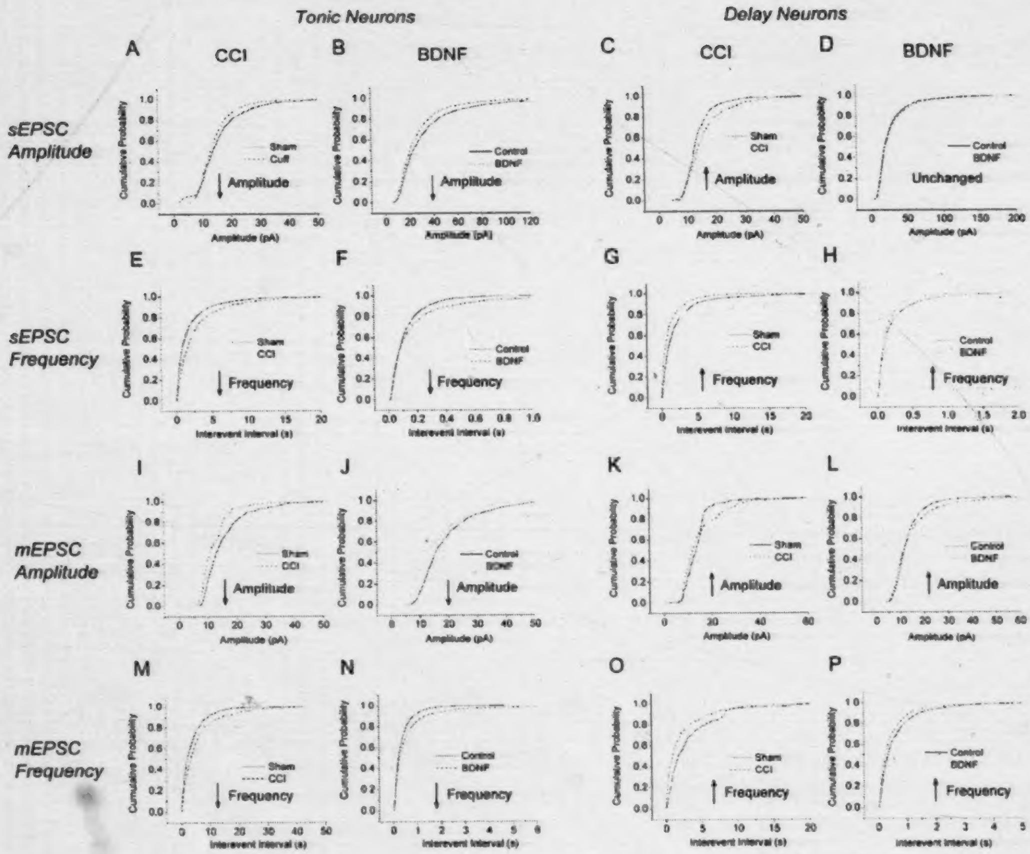
Tonic Neurons
Delay Neurons
A
CCI
B
BDNF
C
CCI
D
BDNF
sEPSC Amplitude
sEPSC Frequency
mEPSC Amplitude
mEPSC Frequency
Cumulative Probability
Sham
Cuff
Amplitude
Control
BDNF
Sham
CCI
Unchanged
Amplitude (pA)
E
F
G
H
Frequency
Interevent Interval (s)
I
J
K
L
M
N
O
P

Figure 8-2: Further analysis of the effects of CCI on mEPSCs of tonic neurons.

A: Distribution histogram (1 pA bins) for amplitudes of 300 mEPSCs from control sham tonic neurons. Fit of the data to two Gaussian distributions represented by black lines. B: Similar histogram and fit to two Gaussian functions for 268 mEPSCs from CCI neurons. *Insets* in A and B: Graphs to show effect of number of Gaussian fits (peaks) on the corrected value of χ^2. C: Superimposition of the two Gaussian peaks obtained in (A) with those obtained in (B). D: Graph to show the mean mEPSC decay time constant (τ) for control sham, white bar, and CCI, grey bar, tonic neurons. Error bars indicate SEM. For unpaired t-test, § = $p<0.001$. E and F: Modelled mEPSCs to represent the two peak Gaussian amplitudes obtained in (A) and (B). Solid black lines are for control events (from A), dashed lines are for events in CCI (from B) and dotted lines illustrate effect of a 32% reduction of $\tau 2$ on the control events.

Data from acute slices kindly provided by S. Balasubramanyan.

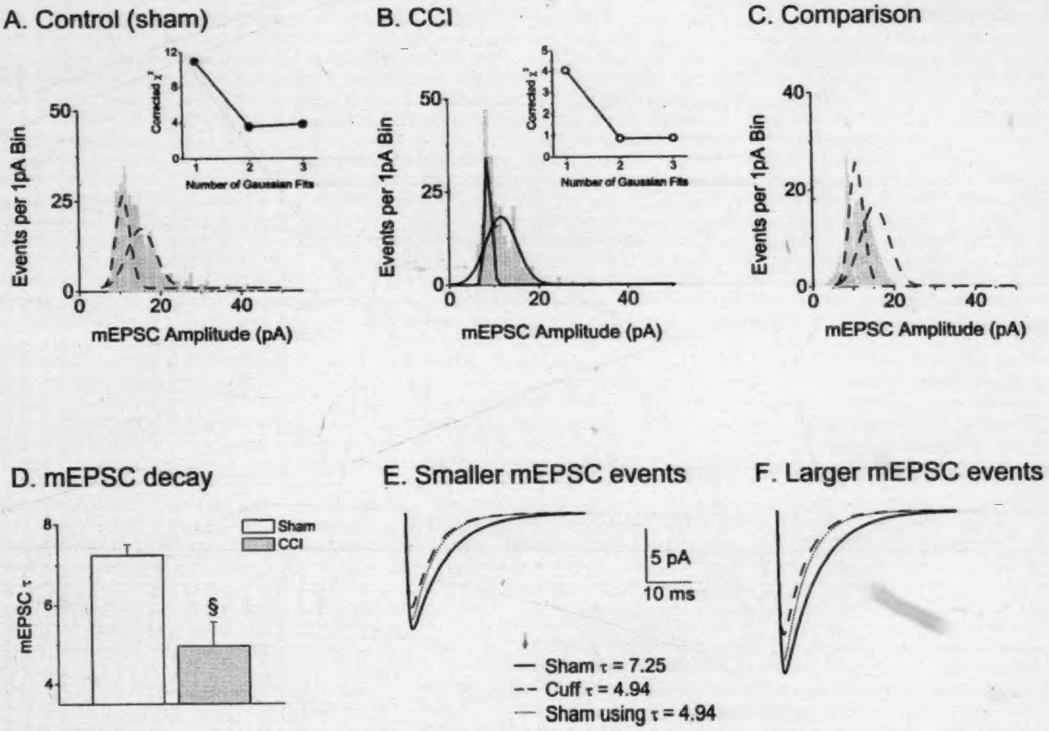
A. Control (sham)
B. CCI
C. Comparison
Events per 1pA Bin
mEPSC Amplitude (pA)
Corrected χ²
Number of Gaussian Fits
D. mEPSC decay
Sham
CCI
mEPSC τ
§
E. Smaller mEPSC events
5 pA
10 ms
Sham τ = 7.25
Cuff τ = 4.94
Sham using τ = 4.94
F. Larger mEPSC events

Figure 8-3: Further analysis of the effects of CCI on mEPSCs of delay neurons.

A: Distribution histogram (1 pA bins) for amplitudes of 730 mEPSCs from control delay neurons. Fit of the data to three Gaussian distributions represented by black lines. B: Similar histogram and fit to three Gaussian functions for 750 mEPSCs from CCI neurons. *Insets in* A and B: Graphs to show effect of number of Gaussian fits (peaks) on the value of corrected χ^2. C: Superimposition of the three Gaussian peaks obtained in (A) with those obtained in (B).

Data from acute slices kindly provided by S. Balasubramanyan.

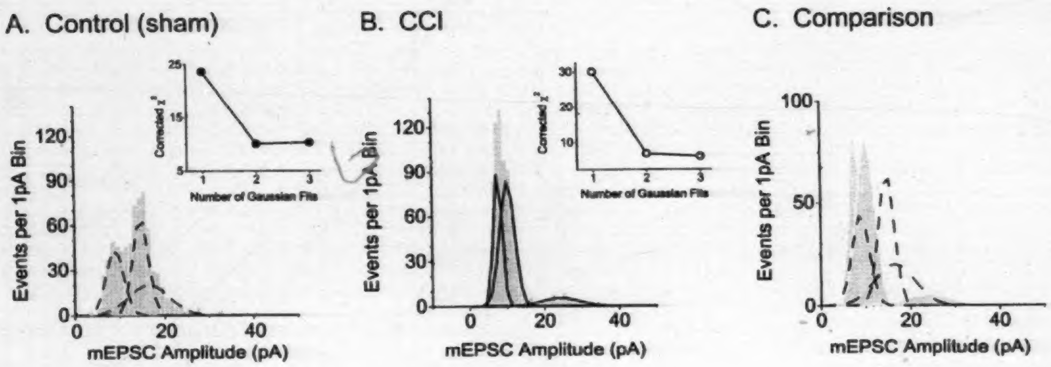
A. Control (sham)
B. CCI
C. Comparison
Events per 1pA Bin
mEPSC Amplitude (pA)
Corrected χ²
Number of Gaussian Fits
0
20
40
30
60
90
120
50
100
1
2
3
5
15
25
10
20
30

Figure 8-4: Population excitability of dorsal horn cells as measured by real-time Ca^{2+} responses to 35 mM K^{+}.

A and B: Confocal images of fields of DMOTC neurons prior to and immediately following exposure to 35 mM K^{+}. Note strong Fluo-4 signal (shown in lighter shade) from individual neurons in response to superfusion of K^{+}. Data records in remainder of figure are real time recordings of Fluo-4 Ca^{2+} signals evoked by 35 mM K^{+} from representative neurons in each experimental situation. C: Response of 3 control neurons. Calibration bar in time and arbitrary units (A.U.) refers to all data records. D: Response of 3 neurons from BDNF-treated DMOTC. E: Summary data from ~ 30 neurons in each situation. F: Response of another 3 control neurons. Calibration bar in time and arbitrary units (A.U.) refers to all data records. G. Response of 3 neurons in DMOTC exposed to activated microglia conditioned medium (MCM). H: Response of 3 neurons exposed to MCM that had been pre-incubated with 7.5 μM TrkB-d5 to bind any BDNF in the medium. I: Summary data from 11 – 20 neurons in each situation. Error bars indicate SEM. For paired t-test, § = $p<0.001$.

Microglial and TrkB-d5 data kindly provided by J. Biggs. TrkB-d5 was a kind gift from D. Dawbarn, University of Bristol and microglial cultures kindly provided by A. Lai.

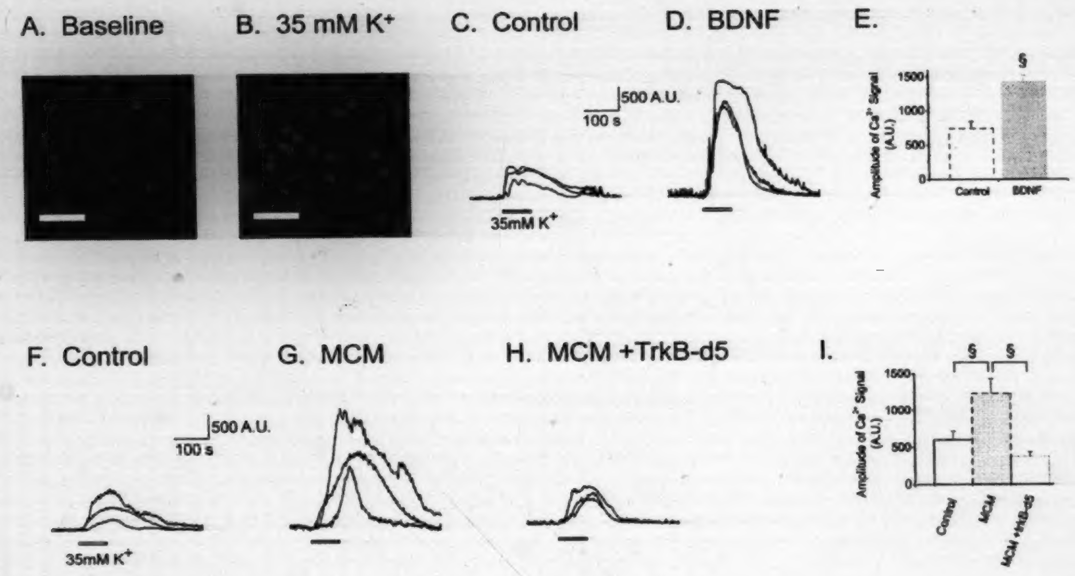
A. Baseline
B. 35 mM K⁺
C. Control
D. BDNF
E.
500 A.U.
100 s
35mM K⁺
§
1500
1000
500
0
Amplitude of Ca²⁺ Signal (A.U.)
Control
BDNF
F. Control
G. MCM
H. MCM +TrkB-d5
I.
500 A.U.
100 s
35mM K⁺
§
§
1500
1000
500
0
Amplitude of Ca²⁺ Signal (A.U.)
Control
MCM
MCM +TrkB-d5

Figure 8-5: Calculated charge transfer for TIC and DR neurons at resting membrane potential.

A and B: Averages from the summation of sEPSC, sIPSC and net charge transfer from 1 min recordings of tonic firing islet-central neurons (A) and delay firing radial neurons (B). Charge transfer was calculated from the area under sPSC events adjusted to the proportion of driving force from resting membrane potential. Average values represented for controls (dashed blue bars) and BDNF-treated (orange bars) neurons. Error bars indicate SEM.

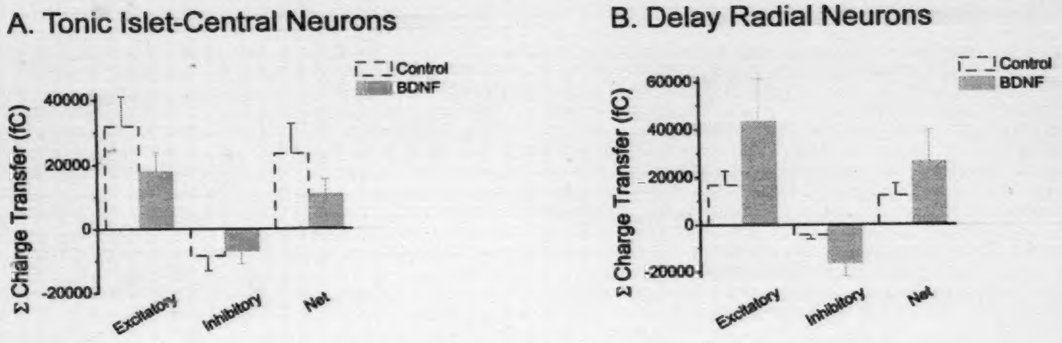
A. Tonic Islet-Central Neurons
Control
BDNF
Σ Charge Transfer (fC)
40000
20000
0
-20000
Excitatory
Inhibitory
Net
B. Delay Radial Neurons
Control
BDNF
Σ Charge Transfer (fC)
60000
40000
20000
0
-20000
Excitatory
Inhibitory
Net

8.6 References

Baccei ML, Fitzgerald M (2004) Development of GABAergic and glycinergic transmission in the neonatal rat dorsal horn. J Neurosci 24: 4749-4757.

Bailey AL, Ribeiro-da-Silva A (2006) Transient loss of terminals from non-peptidergic nociceptive fibers in the substantia gelatinosa of spinal cord following chronic constriction injury of the sciatic nerve. Neuroscience 138: 675-690.

Balasubramanyan S, Stemkowski PL, Stebbing MJ, Smith PA (2006) Sciatic chronic constriction injury produces cell-type-specific changes in the electrophysiological properties of rat substantia gelatinosa neurons. J Neurophysiol 96: 579-590.

Banfield MJ, Naylor RL, Robertson AG, Allen SJ, Dawbarn D, Brady RL (2001) Specificity in Trk receptor:neurotrophin interactions: the crystal structure of TrkB-d5 in complex with neurotrophin-4/5. Structure 9: 1191-1199.

Bardoni R, Ghirri A, Salio C, Prandini M, Merighi A (2007) BDNF-mediated modulation of GABA and glycine release in dorsal horn lamina II from postnatal rats. Dev Neurobiol 67: 960-975.

Beggs S, Salter MW (2007) Stereological and somatotopic analysis of the spinal microglial response to peripheral nerve injury. Brain Behav Immun 21: 624-633.

Blum R, Kafitz KW, Konnerth A (2002) Neurotrophin-evoked depolarization requires the sodium channel Na(V)1.9. Nature 419: 687-693.

Bregman BS, McAtee M, Dai HN, Kuhn PL (1997) Neurotrophic factors increase axonal growth after spinal cord injury and transplantation in the adult rat. Exp Neurol 148: 475-494.

Cho HJ, Kim JK, Park HC, Kim JK, Kim DS, Ha SO, Hong HS (1998) Changes in brain-derived neurotrophic factor immunoreactivity in rat dorsal root ganglia, spinal cord, and gracile nuclei following cut or crush injuries. Exp Neurol 154: 224-230.

Coull JA, Beggs S, Boudreau D, Boivin D, Tsuda M, Inoue K, Gravel C, Salter MW, De Koninck Y (2005) BDNF from microglia causes the shift in neuronal anion gradient underlying neuropathic pain. Nature 438: 1017-1021.

Dalal A, Tata M, Allegre G, Gekiere F, Bons N, Albe-Fessard D (1999) Spontaneous activity of rat dorsal horn cells in spinal segments of sciatic projection following transection of sciatic nerve or of corresponding dorsal roots. Neuroscience 94: 217-228.

Deng YS, Zhong JH, Zhou XF (2000) BDNF is involved in sympathetic sprouting in the dorsal root ganglia following peripheral nerve injury in rats. Neurotox Res 1: 311-322.

Dougherty KD, Dreyfus CF, Black IB (2000) Brain-derived neurotrophic factor in astrocytes, oligodendrocytes, and microglia/macrophages after spinal cord injury. Neurobiol Dis 7: 574-585.

Fukuoka T, Kondo E, Dai Y, Hashimoto N, Noguchi K (2001) Brain-derived neurotrophic factor increases in the uninjured dorsal root ganglion neurons in selective spinal nerve ligation model. J Neurosci 21: 4891-4900.

Gordon GR, Baimoukhametova DV, Hewitt SA, Rajapaksha WR, Fisher TE, Bains JS (2005) Norepinephrine triggers release of glial ATP to increase postsynaptic efficacy. Nat Neurosci 8: 1078-1086.

Grudt TJ, Perl ER (2002) Correlations between neuronal morphology and electrophysiological features in the rodent superficial dorsal horn. J Physiol 540: 189-207.

Guo W, Zou S, Guan Y, Ikeda T, Tal M, Dubner R, Ren K (2002) Tyrosine phosphorylation of the NR2B subunit of the NMDA receptor in the spinal cord during the development and maintenance of inflammatory hyperalgesia. J Neurosci 22: 6208-6217.

Ha SO, Kim JK, Hong HS, Kim DS, Cho HJ (2001) Expression of brain-derived neurotrophic factor in rat dorsal root ganglia, spinal cord and gracile nuclei in experimental models of neuropathic pain. Neuroscience 107: 301-309.

Hains BC, Waxman SG (2006) Activated microglia contribute to the maintenance of chronic pain after spinal cord injury. J Neurosci 26: 4308-4317.

Hayashi Y, Shi SH, Esteban JA, Piccini A, Poncer JC, Malinow R (2000) Driving AMPA receptors into synapses by LTP and CaMKII: requirement for GluR1 and PDZ domain interaction. Science 287: 2262-2267.

Heinke B, Ruscheweyh R, Forsthuber L, Wunderbaldinger G, Sandkuhler J (2004) Physiological, neurochemical and morphological properties of a subgroup of GABAergic spinal lamina II neurones identified by expression of green fluorescent protein in mice. J Physiol 560: 249-266.

Hwang JH, Yaksh TL (1997) The effect of spinal GABA receptor agonists on tactile allodynia in a surgically-induced neuropathic pain model in the rat. Pain 70: 15-22.

Ikeda O, Murakami M, Ino H, Yamazaki M, Nemoto T, Koda M, Nakayama C, Moriya H (2001) Acute up-regulation of brain-derived neurotrophic factor expression resulting from experimentally induced injury in the rat spinal cord. Acta Neuropathol (Berl) 102: 239-245.

Ji RR, Kohno T, Moore KA, Woolf CJ (2003) Central sensitization and LTP: do pain and memory share similar mechanisms? Trends Neurosci 26: 696-705.

Karchewski LA, Gratto KA, Wetmore C, Verge VM (2002) Dynamic patterns of BDNF expression in injured sensory neurons: differential modulation by NGF and NT-3. Eur J Neurosci 16: 1449-1462.

Keller AF, Coull JA, Chery N, Poisbeau P, De Koninck Y (2001) Region-specific developmental specialization of GABA-glycine cosynapses in laminas I-II of the rat spinal dorsal horn. J Neurosci 21: 7871-7880.

King VR, Bradbury EJ, McMahon SB, Priestley JV (2000) Changes in truncated trkB and p75 receptor expression in the rat spinal cord following spinal cord hemisection and spinal cord hemisection plus neurotrophin treatment. Exp Neurol 165: 327-341.

Lai AY, Todd KG (2006) Microglia in cerebral ischemia: molecular actions and interactions. Can J Physiol Pharmacol 84: 49-59.

Laird JM, Bennett GJ (1993) An electrophysiological study of dorsal horn neurons in the spinal cord of rats with an experimental peripheral neuropathy. J Neurophysiol 69: 2072-2085.

Lessmann V (1998) Neurotrophin-dependent modulation of glutamatergic synaptic transmission in the mammalian CNS. Gen Pharmacol 31: 667-674.

Lever IJ, Bradbury EJ, Cunningham JR, Adelson DW, Jones MG, McMahon SB, Marvizon JC, Malcangio M (2001) Brain-derived neurotrophic factor is released in the dorsal horn by distinctive patterns of afferent fiber stimulation. J Neurosci 21: 4469-4477.

Levine ES, Dreyfus CF, Black IB, Plummer MR (1995) Brain-derived neurotrophic factor rapidly enhances synaptic transmission in hippocampal neurons via postsynaptic tyrosine kinase receptors. Proc Natl Acad Sci U S A 92: 8074-8077.

Lohof AM, Ip NY, Poo MM (1993) Potentiation of developing neuromuscular synapses by the neurotrophins NT-3 and BDNF. Nature 363: 350-353.

Lu B, Chow A (1999) Neurotrophins and hippocampal synaptic transmission and plasticity. J Neurosci Res 58: 76-87.

Lu VB, Chee MJS, Gustafson SL, Colmers WF, Smith PA (2005) Concentration-dependent effects of long-term interleukin-1 treatment on spinal dorsal horn neurons in organotypic slice cultures. Abstract Viewer/Itinerary Planner Washington, DC: Society for Neuroscience, Online 292.3.

Lu VB, Moran TD, Balasubramanyan S, Alier KA, Dryden WF, Colmers WF, Smith PA (2006) Substantia Gelatinosa neurons in defined-medium organotypic slice culture are similar to those in acute slices from young adult rats. Pain 121: 261-275.

Lu Y, Perl ER (2003) A specific inhibitory pathway between substantia gelatinosa neurons receiving direct C-fiber input. J Neurosci 23: 8752-8758.

Lu Y, Perl ER (2005) Modular organization of excitatory circuits between neurons of the spinal superficial dorsal horn (laminae I and II). J Neurosci 25: 3900-3907.

Lynch AM, Walsh C, Delaney A, Nolan Y, Campbell VA, Lynch MA (2004) Lipopolysaccharide-induced increase in signalling in hippocampus is abrogated by IL-10--a role for IL-1 beta? J Neurochem 88: 635-646.

Maione S, Siniscalco D, Galderisi U, de N, V, Uliano R, Di Bernardo G, Berrino L, Cascino A, Rossi F (2002) Apoptotic genes expression in the lumbar dorsal horn in a model neuropathic pain in rat. Neuroreport 13: 101-106.

Malcangio M, Lessmann V (2003) A common thread for pain and memory synapses? Brain-derived neurotrophic factor and trkB receptors. Trends Pharmacol Sci 24: 116-121.

Mannion RJ, Costigan M, Decosterd I, Amaya F, Ma QP, Holstege JC, Ji RR, Acheson A, Lindsay RM, Wilkinson GA, Woolf CJ (1999) Neurotrophins: peripherally and centrally acting modulators of tactile stimulus-induced inflammatory pain hypersensitivity. Proc Natl Acad Sci U S A 96: 9385-9390.

Matayoshi S, Jiang N, Katafuchi T, Koga K, Furue H, Yasaka T, Nakatsuka T, Zhou XF, Kawasaki Y, Tanaka N, Yoshimura M (2005) Actions of brain-derived neurotrophic factor on spinal nociceptive transmission during inflammation in the rat. J Physiol 569: 685-695.

Merighi A (2002) Costorage and coexistence of neuropeptides in the mammalian CNS. Prog Neurobiol 66: 161-190.

Michael GJ, Averill S, Shortland PJ, Yan Q, Priestley JV (1999) Axotomy results in major changes in BDNF expression by dorsal root ganglion cells: BDNF expression in large trkB and trkC cells, in pericellular baskets, and in projections to deep dorsal horn and dorsal column nuclei. Eur J Neurosci 11: 3539-3551.

Miletic G, Miletic V (2002) Increases in the concentration of brain derived neurotrophic factor in the lumbar spinal dorsal horn are associated with pain behavior following chronic constriction injury in rats. Neurosci Lett 319: 137-140.

Moore KA, Kohno T, Karchewski LA, Scholz J, Baba H, Woolf CJ (2002) Partial peripheral nerve injury promotes a selective loss of GABAergic inhibition in the superficial dorsal horn of the spinal cord. J Neurosci 22: 6724-6731.

Naylor RL, Robertson AG, Allen SJ, Sessions RB, Clarke AR, Mason GG, Burston JJ, Tyler SJ, Wilcock GK, Dawbarn D (2002) A discrete domain of the human TrkB receptor defines the binding sites for BDNF and NT-4. Biochem Biophys Res Commun 291: 501-507.

Polgar E, Gray S, Riddell JS, Todd AJ (2004) Lack of evidence for significant neuronal loss in laminae I-III of the spinal dorsal horn of the rat in the chronic constriction injury model. Pain 111: 144-150.

Polgar E, Hughes DI, Arham AZ, Todd AJ (2005) Loss of neurons from laminas I-III of the spinal dorsal horn is not required for development of tactile allodynia in the spared nerve injury model of neuropathic pain. J Neurosci 25: 6658-6666.

Polgar E, Hughes DI, Riddell JS, Maxwell DJ, Puskar Z, Todd AJ (2003) Selective loss of spinal GABAergic or glycinergic neurons is not necessary for development of thermal hyperalgesia in the chronic constriction injury model of neuropathic pain. Pain 104: 229-239.

Prescott SA, De Koninck Y (2002) Four cell types with distinctive membrane properties and morphologies in lamina I of the spinal dorsal horn of the adult rat. J Physiol 539: 817-836.

Prescott SA, Sejnowski TJ, De Koninck Y (2006) Reduction of anion reversal potential subverts the inhibitory control of firing rate in spinal lamina I neurons: towards a biophysical basis for neuropathic pain. Mol Pain 2: 32.

Rose CR, Blum R, Kafitz KW, Kovalchuk Y, Konnerth A (2004) From modulator to mediator: rapid effects of BDNF on ion channels. Bioessays 26: 1185-1194.

Ruangkittisakul A, Schwarzacher SW, Secchia L, Poon BY, Ma Y, Funk GD, Ballanyi K (2006) High sensitivity to neuromodulator-activated signaling pathways at physiological [K+] of confocally imaged respiratory center neurons in on-line-calibrated newborn rat brainstem slices. J Neurosci 26: 11870-11880.

Salio C, Averill S, Priestley JV, Merighi A (2007) Costorage of BDNF and neuropeptides within individual dense-core vesicles in central and peripheral neurons. Dev Neurobiol 67: 326-338.

Salio C, Lossi L, Ferrini F, Merighi A (2005) Ultrastructural evidence for a pre- and postsynaptic localization of full-length trkB receptors in substantia gelatinosa (lamina II) of rat and mouse spinal cord. Eur J Neurosci 22: 1951-1966.

Scholz J, Broom DC, Youn DH, Mills CD, Kohno T, Suter MR, Moore KA, Decosterd I, Coggeshall RE, Woolf CJ (2005) Blocking caspase activity prevents transsynaptic neuronal apoptosis and the loss of inhibition in lamina II of the dorsal horn after peripheral nerve injury. J Neurosci 25: 7317-7323.

Slack SE, Thompson SW (2002) Brain-derived neurotrophic factor induces NMDA receptor 1 phosphorylation in rat spinal cord. Neuroreport 13: 1967-1970.

Tsuda M, Inoue K, Salter MW (2005) Neuropathic pain and spinal microglia: a big problem from molecules in "small" glia. Trends Neurosci 28: 101-107.

Watkins LR, Maier SF (2002) Beyond neurons: evidence that immune and glial cells contribute to pathological pain states. Physiol Rev 82: 981-1011.

Woolf CJ (1983) Evidence for a central component of post-injury pain hypersensitivity. Nature 306: 686-688.

Woolf CJ, Chong MS (1993) Preemptive analgesia--treating postoperative pain by preventing the establishment of central sensitization. Anesth Analg 77: 362-379.

Woolf CJ, Salter MW (2000) Neuronal plasticity: increasing the gain in pain. Science 288: 1765-1769.

Yajima Y, Narita M, Narita M, Matsumoto N, Suzuki T (2002) Involvement of a spinal brain-derived neurotrophic factor/full-length TrkB pathway in the development of nerve injury-induced thermal hyperalgesia in mice. Brain Res 958: 338-346.

Yajima Y, Narita M, Usui A, Kaneko C, Miyatake M, Narita M, Yamaguchi T, Tamaki H, Wachi H, Seyama Y, Suzuki T (2005) Direct evidence for the involvement of brain-derived neurotrophic factor in the development of a neuropathic pain-like state in mice. J Neurochem 93: 584-594.

Zhao J, Seereeram A, Nassar MA, Levato A, Pezet S, Hathaway G, Morenilla-Palao C, Stirling C, Fitzgerald M, McMahon SB, Rios M, Wood JN (2006) Nociceptor-derived brain-derived neurotrophic factor regulates acute and inflammatory but not neuropathic pain. Mol Cell Neurosci 31: 539-548.

APPENDIX

PUBLISHED PAPERS

Pain 121 (2006) 261–275

PAIN

www.elsevier.com/locate/pain

Substantia Gelatinosa neurons in defined-medium organotypic slice culture are similar to those in acute slices from young adult rats

Van B. Lu [1], Timothy D. Moran [1,2], Sridhar Balasubramanyan [1], Kwai A. Alier [1],
William F. Dryden, William F. Colmers, Peter A. Smith *

Centre for Neuroscience and Department of Pharmacology, University of Alberta, Edmonton, Alta., Canada

Received 29 July 2005; received in revised form 12 December 2005; accepted 3 January 2006

Abstract

Peripheral nerve injury promotes an enduring increase in the excitability of the spinal dorsal horn. This change, that likely underlies the development of chronic pain, may be a consequence of prolonged exposure of dorsal horn neurons to mediators such as neurotrophins, cytokines, and neurotransmitters. The long-term effects of such mediators can be analyzed by applying them to spinal neurons in organotypic slice culture. To assess the validity of this approach, we established serum-free, defined-medium organotypic cultures (DMOTC) from E13-14 prenatal rats. Whole-cell recordings were made from neurons maintained in DMOTC for up to 42 days. These were compared with recordings from neurons of similar age in acute spinal cord slices from 15- to 45-day-old rats. Five cell types were defined in acute slices as 'Tonic', 'Irregular', 'Delay', 'Transient' or 'Phasic' according to their discharge patterns in response to depolarizing current. Although fewer 'Phasic' cells were found in cultures, the proportions of 'Tonic', 'Irregular', 'Delay', and 'Transient' were similar to those found in acute slices. GABAergic, glycinergic, and 'mixed' inhibition were observed in neurons in acute slices and DMOTC. Pure glycinergic inhibition was absent in 7d cultures but became more pronounced as cultures aged. This parallels the development of glycinergic inhibition in vivo. These and other findings suggest that fundamental developmental processes related to neurotransmitter phenotype and neuronal firing properties are preserved in DMOTC. This validates their use in evaluating the cellular mechanisms that may contribute to the development of chronic pain.

© 2006 International Association for the Study of Pain. Published by Elsevier B.V. All rights reserved.

Keywords: Neuropathic pain; Dorsal horn; *Substantia gelatinosa*; Superficial lamina; Primary afferent

1. Introduction

Understanding the processing of nociceptive information in the superficial spinal laminae is of paramount importance to the elucidation of pain mechanisms. A common approach to the study of chronic, nerve injury-induced pain involves analysis of the long-term changes that are invoked by sciatic nerve injury (Mosconi and Kruger, 1996; Amir et al., 1999; Abdulla et al., 2003; Ma et al., 2003). Days or weeks after this lesion, the electrophysiological properties of dorsal horn neurons are studied in acutely prepared spinal cord slices (Coull et al., 2003). These and other types of experiments have established that peripheral nerve damage is associated with long-term increases in dorsal horn excitability (Woolf, 1983; Laird and Bennett, 1992, 1993; Dalal et al., 1999). Such hyperactivity may reflect altered availability of growth factors, neurotransmitters, neuropeptides, and/or inflammatory mediators (Kerr et al., 1999; Cahill and Coderre, 2002; Miletic and Miletic, 2002; Pezet et al., 2002; Lever et al., 2003b). Organotypic cultures (OTC) of rat spinal cord represent a novel approach to studying the long-term effects of such mediators (Gahwiler et al., 1997; Avossa et al., 2003).

---

* Corresponding author. Tel.: +1 780 492 2643; fax: +1 780 492 4325. *E-mail address:* peter.a.smith@ualberta.ca (P.A. Smith).

[1] First four authors contributed equally to the work.

[2] Present address: Programme in Brain and Behaviour, The Hospital for Sick Children, Toronto, Ont., Canada M5G 1X8.

0304-3959/$32.00 © 2006 International Association for the Study of Pain. Published by Elsevier B.V. All rights reserved.
doi:10.1016/j.pain.2006.01.009

Whereas experiments involving sciatic nerve lesions must be done using adult rats (Howard et al., 2005), OTC must normally be prepared from prenatal animals (Gahwiler et al., 1997). For meaningful comparison, the cultured neurons must be allowed to mature until they attain the same age as those used in nerve-injury studies. Neurons in OTC may be subject to different sets of developmental cues compared to those in intact animals (De Simoni et al., 2003). Thus, to evaluate the relevance of spinal OTC to studies of the actions of putative pain mediators, the physiology of neurons of appropriate age in culture must be compared with those in acute spinal cord slices used in nerve-injury studies. The possibility that neurons fail to differentiate or may de-differentiate in OTC is of particular concern as a variety of cell types can be distinguished electrophysiologically, morphologically or histologically in the superficial spinal laminae (Thomson et al., 1989; Grudt and Perl, 2002; Prescott and de Koninck, 2002; Ruscheweyh and Sandkuhler, 2002; Lu and Perl, 2003; Ruscheweyh et al., 2004; Lu and Perl, 2005b; Prescott and De Koninck, 2005). Also, because aspects of inhibitory synaptic transmission are developmentally regulated in the dorsal horn (Keller et al., 2001; Baccei and Fitzgerald, 2004), it is important to know whether this developmental process proceeds normally in organotypic culture.

A further issue relates to the presence of undefined trophic components and cytokines in serum-containing media that are frequently used to maintain neurons in OTC (Gahwiler et al., 1997). This can lead to variable or ambiguous results, particularly when the long-term actions of exogenously applied growth factors are examined. We have therefore refined spinal OTC methodology by developing serum-free, defined-medium culture (DMOTC) for slices of rat spinal cord (Lu et al., 2004) and have found the physiology of cultured neurons to be reassuringly similar to that of age-matched neurons in acutely prepared slices. We therefore argue that this type of culture system will provide useful new insights into long-term regulation of dorsal horn neurons and thereby provide information of relevance to spinal pain mechanisms.

2. Materials and methods

All procedures were approved by the University of Alberta Health Sciences Laboratory Animal Policy and Welfare Committee. As such, they complied with the guidelines of the Canadian Council for Animal Care and the Committee for Research and Ethical Issues of the International Association for the Study of Pain.

2.1. Acute spinal cord slices

Male or female Sprague–Dawley rats (15–42d old) were deeply anesthetized with urethane (1.5 g/kg, i.p.). An incision was made from the base of the tail to the skull and a downward cut made through the vertebral column at the base of the skull. The incision site was irrigated with ~2 ml of ice-cold oxygenated (95% O_2–5% CO_2) dissection solution containing (in mM): 118 NaCl, 2.5 KCl, 26 $NaHCO_3$, 1.3 $MgSO_4$, 1.2 NaH_2PO_4, 1.5 $CaCl_2$, 5 $MgCl_2$, 25 D-glucose, and 1 kynurenic acid. A laminectomy was performed from the thoracic to the sacral portions of the spinal cord. The spinal cord within the dorsal vertebrae and overlying muscle were removed en bloc and transferred to a glass petri dish containing ice-cold oxygenated dissection solution. The spinal cord was carefully removed from the vertebral column and the ventral roots and all dorsal roots except L4–L5, were cut. It was glued with cyanoacrylate glue ('Vetbond', WPI, Sarasota, FL, USA) to a 4% agar block and transverse slices (300–500 μm) cut using a Vibratome (TPI, USA). To prevent the tissue from being pushed or deformed, the blade advance speed was set between 1 and 4 mm/min, and the greatest blade excursion possible was used (~1.25 mm). The slow advance speed was achieved by inserting a 100 Ω resistor at the rheostat control for the blade advance speed. During slicing, the blade advance speed was constantly monitored and changed according to the progress through the tissue. Slices were incubated in a holding chamber (Sakmann and Stuart, 1995; Moran, 2003) at 36 °C for 1 h and subsequently stored at room temperature (~22 °C) in oxygenated dissection solution (see above, without kynurenic acid).

For recording, slices were placed in a glass-bottomed chamber (25 mm diameter, volume of ~1 ml) and held in place with a U-shaped platinum wire frame with attached parallel nylon fibers. They were superfused (flow rate ~1–2 ml/min) at room temperature (~22 °C) with 95% O_2–5% CO_2 saturated artificial cerebrospinal fluid (aCSF) which contained (in mM): 127 NaCl, 2.5 KCl, 1.2 NaH_2PO_4, 26 $NaHCO_3$, 1.3 $MgSO_4$, 2.5 $CaCl_2$, and 25 D-glucose, pH 7.4. For recording evoked excitatory postsynaptic currents (eEPSCs), bicuculline (10 μM) and strychnine (1 μM) were included to block inhibitory synaptic inputs. For recording evoked inhibitory postsynaptic currents (eIPSCs), 6-cyano-7-nitroquinoxaline-2,3-dione (CNQX; 10 μM) and DL-2-amino-5-phosphonovaleric acid (DL-AP5; 50 μM) were included to block excitatory synaptic inputs. Baclofen, QX-314, CNQX, DL-AP5, and bicuculline were from Tocris (Ballwin, MO, USA). All other chemicals, including strychnine hydrochloride, were from Sigma (Oakville, Ont., Canada).

Spinal cord slices were viewed with a Zeiss Axioskop FS upright microscope equipped with infrared differential interference contrast (IR-DIC) optics and an IR-sensitive video camera (NC-70, Dage-MTI, Michigan City, IN, USA). The *substantia gelatinosae* were identifiable as translucent bands across the dorsal horn. Whole-cell recordings were made from visually identified *substantia gelatinosa* neurons with an npi SEC 05 L amplifier (npi Electronic, Tamm, Germany) in discontinuous single-electrode voltage-clamp or bridge-balance current-clamp mode. Switching frequencies were typically between 30 and 40 kHz. Signals were digitized between 5 and 10 kHz, and filtered at 1–2 kHz. Patch pipettes were pulled from thin-walled borosilicate glass (1.5 mm o.d., 1.12 mm i.d.; TW-150F-4, WPI, Sarasota, FL, USA). Pipettes for recording action potentials (APs) had resistances of 5–10 MΩ when filled with an internal solution containing (in mM): 130 potassium gluconate, 2 $CaCl_2$, 10 Hepes, 10 EGTA, 4 Mg-ATP, and 0.3 Na-GTP, pH 7.2 (290–300 mOsm). In some experiments, a Cs^+-based internal solution containing (in mM): 140 CsCl, 5 Hepes, 10 EGTA, 2 $CaCl_2$, 2 Mg-ATP, and 0.3 Na-GTP, pH 7.2 (290–300 mOsm), was used for recording synaptic currents.

Data for *I–V* plots were obtained in voltage-clamp mode using incremental 10 mV, 800 ms commands. Current values were measured from the close-to-steady-state values attained at the end of these commands.

EPSCs were evoked (eEPSCs) at 0.05 Hz with stimulating electrodes made from two twisted strands of Teflon-coated nichrome wire (7620, A-M Systems, Carlsborg, WA, USA). The ends were cut to expose the nichrome within the strand. The electrodes were placed on the dorsal root entry zone to activate primary afferent fibers. Evoked IPSCs (eIPSCs) were generated at 0.05 Hz by focal stimulation with a patch pipette containing 2 M NaCl that was positioned 50–100 μm from the cell body. The stimulating electrode was repositioned until a reliable synaptic input to the cell was found. The orientation of the stimulating electrode, relative to the cell body, varied in the dorso-ventral and latero-medial axes. Stimulus intensity was between 2 and 30 V for both eEPSCs and eIPSCs, and stimulus duration was 100 or 400 μs. Monosynaptic eEPSCs and eIPSCs were identified by their ability to follow high frequency stimulation (10–20 Hz) with constant latency and the absence of failures. Membrane potential was clamped at −70 mV for recording eEPSCs and eIPSCs when a CsCl-based internal solution was used. With this solution, E_{Cl} was ~0 mV so that eIPSCs appeared as inward currents. The voltage-gated Na^+ channel blocker QX-314 (5 mM) (Strichartz, 1973) was included in the internal solution to prevent action potential discharge. When a K^+-gluconate-based internal solution was used, membrane potential was clamped at −70 mV for recording eEPSCs and 0 mV for recording eIPSCs. Under these conditions, E_{Cl} was −88 mV so eIPSPs appeared as outward currents. Current or voltage clamp data were acquired and analyzed using pCLAMP 8 or 9 (Axon Instruments, Burlingame, CA, USA). Figures were produced with Origin 7.0 (OriginLab, Northampton, MA, USA) and Adobe Illustrator 10 (Adobe Software, San Jose, CA, USA).

Spontaneous EPSCs (sEPSCs) and miniature IPSC (mIPSC, recorded in the presence of 1 μM TTX) were digitized at 5 kHz and filtered at 1 kHz. Mini Analysis Program software (Synaptosoft, Decatur, GA, USA) was used to distinguish sEPSC or mIPSCs from the baseline noise and to prepare cumulative probability plots. Data were only included in the analysis if the series resistance was below 25 MΩ and did not change by >20% during the course of an experiment. Spontaneous postsynaptic currents were detected automatically using an amplitude threshold of 10 pA and an area threshold of 15 fC. All detected events were then re-examined and visually accepted or rejected based on subjective visual examination. The Kolmogorov–Smirnov two-sample test (KS test) was used to compare distributions of amplitudes and inter-event intervals in neurons in acute slices and in DMOTC. All comparisons were made using comparable numbers of events for each cell type (for details see legend to Fig. 6). The Kolmogorov–Smirnov method tested the null hypothesis that two independent samples come from populations that are identical with respect to location and distribution. Distributions were considered statistically significant if $p < 0.05$.

2.2. Organotypic cultures

The DMOTC technique was adapted from published methods (Gahwiler, 1981; Braschler et al., 1989; Ballerini and Galante, 1998). Embryonic day 13–14 rat fetuses were delivered by caesarean section from timed-pregnant Sprague–Dawley rats (Charles River, Saint-Constant, PQ, Canada) under 2–5% isoflurane anesthesia. Following the caesarean section, the female rat was euthanized with an overdose of intra-cardiac chloral hydrate (10.5%). Under aseptic conditions, the entire embryonic sac was placed in chilled Hanks' balanced salt solution (BSS) containing (in mM): 138 NaCl, 5.33 KCl, 0.44 KH_2PO_4, 0.5 $MgCl_2$-$6H_2O$, 0.41 $MgSO_4$-$7H_2O$, 4 $NaHCO_3$, 0.3 Na_2HPO_4, 5.6 D-glucose, and 1.26 $CaCl_2$. Individual rat fetuses were removed from their embryonic sacs and rapidly decapitated. Afterwards, the back of each fetus was cut away from the rest of the body and sliced into 275–325 μm transverse slices using a tissue chopper (McIlwain, St. Louis, MO, USA). Only lumbar spinal cord slices with an intact spinal cord, two attached dorsal root ganglia (DRGs), and associated muscle tissue were chosen and transferred to a new dish filled with Hanks' BSS. These slices were trimmed of excess ventral tissue and chilled for 1 h at 4 °C (see Fig. 1A).

Embryonic spinal cord slices, with attached DRGs and some ventral muscle fibers, were plated onto clean glass coverslips (Karl Hecht, Sondheim, Germany) with a clot of reconstituted chicken plasma (lyophilized, 2 mg/L heparin; Cocalico Biologicals Inc., Stevens, PA, USA) and thrombin (200 U/ml; Sigma, St. Louis, MO, USA). Coverslips were inserted into flat-bottomed tissue culture tubes (Nunc-Nalgene International, Mississauga, Ont., Canada) filled with 1 ml of culture medium and then placed into a roller drum (Model # TC-8, New Brunswick Scientific, Edison, NJ, USA) rotating at 120 rotations per hour in a dry heat incubator at 36 °C (regular air-no CO_2; see Fig. 1B). The initial medium in the tubes was composed of 82% Dulbecco's modified Eagle's medium (DMEM), 10% fetal bovine serum, and 8% sterile water to adjust osmolarity (all from Invitrogen-Gibco, Grand Island, NY, USA). This medium was supplemented with 20 ng/ml NGF (Alomone Laboratories, Jerusalem, Israel) for the first 4 days. Antibiotic and antimycotic drugs (5 U/ml penicillin G, 5 U/ml streptomycin, and 12.5 ng/ml amphotericin B; Invitrogen-Gibco) were also included in the medium during the first 4 days of culture. At the end of this 4 day period, the slices were treated with an antimitotic drug cocktail consisting of uridine, cytosine-β-D-arabino-furanoside (AraC), and 5-fluorodeoxyuridine (all from SIGMA, all at 10 μM) for 24 h to retard the overgrowth of glial cells. Also during this treatment, the serum medium was halved with a serum-free, defined medium consisting of Neurobasal medium, 5 mM Glutamax-1, and N-2 supplement (all from Invitrogen-Gibco). Washout of the antimitotic drugs and serum medium was carried out on day 5 with the serum-free, defined medium described above. The medium within these tubes was exchanged with freshly prepared serum-free medium every 4–5 days, and defined-medium OTC (DMOTC) slices were maintained in serum-free, chemically defined conditions until recordings were carried out. This schedule of treatment with different media is illustrated schematically in Fig. 1C.

Recordings from DMOTC spinal cord slices were typically obtained 15–28 days following the start of culture, but suitable recordings could be obtained from DMOTC slices for up to 45

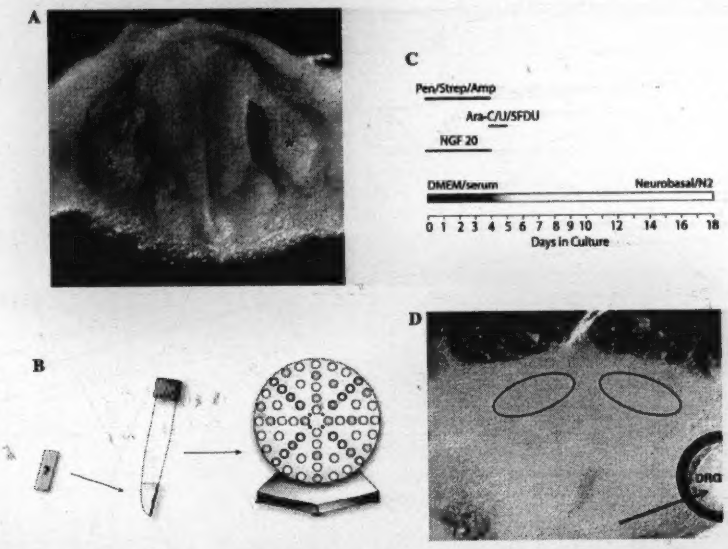

Fig. 1. Organotypic culture methodology. (A) Slice of spinal cord freshly dissected from an E14 rat viewed under IR-DIC optics. Note large size of dorsal root ganglia (indicated by asterisks) compared to size of spinal cord. (B) Schematic diagram for organotypic culture preparation. Slices on coverslips are placed in flat-bottomed culture tubes in modified DMEM. These are rotated on a motor-driven circular drum at 120 revolutions per hour to ensure adequate oxygenation. (C) Scheme to show time course of media changes during preparation of DMOTC slices. NGF 20 denotes period of exposure to 20 ng/ml NGF. AraC-/U/5-FDU denotes period of exposure to uridine, cytosine-β-D-arabino-furanoside (AraC), 5-fluorodeoxyuridine cocktail, and Pen/Strep/Amp denotes period of exposure to 5 U/ml penicillin G, 5 U/ml streptomycin, and 12.5 ng/ml amphotericin B. Slices are initially maintained in DMEM/10% fetal bovine serum and serum progressively halved in each successive change of medium by diluting with neurobasal medium. (D) Organotypic culture of embryonic spinal cord slice maintained for 10 days in vitro. Ovals indicated by dark lines indicate the area from which recordings were obtained. The site of stimulation for evoked EPSCs was as indicated, close to the dorsal root ganglion (DRG).

days in vitro. Cells for recording were chosen from within a light band located across the dorsal region of the slice and stimulating electrodes places closed to the dorsal root ganglion, (DRG, see Fig. 1D). The same electrophysiological recording solutions, procedures, and protocols used on acute adult rat spinal cord slices were applied to DMOTC slices.

Statistical comparisons were made as appropriate using Student's unpaired, two-tailed *t*-test, χ^2 test, ANOVA with the Student Newman–Keuls (SNK) Multiple Comparisons Test or Kolmogorov–Smirnov (KS) test as detailed above.

2.3. Histology

Neurons in acute or OTC slices were routinely filled with biocytin (0.2%) during recordings for post hoc identification. This low concentration was chosen as biocytin has been reported to interfere with postsynaptic drug responses at higher concentrations (Eckert et al., 2001). At the completion of recording, the patch pipette was slowly withdrawn from the cell and the slice transferred to cold (4 °C) 4% paraformaldehyde in phosphate-buffered saline (PBS), pH 7.4, and stored overnight at 4 °C. Slices were rinsed three times with PBS and transferred to a 24-well tissue culture dish for staining. Slices were incubated with 0.3% Triton X-100 and streptavidin–Texas red conjugate (1:50 dilution, Molecular Probes, Eugene, OR, USA) for 50 min on a 3D rotator. Slices were thoroughly rinsed with distilled water, transferred to slides, allowed to dry overnight, and coverslipped with Cytoseal™-60 (Richard-Allan Scientific, Kalamazoo, MI, USA). A Zeiss LSM 510 confocal laser scanning microscope, equipped with an appropriate laser (HeNe1, wavelength 543 nm) and Texas red filter, was used to examine the tissue. Confocal images and 3D reconstructions were acquired using Zeiss LSM image browser software. Figures were converted to black and white to increase contrast and clarity.

3. Results

3.1. Neuronal morphology

Biocytin-filled neurons exhibited a variety of morphologies in DMOTC. Those shown in Fig. 2 had morphologies similar to those of neuronal phenotypes already defined in acutely prepared sections of rodent dorsal horn (Grudt and Perl, 2002; Heinke et al., 2004). Thus, the morphology of the neuron in Fig. 2A is similar to that of a 'dorsoventral' cell, that in

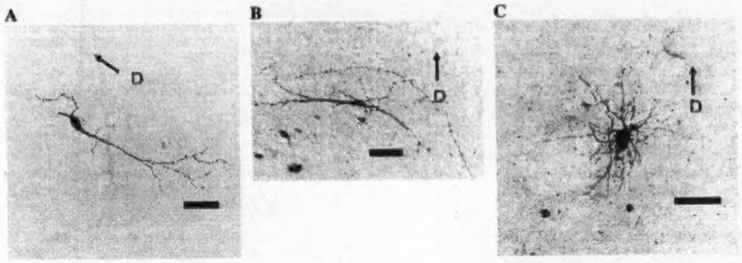

Fig. 2. Confocal images of three biocytin-filled neurons in DMOTC slices. Arrows labeled D point to dorsal surface of culture. Scale bar = 50 µm.

Fig. 2B may be an 'islet' or 'central' cell and that in Fig. 2C is likely a 'radial' cell.

3.2. Observation of living neurons under IR-DIC optics

'Healthy' *substantia gelatinosa* neurons in both acute slices and DMOTC had a 'smooth' appearance, whereas 'unhealthy' cells typically had a high-contrast membrane, appeared swollen or had a 'wrinkled' appearance. Neurons in acute slices could be visualized to a depth of up to 100 µm. However, this distance typically decreased to 40–50 µm as the animals became older (>28d). Neuronal visibility was generally better in the cultures. Whole-cell patch-clamp recordings were obtained from neurons in DMOTC or in acute slices for up to 10 h. Stable recordings were made from individual neurons for up to 3 h.

3.3. Synaptic pharmacology

In both acute slices and in DMOTC, eEPSCs generated in the presence of bicuculline (10 µM) and strychnine (1 µM) were abolished by CNQX (10 µM) plus AP5 (50 µM) (Figs. 3A and D). The amplitude and decay time constant (τ) of eEPSCs were greater in DMOTC neurons than in acute slices (Table 1).

GABA$_A$-mediated eIPSCs generated by focal stimulation in the presence of strychnine (1 µM), AP5 (50 µM), and CNQX (10 µM) were completely blocked by bicuculline in both DMOTC and acute slices (10 µM; Figs. 3B and E). Also, glycine-mediated eIPSCs, generated in the presence of bicuculline (10 µM), AP5 (50 µM), and CNQX (10 µM), were completely blocked by strychnine (1 µM; Figs. 3C and F). Glycinergic eIPSCs decayed more rapidly than GABAergic responses in both acute slices and DMOTC (Table 1).

Decay time constants for glycinergic eIPSCs were greater in DMOTC than in acute slices whereas τ for GABAergic responses were the same in both situations. GABAergic eIPSC amplitude was much larger in cultures than in neurons in acute slices whereas glycinergic events were slightly smaller in the cultures (Table 1, Figs. 3G and H).

To assess the relative contribution of GABA and glycine to the generation of inhibitory responses, eIPSCs in 19–45d acute slices or in 16–28d cultured neurons were studied in the presence of strychnine (1 µM) or bicuculline (10 µM) followed by strychnine (1 µM) + bicuculline (10 µM). Fig. 3I illustrates a plot of the percentage contributions of GABA versus the percentage contribution of glycine to eIPSCs in each neuron studied. Pure GABAergic, mixed, and pure glycinergic responses were observed in neurons from both acute and DMOTC slices. In some cells, application of strychnine or bicuculline produced a slight increase in eIPSC amplitude. For the purposes of Fig. 3I, such cells were defined, respectively, as purely GABAergic or purely glycinergic, respectively. This is because the response persisting in strychnine was 100% antagonized by bicuculline and vice versa. Augmentation of eIPSCs by bicuculline or strychnine was seen in both DMOTC and in acute slices. It may have reflected attenuation of presynaptic inhibitory tone or 'run up' of the response amplitude during continued recording.

In acute slices, the presynaptic GABA$_B$ agonist, baclofen (15–30 µM), suppressed eEPSCs to 57.0 ± 10.3% of control ($n = 4$, Fig. 3J) and suppressed GABA/glycine eIPSCs to 65.2 ± 4.31% of control ($n = 5$, Fig. 3K). Similar effects of baclofen were seen in neurons in DMOTC (Figs. 3L and M). The baclofen-induced suppression of both eEPSCs, (78.07 ± 3.0%; $n = 5$) and eIPSCs, (69.0 ± 6.1%, $n = 7$) in DMOTC was not significantly different from that seen in acute slices.

3.4. Development of glycinergic and GABAergic inhibition in DMOTC

To examine further the development of inhibitory transmission in the cultures, we studied the pharmacology of miniature IPSCs (mIPSCs) in the presence of 1 µM TTX. Miniature IPSCs, which may represent action-potential independent release of single vesicles

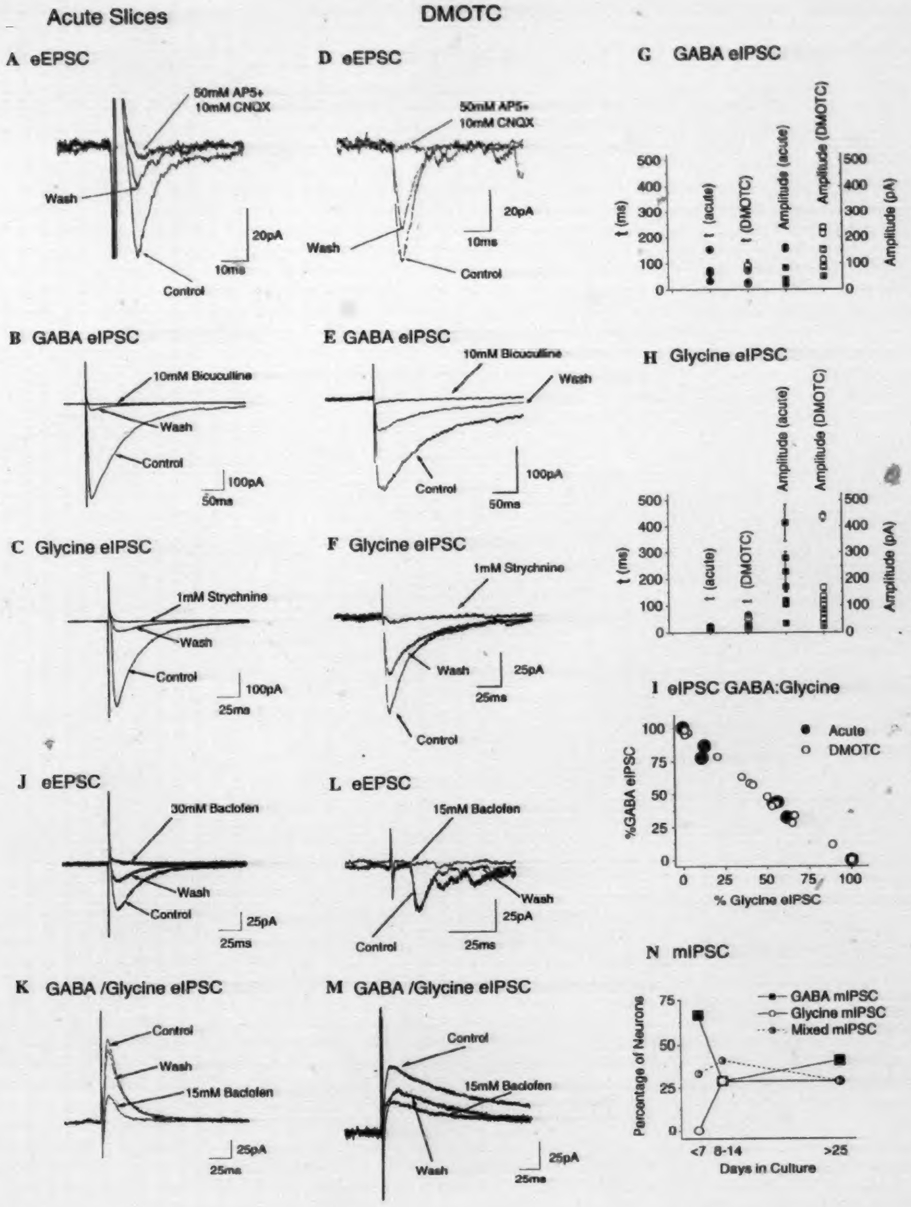
Acute Slices
DMOTC
A eEPSC
50mM AP5+
10mM CNQX
Wash
20pA
10ms
Control
D eEPSC
50mM AP5+
10mM CNQX
20pA
10ms
Wash
Control
G GABA eIPSC
500
400
300
200
100
0
τ (ms)
τ (acute)
τ (DMOTC)
Amplitude (acute)
Amplitude (DMOTC)
Amplitude (pA)
B GABA eIPSC
10mM Bicuculline
Wash
Control
100pA
50ms
E GABA eIPSC
10mM Bicuculline
Wash
Control
100pA
50ms
H Glycine eIPSC
C Glycine eIPSC
1mM Strychnine
Wash
Control
100pA
25ms
F Glycine eIPSC
1mM Strychnine
Wash
25pA
25ms
Control
I eIPSC GABA:Glycine
%GABA eIPSC
% Glycine eIPSC
Acute
DMOTC
0
25
50
75
100
J eEPSC
30mM Baclofen
Wash
Control
25pA
25ms
L eEPSC
15mM Baclofen
Wash
Control
25pA
25ms
N mIPSC
GABA mIPSC
Glycine mIPSC
Mixed mIPSC
Percentage of Neurons
Days in Culture
<7
8-14
>25
K GABA /Glycine eIPSC
Control
Wash
15mM Baclofen
25pA
25ms
M GABA /Glycine eIPSC
Control
15mM Baclofen
Wash
25pA
25ms

Table 1
Properties of evoked synaptic responses in neurons in acute slices and in DMOTC

	Acute slices		DMOTC	
	Amplitude (pA)	τ (ms)	Amplitude (pA)	τ (ms)
eEPSC	88.1 ± 6.0 ($n = 81$ for 14 neurons)	8.3 ± 0.5 ($n = 73$ for 13 neurons)	154.5 ± 7.3 ($n = 188$ for 23 neurons) $P < 0.001$	12.8 ± 1.3 ($n = 166$ for 21 neurons) $P < 0.02$
GABAergic eIPSC	66.9 ± 9.6 ($n = 37$ for 6 neurons)	46.7 ± 4.9 ($n = 37$ for 6 neurons)	243.5 ± 31.4 ($n = 70$ for 7 neurons) $P < 0.0001$	58.4 ± 5.1 ($n = 68$ for 7 neurons) $P > 0.1$
Glycinergic eIPSC	171.6 ± 16.7 ($n = 67$ for 9 neurons)	13.1 ± 0.8 ($n = 67$ for 9 neurons)	129.2 ± 11.8 ($n = 96$ for 10 neurons) $P < 0.05$	34.8 ± 3.3 ($n = 83$ for 10 neurons) $P < 0.001$
	$P < 0.0001$[a]	$P < 0.0001$[a]	$P < 0.002$[a]	$P < 0.001$[a]

Synaptic responses were evoked 4–10 times in each neuron and measurements made of the amplitudes and τ of each individual event, thus the *n* value in the table is always greater than the number of neurons studied. Unless otherwise stated, *P* values = significance of difference between parameters in DMOTC neurons compared to acute neurons.

[a] *P* value comparing glycinergic to GABAergic.

of neurotransmitter (Keller et al., 2001), are exclusively GABA-mediated at birth, whilst glycinergic contribution to the events increases with age (Baccei and Fitzgerald, 2004). If inhibitory transmission is developing normally within the cultures, we would predict that neurons in 7d cultures, which are the same age as neurons in P0 animals in vivo, would not display glycinergic mIPSCs but these should appear in neurons in older cultures. This prediction is borne out by the data illustrated in Fig. 3N. At 7d or less in culture, mIPSCs were either GABAergic or mixed GABA/glycine events (see Keller et al., 2001). Also, the percentage of neurons exhibiting pure, glycine-mediated mIPSCs increased as the cultures aged and there was a downward trend in the percentage of cells exhibiting mixed mIPSCs. These experiments were done by looking at the effects of bicuculline and/or strychnine on overall mIPSC frequency. As for eIPSCs (Table 1), the time to decay for GABAergic mIPSCs ($\tau = 14.5 \pm 0.2$ ms, $n = 5391$) was greater than that for glycinergic events ($\tau = 10.3 \pm 0.37$ ms, $n = 1668$, $P < 0.0001$).

3.5. *Antagonist-induced bursting activity*

Neurons in DMOTC often displayed bursts of action potentials when treated with bicuculline or bicuculline plus strychnine. These bursts lasted for 1–2 s and the inter-burst interval was 20–30 s. A typical example, illustrating burst activity on two different timescales, is presented in Fig. 4A.

Under voltage clamp (at −70 mV), bursts of 'giant' spontaneous EPSCs (sEPSCs) were seen in 13 out of 16 neurons treated with 10 μM bicuculline with or without 1 μM strychnine. These events, which were 2–5 times the amplitude of regular sEPSCs (Fig. 4B), were likely responsible for the appearance of bursts of action potentials under current clamp (Fig. 4A). Although we cannot rule out the possibility that unclamped action potentials

Fig. 3. Pharmacology of synaptic responses in acute slices recorded from 20- to 35-day-old animals and from neurons in DMOTC. (A and D) Stimulation of dorsal root entry zone (A) or primary afferent fibers (D) in the presence of 10 μM bicuculline and 1 μM strychnine generates AMPA and NMDA receptor-mediated eEPSCs in neurons from an acute slice and from a neuron in an 8d DMOTC slice. Averaged traces ($n = 6$ in A and $n = 10$ in D) of eEPSCs before, during, and after application of the AMPA antagonist, CNQX (10 μM) plus the NMDA antagonist, AP5 (50 μM). K-gluconate-based internal solutions $V_h = -70$ in A and D. (B and E). GABA-mediated eIPSCs generated by focal stimulation in the presence of AP5 (50 μM), CNQX (10 μM), and strychnine (1 μM). Averaged traces ($n = 6$ in B and $n = 10$ in E) of eIPSCs before, during, and after application of the $GABA_A$ antagonist, bicuculline (10 μM). $V_h = -70$ mV, CsCl-based internal solutions. B from neuron in acute slice and E from a neuron in a 20d DMOTC slice. (C and F) Glycine-mediated eIPSCs generated by focal stimulation in the presence of AP5 (50 μM), CNQX (10 μM), and bicuculline (10 μM). Averaged traces ($n = 6$ in C, $n = 10$ in F) of eIPSCs before, during and after application of strychnine (1 μM). $V_h = -70$ mV with CsCl-based internal solution. C from neuron in acute slice and F from a neuron in an 18d DMOTC slice. (G and H)Comparison of the rate constants of decay (τ) and amplitudes of GABAergic (G) and glycinergic (H) eIPSCs in neurons in acute slices and in DMOTC. Four to 10 events were measured in each data point represent the mean value for each neuron, error bars = SEM. Note small values for τ for glycinergic events both in acute slices and in DMOTC. See Table 1 for statistical analysis of these data. (I) Plots of percentage contributions of GABA versus percentage contribution of glycine to eIPSCs in each neuron studied. (J and L) eEPSCs generated by stimulating the dorsal root in the presence of 10 μM bicuculline and 1 μM strychnine. Averaged traces ($n = 3$ in J, $n = 10$ in L) of eEPSCs before, during, and after application of 30 or 15 μM baclofen. CsCl-based internal solution, $V_h = -70$ mV. J from neuron in acute slice and L from a neuron in a 11d DMOTC slice. (K and M) eIPSCs generated by focal stimulation in the presence of 10 μM CNQX and 50 μM AP5. Averaged traces ($n = 3$ in K, $n = 10$ in M) of eIPSCs before, during, and after application of 15 μM baclofen. $V_h = 0$ mV, acute 20–42d slice in K, $V_h = -40$ mV, 11d DMOTC slice in M, K^+-gluconate-based internal solution in both. (N) Developmental pharmacology of mIPSCs. Percentage of cells in DMOTC exhibiting GABAergic, glycinergic or mixed mIPSCs in three time periods in culture; <7d, ($n = 9$), 8–14d ($n = 17$), and >25d ($n = 17$). Note emergence of pure glycinergic mIPSCs and that 7d in culture is equivalent to P0 in vivo.

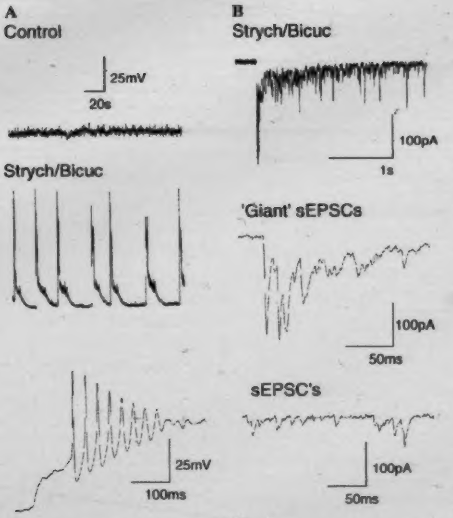

Fig. 4. Spontaneous bursts of action potentials and 'giant' sEPSC in neurons in DMOTC after treatment with strychnine (1 μM) plus bicuculline (10 μM). (A, upper trace) Current-clamp recording prior to administration of antagonists. (Middle trace) Spontaneous bursts of action potentials seen in the presence of strychnine/bicuculline. (Lower trace) A.p.burst on a faster time scale. Recordings from a neuron in a 22d DMOTC. (B, upper trace) Long burst of spontaneous excitatory synaptic activity seen in another neuron at −70 mV in the presence of antagonists. (Middle trace) 'Giant' sEPSCs from the start of the upper record displayed on a faster time scale. (Lower trace) 'Regular sEPSCs recorded towards the end of the upper trace and displayed on an expanded time scale. Recordings from a neuron in a 12d DMOTC slice.

contributed to the total amplitude of 'giant' sEPSCs, this would seem unlikely as the recording pipettes routinely contained QX-314. The bursts occurred at a low frequency with an inter-event interval of $\sim$20 s. They resembled antagonist-induced bursts which have been described in ventral horn interneurons in organotypic culture (Ballerini and Galante, 1998; Ballerini et al., 1999). We never encountered spontaneous bursts of action potentials or 'giant' sEPSCs when neurons in acute slices were treated with strychnine/bicuculline.

3.6. Electrophysiological phenotypes

Data were analyzed from 215 neurons in acute slices. *Substantia gelatinosa* neurons were characterized by five different discharge patterns in response to depolarizing current. 'Tonic' neurons were defined as those that continued to discharge action potentials at constant frequency throughout the duration of the current pulse (i.e., without accommodation; 21.5% of cells studied; Figs. 5A and C). The second group of neurons (27% of those studied) displayed 'irregular' discharge that was characterized by a resumption of discharge following an initial accommodation and/or a rate of discharge that was disproportionate to the amount of injected current (Figs. 5A and C). The third group of neurons (28.5% of those studied) exhibited a clear delay before the initiation of discharge. Although 18 out of 58 of these 'delay' neurons exhibited a tonic discharge pattern after an initial delay whereas 43 out of 58 exhibited irregular firing after a delay, all 'delay' neurons were considered as a single category. The fourth group of neurons discharged only a single action potential no matter how much depolarizing current was applied. These 'transient' neurons comprised 14% of all neurons studied (Figs. 5A and C). The final group of neurons discharged a short burst of action potentials which abated despite the presence of sustained depolarizing current. These 'phasic' neurons comprised 9% of all cells studied (Figs. 5A and C). To formally distinguish them from 'transient' cells, neurons were only identified as 'phasic' if they discharged 3 or more action potentials in response to depolarizing current.

Although the discharge pattern of individual neurons did not change appreciably over 1 h of recording, some cells displayed different discharge patterns when depolarizing current was applied from different initial membrane potentials. This complication has previously been noted in lamina I neurons by Prescott and De Koninck (2005). All cell identifications were therefore based on responses to current commands from a membrane potential artificially set to −60 mV.

All neuronal types characterized in acute slices were present in DMOTC slices (Fig. 5B). Fig. 5D shows the percentage of each of the five cell types in slices that had been in culture for 7–42 days (defined medium started at day 5). There is no significant difference (χ^2 test $P > 0.3$) in the proportions of tonic, irregular, delay, and transient neurons in the cultures. There are significantly fewer phasic neurons ($P < 0.02$; χ^2 test) and the proportion of phasic cells appeared to decline with time in culture (Fig. 5E). Another interesting observation from the data in Fig. 5E is that the relative percentages of different cell types stabilize after 14–28d in culture, again verifying the similarity between DMOTC and acute slices.

3.7. Membrane excitability

The mean resting potential (rmp) of all cells studied in acute slices was ~ -50 mV and there was no significant difference between the rmp of any pair of cell type ($P > 0.05$, ANOVA-SNK test). Similarly, the rmp of all neurons studied in DMOTC was ~ -50 mV and, as with acute slices, there was no significant difference between the membrane potential of any pair of cell types ($P > 0.05$ ANOVA-SNK test, for numerical values see Table 2).

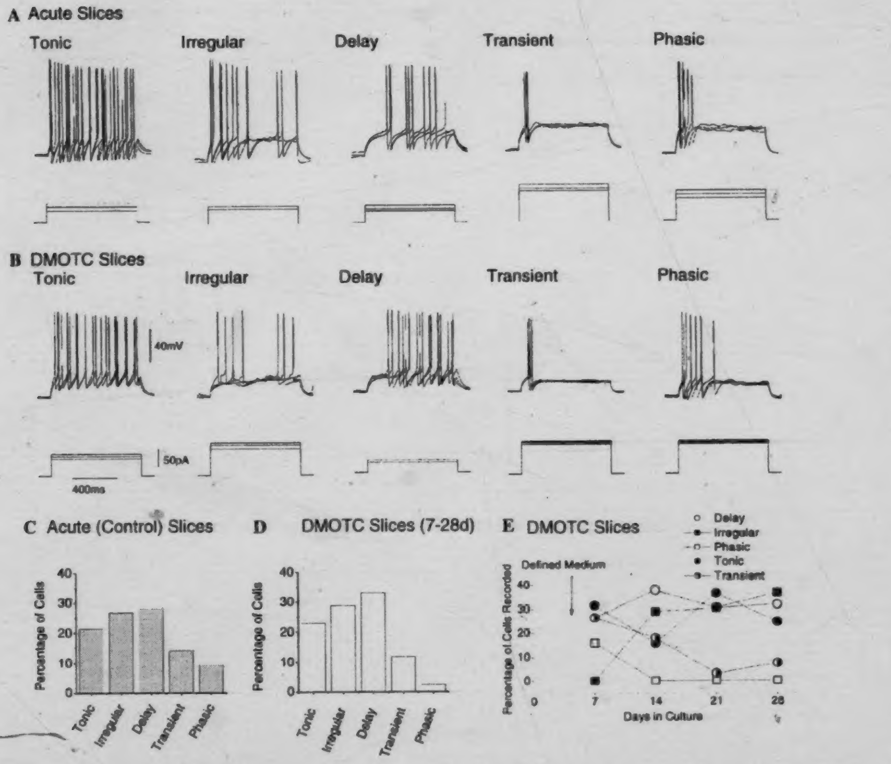

Fig. 5. Sample current-clamp recordings from neurons in acute spinal cord slices and DMOTC. Effects of depolarizing current commands and typical recordings from 'Tonic', 'Irregular', Delay', 'Phasic', and 'Transient' neurons in (A) acute slices, (B) DMOTC. 40 mV, 100 pA, 400 ms calibrations in (B) refer to all traces. (C and D) Bar graphs to illustrate percentages of cells in each category in acute slices ($n = 214$) and DMOTC ($n = 134$). (E) Time course of changes of percentage of cells during DMOTC. For 7d, $n = 19$; for 14d, $n = 45$; for 21d $n = 34$; and for 28d $n = 42$.

In acute slices, rheobase was significantly less in tonic cells than in transient, delay or irregular cells ($P < 0.001$ for all comparisons, ANOVA-SNK test). Similarly, tonic neurons in DMOTC exhibited the lowest rheobase. This was significantly lower than that of delay neurons ($P < 0.001$ ANOVA-SNK test; for numerical values see Table 2).

Comparison of the rheobase and rmp data for each of the five cell types in acute slices and with corresponding cell types in DMOTC revealed only one significant difference; the rmp of tonic cells was significantly less in the cultures than in acute slices ($P < 0.03$: Table 2).

Fig. 6A shows the current–voltage relationships for the five cell types in both acute slices and DMOTC, as well as that for all cells combined. Input resistances (R_{in}) were measured from the slopes of the linear portions of these graphs between −70 and −90 mV, and the values are listed in Table 2. Although the mean values of R_{in} ranged from ~573 MΩ for tonic cells to ~757 MΩ for phasic cells, there was no significant difference between the mean R_{in} values for any pair of neuron types in acute slices. The presence of unclamped spikes at positive clamp voltages complicated measurements for the generation of current–voltage relationships in neurons in DMOTC. Nevertheless, for the values that could be accurately determined, there was less outward current (decreased conductance) at positive voltages in all neuron types in DMOTC compared to those in acute slices. This is illustrated more clearly when data from all cell types are combined (Fig. 6A). R_{in} in the linear range −70 to −90 mV was similar in transient, tonic, and delay cells in acute slices and DMOTC. R_{in} of irregular cells was significantly lower in the cultures than in acute slices.

Table 2
Comparison of properties of cell types in DMOTC with those in acutely dissociated slices

	RMP (mV)	Rheobase (pA)	R_{in} (−70 to −90 mV) (MΩ)
Tonic			
Acute slice	−51.8 ± 1.5 ($n = 46$)	24.8 ± 2.6 ($n = 28$)	573 ± 77 ($n = 22$)
DMOTC	−46.9 ± 1.4 ($n = 31$)^{c}	26.6 ± 2.1 ($n = 31$)	657 ± 60 ($n = 28$)
Irregular			
Acute slice	−51.0 ± 1.3 ($n = 57$)	49.7 ± 3.7 ($n = 42$)^{a}	581 ± 50 ($n = 39$)
DMOTC	−49.4 ± 1.4 ($n = 38$)	50.0 ± 6.7 ($n = 39$)	375 ± 46 ($n = 38$)^{d}
Delay			
Acute slice	46.6 ± 1.0 ($n = 61$)	60.9 ± 3.3 ($n = 52$)^{a}	743 ± 37 ($n = 43$)
DMOTC	−47.4 ± 1.3 ($n = 44$)	64.9 ± 6.6 ($n = 45$)^{b}	624 ± 149 ($n = 44$)
Phasic			
Acute slice	−49.5 ± 2.8 ($n = 20$)	41.0 ± 6.0 ($n = 12$)	757 ± 135 ($n = 13$)
DMOTC	−53.3 ± 6.7 ($n = 3$)	28.3 ± 8.8 ($n = 3$)	1846 ± 850 ($n = 3$)^{c}
Transient			
Acute slice	−49.0 ± 2.1 ($n = 29$)	61.2 ± 7.2 ($n = 21$)^{a}	653 ± 72 ($n = 22$)
DMOTC	−48.2 ± 2.7 ($n = 12$)	54.4 ± 7.6 ($n = 16$)	494 ± 302 ($n = 16$)

[a] $P < 0.001$ compared to rheobase of tonic cells in acute slices.

[b] $P < 0.001$ compared to rheobase of tonic cells in DMOTC.

[c] $P < 0.03$ compared to rmp of tonic cells in acute slices.

[d] $P < 0.005$ compared to R_{in} of irregular cells in acute slices.

[c] $P < 0.03$ compared to R_{in} of phasic cells in acute slices.

Although the difference in R_{in} between phasic neurons in the two situations attained statistical significance, n values were too low to allow us to assign any real meaning to this observation (Table 2).

Membrane excitability was monitored by injecting slow depolarizing current ramps from a preset membrane potential of −60 mV and measuring the latency to the first spike (Fig. 6B). The latency decreased with increasing ramp rates. Data from tonic, irregular, and delay cells are shown in Fig. 6C. Few data were available for transient cells as they only occasionally discharged in response to our ramp protocol. Data from phasic cells are also omitted as so few of them were found in DMOTC (see below and Fig. 5E). Membrane excitability of 'tonic', 'irregular', and 'delay' cells was clearly greater in neurons from DMOTC than in those in acute slices. Fig. 6C shows that these cells displayed significantly shorter latency to first spike in response to depolarizing current ramps than cells in acute slices. The generalized increase in membrane excitability (Fig. 6C) was accompanied by spontaneous action potential discharge in neurons in DMOTC (Fig. 7D). Spontaneous action potentials were not seen in neurons from acute spinal cord slices but occurred quite frequently in cells in DMOTC. These action potentials were seen in the normal extracellular solution and were distinct from the bursts of action potentials seen in bicuculline/strychnine (Fig. 4). Thus, 4/9 neurons after one week in culture, 5/14 neurons after 2 weeks, 23/33 neurons after 3 weeks, 34/41 neurons after 4 weeks, and 4/6 neurons after 5–6 weeks exhibited spontaneous action potentials.

3.8. Spontaneous synaptic activity

Figs. 7A and B illustrate cumulative distribution plots of inter-event interval and amplitude of spontaneous excitatory postsynaptic currents (sEPSCs) for all five cell types. Under our recording conditions, sIPSCs were small and infrequent in acute slices. Although inhibitory events appear larger when Cs^+ rather than K^+ is used as the dominant intracellular cation (Moran et al., 2004), this was not feasible in the present experiments as the presence of intracellular Cs^+ would have affected the discharge characteristics of neurons and therefore precluded their identification.

In all except 'phasic' neurons, sEPSCs were larger and more frequent in DMOTC than in acute slices. This is illustrated by the cumulative distribution plots for sEPSC inter-event interval and amplitude shown in Figs. 7A and B. All differences were statistically significant ($P < 0.0001$; KS test). A sample recording of sEPSCs in a transient cell in DMOTC is shown in Fig. 7C.

We also noted that sIPSCs occurred frequently in DMOTC, even when K^+ was used as the intracellular cation, and large, spontaneous IPSPs were observed in current clamp, indicating an overall increase in spontaneous inhibitory synaptic activity (Fig. 7E). sIPSPs were particularly prevalent when action potentials were elicited with depolarizing current pulses (arrows in Fig. 7E). In some cells, sIPSPs appeared time-locked with preceding action potentials (right-hand records in Fig. 7E). Spontaneous IPSPs were not seen in neurons in acutely isolated slices.

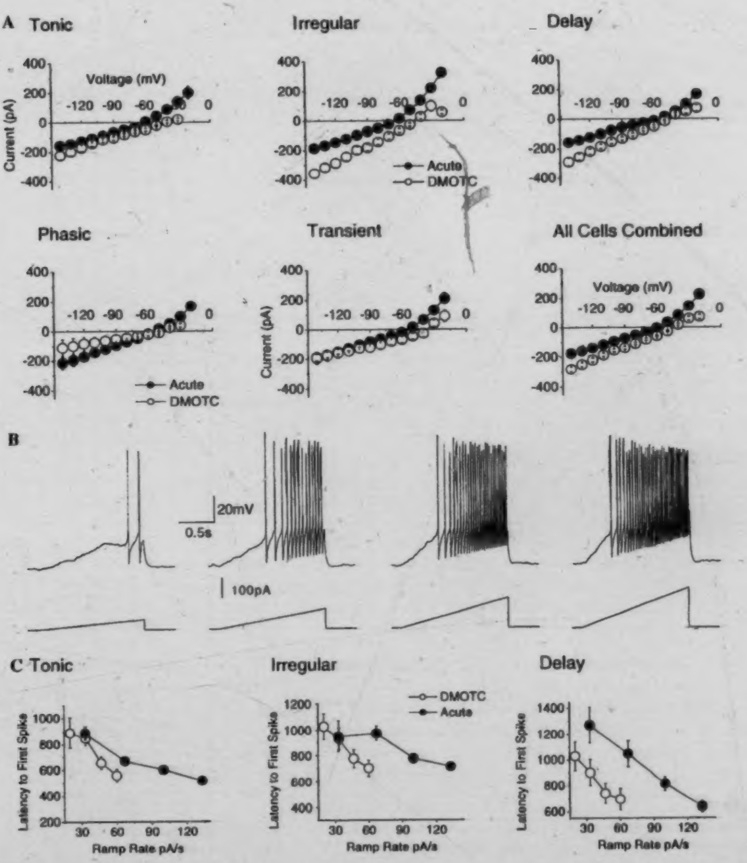

Fig. 6. (A) Current–voltage plots for 'tonic', 'irregular', 'delay', 'phasic', and 'transient' neurons as well as plot for all cell types combined. Filled circles indicate data from neurons in acutely isolated slices and open circles represent data from neurons in OTC. For some values, error bars indicating SEM are smaller than symbols used to designate data points. *N*'s for all plots are the same as those for R_{in} values listed in Table 2. For combined plot, $n = 139$ cells from acute slices and $n = 129$ cells from DMOTC. (B) Sample recordings of responses to current ramp protocols used for quantitative assessment of cell excitability (latency to first spike; recording from a neuron in an acute slice). (C) Plots of latency to first spike versus current ramp rate for tonic irregular and delay cells. Note for neurons in DMOTC (open circles) lower ramp rates produced shorter latencies (increased excitability) compared to neurons from acute slices (filled circles). For some values, error bars indicating SEM are smaller than symbols used to designate data points. Because some cells failed to respond to the slowest ramp rates *n*'s for points on graphs were not constant. Thus for tonic cells, $n = 14$–25 in DMOTC; $n = 18$–25 in acute slices. For irregular cells, $n = 12$–21 in DMOTC; $n = 8$–23 in acute slices. For delay cells, $n = 8$–20 in DMOTC; $n = 3$–17 in acute slices. For all cells combined, $n = 34$–66 in DMOTC; $n = 29$–65 in acute slices. For all cell types, significant differences in latency were seen at 60 pA/S.

4. Discussion

Our main finding is that the physiological characteristics of neurons in DMOTC are remarkably similar to those in acute slices. It is particularly important to note that: (1) A variety of cell morphologies are seen in the cultures (Fig. 2) and these may correspond to morphologically defined cell types in the in vivo dorsal horn; (2) All five neuron types defined electrophysiologically in acute slices are preserved in DMOTC and 4 of the 5 neuron types are seen in similar proportions in both situations (Fig. 5). There do appear to be fewer phasic cells in DMOTC (but see discussion below); (3) with a few exceptions, the rmp, rheobase, and R_{in} of the various neuron types in culture are similar to those of corresponding neuron types in acute slices (Table 2);

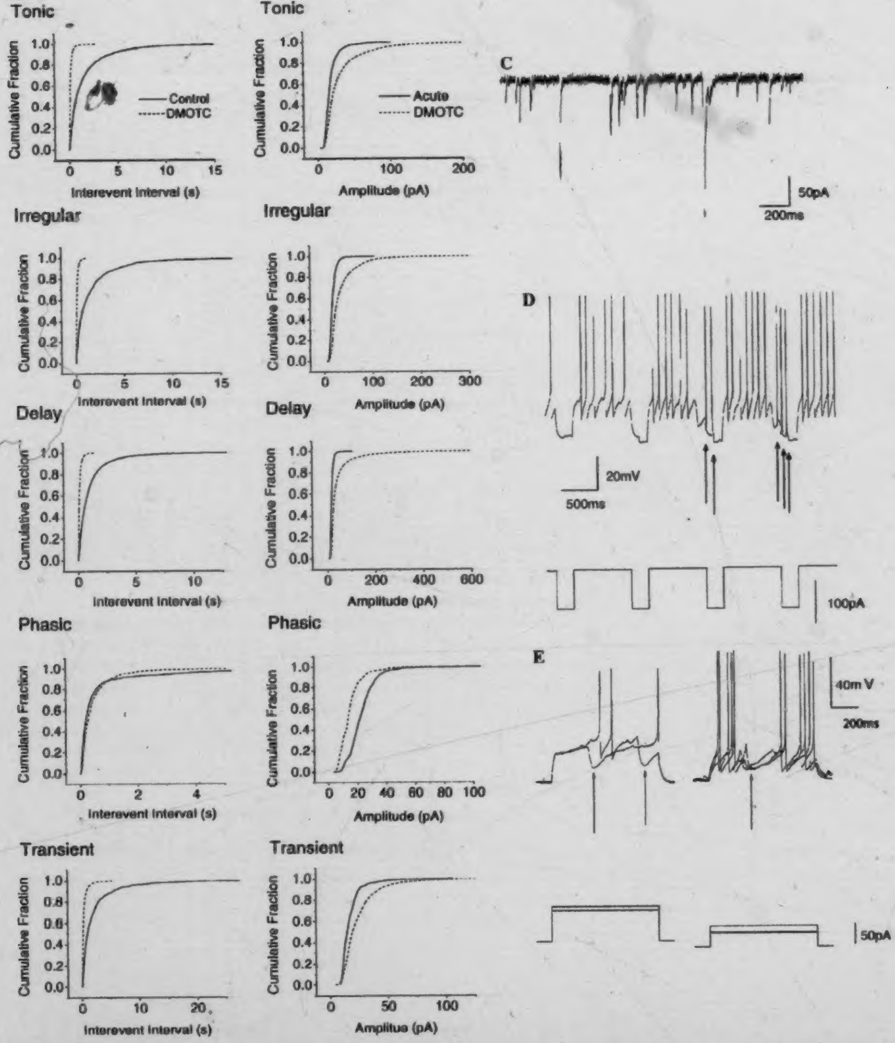

Fig. 7. (A) Cumulative distribution plot of inter-event intervals for all five groups of cells from acute slices and DMOTC. (B) Cumulative distribution histogram of sEPSP amplitudes from the same pool of data. For neurons in acute slices, data were measured from 53 min of recording in tonic and irregular cells, 58 min in delay cells, 15 min in phasic cells, and 29 min in transient cells. For neurons in DMOTC, data were measured from 9 min in phasic cells and 15 min in all other cell types. Numbers of events analyzed were; for tonic cells, 1776 in acute slices, 5430 in DMOTC; for irregular cells, 1402 and 6817 in acute and DMOTC, respectively, for delay cells 3204 in acutes, 6545 in DMOTC, for phasic cells, 1081 in acutes and 1117 in DMOTC, for transient cells, 623 in acutes and 2700 in DMOTC. With the exception of phasic cell inter-event interval, all differences between DMOTC and acute neurons were statistically significant ($P < 0.0001$; KS test). (C) Example of spontaneous excitatory synaptic activity recorded in a transient neuron in a 47d DMOTC at −70 mV. (D) Spontaneous action potentials in a tonic cell after 26d in DMOTC. Neuronal excitability was being studied by passing increasing depolarizing currents into the cell. The arrows indicate persistence of discharge between the current pulses. (E) Sample current-clamp recordings from two neurons in DMOTC illustrating large spontaneous and action potential-related IPSPs (marked by arrows). Left and right traces 22d and 27d in DMOTC, respectively.

(4) inhibitory transmission is similar, as GABAergic, glycinergic, and mixed IPSCs are seen both in culture and in acute slices (Fig. 3). Moreover, previous developmental studies have shown that glycinergic transmission is absent at birth in vivo (Baccei and Fitzgerald, 2004) but develops as animals mature (Keller et al., 2001). A similar developmental sequence appears in the cultures (Fig. 3N) and this further attests to the persistence of normal developmental processes under these conditions. Presynaptic, $GABA_B$-mediated effects of baclofen are also similar in neurons from DMOTC and from acute slices (Figs. 3J–M).

Although methods for preparing organotypic cultures of embryonic spinal cord (Braschler et al., 1989; Spenger et al., 1991; Ballerini and Galante, 1998; Avossa et al., 2003) have been available for some time, we believe we are the first to develop a serum-free, defined-medium culture for this tissue. This system is especially useful for examining the long-term effects of growth factors such as NGF or BDNF, cytokines or neurotransmitters that may be involved in promoting chronic increases in activity in dorsal horn neurons that lead to neuropathic pain (Garraway et al., 2003; Lever et al., 2003a; Lu et al., 2004, 2005a). The defined medium allows us to circumvent complications imposed by the presence of serum that contains an undefined mixture of trophic substances and/or cytokines. Any findings regarding the actions of pain-producing molecules in culture may therefore be related to studies of the effects of nerve injury in vivo which are done in adult animals.

The main difference between neurons in DMOTC and those in acute slices is that membrane excitability and spontaneous synaptic activity are increased in the cultures. Also, slow bursting activity can be induced in cultures in the presence of bicuculline with or without strychnine. The frequency and amplitude of these bursts resemble those generated by strychnine/bicuculline in ventral horn neurons in organotypic culture. Such bursts have been attributed to the synaptic network properties of the cultures rather than to altered properties of individual cultured neurons (Ballerini and Galante, 1998).

4.1. Neuronal phenotypes in DMOTC and in acute slices

Thomson et al. (1989) identified three broad categories of cells in rat dorsal horn which would fit best with the 'tonic', 'phasic', and 'transient' categories described in the present work. More recent work has refined the criteria to identify additional groups of neurons, including those that display an initial delay in the firing response to depolarizing current and which display irregular firing (Grudt and Perl, 2002; Ruscheweyh and Sandkuhler, 2002; Lu and Perl, 2003). Thus, the five electrophysiologically defined neuronal phenotypes found in the *substantia gelatinosa* of acute slices in the present experiments correspond well with previous reports. Also discrete morphological phenotypes can be found in the cultures and the cells illustrated in Fig. 2 are similar to dorsoventral, islet/central, and radial cells defined in acutely prepared sections of rodent dorsal horn (Grudt and Perl, 2002; Heinke et al., 2004).

If differentiation of these morphological and electrophysiological phenotypes occurs before embryonic day 13–14 (when the cultures are prepared), their persistence in DMOTC would indicate that no de-differentiation occurs. Alternatively, if morphological and electrophysiological differentiation occurs after E13-14, these processes would appear to proceed normally in culture. The apparent progressive loss of the 'phasic' cell electrophysiological phenotype in DMOTC may reflect the profound overall increase in membrane excitability seen under these conditions. For example, during electrophysiological classification, hyperexcitable phasic cells may fail to accommodate and appear as irregular or tonic cells in DMOTC.

4.2. Development of inhibitory synaptic transmission

Studies of developmentally regulated markers in organotypic cultures of embryonic mouse spinal cord suggest that inhibitory transmission as well as neuronal development in general proceeds similarly both in DMOTC and *in vivo*. Thus, the pattern of appearance of the GABAergic marker, glutamic acid decarboxylase (GAD), and glial fibrillary acidic protein; a marker for mature astrocytes, paralleled situation in vivo. (Avossa et al., 2003). In agreement with this, the absence of pure glycinergic inhibition in 7d cultures (Fig. 3N) parallels its absence in P0 *substantia gelatinosa* neurons in vivo (Baccei and Fitzgerald, 2004). Although there is a downward trend in the percentage of neurons exhibiting mixed GABA/glycine mIPSCs (Fig. 3N), they were still seen in the oldest (36d) cultures. This might reflect a slight difference between DMOTC and the in vivo situation. Although mixed mIPSCs persist into adulthood, postjunctional detection of GABA released in mixed mIPSCs ceases (Keller et al., 2001). This developmental 'tuning of inhibitory synapses' does not appear to occur in DMOTC.

4.3. Increased synaptic activity and excitability in DMOTC

As yet, we can only speculate as to the mechanisms that underlie increased spontaneous synaptic activity in DMOTC neurons. Decreased inter-event intervals for sEPSCs may reflect the development of increased synaptic contacts (Fig. 7A). Also, large IPSPs appear in current-clamp recordings when neurons are made to discharge by injection of depolarizing current (Fig. 7E). These events are not seen in acute slices where only about 11% of *substantia gelatinosa* interact synaptically (Lu and Perl, 2003). They may therefore reflect the enabling or growth of local synaptic circuits. The probability that altered synaptic circuitry is present in the cultures is also reflected by the ability of strychnine and bicuculline to produce bursting activity (Ballerini and Galante, 1998).

Since increased membrane excitability leads to generation of spontaneous action potentials (Fig. 7D) in DMOTC, this could also lead to increased synaptic activity as more presynaptic action potentials would generate more spontaneous postsynaptic currents. Because outward currents in the *I–V* plots are decreased in DMOTC, alterations in voltage-gated K^+ channels (Fig. 6A) may be one of many mechanisms that contribute to increased membrane excitability (Fig. 6C).

It should also be noted however that neurons in acute slices are likely subject to acute inflammatory reactions, anoxia, and acute trauma following the preparation of slices in a vibratome. On the other hand, neurons in DMOTC have had weeks to recover following the initial establishment of a culture. It has been reported that microglia reassume their inactive, ramified morphology in 9d hippocampal cultures. This may indicate abatement of the inflammatory response at this time (Hailer et al., 1997). The simple 'health' of long-term cultured neurons may therefore be a major determinant of their increased synaptic activity and membrane responsiveness rather than any real phenotypic or developmental difference between them and neurons in acutely prepared slices.

Whatever the cause of increased excitability, the many processes that underlie and/or maintain differentiation of the five distinct electrophysiological phenotypes remain intact in DMOTC. Basic synaptic pharmacology and the development of glycinergic inhibition in DMOTC proceed over a similar time course to the in vivo situation (Keller et al., 2001; Baccei and Fitzgerald, 2004). Lastly, neuronal morphologies corresponding to the in vivo situation can be found in DMOTC. We therefore suggest that experimental findings in these cultures may provide new insights into the changes in *substantia gelatinosa* induced by nerve injury which may, in turn, be relevant to the process of pain centralization.

Acknowledgments

This work was supported by Canadian Institutes of Health Research (CIHR), Christopher Reeve Paralysis Foundation, and Astra Zeneca-Canadian Federation of Biological Societies. S.B. received a studentship award from the Alberta Heritage Foundation for Medical Research (AHFMR). V.B.L. received studentship awards from both CIHR and AHFMR. W.F.C. is an AHFMR Medical Scientist. We thank Dr. Nae Dun (Temple University, Philadelphia, PA, USA) and Dr. Suying Wu (East Tennessee State University, Johnson City, TN, USA) for introducing us to in vitro spinal cord recording techniques, Dr. Laura Ballerini (International School for Advanced Studies, University of Trieste, Trieste, Italy) for generously introducing us to organotypic culture methodology, Dr. William Panenka for initiation of the organotypic culture methodology, Patrick Stemkowski and Ken Wong for skilled technical assistance, Katie Robertson for illustrations, and Dr. John Greer (University of Alberta) for comments on an early version of the manuscript.

References

Abdulla FA, Moran TD, Balasubramanyan S, Smith PA. Effects and consequences of nerve injury on the electrical properties of sensory neurons. Can J Physiol Pharmacol 2003;81:663–82.

Amir R, Michaelis M, Devor M. Membrane potential oscillations in dorsal root ganglion neurons: role in normal electrogenesis and neurópathic pain. J Neurosci 1999;19:8589–96.

Avossa D, Rosato-Siri MD, Mazzarol F, Ballerini L. Spinal circuits formation: a study of developmentally regulated markers in organotypic cultures of embryonic mouse spinal cord. Neuroscience 2003;122:391–405.

Baccei ML, Fitzgerald Maria. Development of GABAergic and glycinergic transmission in the neonatal rat dorsal horn. J Neurosc 2004;24:4749–57.

Ballerini L, Galante M. Network bursting by organotypic spinal slice cultures in the presence of bicuculline and/or strychnine is developmentally regulated. Eur J Neurosci 1998;10:2871–9.

Ballerini L, Galante M, Grandolfo M, Nistri A. Generation of rhythmic patterns of activity by ventral interneurones in rat organotypic spinal slice culture. J Physiol 1999;517(Pt 2):459–75.

Braschler UF, Iannone A, Spenger C, Streit J, Luscher HR. A modified roller tube technique for organotypic cocultures of embryonic rat spinal cord, sensory ganglia and skeletal muscle. J Neurosci Methods 1989;29:121–9.

Cahill CM, Coderre TJ. Attenuation of hyperalgesia in a rat model of neuropathic pain after intrathecal pre- or post-treatment with a neurokinin-1 antagonist. Pain 2002;95:277–85.

Coull JA, Boudreau D, Bachand K, Prescott SA, Nault F, Sik A, et al. Trans-synaptic shift in anion gradient in spinal lamina I neurons as a mechanism of neuropathic pain. Nature 2003;424:938–42.

Dalal A, Tata M, Allègre G, Gekiere F, Bons N, Albe-Fessard D. Spontaneous activity of rat dorsal horn cells in spinal segments of sciatic projection following transection of sciatic nerve or of corresponding dorsal roots. Neuroscience 1999;94:217–28.

De Simoni A, Griesinger CB, Edwards FA. Development of rat CA1 neurones in acute versus organotypic slices: role of experience in synaptic morphology and activity. J Physiol (Lond) 2003;550: 135–47.

Eckert III WA, Willcockson HH, Light AR. Interference of biocytin with opioid-evoked hyperpolarization and membrane properties of rat spinal substantia gelatinosa neurons. Neurosci Lett 2001;297:117–20.

Gahwiler BH. Organotypic monolayer cultures of nervous tissue. J Neurosci Methods 1981;4:329–42.

Gahwiler BH, Capogna M, Debanne D, McKinney RA, Thompson SM. Organotypic slice cultures: a technique has come of age. Trends Neurosci 1997;20:471–7.

Garraway SM, Petruska JC, Mendell LM. BDNF sensitizes the response of lamina II neurons to high threshold primary afferent inputs. Eur J Neurosci 2003;18:2467–76.

Grudt TJ, Perl ER. Correlations between neuronal morphology and electrophysiological features in the rodent superficial dorsal horn. J Physiol 2002;540:189–207.

Hailer NP, Heppner FL, Haas D, Nitsch R. Fluorescent dye prelabelled microglial cells migrate into organotypic hippocampal slice cultures and ramify. Eur J Neurosci 1997;9:863–6.

Heinke B, Ruscheweyh R, Forsthuber L, Wunderbaldinger G, Sandkuhler J. Physiological, neurochemical and morphological properties of a subgroup of GABAergic spinal lamina II neurones identified by expression of green fluorescent protein in mice. J Physiol 2004;560:249–66.

Howard RF, Walker SM, Michael MP, Fitzgerald Maria. The ontogeny of neuropathic pain: Postnatal onset of mechanical allodynia in rat spared nerve injury (SNI) and chronic constriction injury (CCI) models. Pain 2005;115:382–9.

Keller AF, Coull JA, Chery N, Poisbeau P, de Koninck Y. Region-specific developmental specialization of GABA-glycine cosynapses in laminas I–II of the rat spinal dorsal horn. J Neurosci 2001;21:7871–80.

Kerr BJ, Bradbury EJ, Bennett DL, Trivedi PM, Dassan P, French J, et al. Brain-derived neurotrophic factor modulates nociceptive sensory inputs and NMDA-evoked responses in the rat spinal cord. J Neurosci 1999;19:5138–48.

Laird JM, Bennett GJ. An electrophysiological study of dorsal horn neurons in the spinal cord of rats with an experimental peripheral neuropathy. J Neurophysiol 1993;69:2072–85.

Laird JMA, Bennett GJ. Dorsal root potentials and afferent input to the spinal cord in rats with an experimental peripheral neuropathy. Brain Res 1992;584:181–90.

Lever I, Cunningham J, Grist J, Yip PK, Malcangio M. Release of BDNF and GABA in the dorsal horn of neuropathic rats. Eur J Neurosci 2003a;18:1169–74.

Lever IJ, Pezet S, McMahon SB, Malcangio M. The signaling components of sensory fiber transmission involved in the activation of ERK MAP kinase in the mouse dorsal horn. Mol Cell Neurosci 2003b;24:259–70.

Lu, VB, Chee, MJS, Gustafson, SL, Colmers, WF, Smith, PA, 2005a. Concentration-dependent effects of long-term interleukin-1 treatment on spinal dorsal horn neurons in organotypic slice cultures. Abstract Viewer/Itinerary Planner. Washington, DC: Society for Neuroscience, Online, Program No. 292.3.

Lu, VB, Colmers, WF, Dryden, WF, Smith PA, 2004. Brain-derived neurotrophic factor alters the synaptic activity of dorsal horn neurons in long-term organotypic spinal cord slice cultures. Abstract Viewer/Itinerary Planner. Washington, DC: Society for Neuroscience, Online, Program No. 289.15.

Lu Y, Perl ER. A specific inhibitory pathway between substantia gelatinosa neurons receiving direct C-fiber input. J Neurosci 2003;23:8752–8.

Lu Yan, Perl ER. Modular organization of excitatory circuits between neurons of the spinal superficial dorsal horn (Laminae I and II). J Neurosci 2005b;25:3900–7.

Ma C, Shu Y, Zheng Z, Chen Y, Yao H, Greenquist KW, et al. Similar electrophysiological changes in axotomized and neighboring intact dorsal root ganglion neurons. J Neurophysiol 2003;89:1588–602.

Miletic G, Miletic V. Increases in the concentration of brain derived neurotrophic factor in the lumbar spinal dorsal horn are associated with pain behavior following chronic constriction injury in rats. Neurosci Lett 2002;319:137–40.

Moran, TD. Neuropeptide Modulation of Spinal Pain Pathways. 2003. PhD Thesis University of Alberta.

Moran TD, Colmers WF, Smith PA. Opioid-like actions of neuropeptide Y in rat substantia gelatinosa: Y1 suppression of inhibition and Y2 suppression of excitation. J Neurophysiol 2004;92:3266–75.

Mosconi T, Kruger L. Fixed-diameter polyethylene cuffs applied to the rat sciatic nerve induce a painful neuropathy: ultrastructural morphometric analysis of axonal alterations. Pain 1996;64:37–57.

Pezet S, Cunningham J, Patel J, Grist J, Gavazzi I, Lever IJ, et al. BDNF modulates sensory neuron synaptic activity by a facilitation of GABA transmission in the dorsal horn. Mol Cell Neurosci 2002;21:51–62.

Prescott SA, de Koninck Y. Four cell types with distinctive membrane properties and morphologies in lamina I of the spinal dorsal horn of the adult rat. J Physiol 2002;539:817–36.

Prescott SA, De Koninck Yves. Integration time in a subset of spinal lamina I neurons is lengthened by sodium and calcium currents acting synergistically to prolong subthreshold depolarization. J Neurosci. 2005;25:4743–54.

Ruscheweyh R, Sandkuhler J. Lamina-specific membrane and discharge properties of rat spinal dorsal horn neurons in vitro. J Physiol (Lond) 2002;541:231–44.

Ruscheweyh R, Ikeda H, Heinke B, Sandkuhler J. Distinctive membrane and discharge properties of rat spinal lamina I projection neurones in vitro. J Physiol (Lond) 2004;555:527–43.

Sakmann B, Stuart GJ. Patch clamp recordings from the soma, dendrites and axons of neurons in brain slices. In: Sakmann B, Neher E, editors. Single-channel recordings. New York: Plenum; 1995. p. 199–211.

Spenger C, Braschler UF, Streit J, Luscher HR. An organotypic spinal cord—dorsal root ganglion—skeletal muscle coculture of embryonic rat. I. The morphological correlates of the spinal reflex arc. Eur J Neurosci 1991;3:1037–53.

Strichartz GR. The inhibition of sodium currents in myelinated nerve by quaternary derivatives of lidocaine. J Gen Physiol 1973;62:37–57.

Thomson AM, West DC, Headley PM. Membrane characteristics and synaptic responsiveness of superficial dorsal horn neurons in a slice preparation of adult rat spinal cord. Eur J Neurosci 1989;1:479–88.

Woolf CJ. Evidence for a central component of post-injury pain hypersensitivity. Nature 1983;306:686–8.

Neuron type-specific effects of brain-derived neurotrophic factor in rat superficial dorsal horn and their relevance to 'central sensitization'

Van B. Lu[1], Klaus Ballanyi[2,3], William F. Colmers[1,3] and Peter A. Smith[1,3]

[1]Department of Pharmacology, [2]Department of Physiology and [3]Centre for Neuroscience, University of Alberta, Edmonton, Alberta, Canada

Chronic constriction injury (CCI) of the rat sciatic nerve increases the excitability of the spinal dorsal horn. This 'central sensitization' leads to pain behaviours analogous to human neuropathic pain. We have established that CCI increases excitatory synaptic drive to putative excitatory, 'delay' firing neurons in the substantia gelatinosa but attenuates that to putative inhibitory, 'tonic' firing neurons. Here, we use a defined-medium organotypic culture (DMOTC) system to investigate the long-term actions of brain-derived neurotrophic factor (BDNF) as a possible instigator of these changes. The age of the cultures and their 5–6 day exposure to BDNF paralleled the protocol used for CCI *in vivo*. Effects of BDNF (200 ng ml^{-1}) in DMOTC were reminiscent of those seen with CCI *in vivo*. These included decreased synaptic drive to 'tonic' neurons and increased synaptic drive to 'delay' neurons with only small effects on their membrane excitability. Actions of BDNF on 'delay' neurons were exclusively presynaptic and involved increased mEPSC frequency and amplitude without changes in the function of postsynaptic AMPA receptors. By contrast, BDNF exerted both pre- and postsynaptic actions on 'tonic' cells; mEPSC frequency and amplitude were decreased and the decay time constant reduced by 35%. These selective and differential actions of BDNF on excitatory and inhibitory neurons contributed to a global increase in dorsal horn network excitability as assessed by the amplitude of depolarization-induced increases in intracellular Ca^{2+}. Such changes and their underlying cellular mechanisms are likely to contribute to CCI-induced 'central sensitization' and hence to the onset of neuropathic pain.

(Resubmitted 25 July 2007; accepted after revision 23 August 2007; first published online 30 August 2007)

Corresponding author P. A. Smith: Department of Pharmacology, University of Alberta, 9.75 Medical Sciences Building, Edmonton, Alberta, Canada, T6G 2H7. Email: peter.a.smith@ualberta.ca

Neuropathic pain, which is characteristically chronic and frequently intractable, is a major clinical problem. It can be initiated by nerve, brain or spinal cord injury (Kim & Chung, 1992; Kim *et al.* 1997) or by complications associated with diseases such as postherpetic neuralgia, stroke or diabetes (Chen & Pan, 2002).

Much of our understanding of neuropathic pain mechanisms comes from animal models in which experimentally induced peripheral nerve damage is used to initiate behaviours analogous to the signs of human neuropathic pain. It has been shown that injury to primary afferents can give rise to a global increase in excitability of the dorsal horn (Woolf, 1983; Laird & Bennett, 1993; Dalal *et al.* 1999; Kohno *et al.* 2003). Activation of microglia has also been implicated in this process of 'central sensitization' (Baba *et al.* 1999; Tsuda *et al.* 2005; Zhuang *et al.* 2005; Hains & Waxman, 2006). Our work, using chronic constriction injury (CCI) of the sciatic nerve revealed a distinct pattern of altered synaptic drive to electrophysiologically defined populations of neurons in the substantia gelatinosa of the rat dorsal horn; putative excitatory 'delay' firing neurons received more excitation whereas putative inhibitory 'tonic' firing neurons received less (Balasubramanyan *et al.* 2006).

It has been postulated that substances released from damaged primary afferents and/or activated microglia (Coull *et al.* 2005) signal changes in the properties of dorsal horn neurons. Thus, any chemical instigator of 'central sensitization' should affect the dorsal horn in the same way as CCI.

The neurotrophin brain-derived neurotrophic factor (BDNF) may be one such instigator. It is found in the central nerve terminals of primary afferents fibres (Apfel *et al.* 1996), and neuropathic pain-related behaviours, such as allodynia, are attenuated by blocking or sequestering BDNF (Zhou *et al.* 2000; Coull *et al.* 2005; Matayoshi *et al.* 2005). Also, following nerve injury, the expression of BDNF and its high-affinity receptor, TrkB, are up-regulated in the superficial dorsal horn (Cho *et al.* 1998; Michael *et al.* 1999; Dougherty *et al.* 2000; Ha *et al.* 2001;

© 2007 The Authors. Journal compilation © 2007 The Physiological Society

DOI: 10.1113/jphysiol.2007.141267

Fukuoka *et al.* 2001; Miletic & Miletic, 2002). Although elevated levels of BDNF have been shown to persist for several days following nerve injury (Cho *et al.* 1997; Zhou *et al.* 1999; Dougherty *et al.* 2000; Fukuoka *et al.* 2001), most studies examining its action on dorsal horn neurons have used acute, short-term exposures (Kerr *et al.* 1999; Garraway *et al.* 2003; Slack *et al.* 2004). It is yet to be determined whether long-term exposure of dorsal horn neurons to BDNF instigates the same enduring neuron type-specific changes as CCI as would be expected if it contributes to 'central sensitization'.

To test this, we developed a defined-medium organotypic culture (DMOTC) of rat spinal cord that allowed us to expose neurons to elevated levels of BDNF for durations that would mimic the effects of CCI *in vivo* (Lu *et al.* 2006). Reports of some of our findings have appeared in abstract form (Lu *et al.* 2004; Smith *et al.* 2005).

Methods

All procedures were carried out in compliance with the guidelines of the Canadian Council for Animal Care and with the approval of the University of Alberta Health Sciences Laboratory Animal Services Welfare Committee.

Organotypic slice culture preparation

Organotypic cultures (DMOTCs) were prepared as previously described (Lu *et al.* 2006). Briefly, embryonic day 13 (E13) rat fetuses were delivered by caesarean section from timed-pregnant female Sprague–Dawley rats (Charles River, Saint-Constant, QC, Canada) under deep isoflurane anaesthesia. The dam was subsequently killed with an overdose of intracardial chloral hydrate (10.5%). The entire embryonic sac was placed in chilled Hanks' balanced salt solution containing (mM): 138 NaCl, 5.33 KCl, 0.44 KH_2PO_4, 0.5 $MgCl_2$–$6H_2O$, 0.41 $MgSO_4$–$7H_2O$, 4 $NaHCO_3$, 0.3 Na_2HPO_4, 5.6 D-glucose and 1.26 $CaCl_2$. Individual rat fetuses were removed from their embryonic sacs and rapidly decapitated. The spinal cord from each fetus was isolated in the above solution and sliced into 275–325 μm transverse slices using a tissue chopper (McIlwain, St Louis, MO, USA). Only lumbar spinal cord slices with an intact spinal cord and two attached dorsal root ganglia were chosen and trimmed of excess ventral tissue and allowed to recover for 1 h at 4°C.

Each embryonic spinal cord slice was plated on a single glass coverslip (Karl Hecht, Sondheim, Germany) and attached with a clot of reconstituted chicken plasma (lyophilized, 0.2 mg% heparin; Cocalico Biologicals Inc., Stevens, PA, USA) and thrombin (200 units ml^{-1}; Sigma, St Louis, MO, USA). Coverslips were then inserted into flat-bottomed tissue culture tubes (Nunc-Nalgene International, Mississauga, ON, Canada) filled with 1 ml of medium, and then placed into a roller drum rotating at 120 rotations per hour in a dry heat incubator at 36°C. The medium in the tubes was composed of 82% Dulbecco's modified Eagle's medium (DMEM), 10% fetal bovine serum and 8% sterile water (all from Gibco, Grand Island, NY, USA). The medium was supplemented with 20 ng ml^{-1} NGF (Alomone Laboratories, Jerusalem, Israel) for the first 4 days, and omitted thereafter. Antibiotic and antimycotic drugs (5 units ml^{-1} penicillin G, 5 units ml^{-1} streptomycin and 12.5 ng ml^{-1} amphotericin B; Gibco) were also included in the media during the first 4 days of culture. After 4 days in culture, DMOTC slices were treated with an antimitotic drug cocktail consisting of uridine, cytosine-β-D-arabino-furanoside (AraC), and 5-fluorodeoxyuridine (all at 10 μM) for 24 h to prevent the overgrowth of glial cells. During antimitotic treatment, the serum medium was progressively switched (first diluted 50 : 50 after 4 days, then completely exchanged after 5 days) to a defined, neurotrophin- and serum-free medium consisting of Neurobasal medium with N-2 supplement and 5 mM Glutamax-1 (all from Gibco). The medium within these tubes was exchanged regularly with freshly prepared medium every 3–4 days.

BDNF treatment

DMOTC slices were maintained *in vitro* for 3–4 weeks before recording to allow cultures to stabilize as previously reported (Lu *et al.* 2006). Also, the BDNF treatment schedule was chosen to parallel previous whole animal studies (Balasubramanyan *et al.* 2006) so exposure of dorsal horn neurons to BDNF would be congruent with the time course of BDNF elevation following nerve injury (see Fig. 1). Slices were treated after 15–21 days *in vitro* for a period of 5–6 days with 200 ng ml^{-1} BDNF (Alomone Laboratories, Jerusalem, Isreal) in the serum-free medium described above. Thus, the oldest cultures studied were 37 days old. Cultures maintained for longer periods tended to deteriorate. The BDNF medium was exchanged on the third treatment day. Age-matched untreated DMOTC slices served as controls.

Electrophysiology

For whole-cell recordings, DMOTC slices were superfused at room temperature (~22°C) with 95% O_2–5% CO_2-saturated, external recording solution containing (mM): 127 NaCl, 6.5 KCl, 1.2 NaH_2PO_4, 1.3 $MgSO_4$, 26 $NaHCO_3$, 25 D-glucose, 2.5 $CaCl_2$. DMOTC slices assumed a circular shape approximately 5 mm in diameter. Neurons selected for recording were located between 0.5 and 2 mm from the dorsal surface. They were patched under visual guidance using infrared-differential interference contrast (IR-DIC) optics.

Recordings were made using a NPI SEC-05L amplifier (npi Electronics, Tamm, Germany) in whole-cell

© 2007 The Authors. Journal compilation © 2007 The Physiological Society

discontinuous single-electrode voltage-clamp or current-clamp mode. Patch pipettes were pulled from thin-walled borosilicate glass (WPI, Sarasota, FL, USA) to 5–10 MΩ resistances and filled with an internal recording solution containing (mM): 130 potassium gluconate, 1 $MgCl_2$, 2 $CaCl_2$, 10 Hepes, 10 EGTA, 4 Mg-ATP, 0.3 Na-GTP, pH 7.2, 280–310 mosmol l^{-1}.

Current–voltage (I–V) relationships were determined under voltage clamp using a range of 800 ms voltage commands which stepped holding potential from −140 to −20 mV in 10 mV steps. 'Pseudo-steady state' current was measured just prior to the termination of each voltage pulse. Input resistance was measured from the slope of the I–V relationship between −70 and −140 mV. Membrane excitability was quantified by examining discharge rates in response to a 1.5 s current ramp at a rate of 60 pA s^{-1} from a preset membrane potential of −60 mV. Cumulative latencies for the first, second, third and subsequent action potentials were plotted. The rheobase was determined as the minimum amount of current required to initiate firing of an action potential from a membrane potential adjusted to −60 mV.

Spontaneous excitatory postsynaptic currents (sEPSCs) were recorded for 3 min with the neuron clamped at −70 mV. At this voltage, Cl^- mediated inhibitory events would be small outward currents generated by a 13 mV driving force from the estimated E_{Cl} of −83 mV. Miniature excitatory postsynaptic currents (mEPSCs) were recorded in a similar manner but in the presence of 1 μM tetrodotoxin (TTX; Alomone Laboratories, Jerusalem, Isreal) to block action potential-dependent neurotransmitter release. Blockade of action potential generation was confirmed by the cessation of action potential discharges in response to depolarizing current pulses. Also, the percentage of TTX-sensitive sEPSCs in each neuron (i.e. action potential-dependent events) was calculated from two 3 min recording periods in the absence and presence of TTX using the following equation:% TTX-sensitive sEPSCs = (total number of sEPSCs − total number of mEPSCs)/total number of sEPSCs.

Spontaneous excitatory postsynaptic potentials (sEPSPs) and action potentials were recorded at resting membrane potential in current-clamp mode. All data were acquired using Axon Instruments pCLAMP 9.0 software (Molecular Devices, Burlingame, CA, USA).

Data analysis, modelling and statistical testing

All data, except sEPSCs, mEPSCs and sEPSPs, were analysed using pCLAMP 9.0 software. Statistical comparisons were made with Student's unpaired t test or chi-squared (χ^2) test as specified and appropriate, using GraphPad InStat 3.05 (GraphPad Software, San Diego, CA, USA).

Excitatory synaptic events were analysed using Mini Analysis software (Synaptosoft, Decatur, GA, USA). Peaks of events were first automatically detected by the software according to a set of threshold criteria, and then all detected events were visually re-examined and accepted or rejected subjectively (refer to Moran *et al.* 2004 for complete details). To generate cumulative probability plots for both amplitude and interevent time interval, the same number of events (50–200 events acquired after an initial 1 min of recording) from each neuron was pooled for each neuron type, and input into the Mini Analysis program. The Kolmogorov–Smirnov two-sample statistical test (KS test) was used to compare the distribution of events between control and BDNF-treated groups.

All graphs were plotted and fitted using Origin 7.0 (OriginLab Corp., Northampton, MA, USA) and statistical significance was taken as $P < 0.05$. Rise times and decay times of individual mEPSCs were fitted with a double exponential equation of the form:

$$y = y_0 + A(1 - \exp(-(x - x_0)/\tau_1))^{\wedge} P \exp(-(x - x_0)/\tau_2)$$

Where y_0 and x_0 determine the position of the fit relative to the x and y axes, A is an amplitude term, τ_1 and τ_2 are time constants for the rise and decay of the mEPSC, respectively, and P is a value determining the relative importance of the two parts of the equation that was set

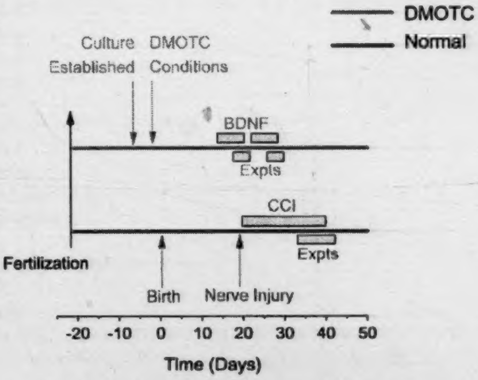

Figure 1. Time course of BDNF treatment parallels time course of nerve injury *in vivo* in a neuropathic pain model (CCI)
Timeline indicated for long-term BDNF DMOTC experiments, shown above, and previous CCI experiments (Balasubramanyan *et al* 2006), shown below. Time indicated in postnatal days. The duration of treatment (which lasted 5–6 days) was chosen to correlate with reports of prolonged BDNF release following nerve injury (see Introduction). BDNF treatment was started either 15 or 21 days after the cultures were established and experiments were conducted after the treatment period.

© 2007 The Authors. Journal compilation © 2007 The Physiological Society

to 1 for all fits and simulations. Fitting was carried out by repeated iterations until the χ^2 value was unchanged for successive fits; this consistently yielded r^2 values > 0.99. Manipulation of the decay time constant τ_2 to assess its contribution to response amplitude (Fig. 7*H–J*) was done using a subroutine written in Microsoft Excel by Dr Gerda de Vries (Department of Mathematics and Statistics, University of Alberta). Analysis of mEPSC amplitude also involved redistributing event lists into 1 pA bins to produce histograms such as those illustrated in Figs 7*E* and *F* and 8*E* and *F*. Gaussian curve fitting protocols available in Origin 7.0 were used to identify peaks within the data. Fitting was carried out by repeating iterations until the χ^2 value was not further reduced. For most experimental situations, best fits were obtained by fitting to three peak amplitudes as changing from two to three Gaussian fits produced large increases in r^2 values but adding a fourth component produced very little change (see insets to Figs 7*E* and *F* and 8*E* and *F*).

Calcium imaging

A single DMOTC slice was incubated for 1 h prior to imaging with 5 μM of the membrane-permeant acetoxymethyl form of the fluorescent Ca^{2+}-indicator dye Fluo-4 (TEF Laboratories Inc., Austin, TX, USA). The conditions for incubating the dye were standardized across different slices to avoid uneven dye loading. After dye loading, the DMOTC slice was transferred to a recording chamber and perfused with external solution containing (mM): 131 NaCl, 2.5 KCl, 1.2 NaH_2PO_4, 1.3 $MgSO_4$, 26 $NaHCO_3$, 25 D-glucose, and 2.5 $CaCl_2$ (20°C, flow rate 4 ml min^{-1}). Changes in Ca^{2+}-fluorescence intensity evoked by a high K^+ solution (20, 35, or 50 mM, 90 s application) were measured in dorsal horn neurons with a confocal microscope equipped with an argon (488 nm) laser and filters (20× XLUMPlanFl-NA-0.95 objective; Olympus FV300, Markham, Ontario, Canada). Full frame images (512 × 512 pixels) in a fixed *xy* plane were acquired at a scanning time of 1.08 s $frame^{-1}$ (Ruangkittisakul *et al.* 2006). Selected regions of interest were drawn around distinct cell bodies and fluorescence intensity traces were generated with FluoView v. 4.3 (Olympus).

Drugs and chemicals

Unless otherwise stated, all chemicals were from Sigma (St Louis, MO, USA). Fluo-4 AM dye was dissolved in a mixture of dimethyl sulfoxide (DMSO) and 20% pluronic acid (Invitrogen, Burlington, Ontario, Canada) to a 0.5 mM stock solution and kept frozen until used. TTX was dissolved in distilled water as a 1 mM stock solution and stored at −20°C until use. TTX was diluted to a final desired concentration of 1 μM in external recording solution on the day of the experiment.

Results

Classification of neurons in the superficial dorsal horn of the cultures

In our previous studies of CCI-induced changes in dorsal horn, we recorded from substantia gelatinosa neurons that were classified on the basis of their action potential discharge pattern in response to depolarizing current steps from a preset membrane potential of −60 mV as 'tonic', 'delay', 'phasic', 'transient' or 'irregular' (Balasubramanyan *et al.* 2006; Fig. 2*A*. Because all five neuron types were also encountered in recordings made 0.5–2.5 mm from the dorsal edge of DMOTCs, this region corresponded well with the substantia gelatinosa of acute slices. As was seen with acute slices (Balasubramanyan *et al.* 2006), delay and tonic cells, which are putative excitatory and inhibitory interneurons, respectively, made up about 60% of the total population in the cultures (Fig. 2*B*).

Apart from an increase in the proportion of 'transient' neurons (χ^2 test, $P < 0.05$), there was no significant change in the contribution of each neuronal cell type (χ^2 test, P values ranged from 0.41 to 0.77) to the total population following BDNF treatment ($n = 120$ for controls, $n = 112$ for BDNF; Fig. 2*C*).

Minimal effects of BDNF on passive membrane properties; small effect on active properties

Treatment of DMOTC with BDNF did not affect resting membrane potential (RMP) input resistance or the *I–V* relationship of any neuronal cell type (Table 1, *t* test, *P* values ranged from 0.18 to 0.95 for RMP, and from 0.19 to 0.81 for input resistance). This was similar to the situation with CCI *in vivo*. Moreover, as seen with CCI, BDNF failed to alter rheobase of 'tonic', 'delay', 'phasic' or 'transient' neurons in DMOTC (Table 1, *t* test, $P > 0.5$). Only 'irregular' neurons had a significantly lower rheobase *versus* control (*t* test, $P < 0.05$). Excitability was evaluated further by examining the firing rate in response to a 60 pA s^{-1} depolarizing current ramp. Firing rate was expressed as the cumulative latency to each action potential spike (Fig. 3). Under these conditions, only 'delay' neurons appeared to show a slight increase in excitability following prolonged BDNF exposure (Fig. 3*B*). Although the data only attained statistical significance at the most positive excursions of the current ramps, its possible importance cannot be ignored as 'delay' neurons tended to display bursts of spontaneous action potentials following BDNF treatment (see Fig. 9).

© 2007 The Authors. Journal compilation © 2007 The Physiological Society

Table 1. Comparison of membrane properties between control and BDNF-treated DMOTC slices

	RMP (mV)	R_{input} (MΩ)	Rheobase (pA)
Tonic			
Control	−51.79 ± 1.66 (29)	419.22 ± 36.02 (28)	29.67 ± 2.56 (30)
BDNF	−51.95 ± 1.70 (21)	435.62 ± 56.31 (22)	32.73 ± 4.93 (22)
Delay			
Control	−47.34 ± 1.70 (38)	319.83 ± 27.09 (37)	73.56 ± 6.21 (45)
BDNF	− 50.61 ± 1.75 (36)	383.68 ± 39.93 (39)	70.38 ± 8.24 (39)
Irregular			
Control	−47.37 ± 2.16 (27)	299.28 ± 43.20 (27)	75 ± 9.98 (29)
BDNF	− 47 ± 2.87 (21)	326.74 ± 30.21 (21)	49.32 ± 5.85* (22)
Phasic			
Control	−44 ± 3.93 (7)	371.12 ± 94.11 (6)	44.29 ± 7.19 (7)
BDNF	−49.88 ± 2.87 (8)	411.61 ± 73.11 (9)	46.67 ± 6.01 (9)
Transient			
Control	−46.17 ± 7.1 (6)	301.13 ± 86.44 (9)	102.78 ± 19.82 (9)
BDNF	−54.06 ± 2.70 (16)	270.22 ± 41.61 (17)	93 ± 8.92 (20)

Values expressed as mean ± S.E.M. *n* values in brackets. For Student's unpaired *t* test, $^{*}P < 0.05$.

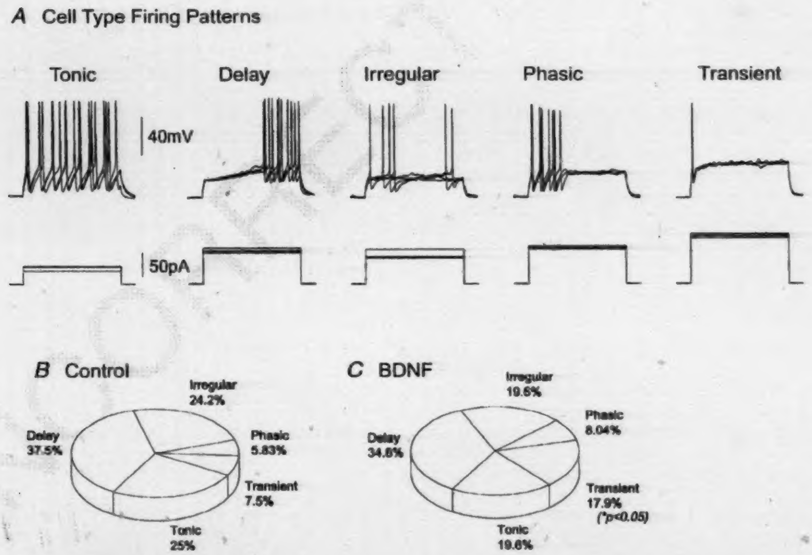

Figure 2. Minimal changes in the proportion of each characterized neuronal cell type within the dorsal horn following BDNF treatment

A, sample current-clamp recordings displaying different discharge firing patterns used to classify neurons within the dorsal horn. Three different recording traces at different current intensities are overlapped for each cell type. Membrane potential was set to −60 mV prior to injection of current pulses. Refer to text for details of characteristic features of each cell type. *B* and *C*, pie graphs showing percentage of each neuronal cell type identified in recordings from control DMOTC slices ($n = 120$) and BDNF treated DMOTC slices ($n = 112$). The only significant shift in the population was in the transient cell type group (χ^2 test, $^{*}P < 0.05$).

© 2007 The Authors. Journal compilation © 2007 The Physiological Society

Effects of BDNF on sEPSCs

CCI produces a specific pattern of changes in excitatory synaptic transmission in the substantia gelatinosa (Table 2); different changes are seen in different cell types. In particular, excitatory synaptic drive to putative inhibitory tonic cells is decreased and that to putative excitatory delay cells is increased. If BDNF is involved in the instigation of such changes, it should alter spontaneous excitatory postsynaptic current (sEPSC) in a neuron type-specific pattern in a similar way to CCI. Effects of BDNF on sEPSC amplitude are illustrated in Fig. 4*A*–*E*, and effects on interevent interval (the reciprocal of frequency) are illustrated in Fig. 4*F*–*J*. As shown, BDNF reduced the amplitude and frequency of sEPSCs in 'tonic' neurons (Fig. 4*A* and *F*). Sample recordings illustrating BDNF's effects on sEPSCs of 'tonic' neurons are shown in Fig. 6*D*. By contrast, BDNF increased the frequency of sEPSCs in 'delay' neurons but did not affect their amplitude (Fig. 4*B* and *G*). Sample recordings illustrating the effect of BDNF on sEPSCs of 'delay' neurons are shown in Fig. 6*E*.

BDNF also increased the amplitude and frequency of sEPSCs in 'irregular' (Fig. 4*C* and *H*), 'phasic' (Fig. 4*D* and *I*) and 'transient' (Fig. 4*E* and *J*) neurons. All changes were significant according to the Kolmogorov–Smirnoff two-sample test (KS test, *P* values presented in the figures).

Further statistical analysis by means of a parametric *t* test of all data sets was also applied (Fig. 4*K* and *L*). The trends of changes of sEPSC amplitude and interevent interval identified in the KS-test were also apparent from the *t* test.

Thus, BDNF did not produce identical changes in the synaptic excitation of all neuron groups, but rather induced neuron type-specific effects. 'Tonic' neurons received reduced spontaneous excitatory synaptic activity and all other neuron types, 'delay', 'irregular', 'phasic' and 'transient' neurons, generally displayed increased synaptic activity. This pattern of BDNF-induced changes in sEPSCs across all cell types was quite similar to that produced by CCI *in vivo* (Table 2). The correlation was particularly clear for sEPSC frequency; CCI and BDNF increased frequency in all cell types except tonic cells where both produced a decrease.

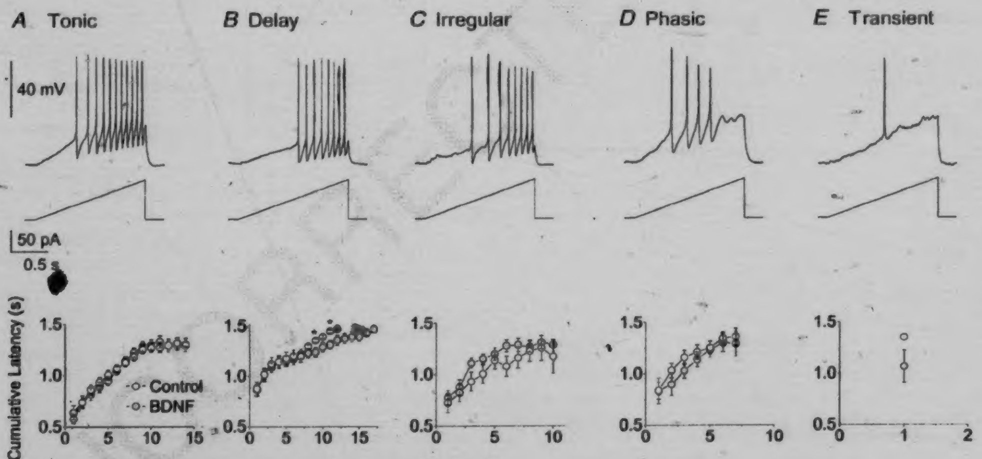

Figure 3. Minimal effects of BDNF membrane excitability
Membrane excitability was measured as the cumulative latency of action potential discharges in response to a depolarizing current ramp from −60 mV. Top panels show sample records of a typical response of tonic, delay, irregular, phasic and transient cells to a 60 pA s^{-1} current ramp injection for 1.5 s. With the exception of transient cells, all cell types discharged ≥ 3 spikes in response to the current ramp. Lower panels are graphs of cumulative latency against spike number for each cell type. Not all cells produced the same number of action potential spikes during ramps. For example in *A*, of the 27 tonic cells examined only 5 of them fired 15 action potentials. The mean cumulative latencies for each spike number therefore have different sample sizes. *A*, for tonic cells, $n = 5$–27 for controls, $n = 11$–22 for BDNF. *B*, for delay cells, $n = 6$–27 for controls, $n = 10$–32 for BDNF. *C*, for irregular cells, $n = 5$–18 for controls, $n = 5$–19 for BDNF. *D*, for phasic cells, $n = 5$–7 for controls, $n = 5$–9 for BDNF. *E*, for transient cells, $n = 3$ for controls, $n = 4$ for BDNF. The only increase in excitability after BDNF treatment was observed in delay cells (*t* test, $^{*}P < 0.05$). In some cases, error bars indicating S.E.M. are smaller than the symbols used to plot the data.

© 2007 The Authors. Journal compilation © 2007 The Physiological Society

Table 2. Summary of comparison between sEPSCs and mEPSCs following chronic constriction nerve injury (CCI) and long-term BDNF exposure.

	Tonic	Delay	Irregular	Phasic	Transient
sEPSC amplitude					
CCI	↓	↑	↑	↓	↑
BDNF	↓	↔	↑	↑	↑
sEPSC frequency					
CCI	↓	↑	↑	↑	↑
BDNF	↓	↑	↑	↑	↑
mEPSC amplitude					
CCI	↓	↑	↑	nd	↑
BDNF	↓	↑	↓	↓	↑
mEPSC frequency					
CCI	↓	↑	↔	nd	↑
BDNF	↓	↑	↓	↑	↑

Data for changes induced by CCI from Balasubramanyan *et al.* (2006). ↑ indicates a significant increase compared to control; ↓ indicates a significant decrease compared to control; ↔ indicates no change compared to control and nd indicates not determined because *n* values were too low.

Effects of BDNF on mEPSCs

Miniature excitatory postsynaptic currents (mEPSCs) represent the action potential independent release of neurotransmitter (Colomo & Erulkar, 1968). To further characterize the changes in synaptic excitation induced by BDNF, mEPSCs were recorded in the presence of 1 μM TTX and analysed in a similar manner to sEPSC events.

The effects of BDNF on mEPSC amplitude are illustrated in Fig. 5*A*–*E*, and its effects on inter-event interval are illustrated in Fig. 5*F*–*J*. Similar to its action on sEPSCs, BDNF reduced the amplitude and frequency of mEPSCs in 'tonic' neurons (Fig. 5*A* and *F*). Sample recordings illustrating BDNF-induced decreases in mEPSCs on 'tonic' neurons are shown in Fig. 6*D*. Conversely, long-term BDNF exposure increased the amplitude and frequency of mEPSCs in 'delay' neurons (Fig. 5*B* and *G*). Sample recordings illustrating BDNF-induced increases in mEPSCs on 'delay' neurons are shown in Fig. 6*E*.

In addition, BDNF reduced the amplitude and frequency of mEPSCs in 'irregular' neurons (Fig. 5*C* and *H*), reduced the amplitude but increased the frequency of mEPSCs in 'phasic' neurons (Fig. 5*D* and *I*) and increased both the frequency and amplitude in 'transient' neurons (Fig. 5*E* and *J*). All changes mentioned were significant and the *P* values from KS tests are presented in the figures. The results from *t* tests on the same data sets are in agreement with the conclusions from the KS test (Fig. 5*K* and *L*). As was seen with sEPSCs, the pattern of the action of BDNF on mEPSCs across all cell types was similar to that seen with CCI *in vivo* (Table 2).

BDNF-induced alterations in the frequency of presynaptic action potentials does not account for changes in sEPSCs of tonic and delay neurons

The sEPSC population is composed of synaptic events generated in response to presynaptic action potentials, as well as mEPSCs resulting from action potential-independent release. TTX significantly reduced the mean sEPSC amplitude (Fig. 6*A*, *t* test, $P < 0.001$) and produced the expected increase in interevent interval (Fig. 6*B*, *t* test, $P < 0.001$) in all neuron types.

BDNF-induced changes in the mEPSC population (Fig. 5) may not be solely responsible for the changes in sEPSCs (Fig. 4). We cannot exclude the possible contribution of changes in presynaptic action potential activity. This would alter the proportion of action potential-dependent synaptic events that are removed by the addition of TTX.

The observed decrease in sEPSC frequency observed in 'tonic' neurons with chronic BDNF treatment (Fig. 4*F*) could not be accounted for by a decrease in action potential-dependent events as the percentage of TTX-sensitive sEPSCs was increased (Fig. 6*C*, *t* test, $P < 0.05$). Sample recordings illustrating this effect of BDNF on relative sEPSC and mEPSC frequency are shown in Fig. 6*D*.

In 'delay' neurons, an increase in action potential-dependent release is unlikely to contribute to the observed increase in sEPSC frequency (Fig. 4*G*) since the percentage of TTX-sensitive sEPSCs decreased significantly with BDNF treatment (Fig. 6*C*, *t* test, $P < 0.05$). Sample recordings illustrating this effect of BDNF on relative sEPSC and mEPSC frequency are shown in Fig. 6*E*. Thus, the increased frequency of sEPSCs in

© 2007 The Authors. Journal compilation © 2007 The Physiological Society

'delay' neurons (Fig. 4*G*) is most likely attributable to an increase in mEPSC frequency (Fig. 5*G*) and thus perhaps to changes in the release process.

In the case of 'irregular' neurons, BDNF increased the frequency of sEPSCs but decreased the frequency of their corresponding mEPSCs. Thus, an increase in the action potential-dependent events is mainly responsible for the increase in synaptic activity in these neuron cell types.

Lastly for 'phasic' and 'transient' neurons, there was no change in the percentage of TTX-sensitive sEPSCs with BDNF treatment (*t* test, $P > 0.1$). Since mEPSC frequency increased (Fig. 5*I* and *J*), it is possible that this, as well as an increase in action potential-dependent events, occurred in both cell types.

Further analysis of the mechanism of action of BDNF on tonic cells

Since tonic and delay cells comprise ~60% of the neurons studied, and they likely represent inhibitory and excitatory neurons, respectively, mEPSC data from these two cell types were analysed more thoroughly.

Besides the reduction in mEPSC amplitude and frequency (Fig. 5*A* and *F*), BDNF reduced the time constant for mEPSC decay (τ_2) by 35%. $\tau_2 = 10.5 \pm 0.43$ ms ($n = 1151$) for control and 6.8 ± 0.28 ms ($n = 631$) for mEPSCs recorded after BDNF treatment (*t* test, $P < 0.0001$). Superimposed events from a typical control 'tonic' neuron and from

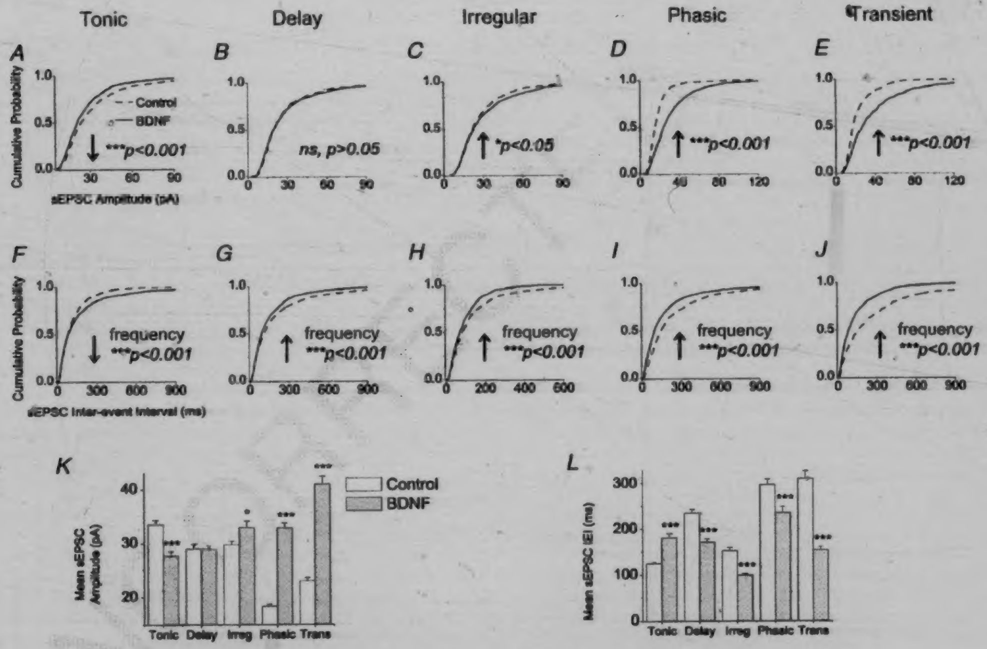

Figure 4. Effects of BDNF on amplitude and interevent interval of spontaneous excitatory postsynaptic currents (sEPSCs)

A–E, cumulative probability plots for sEPSC amplitude. The first 50 events following the 1st minute of recordings from each cell were pooled in order to construct cumulative distribution plots, except for phasic and transient cells where the first 200 or 100 events following the 1st minute of recording were taken, respectively. *A*, tonic cells; 1450 events from control DMOTC slices, 1950 events from BDNF-treated DMOTC slices. *B*, delay cells; 1900 events for controls, 1100 events for BDNF. *C*, irregular cells; 1350 events for controls, 1100 events for BDNF. *D*, phasic cells; 1356 events for controls, 1670 events for BDNF. *E*, transient cells; 800 events for controls, 800 events for BDNF. An equal number of BDNF-treated transient cells as controls were chosen at random to analyse sEPSC events. *P* values derived from the KS test indicated on graphs. *F–J*, cumulative probability plots for sEPSC interevent interval (IEI). *P* values derived from the KS test indicated on graphs. *K* and *L*, effects of BDNF on mean amplitude (*K*) and IEI (*L*) of sEPSC events. The same events used to construct cumulative probability plots were used, so the same *n* values apply. For Student's unpaired *t* test, $^{*}P < 0.05$, $^{***}P < 0.001$. Error bars indicate S.E.M.

© 2007 The Authors. Journal compilation © 2007 The Physiological Society

another neuron from a BDNF-treated culture are shown in Fig. 7*A* and *B*. The white traces show superimposed average data from the two cells and these are compared in Fig. 7*C*. The scaled averages presented in Fig. 7*D* emphasize the increased rate of mEPSC decay in 'tonic' neurons from BDNF-treated cultures.

Three populations of mEPSC amplitudes of 12.1 ± 0.28, 19.7 ± 2.22 and 35.7 ± 7.38 pA were seen in control 'tonic' cells (Fig. 7*E*). These may reflect three different populations of vesicles in presynaptic terminals, different sizes of vesicles in different types of afferents, i.e. various intraspinal inputs such as primary afferents or local interneurons, or different populations of terminals at different distances from the site of recording. Three populations of mEPSC amplitude were also seen in BDNF-treated neurons (Fig. 7*F*) but these had smaller peak amplitudes at 7.3 ± 0.19, 10.9 ± 1.19 and 19.4 ± 2.35 pA. The insets to Fig. 7*E* and *F* show that fitting with three peaks produced the optimal reduction in χ^2 (see Methods). Figure 7*G* shows a replot of the three Gaussian distributions of mEPSC amplitude from control and BDNF 'tonic' cells for comparison.

The apparent leftward shift in the three distributions raised the possibility that the reduction in time constant for mEPSC recovery contributed to the observed decrease in amplitude. To test this, we modelled three different mEPSCs using two exponential equations (Fig. 7*I*–*J*; see Methods). We used the mean value of τ_2 as 10.5 ms and modelled the event amplitudes to represent the three peak mEPSC amplitudes seen in control neurons (Figs 7*E*

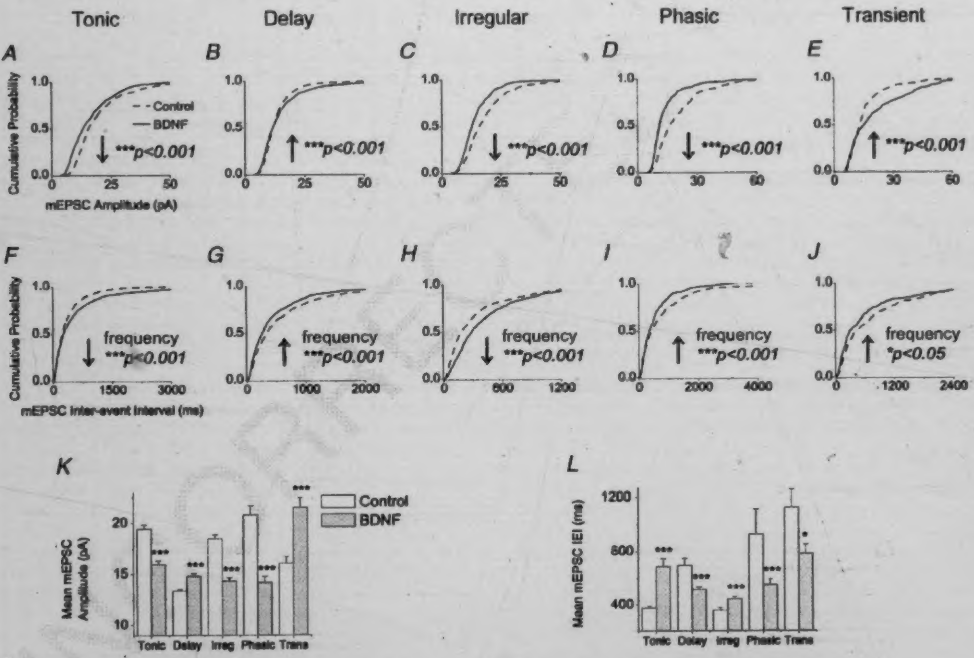

Figure 5. Effects of BDNF on amplitude and interevent interval of miniature excitatory postsynaptic currents (mEPSCs)

A–*E*, cumulative probability plots for mEPSC amplitude. The first 50 events following the 1st minute of recordings from each cell were pooled in order to construct cumulative distribution plots. *A*, tonic cells; 1100 events from control DMOTC slices, 877 events from BDNF-treated DMOTC slices. *B*, delay cells; 1074 events for controls, 1554 events for BDNF. *C*, irregular cells; 700 events for controls, 800 events for BDNF. *D*, phasic cells; 303 events for controls, 300 events for BDNF. *E*, transient cells; 300 events for controls, 300 events for BDNF. An equal number of BDNF-treated transient cells as controls were chosen at random to analyse mEPSC events. *P* values derived from the KS test indicated on graphs. *F*–*J*, cumulative probability plots for mEPSC interevent interval (IEI). *P* values derived from the KS test indicated on graphs. *K* and *L*, effects of BDNF on mean amplitude (*K*) and IEI (*L*) of mEPSC events. The same events used to construct cumulative probability plots were used, so the same *n* values apply. For Student's unpaired *t* test, $^*P < 0.05$, $^{***}P < 0.001$. Error bars indicate S.E.M.

© 2007 The Authors. Journal compilation © 2007 The Physiological Society

and *G*). We next modelled mEPSCs based on the three peak amplitudes for events in BDNF-treated neurons using the reduced mean value of 6.8 ms for τ_2. Lastly, we remodelled the control events using the τ_2 value of 6.8 ms from events acquired in BDNF. Since this increase in decay rate produced only slight reductions in the calculated amplitudes of peaks 1, 2 and 3, a decrease in the decay time constant τ_2 for mEPSC decay cannot account for the substantially reduced peak amplitudes seen in BDNF-treated cells; other pre- or postsynaptic mechanisms must contribute to this effect.

Further analysis of the mechanism of action of BDNF on delay cells

Unlike 'tonic' cells, the overall τ for recovery of mEPSC amplitude was unchanged in 'delay' cells (control $\tau = 10.73 \pm 0.55$ ms, $n = 766$; BDNF $\tau = 9.5 \pm 0.82$ ms, $n = 1177$; *t* test, $P > 0.2$). Superimposed events from a typical control and a typical BDNF-treated 'delay' neuron are shown in Fig. 8*A* and *B*. Figure 8*C* shows superimposed average data from these cells and scaled averages are presented in Fig. 8*D*.

As with 'tonic' cells, three populations of mEPSC amplitude were identified in control 'delay' cells by fitting Gaussian curves to binned histogram data. These appeared at 9.26 ± 1.51, 12.7 ± 9.0 and 19.0 ± 12.3 pA in control 'delay' cells (Fig. 8*E*) and at very similar amplitudes (8.14 ± 0.24, 12.5 ± 1.38 and 20.5 ± 4.3 pA) in BDNF-treated cells (Fig. 8*F*). Insets to Fig. 8*E* and *F* show optimized χ^2 values for using three peaks to fit the data. Figure 8*G* is a replot of the distributions for comparison between control and BDNF-treated cells. Since overall mEPSC amplitude is increased in 'delay' cells

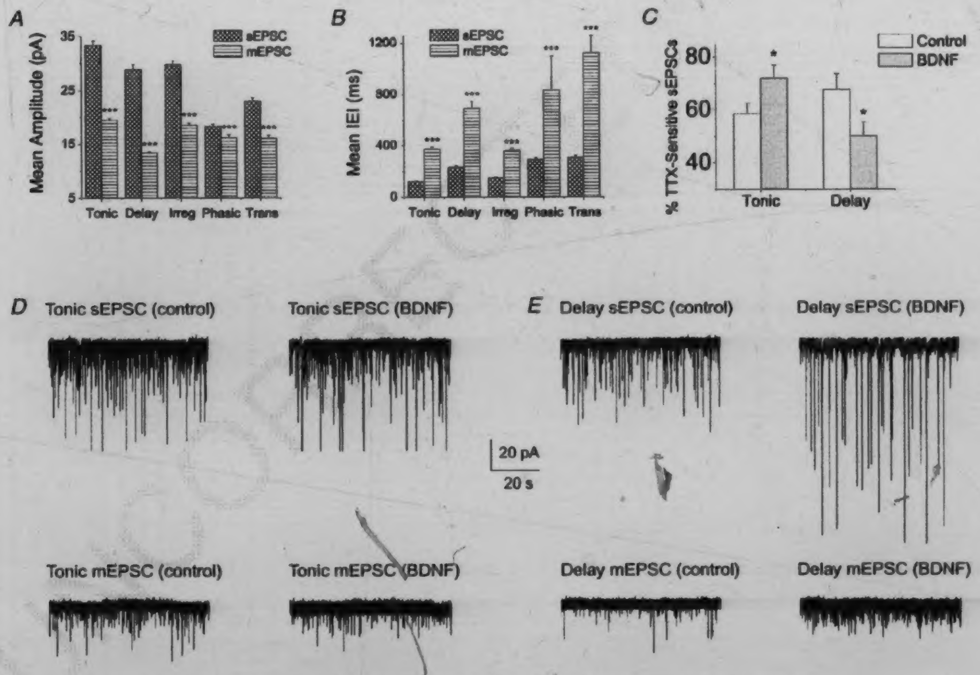

Figure 6. Effects of BDNF on the action potential-dependent (TTX-sensitive) sEPSCs population

A–B, comparison of sEPSCs to mEPSCs for controls. Comparison of mean amplitudes (*A*) and mean interevent intervals, IEI (*B*) are shown. Cross-hatched bars indicate values for sEPSCs and horizontal lined bars indicate values for mEPSCs. *C*, the percentage of TTX-sensitive sEPSCs was calculated as the number of mEPSCs subtracted from the total number of sEPSCs over the total sEPSCs for each cell. The mean percentages are shown for controls, white bars, and the BDNF-treated group, grey bars. For Student's unpaired *t* test, $^{*}P < 0.05$, $^{***}P < 0.001$. Error bars indicate S.E.M. *D* and *E*; sample recording traces from tonic (*D*) and delay (*F*) cells under control and long-term BDNF exposure conditions. Sample mEPSC recording traces were from the same cell represented in the above sample sEPSC recording trace.

© 2007 The Authors. Journal compilation © 2007 The Physiological Society

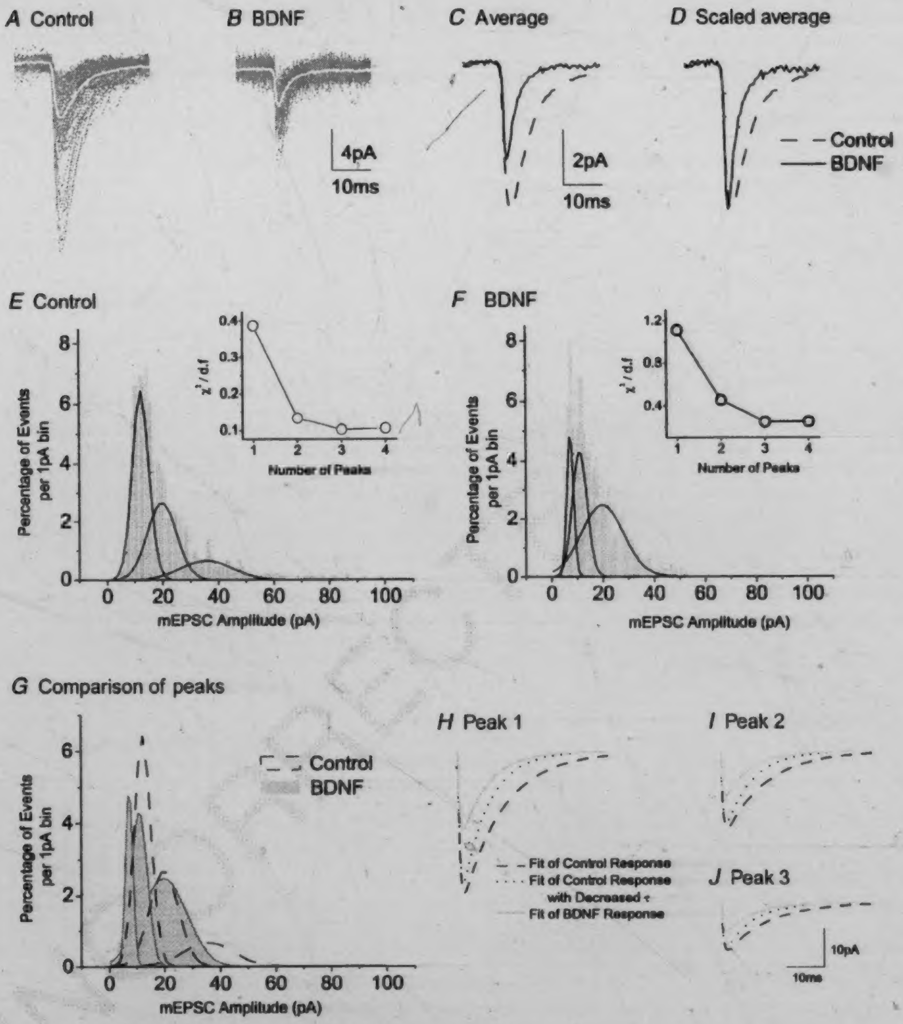

Figure 7. Analysis of the effects of BDNF on mEPSCs of tonic neurons

A, superimposed recordings of 3 min of mEPSC activity in a control tonic neuron; average of events presented as superimposed white trace. *B*, similar superimposed recordings from a tonic neuron in a BDNF-treated culture. C, averaged events from the neurons illustrated in *A* and *B*. *D*, averaged events normalized to control size. Note marked increased rate of decay of current. *E*, distribution histogram (1 pA bins) for amplitudes of 1100 mEPSCs from control tonic neurons. Fit of the data to three Gaussian distributions represented by continuous lines. *F*, similar histogram and fit to three Gaussian functions for 877 mEPSCs from BDNF-treated neurons. Insets in *E* and *F*, graphs to show effect of number of Gaussian fits (peaks) on the value of χ^2 divided by the number of degrees of freedom. G, superimposition of the three Gaussian peaks obtained in *E* with those obtained in *F*. *H–J*, modelled mEPSCs to represent the three peak Gaussian amplitudes obtained in E and *F*; dashed lines are for control events (from *E*), grey lines are for events in BDNF (from *F*) and dotted lines illustrate effect of a 35% reduction of τ_2 on the control events.

© 2007 The Authors. Journal compilation © 2007 The Physiological Society

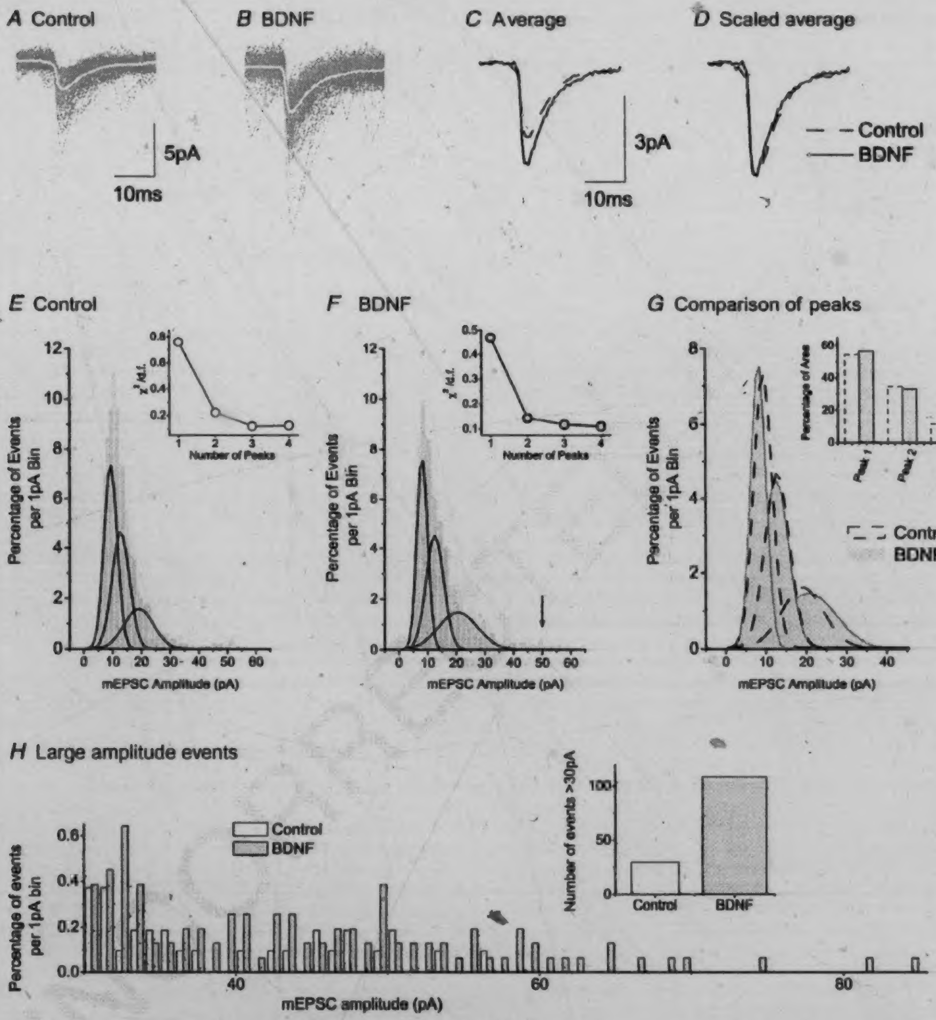

Figure 8. Analysis of the effects of BDNF on mEPSCs of delay neurons
A, superimposed recordings of 3 min of mEPSC activity in a control delay neuron; average of events presented as superimposed white trace. *B*, similar superimposed recordings from a delay neuron in a BDNF-treated culture. *C*, averaged events from the neurons illustrated in *A* and *B*. *D*, averaged events normalized to control size. Note no change in the rate of decay of current. *E*, distribution histogram (1 pA bins) for amplitudes of 1074 mEPSCs from control delay neurons. Fit of the data to three Gaussian distributions represented by black lines. *F*, similar histogram and fit to three Gaussian functions for 1554 mEPSCs from BDNF treated neurons; arrow points out small number of very large events that appear in BDNF. Insets in *E* and *F*, graphs to show effect of number of Gaussian fits (peaks) on the value of χ^2 divided by the number of degrees of freedom. *G*, superimposition of the three Gaussian peaks obtained in *E* with those obtained in *F*. Inset, comparison of area under curves for the three peaks (normalized to total area under peaks). *H*, data for control and BDNF mEPSCs > 30 pA replotted and compared on the same axes. Inset, number of mEPSC events larger than 30 pA.

© 2007 The Authors. Journal compilation © 2007 The Physiological Society

(Fig. 5*B*), we tested whether changes in the number of events contributing to each of the three distributions could explain this increase. This was done by measuring the area under the Gaussian curves in Fig. 8*G* and expressing the results as a percentage of the total area (Fig. 8*G* inset). Surprisingly, similar proportions of the total events made up each of the three peaks under control and BDNF-treated conditions. However, further inspection of the histogram data obtained from BDNF-treated cells revealed a new population of very large events (indicated by arrow in Fig. 8*F*). Whereas only 30 events in the control data had amplitudes > 30 pA, 106 events in data from BDNF-treated cells fell into this category. The appearance of this new population of large events is emphasized by the presentation of data for mEPSCs > 30 pA in Fig. 8*H* and *I*. Although few events appear in this group, those that do, have large amplitudes. Thus, the emergence of a new group of large mEPSC amplitude events in BDNF may have a noticeable effect on overall mEPSC amplitude.

Alterations in synaptic activity can affect spontaneous action potential activity of dorsal horn neurons

If BDNF-induced changes in spontaneous synaptic activity are responsible for the overall increased excitability of the dorsal horn that follows CCI (Dalal *et al.* 1999) one would also expect to observe changes in spontaneous action potential activity in neurotrophin-treated cultures.

As would predicted from the sEPSC data (Fig. 4*A* and *F*), long-term BDNF treatment significantly reduced the mean number of sEPSPs per minute in 'tonic' neurons (Fig. 9*A*, *t* test, $P < 0.05$). More importantly however, the mean number of spontaneous action potentials generated from these sEPSPs significantly decreased following BDNF treatment (Fig. 9*B*, *t* test, $P < 0.01$). Therefore, long-term BDNF treatment significantly reduced the spontaneous firing of 'tonic' neurons.

There was also the anticipated significant increase in the number of sEPSPs per minute in 'delay' neurons following BDNF treatment (Fig. 9*C*, *t* test, $P < 0.05$). The mean number of spontaneous action potentials observed during the recording period also increased but did not reach statistical significance (Fig. 9*D*, *t* test, $P > 0.1$). However, there was a change in the pattern of spontaneous action potential activity following BDNF treatment. A typical sEPSP triggering a single action potential in a control 'delay' neuron is illustrated in Fig. 9*E*. However in BDNF-treated cultures, sEPSPs often produced bursts of three to four action potentials in 'delay' neurons (Fig. 9*F*). There was a 15% increase in the number of 'delay' neurons that displayed such bursts following long-term BDNF exposure (Fig. 9*G*). A low percentage of control 'tonic' neurons displayed bursting behaviour but the percentage did not change following BDNF treatment. Therefore, long-term BDNF treatment selectively increased the spontaneous bursting activity of 'delay' neurons.

Enhanced overall excitability of BDNF-treated DMOTC slices

BDNF-induced increased burst firing of 'delay' cells and reduced firing of 'tonic' cells would only be expected to increase overall dorsal horn network excitability if 'delay' cells are excitatory and 'tonic' cells are inhibitory. Although this idea is generally well accepted, we do not know whether these effects, seen in 60% of the neuronal population, are sufficient to generate a global increase in dorsal horn excitability. BDNF also has effects on 'phasic', 'transient' and 'irregular' cells, all of which have undefined function. It is possible therefore that the changes in tonic and delay cells described above are insufficient to produce an overall excitatory effect. We therefore used confocal Ca^{2+} imaging techniques (Ruangkittisakul *et al.* 2006) to monitor the responses of both control and BDNF-treated DMOTC slices to depolarizing stimuli of varying strength (20, 35, or 50 mm K^+ solution for 90 s). If overall network excitability is increased, we predicted that depolarizing stimuli should produce larger Ca^{2+} signals.

With identical stimuli, networks of dorsal horn neurons in BDNF-treated DMOTC slices exhibited a larger increase in Fluo-4 fluorescence intensity compared to cells in the same region in control untreated DMOTC slices. This is clear from the images and sample traces of Fluo-4 fluorescence intensity signal for control (Fig. 10*A* and *C*) and BDNF-treated cells (Fig. 10*B* and *D*). Quantification of the peak amplitude revealed a significant increase in the Ca^{2+} response in the BDNF-treated group at all K^+ concentrations tested (Fig. 10*E*, *t* test, $P < 0.001$). As well, the area under the Ca^{2+} intensity signal was significantly larger for the BDNF-treated DMOTC slices for all challenges (Fig. 10*F*, *t* test, $P < 0.05$).

During the course of Ca^{2+} imaging experiments, synchronous oscillations in the Ca^{2+} signal were observed in BDNF-treated slices (Fig. 10*H*). These synchronous oscillations, which were not usually present in control slices (Fig. 10*G*), were observed across the entire dorsal region of the slice at a frequency of 0.05–0.1 Hz. All 7/7 BDNF-treated DMOTC slices tested, compared to only 2/9 control DMOTC slices, displayed this phenomenon. Because these effects were blocked by TTX (1 μm) and glutamatergic receptor blockers kyneurinic acid (1 mm) or NBQX (10 μm) (data not shown), they ate likely to represent oscillations in neuronal $[Ca^{2+}]_i$ rather than glial $[Ca^{2+}]_i$.

© 2007 The Authors. Journal compilation © 2007 The Physiological Society

Discussion

The main findings of this study are as follows. (1) BDNF produces a pattern of neuron type-specific changes that resembled those seen with CCI *in vivo*. This suggests that the actions of BDNF in DMOTCs are not a general neurotrophic effect but are instead more relevant to its putative role as a harbinger of neuropathic pain (Coull *et al.* 2005; Yajima *et al.* 2005). (2) BDNF increases excitatory synaptic drive to most neuron types except putative inhibitory 'tonic' cells, where synaptic drive decreases. (3) Effects of BDNF on putative excitatory 'delay' cells may be exclusively presynaptic whereas both pre- and post-components are involved in its action on putative inhibitory 'tonic' neurons. (4) BDNF does not increase the sensitivity of 'delay' cells to glutamate. (5) BDNF-induced changes in synaptic drive to discrete neuronal populations contribute to an overall increase in dorsal horn excitability.

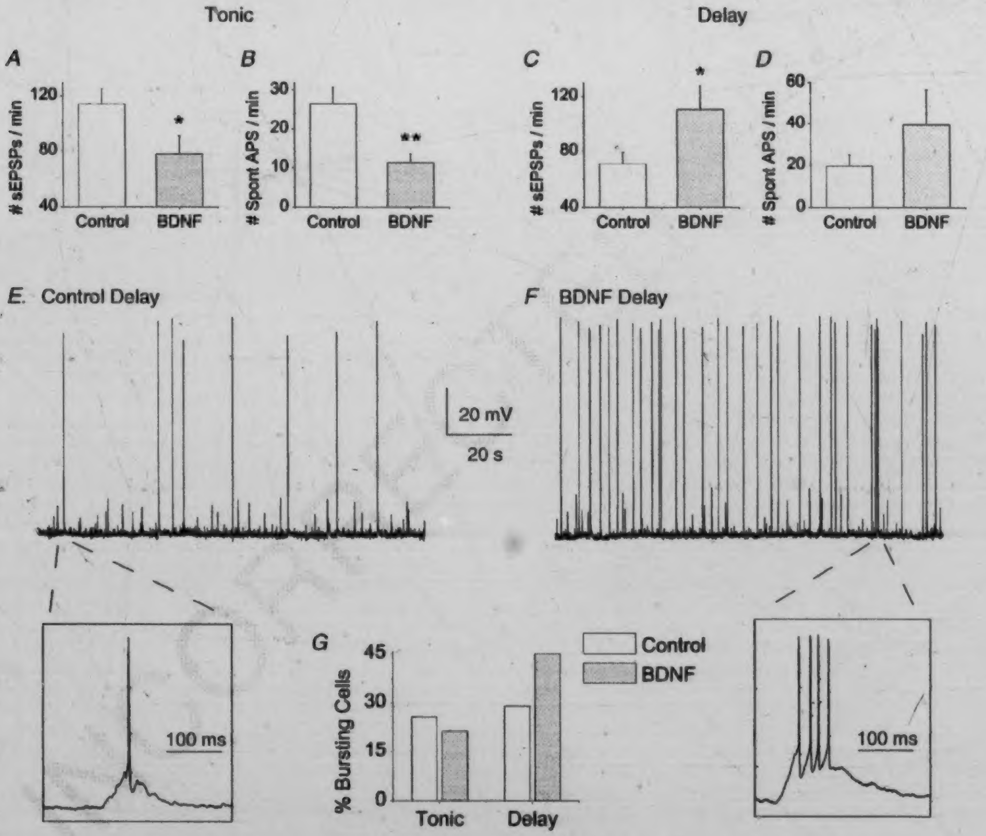

Figure 9. Effect of BDNF on spontaneous activity of tonic and delay neurons
Spontaneous activity was measured as the number of depolarizations or action potential discharges at resting membrane potential in current-clamp mode. The mean number of spontaneous excitatory postsynaptic potentials (sEPSPs) and spontaneous action potentials generated from sEPSPs are shown for tonic (*A* and *B*, respectively) and delay neurons (C and *D*, respectively). For tonic neurons, $n = 36$ for controls, $n = 15$ for BDNF. For delay neurons, $n = 35$ for controls, $n = 27$ for BDNF. *E and F*, sample 2 min recording of spontaneous activity from a control (*E*) and BDNF-treated (*F*) delay neuron. Lower panels show on an expanded time scale a large sEPSP generating an action potential. Note under long-term BDNF treatment conditions, the probability of a large sEPSP generating a burst of action potentials is greater. G, percentage of cells in the tonic and delay group firing a burst of action potentials. White bars indicate controls and grey bars indicate BDNF-treated neurons.

© 2007 The Authors. Journal compilation © 2007 The Physiological Society

To the best of our knowledge, all studies of injury-induced increases in spinal BDNF levels have relied on immunological or immunohistochemical techniques (Cho *et al.* 1997; Cho *et al.* 1998; Ha *et al.* 2001) and this has precluded measurements of exact neurotrophin concentration. The nature of our study dictated the use of a relatively high concentration of BDNF to assure that a robust effect would be observed. Extensive data analysis from large numbers of neurons was required to document the actions of BDNF. Had a lower concentration been used, considerable effort may have been wasted in attempting to statistically distinguish some potentially small effects. Also, because it was not feasible to routinely maintain sterile viable cultures for more than 40 days, the age of neurons used in the BDNF experiments only approximates that of the *in vivo* neurones used in the CCI study (Fig. 1). Neuronal age in the *in vivo* studies is dictated by the need to use animals > 20 days old to produce behavioural manifestations of neuropathic pain (Balasubramanyan *et al.* 2006). Although there are inevitable physiological differences between age-matched substantia gelatinosa neurons *in vivo* and in DMOTCs, these are surprisingly minor (Lu *et al.* 2006). We therefore contend that our comparison of CCI *in vivo* and BDNF's effects in DMOTCs is the best feasible methodology given the constraints imposed by the two experimental systems.

Cell type-specific effects of BDNF on excitatory synaptic transmission

Because input resistance, rheobase and firing latency were unchanged in most neuron types (Fig. 3 and Table 1), alterations in the intrinsic membrane excitability of individual neurons may play only a minor role in the increase in overall excitability of the dorsal horn produced by BDNF. An exception may be the increased excitability of 'delay' neurons (Fig. 3*B*) as these tended to display bursts of action potentials in response to spontaneously occurring EPSPs (Fig. 9*D*–*G*).

Thus, the actions of BDNF are dominated by its effects on synaptic activity (Figs 4–9). Spontaneous excitatory synaptic activity increased in all neuron types except 'tonic' cells where a decrease was observed (Fig. 4*A*, *F*, *K* and *L*). Interestingly, similar changes in excitatory synaptic activity were observed following sciatic nerve CCI (Balasubramanyan *et al.* 2006). Table 2 compares the changes seen in five defined types of substantia gelatinosa neurons in CCI with those seen with long-term BDNF exposure. The degree of similarity, which is especially clear for 'tonic', 'delay' and 'transient' neurons and for sEPSC frequency in all cell types, supports the role of BDNF in instigating changes in dorsal horn neurons which can lead to neuropathic pain.

It could of course be argued that any potentially traumatic manipulation of the cultures would produce a similar pattern of changes, so that the similarity between the actions of CCI and BDNF is of little significance. However, in other experiments we have maintained DMOTC in the presence of interleukin-1β. Although it has been suggested that this cytokine may be responsible for the development of various types of chronic inflammatory pain (Watkins *et al.* 1995; Ledeboer *et al.* 2005), it is probably not responsible for the allodynia associated with neuropathic pain (Ledeboer *et al.* 2006). Consistent with this, we found that the pattern of changes produced by IL-1β, was quite dissimilar to that produced by BDNF and CCI (Lu *et al.* 2005). This underlines the significance of the similarity between the actions of BDNF and CCI which produces neuropathic pain.

Effect of BDNF on 'tonic' neurons

Several lines of evidence are consistent with the possibility that 'tonic' neurons are inhibitory. Specifically, 'tonic' neurons often exhibit the morphology of dorsal horn islet cells (Grudt & Perl, 2002), and many islet cells express markers for GABAergic neurons (Todd & McKenzie, 1989; Heinke *et al.* 2004). Moreover, simultaneous paired whole-cell recordings of Lamina II neurons have revealed the generation of inhibitory postsynaptic potentials following stimulation of 'tonic' neurons (Lu & Perl, 2003).

Our finding that BDNF reduced excitatory synaptic transmission to 'tonic' neurons would predict decreased release of inhibitory neurotransmitters and a reduction in inhibitory tone within the dorsal horn network. Loss of inhibition has been implicated in the generation of pain-like behaviours in nerve injury models of neuropathic pain (Sivilotti & Woolf, 1994; Moore *et al.* 2002; Baba *et al.* 2003) and as shown in Table 2, a reduction in synaptic drive to 'tonic' neurons also occurs following CCI (Balasubramanyan *et al.* 2006).

The decrease in sEPSC and mEPSC frequency of 'tonic' neurons implicates a presynaptic site of action for BDNF. A loss of vesicular glutamate transporter 1 (VGLUT1), which has been observed following nerve injury (Oliveira *et al.* 2003; Alvarez *et al.* 2004), could account for the observed decrease in sEPSC and mEPSC frequency, but other mechanisms such as loss of presynaptic release sites may also be involved (Bailey *et al.* 2006). Reduced sEPSC frequency is unlikely to reflect a decrease in the frequency of presynaptic action potentials because a greater percentage of TTX-sensitive spontaneous events appeared in 'tonic' neurons after BDNF treatment (Fig. 9*C*).

Because the decrease in the time constant for mEPSC decay (τ_2) has little effect on event amplitude (Fig. 7*H*–*J*), other pre- or postsynaptic mechanisms must be invoked to explain the BDNF-induced in mEPSC amplitude. One

© 2007 The Authors. Journal compilation © 2007 The Physiological Society

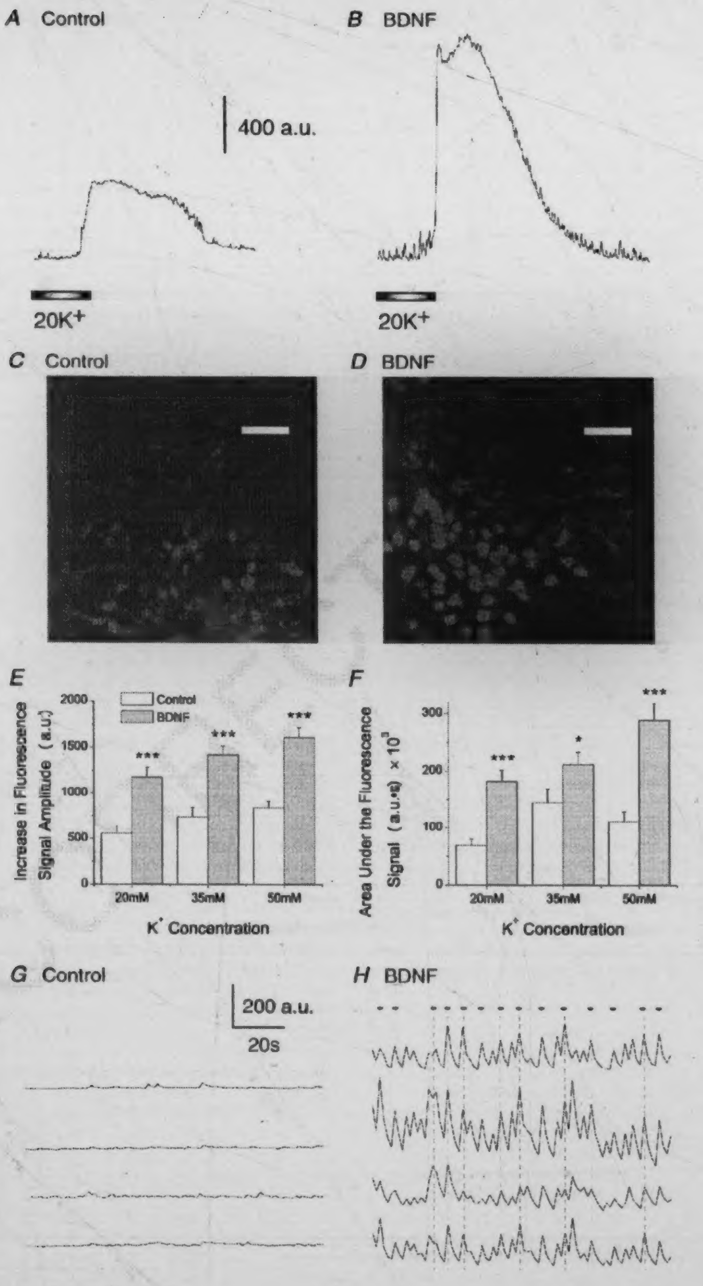

© 2007 The Authors. Journal compilation © 2007 The Physiological Society

possibility is dendritic shunting, as this would reduce the amplitude as well as increasing the rate of decay of mEPSCs. This could occur, for example, as a result of BDNF-induced increases in dendritic K^+ conductance(s).

Thus, effects of BDNF on mEPSC in 'tonic' cells include a presynaptic component, which accounts for their decrease in frequency, a postsynaptic component, which accounts for their increased rate of decay, and a third component that may be either pre- or postsynaptic, which accounts for much of their reduction in amplitude.

Effect of BDNF on 'delay' neurons

Less than 1% of GAD-positive neurons in the substantia gelatinosa display a 'delay' firing pattern (Hantman *et al.* 2004; Heinke *et al.* 2004; Dougherty *et al.* 2005), and since simultaneous paired recordings show the production of an excitatory postsynaptic potential following stimulation of 'delay' neurons (Lu & Perl, 2005), these are likely to represent a population of excitatory neurons.

In contrast to 'tonic' neurons, long-term BDNF exposure produced a significant increase in excitatory synaptic drive to 'delay' neurons. As illustrated in Table 2, a similar effect was seen following CCI (Balasubramanyan *et al.* 2006). Lu & Perl (2005) have suggested Lamina II 'delay' neurons form excitatory connections with Lamina I neurons, which may include projection neurons that signal to higher pain centres. Therefore, enhanced activation of 'delay' neurons following BDNF treatment could lead to increased transmission of nociceptive information at the spinal level.

The increased frequency of sEPSCs in 'delay' neurons following BDNF treatment (Fig. 5*G*) implies a presynaptic site of action. However, the proportion of TTX-sensitive sEPSC events decreased (Fig. 6*C*), indicating a smaller proportion of spontaneous synaptic events were action potential dependent. This argues against an increase in presynaptic action potential activity as a mechanism of BDNF action. Noxious stimulation induces phosphorylation of the GluR1 subunit of AMPA receptors and subsequently enhances recruitment and surface expression of functional AMPA receptors (Nagy *et al.* 2004; Galan *et al.* 2004). Interestingly, BDNF has also been shown to enhance phosphorylation of the GluR1 subunit (Wu *et al.* 2004). GluR1 is strongly associated with nociceptive primary afferents and its distribution in the dorsal horn is restricted to Lamina II (Lee *et al.* 2002; Nagy *et al.* 2004). Possible recruitment of Ca^{2+}-permeable AMPA receptors presynaptically could increase intracellular Ca^{2+} levels in the terminal and thereby enhance action potential-independent glutamate release. This could explain action of BDNF on mEPSC amplitude and frequency. If expression of GluR1 is specific to primary afferent terminals that contact 'delay' neurons, this could represent a possible mechanism by which BDNF can differentially affect one neuron type in the dorsal horn and not another.

Increased insertion of postsynaptic AMPA receptors is unlikely to occur as the mean amplitudes of the three populations of mEPSCs in delay neurons were unchanged (Fig. 8*E*–*G*) and a new population of events appeared in BDNF-treated neurons. These large events may reflect coincident release of two or more vesicles from terminals contacting 'delay' cells. Mechanistically, this could reflect increased levels of ambient Ca^{2+} in the presynaptic terminal as described above, or perhaps BDNF-induced sprouting of presynaptic terminals such that coincidental release of vesicles occurs more frequently.

These observations are important as they imply that BDNF treatment does not change the postsynaptic sensitivity of 'delay' cells to glutamate (Fig. 8*G*). This further suggests that its actions do not invoke an LTP-type phenomenon involving the insertion of new postsynaptic AMPA receptors (Hayashi *et al.* 2000). We therefore attribute all actions of BDNF on synaptic activity in 'delay' cells to presynaptic mechanisms.

Effect of BDNF on 'irregular', 'phasic' and 'transient' neurons

There is currently no consensus as to the transmitter phenotype of neurons that exhibit an 'irregular', 'phasic' or 'transient' firing pattern. Rather, evidence has been found to support these neurons as both excitatory or inhibitory

Figure 10. Enhanced K^+-induced Ca^{2+} rise in BDNF-treated DMOTC slices
A–*B*, sample fluorescent Ca^{2+} intensity traces during a 90 s, 20 mM K^+ challenge for a cell in a control DMOTC slice (*A*), and a BDNF-treated DMOTC slice (*B*). *C* and *D*, sample fluorescence images (512 × 512 pixels) of the dorsal region of a control slice (*C*) and a BDNF-treated DMOTC slice (*D*), loaded with Fluo-4 AM, during a 20 mM K^+ solution challenge. White scale bar is 50 μm. *E*, comparison of Ca^{2+} fluorescence signal amplitude over a range of high K^+ solutions tested. Amplitude of the signal was measured from baseline to peak of each trace recorded from cells in control and BDNF-treated DMOTC slices ($n = 30$ cells for control, $n = 41$ cells for BDNF). Scaling is in arbitrary units (a.u.) *F*, comparison of area under the Ca^{2+} fluorescence signal traces over a range of high K^+ solutions in control and BDNF-treated DMOTC slices. At all concentrations tested, both area and amplitude of the Ca^{2+} signal were significantly larger in BDNF-treated cells (*t* test; $^*P < 0.05$; $^{***}P < 0.001$). Error bars indicate S.E.M. *G* and *H*, sample baseline recordings from four cells in the same control DMOTC slice (*G*) and a BDNF-treated DMOTC slice (*H*). Dots with dashed lines indicate synchronous oscillations in Ca^{2+}.

© 2007 The Authors. Journal compilation © 2007 The Physiological Society

(Hantman *et al.* 2004; Heinke *et al.* 2004; Dougherty *et al.* 2005). Regardless, the magnitude and frequency of spontaneous excitatory neurotransmission to all three neuron types increased significantly following BDNF treatment (Fig. 5*C–E* and *H–J*). Because of the ambiguity of these neuronal populations, it is unclear if an increase in the excitatory drive to any of them would enhance excitation in the dorsal horn. Nevertheless, it would appear that the action potential-dependent population of synaptic events mainly contributed to the increase in synaptic events for 'irregular' neurons. This implicates BDNF in increasing the activity of presynaptic excitatory neurons, either primary afferents or excitatory spinal interneurons such as 'delay' neurons.

Several underlying mechanisms may underlie the differential actions of BDNF on the various cell types in dorsal horn. First, as already mentioned, GluR1 receptors which are phosphorylated following BDNF exposure (Wu *et al.* 2002) are strongly associated with nociceptive primary afferents (Lee *et al.* 2002). This implies that BDNF may not affect terminals that do not express these receptors. Second, BDNF exerts its actions both by TrkB and via the p75 neurotrophin receptor. Whereas TrkB activation generally produces positive actions on neuronal growth and sprouting, activation of p75 can sometimes produce effects that are deleterious and can even include apoptosis (Huang & Reichardt, 2003). Thus, in order to determine how the differential effects of BDNF on various neurons terminals and cell bodies in the dorsal horn are generated, it will be necessary to determine which AMPA receptor subtypes and which BDNF receptors are expressed on the cell bodies and afferent terminals of various types of electrophysiologically defined dorsal horn neuron. Such information is not yet available.

Long-term BDNF exposure increases overall dorsal horn excitability

The Ca^{2+} responses to high K^{+} stimulation were significantly larger in BDNF-treated DMOTC slices than in age-matched controls (Fig. 10). Therefore, the cellular changes produced by BDNF contributed to an overall increase in the excitability of the dorsal horn.

Even though the [Ca^{2+}]$_i$ was not determined, the relative increase in Fluo-4 fluorescence signal intensity still provided a good measure of a slice's excitability since Fluo-4 fluorescence intensity correlates well with Ca^{2+} concentration at physiological ranges (Gee *et al.* 2000). Also, it is unlikely that the dye saturated since there was a progressive increase in the Ca^{2+} signal amplitude at higher K^{+} concentrations.

Although other studies have examined the acute effects of BDNF on dorsal horn neurons (Kerr *et al.* 1999; Garraway *et al.* 2003; Slack *et al.* 2004), we are the first to show that long-term, 5–6 days exposure to BDNF, which resembles the time course of nerve injury-induced BDNF elevation (Cho *et al.* 1997; Zhou *et al.* 1999; Dougherty *et al.* 2000; Fukuoka *et al.* 2001), can induce persistent, and possibly permanent, changes to the dorsal horn network. BDNF is also well known to attenuate GABAergic transmission in dorsal horn (Coull *et al.* 2005) and such effects could contribute to increased excitability seen in our experiments. The long-term effects of BDNF on spinal GABAergic function in 'tonic', 'delay', 'phasic', 'transient' and 'irregular' cells are currently being investigated.

The phenomenon of rhythmic Ca^{2+} oscillations has been reported in the spinal cord following various pharmacological manipulations (Ruscheweyh & Sandkuhler, 2005) or during development (Fabbro *et al.* 2007). Our observation that the probability of synchronous Ca^{2+} oscillations increased notably in BDNF-treated DMOTC slices shows that they may play a role in the pathology of chronic pain in adults. Similar oscillations have also been described in hippocampal slices under epileptiform conditions (Kovacs *et al.* 2005) suggesting they may be indicative of hyperexcitable networks.

Conclusions

BDNF induced significant changes in excitatory neurotransmission that reflected both pre- and postsynaptic mechanisms but there was no obvious increase in sensitivity of postsynaptic neurons to glutamate. The pattern of changes was specific to different neuronal populations and was not uniform across the entire dorsal horn. This distinct pattern of changes contributes to an increase in overall excitability in BDNF-treated DMOTC slices. Moreover, the similarity between this pattern of changes and that seen in CCI are consistent with a role for BDNF in the induction of neuropathic pain.

References

Alvarez FJ, Villalba RM, Zerda R & Schneider SP (2004). Vesicular glutamate transporters in the spinal cord, with special reference to sensory primary afferent synapses. *J Comp Neurol* **472**, 257–280.

Apfel SC, Wright DE, Wiideman AM, Dormia C, Snider WD & Kessler JA (1996). Nerve growth factor regulates the expression of brain-derived neurotrophic factor mRNA in the peripheral nervous system. *Mol Cell Neurosci* **7**, 134–142.

Baba H, Doubell TP & Woolf CJ (1999). Peripheral inflammation facilitates Aβ fiber-mediated synaptic input to the substantia gelatinosa of the adult rat spinal cord. *J Neurosci* **19**, 859–867.

© 2007 The Authors. Journal compilation © 2007 The Physiological Society

Baba H, Ji RR, Kohno T, Moore KA, Ataka T, Wakai A, Okamoto M & Woolf CJ (2003). Removal of GABAergic inhibition facilitates polysynaptic A fiber-mediated excitatory transmission to the superficial spinal dorsal horn. *Mol Cell Neurosci* **24**, 818–830.

Bailey AL & Ribeiro-da-Silva A (2006). Transient loss of terminals from non-peptidergic nociceptive fibers in the substantia gelatinosa of spinal cord following chronic constriction injury of the sciatic nerve. *Neuroscience* **138**, 675–690.

Balasubramanyan S, Stemkowski PL, Stebbing MJ & Smith PA (2006). Sciatic chronic constriction injury produces cell-type-specific changes in the electrophysiological properties of rat substantia gelatinosa neurons. *J Neurophysiol* **96**, 579–590.

Chen SR & Pan HL (2002). Hypersensitivity of spinothalamic tract neurons associated with diabetic neuropathic pain in rats. *J Neurophysiol* **87**, 2726–2733.

Cho HJ, Kim JK, Park HC, Kim JK, Kim DS, Ha SO & Hong HS (1998). Changes in brain-derived neurotrophic factor immunoreactivity in rat dorsal root ganglia, spinal cord, and gracile nuclei following cut or crush injuries. *Exp Neurol* **154**, 224–230.

Cho HJ, Kim JK, Zhou XF & Rush RA (1997). Increased brain-derived neurotrophic factor immunoreactivity in rat dorsal root ganglia and spinal cord following peripheral inflammation. *Brain Res* **764**, 269–272.

Colomo F & Erulkar SD (1968). Miniature synaptic potentials at frog spinal neurones in the presence of tertodotoxin. *J Physiol* **199**, 205–221.

Coull JA, Beggs S, Boudreau D, Boivin D, Tsuda M, Inoue K, Gravel C, Salter MW & De Koninck Y (2005). BDNF from microglia causes the shift in neuronal anion gradient underlying neuropathic pain. *Nature* **438**, 1017–1021.

Dalal A, Tata M, Allegre G, Gekiere F, Bons N & Albe-Fessard D (1999). Spontaneous activity of rat dorsal horn cells in spinal segments of sciatic projection following transection of sciatic nerve or of corresponding dorsal roots. *Neuroscience* **94**, 217–228.

Dougherty KD, Dreyfus CF & Black IB (2000). Brain-derived neurotrophic factor in astrocytes, oligodendrocytes, and microglia/macrophages after spinal cord injury. *Neurobiol Dis* **7**, 574–585.

Dougherty KJ, Sawchuk MA & Hochman S (2005). Properties of mouse spinal lamina I GABAergic interneurons. *J Neurophysiol* **94**, 3221–3227.

Fabbro A, Pastore B, Nistri A & Ballerini L (2007). Activity-independent intracellular Ca^{2+} oscillations are spontaneously generated by ventral spinal neurons during development in vitro. *Cell Calcium* **41**, 317–329.

Fukuoka T, Kondo E, Dai Y, Hashimoto N & Noguchi K (2001). Brain-derived neurotrophic factor increases in the uninjured dorsal root ganglion neurons in selective spinal nerve ligation model. *J Neurosci* **21**, 4891–4900.

Galan A, Laird JM & Cervero F (2004). In vivo recruitment by painful stimuli of AMPA receptor subunits to the plasma membrane of spinal cord neurons. *Pain* **112**, 315–323.

Garraway SM, Petruska JC & Mendell LM (2003). BDNF sensitizes the response of lamina II neurons to high threshold primary afferent inputs. *Eur J Neurosci* **18**, 2467–2476.

Gee KR, Brown KA, Chen WN, Bishop-Stewart J, Gray D & Johnson I (2000). Chemical and physiological characterization of fluo-4 Ca^{2+}-indicator dyes. *Cell Calcium* **27**, 97–106.

Grudt TJ & Perl ER (2002). Correlations between neuronal morphology and electrophysiological features in the rodent superficial dorsal horn. *J Physiol* **540**, 189–207.

Ha SO, Kim JK, Hong HS, Kim DS & Cho HJ (2001). Expression of brain-derived neurotrophic factor in rat dorsal root ganglia, spinal cord and gracile nuclei in experimental models of neuropathic pain. *Neuroscience* **107**, 301–309.

Hains BC & Waxman SG (2006). Activated microglia contribute to the maintenance of chronic pain after spinal cord injury. *J Neurosci* **26**, 4308–4317.

Hantman AW, van den Pol AN & Perl ER (2004). Morphological and physiological features of a set of spinal substantia gelatinosa neurons defined by green fluorescent protein expression. *J Neurosci* **24**, 836–842.

Hayashi Y, Shi SH, Esteban JA, Piccini A, Poncer JC & Malinow R (2000). Driving AMPA receptors into synapses by LTP and CaMKII: requirement for GluR1 and PDZ domain interaction. *Science* **287**, 2262–2267.

Heinke B, Ruscheweyh R, Forsthuber L, Wunderbaldinger G & Sandkuhler J (2004). Physiological, neurochemical and morphological properties of a subgroup of GABAergic spinal lamina II neurones identified by expression of green fluorescent protein in mice. *J Physiol* **560**, 249–266.

Huang EJ & Reichardt LF (2003). Trk receptors: roles in neuronal signal transduction. *Annu Rev Biochem* **72**, 609–642.

Kerr BJ, Bradbury EJ, Bennett DL, Trivedi PM, Dassan P, French J, Shelton DB, McMahon SB & Thompson SW (1999). Brain-derived neurotrophic factor modulates nociceptive sensory inputs and NMDA-evoked responses in the rat spinal cord. *J Neurosci* **19**, 5138–5148.

Kim SH & Chung JM (1992). An experimental model for peripheral neuropathy produced by segmental spinal nerve ligation in the rat. *Pain* **50**, 355–363.

Kim KJ, Yoon YW & Chung JM (1997). Comparison of three rodent neuropathic pain models. *Exp Brain Res* **113**, 200–206.

Kohno T, Moore KA, Baba H & Woolf CJ (2003). Peripheral nerve injury alters excitatory synaptic transmission in lamina II of the rat dorsal horn. *J Physiol* **548**, 131–138.

Kovacs R, Kardos J, Heinemann U & Kann O (2005). Mitochondrial calcium ion and membrane potential transients follow the pattern of epileptiform discharges in hippocampal slice cultures. *J Neurosci* **25**, 4260–4269.

Laird JM & Bennett GJ (1993). An electrophysiological study of dorsal horn neurons in the spinal cord of rats with an experimental peripheral neuropathy. *J Neurophysiol* **69**, 2072–2085.

Ledeboer A, Mahoney JH, Milligan ED, Martin D, Maier SF & Watkins LR (2006). Spinal cord glia and interleukin-1 do not appear to mediate persistent allodynia induced by intramuscular acidic saline in rats. *J Pain* **7**, 757–767.

Ledeboer A, Sloane EM, Milligan ED, Frank MG, Mahony JH, Maier SF & Watkins LR (2005). Minocycline attenuates mechanical allodynia and proinflammatory cytokine expression in rat models of pain facilitation. *Pain* **115**, 71–83.

© 2007 The Authors. Journal compilation © 2007 The Physiological Society

Lee CJ, Bardoni R, Tong CK, Engelman HS, Joseph DJ, Magherini PC & MacDermott AB (2002). Functional expression of AMPA receptors on central terminals of rat dorsal root ganglion neurons and presynaptic inhibition of glutamate release. *Neuron* **35**, 135–146.

Lu VB, Chee MJS, Gustafson SL, Colmers WF & Smith PA (2005). Concentration-dependent effects of long-term interleukin-1 treatment on spinal dorsal horn neurons in organotypic slice cultures. *2005 Abstract Viewer/Itinerary Planner*, Program No. 292.3. Society for Neuroscience, Washington, DC.

Lu VB, Colmers WF, Dryden WF & Smith PA (2004). Brain – derived neurotrophic factor alters the synaptic activity of dorsal horn neurons in long-term organotypic spinal cord slice cultures. *2004 Abstract Viewer/Itinerary Planner*, Program No. 289,15. Society for Neuroscience, Washington, DC.

Lu VB, Moran TD, Balasubramanyan S, Alier KA, Dryden WF, Colmers WF & Smith PA (2006). Substantia gelatinosa neurons in defined-medium organotypic slice culture are similar to those in acute slices from young adult rats. *Pain* **121**, 261–275.

Lu Y & Perl ER (2003). A specific inhibitory pathway between substantia gelatinosa neurons receiving direct C-fiber input. *J Neurosci* **23**, 8752–8758.

Lu Y & Perl ER (2005). Modular organization of excitatory circuits between neurons of the spinal superficial dorsal horn (laminae I and II). *J Neurosci* **25**, 3900–3907.

Matayoshi S, Jiang N, Katafuchi T, Koga K, Furue H, Yasaka T, Nakatsuka T, Zhou XF, Kawasaki Y, Tanaka N & Yoshimura M (2005). Actions of brain-derived neurotrophic factor on spinal nociceptive transmission during inflammation in the rat. *J Physiol* **569**, 685–695.

Michael GJ, Averill S, Shortland PJ, Yan Q & Priestley JV (1999). Axotomy results in major changes in BDNF expression by dorsal root ganglion cells: BDNF expression in large trkB and trkC cells, in pericellular baskets, and in projections to deep dorsal horn and dorsal column nuclei. *Eur J Neurosci* **11**, 3539–3551.

Miletic G & Miletic V (2002). Increases in the concentration of brain derived neurotrophic factor in the lumbar spinal dorsal horn are associated with pain behavior following chronic constriction injury in rats. *Neurosci Lett* **319**, 137–140.

Moore KA, Kohno T, Karchewski LA, Scholz J, Baba H & Woolf CJ (2002). Partial peripheral nerve injury promotes a selective loss of GABAergic inhibition in the superficial dorsal horn of the spinal cord. *J Neurosci* **22**, 6724–6731.

Moran TD, Colmers WF & Smith PA (2004). Opioid-like actions of neuropeptide Y in rat substantia gelatinosa: Y1 suppression of inhibition and Y2 suppression of excitation. *J Neurophysiol* **92**, 3266–3275.

Nagy GG, Al Ayyan M, Andrew D, Fukaya M, Watanabe M & Todd AJ (2004). Widespread expression of the AMPA receptor GluR2 subunit at glutamatergic synapses in the rat spinal cord and phosphorylation of GluR1 in response to noxious stimulation revealed with an antigen-unmasking method. *J Neurosci* **24**, 5766–5777.

Oliveira AL, Hydling F, Olsson E, Shi T, Edwards RH, Fujiyama F, Kaneko T, Hokfelt T, Cullheim S & Meister B (2003). Cellular localization of three vesicular glutamate transporter mRNAs and proteins in rat spinal cord and dorsal root ganglia. *Synapse* **50**, 117–129.

Ruangkittisakul A, Schwarzacher SW, Secchia L, Poon BY, Ma Y, Funk GD & Ballanyi K (2006). High sensitivity to neuromodulator-activated signaling pathways at physiological $[\text{K}^+]$ of confocally imaged respiratory center neurons in on-line-calibrated newborn rat brainstem slices. *J Neurosci* **26**, 11870–11880.

Ruscheweyh R & Sandkuhler J (2005). Long-range oscillatory Ca^{2+} waves in rat spinal dorsal horn. *Eur J Neurosci* **22**, 1967–1976.

Sivilotti L & Woolf CJ (1994). The contribution of GABA_A and glycine receptors to central sensitization: disinhibition and touch-evoked allodynia in the spinal cord. *J Neurophysiol* **72**, 169–179.

Slack SE, Pezet S, McMahon SB, Thompson SW & Malcangio M (2004). Brain-derived neurotrophic factor induces NMDA receptor subunit one phosphorylation via ERK and PKC in the rat spinal cord. *Eur J Neurosci* **20**, 1769–1778.

Smith PA, Lu VB & Balasubramanyan S (2005). Chronic constriction injury and brain-derived neurotrophic factor (BDNF) generate similar 'pain footprints' in dorsal horn neurons. *2005 Abstract Viewer/Itinerary Planner*, Program No. 748,2. Society for Neuroscience, Washington, DC.

Todd AJ & McKenzie J (1989). GABA-immunoreactive neurons in the dorsal horn of the rat spinal cord. *Neuroscience* **31**, 799–806.

Tsuda M, Inoue K & Salter MW (2005). Neuropathic pain and spinal microglia: a big problem from molecules in 'small' glia. *Trends Neurosci* **28**, 101–107.

Watkins LR, Maier SF & Goehler LE (1995). Immune activation: the role of pro-inflammatory cytokines in inflammation, illness responses and pathological pain states. *Pain* **63**, 289–302.

Woolf CJ (1983). Evidence for a central component of post-injury pain hypersensitivity. *Nature* **306**, 686–688.

Wu K, Len GW, McAuliffe G, Ma C, Tai JP, Xu F & Black IB (2004). Brain-derived neurotrophic factor acutely enhances tyrosine phosphorylation of the AMPA receptor subunit GluR1 via NMDA receptor-dependent mechanisms. *Brain Res Mol Brain Res* **130**, 178–186.

Yajima Y, Narita M, Usui A, Kaneko C, Miyatake M, Narita M, Yamaguchi T, Tamaki H, Wachi H, Seyama Y & Suzuki T (2005). Direct evidence for the involvement of brain-derived neurotrophic factor in the development of a neuropathic pain-like state in mice. *J Neurochem* **93**, 584–594.

Zhou XF, Chie ET, Deng YS, Zhong JH, Xue Q, Rush RA & Xian CJ (1999). Injured primary sensory neurons switch phenotype for brain-derived neurotrophic factor in the rat. *Neuroscience* **92**, 841–853.

Zhou XF, Deng YS, Xian CJ & Zhong JH (2000). Neurotrophins from dorsal root ganglia trigger allodynia after spinal nerve injury in rats. *Eur J Neurosci* **12**, 100–105.

Zhuang ZY, Gerner P, Woolf CJ & Ji RR (2005). ERK is sequentially activated in neurons, microglia, and astrocytes by spinal nerve ligation and contributes to mechanical allodynia in this neuropathic pain model. *Pain* **114**, 149–159.

© 2007 The Authors. Journal compilation © 2007 The Physiological Society

Acknowledgements

We thank Ms Araya Ruangkittisakul for skilled assistance with calcium imaging experiments, Dr Gerda deVries for help with curve fitting and Dr Kwai Alier for comments on an earlier version of the manuscript. Funding support was provided by the Canadian Institutes for Health Research (CIHR, MOP 13456 and MT10520), the Christopher Reeve Paralysis Foundation and the Alberta Heritage Foundation for Medical Research (AHFMR). V.B.L. received studentship stipends from the CIHR and AHFMR. W.F.C. and K.B. are AHFMR Medical Scientists. Funding for equipment in K.B.'s laboratory provided by AHFMR, the Canadian Foundation for Innovation and the Alberta Science and Research Authority (ASRA).

UNCORRECTED

© 2007 The Authors. Journal compilation © 2007 The Physiological Society